Marinisation of Solix Oxide Fuel Cells
Inclination Experiments, Thermodynamic analysis, and Power Plant Design

van Veldhuizen, B.N.

DOI
10.4233/uuid:879dfbd9-beef-40ea-98e7-f6a3da152b50

Publication date
2025

Document Version
Final published version

Citation (APA)
van Veldhuizen, B. N. (2025). *Marinisation of Solix Oxide Fuel Cells: Inclination Experiments, Thermodynamic analysis, and Power Plant Design*. [Dissertation (TU Delft), Delft University of Technology]. https://doi.org/10.4233/uuid:879dfbd9-beef-40ea-98e7-f6a3da152b50

Marinisation of Solid Oxide Fuel Cells

Inclination Experiments, Thermodynamic Analysis, and Power Plant Design

Marinisation of Solid Oxide Fuel Cells

Inclination Experiments, Thermodynamic Analysis, and Power Plant Design

Dissertation

for the purpose of obtaining the degree of doctor
at Delft University of Technology
by the authority of the Rector Magnificus prof. dr. ir. T.H.J.J. van der Hagen
chair of the Board for Doctorates
to be defended publicly on
Tuesday 25 February 2025 at 12:30 o'clock

by

Berend Nathan van Veldhuizen

Master of Science in Marine Technology
Delft University of Technology, The Netherlands
born in Delft, The Netherlands

This dissertation has been approved by the promotors.

Composition of the doctoral committee:

Rector Magnificus	chairperson
Prof. ir. J.J. Hopman	Delft University of Technology, promotor
Prof. dr. ir. A. Purushothaman Vellayani	University of Groningen / Delft University of Technology, promotor
Dr. ir. L. van Biert	Delft University of Technology, copromotor
Independent members:	
Prof. dr. ir. L.L.M. Veldhuis	Delft University of Technology
Dr. F. Ruzzenenti	University of Groningen
Dr. S.A. Ansar	Deutsches Zentrum für Luft- und Raumfahrt
Prof. dr. ir. B.J. Boersma	Delft University of Technology
Dr. ir. A. Coraddu	Delft University of Technology, reserve member

This research is supported by the European Nautilus Project (grant number 861647), which aims at developing, evaluating, and validating a highly efficient and dynamic integrated SOFC fuelled by LNG for long-haul passenger ships.

Keywords: Solid oxide fuel cells, system integration, ships, marine applications, emission reduction cathode off-gas recirculation, thermodynamic analysis, inclination experiment.

Printed by: Ridderprint B.V.

Front & Back: The cover artwork by Kees Fritschy captures the essence of sea waves, merging their natural flow with a green palette to reflect a commitment to sustainability.

ISBN 978-94-6506-928-9

An electronic version of this dissertation is available at
http://repository.tudelft.nl/.

A master in the art of living draws no sharp distinction between his work and his play. He hardly knows which is which. He simply pursues his vision of excellence through whatever he is doing, and leaves others to determine whether he is working or playing. To himself, he always appears to be doing both.

Lawrence Pearsall Jacks

Contents

Summary xi

Samenvatting xiii

Nomenclature xvii

1 Introduction 1
- 1.1 Emissions in the marine industry . . . 2
- 1.2 Developments towards emission reduction . . . 2
- 1.3 Fuel cells for marine applications . . . 3
- 1.4 Potential of SOFCs for marine applications . . . 3
- 1.5 Research objectives . . . 4
- 1.6 Thesis outline . . . 7

2 Solid oxide fuel cells for marine applications 9
- 2.1 Introduction . . . 10
- 2.2 SOFC power plants . . . 10
  - 2.2.1 SOFC stacks . . . 10
  - 2.2.2 Balance of plant components . . . 12
  - 2.2.3 Combined cycles . . . 15
  - 2.2.4 Fuel possibilities for SOFCs . . . 17
- 2.3 SOFC in marine applications . . . 21
  - 2.3.1 Marine power plants . . . 25
  - 2.3.2 SOFC ship integration . . . 28
  - 2.3.3 SOFC impact . . . 34
  - 2.3.4 Research projects . . . 36
- 2.4 Addressing marine challenges . . . 40
  - 2.4.1 SOFC operation . . . 42
  - 2.4.2 Power density . . . 43
  - 2.4.3 Lifetime . . . 44
  - 2.4.4 Transient capabilities . . . 45
  - 2.4.5 Capital cost . . . 46
- 2.5 Overview of suggested research directions . . . 47
- 2.6 Conclusion . . . 49

3 The influence of inclinations and accelerations on SOFC systems 51
- 3.1 Introduction . . . 52
- 3.2 Methodology . . . 53
  - 3.2.1 Tested SOFC system . . . 53
  - 3.2.2 Experimental set-up . . . 53

3.2.3 Test conditions . . . 54
3.2.4 Degradation rate prediction . . . 55
3.3 Results & discussion . . . 57
3.3.1 Static inclination test. . . . 57
3.3.2 Dynamic inclination tests . . . 57
3.3.3 Degradation test . . . 60
3.3.4 Acceleration test . . . 62
3.3.5 Comparing normal and inclined operation . . . 62
3.4 Guidance for development and regulations . . . 64
3.4.1 Generalizability of experiment . . . 64
3.4.2 Implications for stack development . . . 65
3.4.3 Implications for system operation . . . 66
3.4.4 Implications for ship design and regulations . . . 68
3.5 Conclusion . . . 69

4 Fuel efficiency of SOFC system with COGR for alternative fuels 71
4.1 Introduction . . . 72
4.1.1 Heat integration of SOFC systems . . . 72
4.1.2 Cathode off-gas recirculation . . . 72
4.1.3 Objective & Outline . . . 73
4.2 Description of selected SOFC systems . . . 74
4.2.1 Methane system . . . 76
4.2.2 Methanol system. . . . 76
4.2.3 Diesel system . . . 76
4.2.4 Ammonia system . . . 77
4.2.5 Hydrogen system . . . 77
4.3 Methodology . . . 77
4.3.1 SOFC model . . . 77
4.3.2 Balance of plant components . . . 80
4.3.3 Cathode recirculation system . . . 80
4.3.4 System performance . . . 80
4.4 Results . . . 81
4.4.1 Electrical and heat efficiency. . . . 81
4.4.2 Oxygen utilisation and blower losses. . . . 83
4.4.3 Effect of cathode off-gas recirculation . . . 84
4.5 Discussion . . . 87
4.5.1 Model limitations . . . 87
4.5.2 Model verification . . . 90
4.5.3 Result validation . . . 90
4.6 Conclusion . . . 94

5 Scaling of SOFC systems to high rated power 95
5.1 Introduction . . . 96
5.2 SOFC system . . . 96
5.2.1 System definition . . . 96
5.2.2 Scaling of SOFC system . . . 97

5.3 Design of scaled SOFC system . . . 99
5.3.1 Design considerations . . . 101
5.3.2 Design considerations . . . 101
5.3.3 Concept design SOFC unit . . . 103
5.3.4 Concept design of SOFC room . . . 107
5.4 Conclusion . . . 110

6 Dynamic simulation of hybrid SOFC power plant **111**
6.1 Introduction . . . 112
6.2 Methodology . . . 115
6.2.1 Design scenarios . . . 115
6.2.2 Component sizing model . . . 117
6.2.3 Power plant simulation model . . . 119
6.2.4 Adaptation of battery and boiler components . . . 127
6.3 Results . . . 127
6.3.1 Volume and mass of power plant. . . . 127
6.3.2 Power and energy balance . . . 131
6.3.3 Degradation effects . . . 133
6.3.4 Fuel consumption and emissions . . . 133
6.4 Discussion . . . 137
6.4.1 Range and installed power requirements. . . . 137
6.4.2 Advanced energy management . . . 137
6.4.3 Applicability of simulation model . . . 138
6.5 Conclusion . . . 139

7 Application discussion **141**
7.1 Power plant performance . . . 142
7.2 Ship applications . . . 144
7.3 Conclusion . . . 149

8 Conclusions and recommendations **151**
8.1 Conclusions. . . . 152
8.2 Recommendations for future research . . . 155

A Appendix **157**
A.1 Emission data review . . . 157
A.2 Marine inclination conditions and regulations . . . 157
A.3 Data processing of inclination experiment . . . 159
A.4 Simulation parameters of validation studies . . . 160
A.5 Derivation of initial battery capacity sizing . . . 164
A.6 Emission data for power plant simulation. . . . 165

Bibliography **169**

Acknowledgements **193**

Curriculum Vitæ **195**

List of Publications **197**

SUMMARY

Ships have been, are, and will be crucial in transporting materials, goods, energy, and people. 90% of the things people directly or indirectly use in their daily lives once were on a ship, may it be a fish for dinner, a wind turbine blade that converts wind to electric energy, or the hydrogen that fuels a car. All these ships contribute significantly to the global emissions of greenhouse gases and toxic airborne pollutants. Consequently, the International Maritime Organisation sets stringent limits on sulphurous and nitrous oxide emissions, especially in sensitive areas, and aims to reach net-zero greenhouse gas emissions by 2050.

Solid oxide fuel cell (SOFC) systems are a high-potential solution for reducing emissions. Compared to marine diesel engines, SOFC systems convert fuel with a higher efficiency, which results in a substantial decrease in carbon emissions. Furthermore, SOFCs emit negligible amounts of toxic airborne pollutants. Other benefits for marine use include high system redundancy, along with the absence of noise and vibrations. State-of-the-art systems are fuelled with natural gas, which has been adopted across many ship types in recent years. Further decarbonisation is achievable with bio- or synthetic methane, or by transitioning to SOFC systems powered by hydrogen, methanol or ammonia, for which systems are under development. In short, significant emission reductions are already possible with the existing fuel infrastructure and carbon neutrality can be achieved as SOFC technologies and renewable fuel infrastructure continue to advance.

In this dissertation, it is evaluated how SOFC systems can be effectively integrated into ships to reduce emissions. Marine SOFC research and industry projects are extensively reviewed, covering the characteristics and challenges of SOFC power plants, fuel possibilities, and ship integration opportunities. Subsequently, the influence of ship motions on the operation, safety, and lifetime of SOFC systems is studied experimentally. The electric and heat efficiency of SOFC systems are compared for several fuels using thermodynamic analysis and it is investigated how SOFC modules can be scaled to a megawatt-size marine power plant. Such a power plant, including SOFCs, generators, batteries and boilers is simulated for different hybrid scenarios. Finally, a qualitative analysis discusses the applicability of SOFC systems for a wide variety of ship types.

The review identifies that using SOFCs in ships introduces challenges compared to land-based systems, such as exposing the system to inclinations, accelerations, and highly varying load profiles. A comparison with state-of-the-art marine power plants shows that power density, capital cost, and lifetime improvements are necessary to compete with marine combustion engines. Cathode off-gas recirculation is proposed as a research topic to reduce the system's footprint by decreasing the primary process air requirements. The hybridisation of SOFC systems with generator sets and batteries is suggested to reach feasibility in terms of cost, size and transient capabilities.

A 1.5 kW SOFC module is operated on an inclination platform to evaluate the influence of ship motions. There were no detectable gas leakages or safety hazards during all test conditions. Nevertheless, dynamic inclinations resulted in forced oscillations in system parameters such as power supply and electric efficiency. This was caused by the natural frequency of a plunger in the fuel supply and was solved by changing the valve. The following is proposed for design practices and regulations: besides the stack technology, balance of plants components and their interaction with the stacks should also be evaluated on inclinations. Furthermore, the control feedback should be designed such that potential periodical deviations in operational parameters do not propagate through the system. All in all, SOFC systems can be exposed to ship motions after relatively simple design modifications.

The thermodynamic performance of an SOFC system is compared for methane, methanol, diesel, ammonia, and hydrogen. The highest net electrical efficiency is achieved with methane, in which the parasitic losses of the air blower have a major influence. The highest heat efficiency is found for ammonia. Fuels operating on a lower oxygen utilisation (methanol, diesel, and hydrogen) require significant exhaust heat to warm the process air, resulting in exhaust temperatures insufficient to produce steam for high-temperature applications on the ship. To conclude, ammonia yields the highest fuel efficiency if the dedicated ship has a significant heat demand, otherwise, methane is preferable. Cathode off-gas recirculation is also examined as a potential system configuration, which leads to a reduction in primary airflow and an improvement in thermal efficiency.

A concept design of a megawatt-size SOFC system is developed, with the aim of improving the power density by smartly centralising components. The preference for handleable stack replacement forces a limitation in scaling the SOFC system to a high-rated power. By using a large stack footprint and centralising BOP components on different levels, it is possible to significantly improve the power density.

A power plant simulation model is developed to evaluate different hybrid scenarios on size, weight, fuel efficiency and emissions. The results show that using SOFCs for the auxiliary consumers significantly reduces emissions of greenhouse gas and toxic airborne pollutants. This satisfies the greenhouse gas emission reduction target of 30% by 2030 with limited consequences for the size of the power plant.

Finally, the applicability of SOFCs on different ship types is discussed based on range requirements, load profile, and auxiliary and heat demand. Ships with high range requirements and stable, predictable propulsion or auxiliary loads offer the greatest potential for significant efficiency gains, for instance: container ships, gas carriers, bulk carriers, tankers, cruise ships, and research vessels.

This dissertation highlights several integration concepts and opportunities for an effective SOFC system, focusing on size, weight, fuel efficiency and emissions. Using the SOFC system solely for the auxiliary load contributes to large emission reduction while requiring limited battery capacity and space. This is possible with currently available technology and infrastructure. However, to achieve further emission reductions, the development of SOFC systems using alternative fuels is essential, alongside improvements in power density and transient capabilities.

SAMENVATTING

Schepen waren, zijn, en zullen essentieel zijn voor het transporteren van grondstoffen, producten, energie en mensen. 90% van alles wat men dagelijks gebruikt was ooit op een ship, van een vis die we bereiden, een wind turbine blad die energie genereert, tot de waterstof die we tanken voor onze auto. Al deze schepen dragen significant bij aan de globale emissie van broeikasgassen en schadelijke stoffen. In reactie heeft de International Maritime Organisation een plan opgesteld om emissies te reduceren. Ze introduceerden strenge limieten op zwavel- en stikstofoxiden en streven dat de scheepsvaartindustrie emissieneutraal vaart in 2050.

Solid oxide fuel cell (SOFC) systemen hebben potentie om scheepsemissies drastisch te reduceren. Vergeleken met scheepsmotoren, converteren SOFC systemen brandstof met hoge efficiëntie, wat leidt tot een reductie in koolstofdioxide emissies. Bovendien stoten SOFC systemen erg weinig schadelijke emissies uit. Andere voordelen voor de scheepstoepassing zijn een hoge systeem redundantie, samen met een laag geluids- en trillingsniveau. Commerciële SOFC system worden aangedreven door aardgas, wat de laatste 10 jaar is veel schepen is toegepast. Verdere decarbonisatie is mogelijk met bio-of synthetische methaan, of door over te schakelen naar waterstof, methanol, of ammoniak. Kortom, aanzienlijke emissie reductie is binnen bereik met bestaande infrastructuur, en voor koolstofneutraliteit is verdere ontwikkeling van SOFC technologie nodig gepaard met alternatieve brandstof productie en distribute.

Deze dissertatie behandeld de integratie van SOFC systemen in schepen. De huidige staat in onderzoek en industriële projecten wordt eerst uitgebreid besproken, waarbij de kenmerken en uitdagingen van SOFC systemen, brandstof opties en integratie mogelijkheden aan bod komen. Vervolgens wordt met behulp van een inclinatie testopstelling onderzocht hoe scheepsbewegingen de operatie, veiligheid en levensduur van SOFC systemen beïnvloeden. De brandstof efficiëntie wordt vergeleken voor SOFC systemen met vijf verschillende brandstoffen, waarvoor thermodynamische modellen zijn ontwikkeld. Gebaseerd op deze analyse wordt er een concept ontwerp gepresenteerd waarbij modules van enkele kilowatt worden geschaald naar een megawatt schaal machine ruimte voor schepen. De operatie van het hele energy systeem, wat generatoren, SOFC's, batterijen en boilers bevat, wordt vervolgens gesimuleerd voor verschillende hybride architecturen. Tot slot wordt de toepasbaarheid van SOFC systemen voor verschillende scheepstypes besproken.

Uit het literatuuronderzoek blijkt dat het gebruik van SOFC's in schepen nieuwe uitdagingen met zich meebrengt vergeleken met systemen op land, bijvoorbeeld blootstelling aan hellingen en versnellingen en sterk variërende belastingprofielen. Een vergelijking met huidige scheepsgeneratoren laat zien dat verbeteringen in vermogensdichtheid, aanschafprijs en levensduur nodig zijn om te kunnen concurreren. Kathode recirculatie wordt voorgesteld als een onderzoeksonderwerp omdat het de benodigde lucht toevoer verminderd. Hybridisatie van SOFC systemen met generatoren en batterijen

wordt aanbevolen om tot een haalbaar systeem te komen op het gebied van kosten, omvang en het voldoen aan variërende belastingen.

Een 1,5 kW SOFC-module is getest op een inclinatieplatform om de invloed van scheepsbewegingen te evalueren. Er werden geen detecteerbare gaslekken of veiligheidsrisico's waargenomen tijdens de verschillende testen. Dynamische inclinaties leidden echter tot oscillaties in systeemparameters, zoals stroom en elektrische efficiëntie. Dit werd veroorzaakt door de eigenfrequentie van de klep in de brandstoftoevoer en was voorkomen door de klep aan te passen. Voor de ontwerpfase en regelgeving wordt het volgende aanbevolen: naast de stacktechnologie moeten ook ondersteunende componenten en hun interactie met de stacks op inclinaties worden geëvalueerd. Daarnaast moet het regelsysteem zodanig worden ontworpen dat periodieke afwijkingen in operationele parameters niet door het systeem propageren. Al met al kunnen SOFC-systemen na relatief eenvoudige ontwerpaanpassingen worden blootgesteld aan scheepsbewegingen.

De thermodynamische prestaties van een SOFC systeem worden vergeleken voor methaan, methanol, diesel, ammoniak en waterstof. De hoogste netto elektrische efficiëntie wordt bereikt met methaan, waarvoor de energie consumptie van de ventilator een grote invloed hebben. De hoogste warmte-efficiëntie is gevonden bij ammoniak. Brandstoffen met een lagere zuurstofgebruik factor (methanol, diesel en waterstof) vereisen een aanzienlijke hoeveelheid warmte om de proceslucht op temperatuur te brengen, wat resulteert in uitlaattemperaturen die onvoldoende zijn om warmte terug te winnen voor het stoom net van het schip. Samenvattend levert ammoniak de hoogste brandstofefficiëntie als het schip een aanzienlijke warmtebehoefte heeft; anders heeft methaan de voorkeur. Kathode recirculatie is ook onderzocht als een potentiële systeemconfiguratie, wat resulteerde in een lagere primaire luchtstroom, een kleinere warmtewisselaar en verbetering van de thermische efficiëntie.

Er is een conceptontwerp ontwikkeld voor een SOFC-systeem van megawatt formaat, met als doel de vermogensdichtheid te verhogen door bepaalde componenten te centraliseren. Het ontwerpproces toonde aan dat het vermogen van de SOFC modules gelimiteerd is door de voorkeur om het vervangen van modules hanteerbaar te houden. Door een groot cel oppervlak te gebruiken en de ondersteunende componenten op verschillende niveaus te centraliseren, is de vermogensdichtheid aanzienlijk verbeterd.

Een simulatiemodel wordt gebruikt om verschillende hybride scenario's te beoordelen op basis van volume, gewicht, brandstofefficiëntie en emissies. De resultaten tonen aan dat als SOFC's worden ingezet om alleen te voldoen aan de hulp vermogensvraag, de uitstoot van broeikasgassen en verontreinigende stoffen al aanzienlijk verminderen. Dit voldoet het reductiedoel van 30% minder broeikasgasemissies in 2030, met een overzienbare impact op de grootte van het systeem.

Tot slot wordt de toepasbaarheid van SOFC's voor verschillende scheepstypes besproken, gebaseerd op de vereisten voor actieradius, het belastingprofiel, en de behoefte aan hulpvermogen en warmte. Schepen met een grote actieradius, en stabiel en voorspelbaar voortstuwings- of hulpvermogensvraag bieden het meeste potentieel voor efficiëntiewinst, bijvoorbeeld containerschepen, gastankers, bulkschepen, tankers, cruiseschepen en onderzoeksschepen.

Deze dissertatie belicht verschillende integratieconcepten die bijdragen aan een effectief SOFC-systeem, met een focus op omvang, gewicht, brandstofefficiëntie en emissies. Het inzetten van het SOFC-systeem voor de hulp vermogensvraag draagt al sterk bij aan emissiereductie, terwijl dit slechts een beperkte batterijcapaciteit en ruimte vraagt. Dit is binnen bereik met de huidige technologie en bestaande infrastructuur. Voor verdere emissiereducties is echter de ontwikkeling van SOFC-systemen op alternatieve brandstoffen noodzakelijk, gepaard met verbeteringen in vermogensdichtheid en de capaciteit om belasting te volgen.

Nomenclature

In this dissertation, symbols and parameters are consistently defined in the text when applied. Abbreviations are explained per chapter and common abbreviations are summarised below:

AC	alternating current
AOGR	anode off-gas recirculation
APU	auxiliary power unit
BAT	battery
BOP	balance of plant
CHP	combined heat and power
CO	carbon monoxides
COGR	cathode off-gas recirculation
DC	direct current
DFG	dual-fuel generator
DG	diesel generator
DME	dimethyl ether
DOD	depth of discharge
ECA	emission control area
ER	external reforming
FT	Fischer-Tropsch
GG	gas generator
GHG	greenhouse gases
GPR	gaussian process regression
GT	gas turbine
HDS	hydrodesulphurisation

HRSG	heat recovery steam generator
HT	high temperature
HVAC	heating, ventilation and air conditioning
HW	hot water
ICE	internal combustion engine
IMO	International Marine Organisation
IR	internal reforming
LCA	life cycle analysis
LHV	lower heating value
LNG	liquefied natural gas
LT	low temperature
MeOH	methanol
MGO	marine gas oil
NO_X	nitrous oxides
PEMFC	proton exchange membrane fuel cell
PM	particulate matter
RE	reciprocating engine
RR	recirculation ratio
S/C	steam to carbon ratio
SO_X	sulphurous oxides
SOC	state of charge
SOFC	solid oxide fuel cell
SOH	state of health
ST	steam (turbine)
TRL	technological readiness level
TTE	tank-to-electricity
TTW	tank-to-wake
WGS	water gas shift

WHR	waste heat recovery
WTT	well-to-tank
WTW	well-to-wake

1

INTRODUCTION

The journey of a thousand miles begins with one step.

Lao Tzu

Parts of this chapter have been published in the International Journal of Energy Research **2023**, 5163448 [1].

1.1. EMISSIONS IN THE MARINE INDUSTRY

Currently, marine transport accounts for over 90% of global trade in weight [2]. Although shipping is a very efficient and cost-effective method of international transportation [3], it is also associated with much emission of greenhouse gases and toxic airborne pollutants [4]. Between 2012 and 2018, the carbon efficiency of shipping operations improved by approximately 11%. However, this progress was surpassed by a growth in activity. In the same period, carbon dioxide equivalent emissions (including carbon dioxide, methane, and nitrogen oxide) from shipping increased by 9.6%, from 977 million tonnes to 1,076 million tonnes [5]. More recently, in 2022, international shipping accounted for approximately 2% of global CO_2 emissions [6]. Besides greenhouse gasses, European shipping contributed 19% for nitrogen oxides (NO_X), 11% for sulphur oxides (SO_X) and 8% for particulate matter (PM) to the total European emissions in 2017 [7].

Consequently, in 2018, the International Maritime Organisation (IMO) adopted an ambitious strategy to reduce the greenhouse gases (GHG) and toxic airborne pollutants emitted by the shipping industry. The targets had been set to reduce carbon dioxide emissions by 40% by 2030 and 70% by 2050 (compared to 2008) [8]. In 2023, this strategy was revised. IMO now strives to reduce GHG emissions by 30% by 2030 and 80% by 2040 and reach net-zero GHG emissions by 2050 [9]. Importantly, the targets now adopt a well-to-wake approach to GHG emissions, accounting for the entire fuel lifecycle from production to combustion. Moreover, since 1 January 2023, all ships must report their Energy Efficiency Existing Ship Index (EEXI) and Carbon Intensity Indicator (CII) [10]. This forces shipbuilders and shipowners to monitor and gradually reduce carbon emissions from their ships. Furthermore, stringent limits restrict the NO_X and PM emissions from ships, especially in specific emission control areas where only 0.1% m/m is allowed [11]. Furthermore, a global sulphur cap of 0.5% for marine fuels was implemented on January 1, 2020.

1.2. DEVELOPMENTS TOWARDS EMISSION REDUCTION

Four areas can be defined for emission reduction in marine applications. Firstly, the energy consumption can be reduced, for instance, with hull and propeller optimisation [12, 13], routing optimisation [14, 15], energy regeneration [16, 17], and grid optimisation [18]. Secondly, alternative bunker fuels can be applied, for example, natural gas [19], bio-diesel [20], and low sulphur diesels [21]. CO_2 and sulphur emissions mainly depend on the fuel composition and the conversion efficiency. Methane, NO_X, and PM emissions also depend heavily on the conversion process, for instance, combustion conditions [22]. Consequently, the selection of an alternative marine fuel should be combined with the fuel conversion technology. Thirdly, fuel conversion can be improved (e.g., two-stage turbocharging, heat recovery, late miller-timing). Fourthly, exhaust gases can be treated. Scrubbers or selective catalytic reduction can be used to reduce NO_X and SO_X emissions [23]. Moreover, onboard carbon capture could offer a transitional solution to reduce carbon emissions in the short term [24].

Although remarkable improvements have been made, ship operators and shipbuilders indicate that radical changes in the power generation system and its fuel source might be necessary to reach these future regulations and goals. Battery-powered ships are an example of such a radical innovation. Charging from the coastal power grid may achieve zero emissions during sailing, and when renewable electricity is used to charge the batteries, low life cycle emissions can be guaranteed as well. So far, batteries have been applied in ships with short mission requirements, for instance, tugs and ferries [25]. However, due to their low energy density and high cost, fully battery-powered propulsion is not considered a viable solution for large ocean-going vessels [26], and will not be considered in this disseration.

1.3. Fuel cells for marine applications

Many researchers consider fuel cells a promising solution for low-emission power generation on ships [27–31]. Fuel cells convert chemical energy directly into electrical energy, enabling high efficiencies compared with combustion technology (see Figure 1.1). Besides high efficiency, these devices have several advantages for marine applications compared to diesel engines: low emissions, good part-load characteristics, high redundancy, low maintenance, and low noise and vibrations [28]. However, implementing fuel cells in combination with alternative fuels still struggles with high capital expenses, large fuel storage, lack of alternative fuel infrastructure, short lifetime, and slow transient behaviour [28, 32].

The low-temperature proton exchange membrane fuel cell (LT-PEMFC) is currently the most common fuel cell in transport applications, due to its relatively high power density, low price, and quick response to load transients. However, fuel flexibility is its main limitation [27]. LT-PEMFC only tolerates low contamination concentrations, due to its low operating temperature of 60-80 °C [33]. This means it operates best on pure hydrogen, which requires expensive and voluminous storage, which makes it impractical for ships with high range requirements. On top of that, hydrogen is currently very expensive. Alternatively, using hydrogen carriers in combination with LT-PEMFC, requires a large, complex, and expensive fuel processing plant [28]. Therefore, the interest in high-temperature fuel cells in combination with other bunker fuels has been increasing.

1.4. Potential of SOFCs for marine applications

Solid oxide fuel cells (SOFCs) are characterized by a higher fuel impurity tolerance than LT-PEMFCs [27, 28]. High-temperature PEMFCs operating at intermediate temperatures (120 - 200 °C) also inherit an increased impurity tolerance, but in general, do not have internal reforming capabilities [33]. Natural gas (NG) and ammonia can be fed directly to SOFC systems [34], omitting the need for a large and costly fuel processing plant. Moreover, SOFCs have demonstrated high system efficiencies of 50-65%, which can be even increased to 70% with combined gas turbine cycles [35, 36]. Currently, SOFC systems struggle with low power density, high investment cost, limited lifetime, and slow response to dynamic loads [27, 28]. Nevertheless, these four challenges can be mitigated. Firstly, a high efficiency compensates for the low power-to-volume ratio. This results in lower fuel consumption, which leads to relatively smaller fuel tanks [37]. Moreover, SOFC's fuel flexibility makes it possible to use a fuel with a higher energy density at high efficiency, further decreasing the required ship volume compared to LT-PEMFC. Secondly, investment costs are expected to drop when production increases [38]. Thirdly,

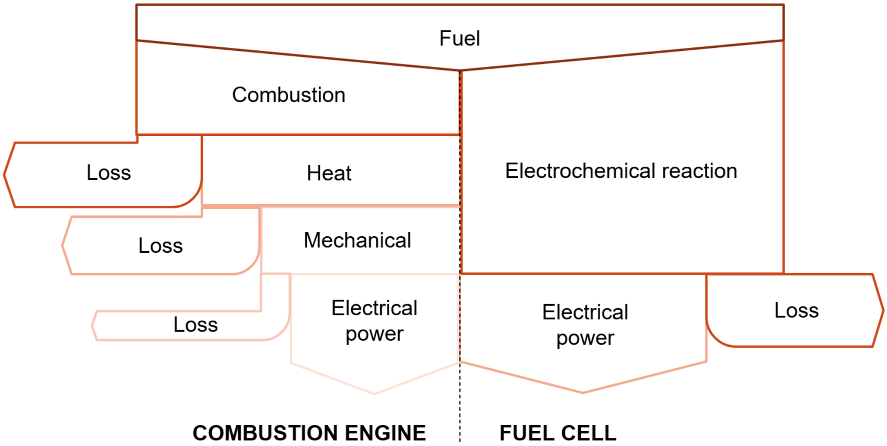

Figure 1.1: Schematic diagram of losses in fuel cell and combustion technology.

the lifetime of SOFC stacks, 30000 to 60000 hours [39], is sufficient to reach the typical five-year docking interval for most ship applications. Using a modular system design and stacks of manageable sizes the relatively short lifetime poses no significant challenge. Fourthly, SOFCs can be combined with batteries or internal combustion engines to ensure the dynamic capabilities of the power plant [28, 40, 41]. Hence, SOFCs are considered a promising power generation solution to reduce emissions from long-haul shipping.

1.5. RESEARCH OBJECTIVES

This dissertation aims to contribute to the scientific challenges of applying SOFCs in ships. Effectively integrating SOFCs in ships must result in a propulsion system with high fuel efficiency, low emissions (greenhouse gas and airborne toxic pollutants), adequate transient performance, and a sufficient operational lifespan. This is covered by the following research question:

How can SOFC systems be effectively integrated in ships in order to reduce emissions?

To identify the integration challenges already addressed and those unresolved at the outset of this doctoral research, the research field of SOFCs in marine applications was explored. This is tackled with research objective one. The subsequent research objectives emerged from this gap analysis. While the research objectives are briefly introduced below, it is recommended to read the literature review in Chapter 2 for comprehensive understanding.

1. Identify the main technical challenges of integrating SOFCs in ships.

Marine SOFC research and industry projects are extensively reviewed in Chapter 2, covering the characteristics and challenges of SOFC power plants, fuel possibilities, and ship integration opportunities. To compare SOFC systems with other technologies they need to be evaluated on efficiency, size, weight, load-following capability, maintenance intensity, safety, reliability, economics and environmental impact. Although SOFC systems perform well on efficiency and emissions, compared with state-of-the-art power generation in ships, they lack volumetric and gravimetric power density, lifetime, transient capability and cost competitiveness. Moreover, compared to land-based systems, the marinisation of SOFC systems introduces new challenges in design and integration:

- The SOFC systems must be able to withstand inclinations and accelerations, which most commercial systems are currently not designed for.
- To compete with a marine engine on fuel efficiency, an SOFC system must have the highest possible electrical efficiency and sufficient heat recovery capability. Various bunker fuels are being considered in the marine industry, and it is important to evaluate the electrical and thermal efficiency that SOFC systems can achieve with these fuels.
- The low oxygen utilisation of SOFCs leads to large air and exhaust flows. Reducing these flows would save ship space. Cathode off-gas recirculation has been suggested as a possible method as it improves the overall oxygen utilisation of the system and thus the primary airflow.
- Current SOFC systems must be scaled to high-power modular marine systems with increased power density while ensuring system redundancy.
- For a feasible system, SOFCs are expected to be coupled with batteries to ensure transient capability. Alternatively, a power plant hybridised with engines would limit the impact on the size and cost.
- The degradation of the stacks should be included in the system sizing and system operation.

These integration challenges are covered by the five research objectives below.

2. Evaluate the influence of marine conditions in terms of static and dynamic inclinations on the operation, safety, and lifetime of SOFC systems.

Most SOFC systems are designed for static land-based applications and the effect of inclinations and accelerations is not widely studied. A 1.5 kW SOFC module is operated on an inclination platform that emulates ship motions. The conditions and regulations of marine power plants have been used to define the test conditions. The test campaign consists of a static inclination test, a dynamic test, a degradation test, and a high acceleration test. Although the SOFC module does not fail in any test condition, dynamic inclinations result in forced oscillations in the fuel regulation. These variations propagate through the system by different feedback loops in the control architecture, leading to significant deviations in the operational parameters of the system. Several enhancements are recommended to improve the design of SOFCs and marine fuel cell regulations to ensure their safe operation on ships.

3. Evaluate the electric and heat efficiency of a marine SOFC power plant using alternative fuels and COGR.

It is often reported that SOFC systems operate on a high fuel efficiency and can cater for the electrical and heat demand in ships. Nevertheless, in an integrated system, the supporting components also use heat and electricity. Moreover, the used fuel also determines which supporting components are necessary. To compare the fuel efficiency, a 100 kW SOFC stack and its balance of plant components have been thermodynamically modelled for LNG, methanol, FT-diesel, ammonia and hydrogen. Although, the highest net electrical efficiency was found for methane (58.1%), when including heat efficiency, ammonia results in the highest fuel efficiency. In addition, COGR is investigated to tackle low oxygen utilisation, which greatly improves heat efficiency. Moreover, the primary airflow was reduced significantly. This is beneficial for the SOFC system because it decreases the size and cost of the air pre-heater. It is also beneficial for the ship because it reduces the space required for ducting.

4. Identify the scale advantages of high-power modular SOFC systems for ships.

Most commercial systems are not available on the power scale required for large ships. There is a need to scale SOFC systems from kW to MW scale marine power plants while exploiting scale effects to improve the power density and specific cost of these systems. A concept of a modular 125kW SOFC unit and a 1.125 MW SOFC room has been developed. This includes centralising certain components such as fuel treatment and air blowers to increase the space and cost efficiency of the system. It is found that the high weight of SOFC stacks, combined with their regular replacement interval, has a significant impact on the sizing of the modular parts in the system. Moreover, applying COGR significantly decreases the space needed for process air and exhaust piping.

5. Evaluate the volume, mass, fuel consumption, and emissions of hybrid SOFC power plants while taking into account component degradation.

SOFC systems compete with conventional combustion technologies. To assess its advantages and shortcomings, different hybrid SOFC power plants are compared in terms of volume, mass, fuel consumption, and emissions. The scope of emissions includes greenhouse gases and airborne toxic pollutants NO_x, SO_x, CO, and PM. A component sizing model and a dynamic power plant simulation model are developed to estimate these performance metrics. An energy management strategy based on the battery state of charge allocates the power between the fuel cells, engines, batteries, and boilers. The electric and heat balance are simulated for five operational years of a cruise ship, including part-load operation and component degradation. The results emphasise the importance of dynamic simulation for accurate battery sizing. Moreover, significant emission reduction can be achieved with a limited amount of installed SOFC power, minimising the impact on ship design and cost.

6. Identify which ship applications match the technical specifications of SOFC systems.

The ship type and its operational profile dictate which power-generating device and fuel type are best applied to its propulsion system. SOFCs are typically most suitable for long-range applications, primarily due to the limitations of other low-emission solutions. Moreover, a predictable load profile with little variations is beneficial for SOFCs. Lastly, ships with significant heat demand can benefit from the heat recovery capacity of SOFC systems. The applicability of SOFCs on different ship types is discussed on the range requirements, predictability of load profile, and size of auxiliary and heat demand. Container ships, gas carriers, bulk carriers, tankers, cruise ships, and research vessels are identified as suitable applications for SOFC systems.

1.6. THESIS OUTLINE

The research objectives are addressed in separate chapters, as shown in Figure 1.2. Chapter 2 extensively examines the research field and this understanding is used to define the remaining research objectives. First, in Chapter 3, it is assessed whether SOFCs can handle the inclinations and accelerations that a ship power plant is exposed to. A wide scalar of ship motions is considered to ensure applicability to a wide range of ship types. The potential conversion efficiency of the system is assessed in Chapter 4, where an SOFC system is thermodynamically evaluated for five different fuel types. After proving that an SOFC system can convert fuel very efficiently. The SOFC system is scaled to a high-power marine plant in Chapter 5. A concept design is presented for a SOFC cabinet with replaceable stacks, which can be scaled to a high-power solution. This concept is integrated into the ship in Chapter 6, where the SOFC system is hybridised with batteries and engines, and dynamically simulated. Different design scenarios are evaluated based on volume, mass fuel consumption and emissions. In Chapter 7, it is discussed for which ship types SOFC systems are best applicable and finally in Chapter 8, the conclusions are presented and future research directions are proposed.

1

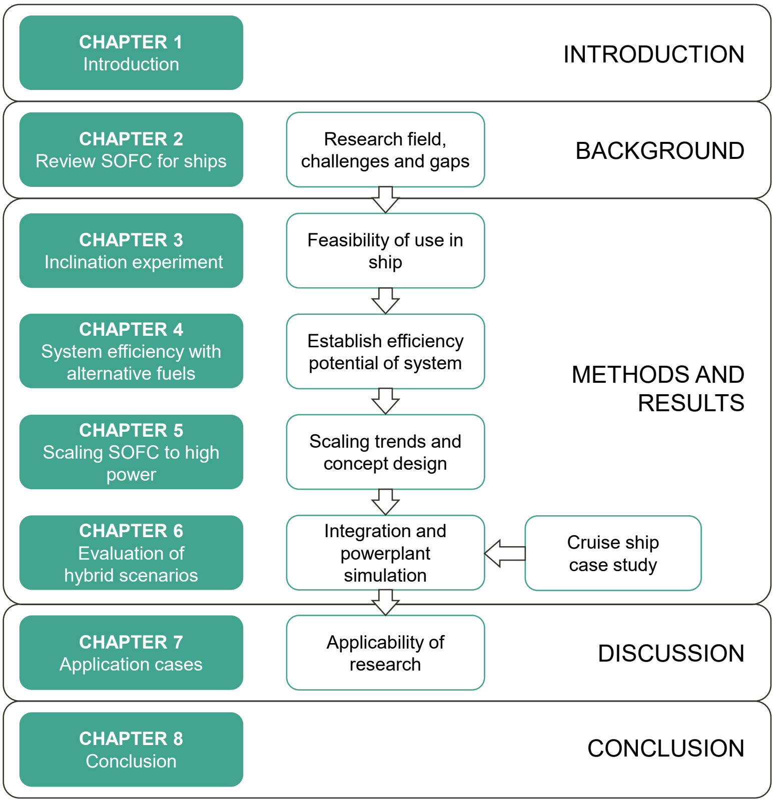

Figure 1.2: Dissertation outline.

2

SOLID OXIDE FUEL CELLS FOR MARINE APPLICATIONS

Discovery consists of seeing what everybody has seen and thinking what nobody has thought.

Albert Szent-Györgyi

Parts of this chapter have been published in the International Journal of Energy Research **2023**, 5163448 [1].

2.1. INTRODUCTION

SOFCs are considered a promising power generation solution for long-haul marine applications [27–29, 42]. This chapter contains a review of literature and research projects regarding SOFC in marine applications. The technical, economical, and societal challenges of SOFC implementation are identified and are used to form a guidance for future research. These insights support marine actors in their consideration of applying SOFCs in ships.

First, general developments in SOFC systems are examined, which covers SOFC stacks, combined cycles, power plant components, and fuel possibilities. Next, previous studies on SOFCs in ships are discussed, which includes marine power plant considerations, ship integration opportunities, and financial and environmental impact. Finally, gaps in the current literature are identified from the review and propositions are made for future research. This chapter mainly covers system considerations and developments relevant for the marinisation of SOFC systems. Recent developments in cell materials, cell manufacturing, and stack assembly are outside the scope as these are not specific to marine applications and are often reviewed.

2.2. SOFC POWER PLANTS

The SOFCs provide electrical power and many components support the fuel cells in their operation. Moreover, there are many options in system design and system integration for an SOFC power plant. This section discusses the important characteristics and developments in the main components of SOFC systems, to get an understanding of the possibilities for a marine SOFC power plant. SOFC stacks, balance of plant components, and combined cycles are discussed. Figure 2.1 shows the most relevant components in an SOFC power plant.

2.2.1. SOFC STACKS

An SOFC is a full solid-state device with a ceramic oxide ion-conducting electrolyte. SOFCs operate at high temperatures (500-1000°C), which offers several advantages. Firstly, precious metals are not required for the catalyst. These usually form a large contribution to the expenses of low-temperature fuel cells and reduce the tolerance to fuel impurities [43]. Secondly, high-temperature exhaust gas can be utilised in combined cycles, heating purposes or cooling purposes to increase efficiency [44]. Thirdly, some fuels such as methane and ammonia can be reformed internally [28]. Although the high operating temperature of SOFCs brings opportunities, it also introduces large design challenges. All stack components need to be mechanically and chemically stable while being compatible in terms of thermal expansion, for a large range of temperatures [45]. The fuel cell stacks often form a large contribution to the fuel cell system cost, which Battelle Memorial Institute [46] concluded to be 30% for a 250 kW NG-fuelled SOFC system.

2

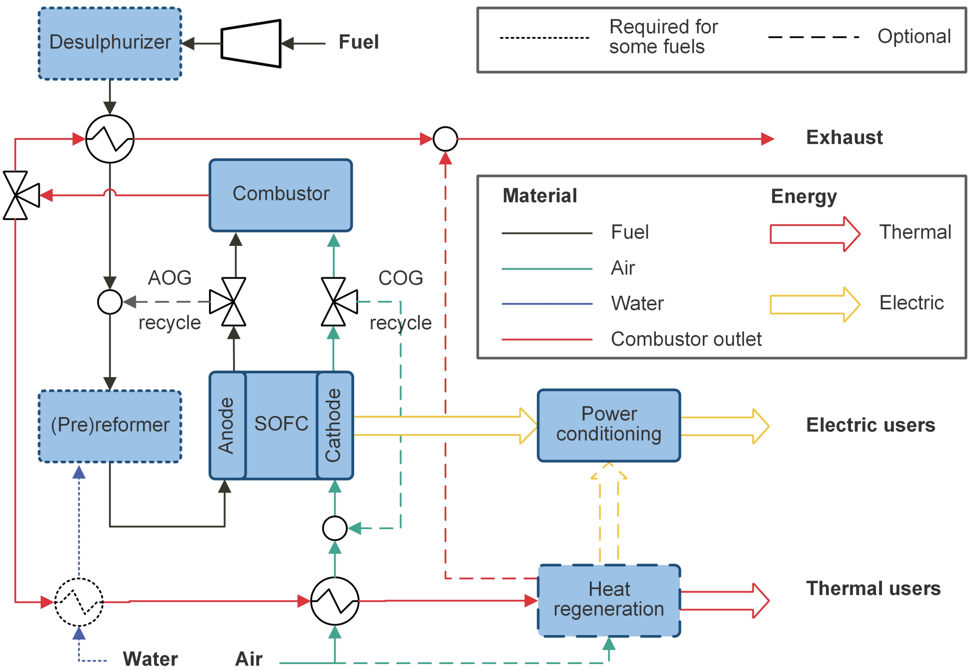

Figure 2.1: Schematic overview of SOFC power plants. AOG = Anode Off-Gas, COG = Cathode Off-Gas, [own image].

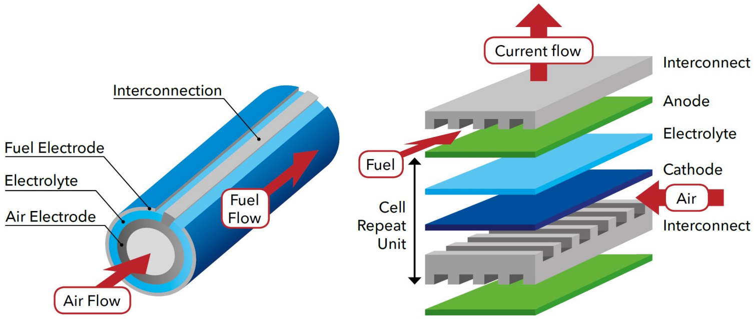

Figure 2.2: Tubular SOFC design (left) and planar SOFC design (right) [47].

Figure 2.2 shows that SOFC stack design is distinguished in planar (PSOFC) and tubular (TSOFC); the former is most often researched [48] and is dominantly used in commercial products. PSOFC has a higher power density and is easier to manufacture. Its challenges are the expensive gas-tight interconnects and mechanical stability of the cells. TSOFC eliminates gas-tight interconnects, since the fuel cell itself seals the air from the fuel and has a better mechanical strength. However, the result is a lower power density and higher manufacturing cost [49]. Welaya et al. [42] indicated the differences between PSOFC and TSOFC for marine applications by means of a thermodynamic analysis for hydrogen and LNG. Using tubular SOFC stacks resulted in higher system efficiency and thermal efficiency compared with planar stacks.

2.2.2. BALANCE OF PLANT COMPONENTS

Components that support the fuel cells in power generation are called balance of plant (BOP) components. This includes fuel processing equipment, airflow control, thermal management systems, water management systems, and power conditioning equipment [50]. These systems contain many different components (e.g., reformers, burners, blowers, evaporators, heat exchangers, generators, sensors, and valves) and form a large part of the whole system. The components have a significant effect on system efficiency, power density, cost and transient capabilities.

When liquid fuels are applied, the fuel is transferred to its gaseous phase with evaporators. Recuperators (i.e., counterflow heat exchangers) are often deployed to preheat fuel and air before these enter the SOFC by utilising the thermal energy in the SOFC outlets. This reduces carbon formation and thermal gradients in the SOFC. The external air and fuel are compressed up to the operating pressure of the fuel cell before they enter the stack. The non-reacted fuel and unused air are often combined and burned in a combustor to increase the thermal energy in the exhaust stream. Diffusion- or catalytic burners are often deployed since the fuel is highly diluted [51]. When anode recirculation is applied, the fuel is recycled before combustion. The gas flows in the fuel cell system are controlled with blowers, valves, and pressure regulators.

DESULPHURISATION

Most fossil fuels contain sulphur particles. For such fuels, desulphurisation must occur before any fuel reforming steps (see Figure 2.1), because sulphur poisons the catalysts used in reformers, shift reactors and fuel cells [44]. The most suitable desulphurisation method depends on the fuel type and the sulphur tolerance of the fuel cell. Researchers and suppliers state that SOFCs require a sulphur content below 1 to 10 ppm, which is much more tolerant than LT-PEMFC. Hydrodesulphurisation (HDS) is employed in refineries to reduce sulphur content. However, this process is not desirable for marine applications due to its size and cost [52]. Moreover, HDS is inconvenient for internally reformed SOFC (see section 2.2.2), since a hydrogen-rich stream must be fed to the HDS reactor. Another option is to use sorbents for the selective removal of sulphur particles. Rheinberg et al. [52] compared several commercial sorbents with experiments and proposed nickel-based selective adsorbents for fuel cell applications to reach the desired <1 ppm sulphur content. Nevertheless, the adsorbent requires to be regenerated and they criticized adsorbents for high sulphur fuels, since the sorbent would not have sufficient capacity and the adsorption would require much time.

REFORMING STRATEGY

A fuel cell converts the chemical energy that is stored in hydrogen to electrical energy. Fuel cells are fuelled with pure hydrogen or with a fuel that contains hydrogen. There are several methods to convert hydrogen carriers to a hydrogen-rich mixture, of which steam reforming is the most efficient for SOFC [53]. Steam reforming is an endothermic reaction that needs a constant supply of heat and steam.

The conversion can occur in an external reformer. Alternatively, the heat and steam produced by the electrochemical reaction in the SOFC can be used to reform the fuel internally. Internal reforming significantly decreases system capital cost and system complexity, since no external reformer is needed [35]. For internal reforming, a distinction is made between direct and indirect reforming, see Figure 2.3. Indirect internal (IIR) reforming only makes use of the heat released from the fuel cells. With direct internal reforming (DIR), the fuel is directly fed to the anode, where the reforming occurs. DIR simplifies the system and lowers the capital cost [44]. An increased risk of carbon deposition on the anode and larger temperature gradients in the stacks (i.e., deterioration of the ceramic cell material) are challenges of direct internal reforming [35]. A pre-reformer is used in some studies to accelerate the electrochemical reactions in the fuel cell, improving the power production [36, 54].

ANODE OFF-GAS RECIRCULATION

Steam is often necessary for the reforming process. The steam demand can be satisfied with a heat recovery steam generator (HRSG), driven by the exhaust heat and using demineralised water [55, 56]. However, the anode off-gas of an SOFC already contains steam, since water is produced at the anode during the electrochemical reaction. The anode off-gas (AOG) can be recirculated using blowers or ejectors, mixed with new fuel and fed back into the fuel cell. This lowers the steam generator requirements, leading to lower capital cost [57]. Recycling the fuel also leads to lower local fuel utilisation [58] and a more homogeneous temperature and particle concentration distribution through the stack [59], which are beneficial for the cell lifetime [60]. In addition, a fuel cell does not utilise all fuel that is fed to its anode. By recycling the fuel, non-reacted fuel is utilised, slightly enhancing the overall system efficiency [61–63]. There are other advantages of anode recirculation. Firstly, less preheating of the fuel is needed. Secondly, fuel that

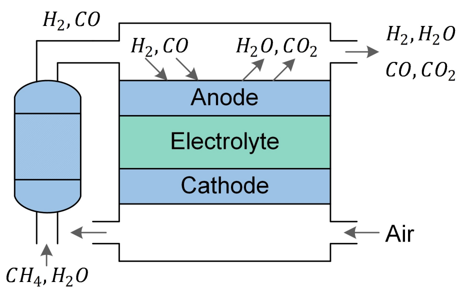

(a) External reforming.

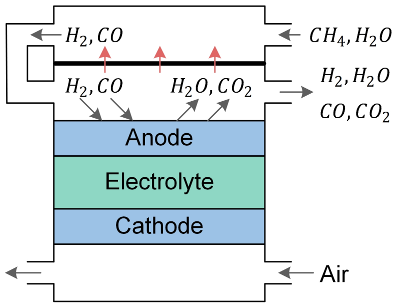

(b) Indirect internal reforming.

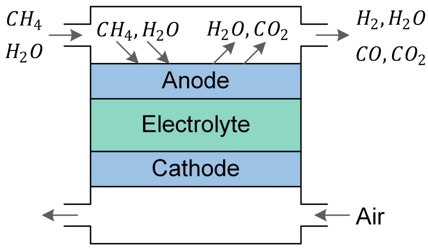

(c) Direct internal reforming.

Figure 2.3: SOFC reforming types [own images based on Choudhury et al. [44]].

enters the fuel cell is already partially reformed, which reduces the stress on the reformation catalyst [64]. In the studies by Jia et al. [57] and Peters et al. [65] it was found that an SOFC system with internal reforming and anode off-gas recirculation results in a 16-20% higher system efficiency compared with an externally reformed SOFC system without AOG recirculation. However, steam-to-carbon ratio control, which is required to prevent carbon deposition, might be less accurate [54]. On top of that, the high operating temperature adds challenges to the blower or injector design in the recirculation system. Peters et al. [62] and Hollmann et al. [66] proposed to reduce the temperature of the recirculation loop to enable the use of commercial blowers, which are available at operating temperatures up to 300 °C.

POWER CONDITIONING

Fuel cells deliver direct current and their voltage varies among others with current and age. On top of that, fuel cells do not handle reverse currents and ripple currents well [67]. Consequently, power conditioning equipment is necessary for an adequate and stable power source. Power converters are used to boost and regulate voltage. Transformers are often incorporated in these converters to protect the fuel cells from substantial voltage differences. Next, DC/AC inverters (three-phase inverters for non-residential applications) are used when AC power is required. Diodes can be used to prevent reverse current flow to the fuel cell, but introduce additional losses [68]. Capacitors can be used to filter current ripple, but increase the size and cost of the system [69].

START-UP AND COOL-DOWN

During a start-up, the SOFC needs to heat up to its operating temperature. There are two common methods to heat the SOFC. Firstly, the heating elements of the bipolar plate can be connected to an electrical power source. Secondly, the cathode air can be preheated by an electric burner and channelled through the stack, during which the inlet pressure needs to be tuned during heat-up, since the flow resistance in the stack increases with temperature. For both methods, the heating rates should be limited to the allowable thermal stress of the SOFC stack and both require similar heating energy [70]. During a shutdown, the stacks must be gradually cooled. The SOFC stack can be cooled over its cathode with air. A smaller thermal mass of the hot components decreases the start-up and cool-down time [71]. During start-up and shutdown, no air may reach the anode to prevent oxidation. This can be ensured by using a nitrogen supply system that flushes the anode or with advanced flow control. However, a nitrogen supply adds additional piping and mixing components to the system [72].

2.2.3. COMBINED CYCLES

The anode off-gas contains unused fuel and thermal energy. Even when anode recirculation is applied, not all fuel fed to the anode can be converted. To improve the electrical efficiency of the SOFC system, researchers have investigated the utilisation of this exhaust gas for combined cycles (see heat regeneration in Figure 2.1). A variety of systems have been proposed. Earlier studies focused on integration with gas or steam turbines [35], which leads to a significant increase in efficiency accompanied by poor performance at part load. Next, research increased in combined cycles with Stirling engines or reciprocating engines. These offer a significant increase in efficiency at better economics and part-load performance. Baldi [73] and Tan et al. [74, 75] studied an integration concept where purified anode off-gas of the SOFC is fed to the LT-PEMFC. The aim of this concept is to decrease the cost per kW, increase SOFC lifetime, and increase the transient capability. The concept was positively evaluated and is recently also introduced by Hagen et al. [76] for marine applications. The combined cycles that have more often been investigated for marine applications will be discussed in the following sections.

SOFC-GT

SOFC-Gas Turbine (GT) is the most studied combined cycle plant. In this concept, the SOFC generates electrical power with high efficiency, while the anode-off gas is combusted and expanded in a gas turbine to generate additional power. Most of the analyzed SOFC-GT plants operate under pressure, which couples the operation of the SOFC and GT. This has the negative consequence that the transient behaviour of the slowest component depends on the overall system dynamics. A pressurized SOFC system also decreases system simplicity and reliability [35]. Nevertheless, pressurized operation increases the efficiency of the SOFC by increasing its cell voltage [42, 77]. Combined cycle research shows an electrical efficiency of 58% to 76% for SOFC-GT systems [36]. Kawabata et al. [78] published the testing evaluation of the first commercially available SOFC-GT system. They tested the load-following behaviour, SOFC degradation, emissions, noise, and vibrations. The safety was also evaluated for emergency shutdown events, such as internal errors, electricity blackout, or earthquakes. Safe outdoor operation was demonstrated at 53.6% electrical efficiency (LHV) and a practical durability of 10 years was concluded. Despite the promising numbers, off-design and part-load performance have resulted in a significant efficiency drop. Many studies concluded that high efficiency can only be reached when the turbomachinery is operating at the design condition [35, 79–81]. An absolute decrease in electrical efficiency of 23% was reported by Chen et al. [82] at 50% load with simple fuel flow control. Consequently, sustaining high efficiency requires complex control strategies [83].

SOFC-ST

The combusted anode-off gas can also be used to drive a steam turbine (SOFC-ST). Similar to the SOFC-GT system, the steam turbine can be used to increase SOFC system efficiency [84]. Biert et al. [36] concluded that gas turbine integration is more attractive for SOFCs operating at relatively low fuel utilisation, moderate cell voltages, and high stack temperatures. A steam turbine is the better choice for relative low stack temperatures and high voltage. They also concluded that the average stack power densities for a pressurized SOFC-GT and SOFC-ST are, respectively, 75% and 25% higher compared with a stand-alone system of similar electrical efficiency. However, it is not known how this relates to the power density of the total system. Arsalis [85] mentions that steam turbines (and gas turbines to a lesser extent) are inefficient for relatively small power plants. A significant efficiency difference was found between a 1.5 MW and 5 MW application.

SOFC-RE

It is also possible to integrate an SOFC stack with a reciprocating engine (RE). These generally have better part-load, cost, and durability characteristics than gas turbines [77]. On top of that, the operation of the engine can be decoupled by bypassing the fuel directly into the engine. Rapid load transients cause degradation in the fuel cells, decreasing the SOFC lifetime. Engines can quickly respond to load changes, where SOFCs and turbines respond slower. Consequently, integrating SOFC and RE improves the dynamic capability of the total system and thus the lifetime of the SOFCs. All in all, SOFC-RE leads to a more cost-effective combined cycle than SOFC-GT and SOFC-ST [83].

Research by Biert et al. [36] shows lower efficiencies for SOFC-RE than for SOFC-GT and SOFT-ST for a similar system at nominal operation. Nevertheless, they mention this may be out-weighted by the advantages in transient capability and simplicity in control strategies. Sapra [77] investigated the optimal power split for a SOFC-RE system (RE fuelled with AOG) for three naval applications. A higher power split towards SOFC resulted in higher efficiency, but increased the total volume and weight of the total system. An optimal value was found at 28% SOFC load share, which corresponds to a combined system efficiency of 52%. This resulted in a system with twice the size, similar weight, an efficiency improvement of 9% to 11%, and a NO_2 reduction of 36% to 43%, compared with a conventional system. Sapra et al. [31] further validated the power split with engine experiments. Wu et al. [86] investigated the dynamic behaviour of an integrated SOFC-engine system and concluded that the slow dynamics of the SOFC dominates the overall system dynamics, but they did not use a fuel bypass. They proposed to add a metal hydride reactor for H_2 addition, which improved the overall dynamic capabilities.

Although high system efficiencies were projected for SOFC-combined cycle plants in theoretical studies, most physical demonstrators have not reached the predicted efficiencies [35]. Moreover, combined cycles result in more complex plants with bigger control challenges. On the other hand, stand-alone SOFC systems have been demonstrating higher efficiency as expected [36]. Consequently, recent research has been reconsidering SOFC systems without combined cycles.

2.2.4. Fuel possibilities for SOFCs

Several fuel types are possible in combination with SOFCs, although several reforming and purification processes are needed for some fuels. This section discusses fuels that have been considered for SOFCs in the marine industry. While considering fuels for marine applications, attention must be paid to the associated costs and emissions in the production and distribution phases of fuels and their feedstocks. However, this comparison is outside the scope of this research.

Diesel

Currently, diesel-type fuels are dominantly used in ships. They are relatively cheap and energy-dense compared to alternative fuels. In the past, heavy fuel oil (HFO), a residual from the refinery process, was mostly used in deep-sea shipping. Since 2015, its yearly usage decreased and is partly replaced by cleaner distillates, such as marine gas oil (MGO) or blends of MGO and HFO, called marine diesel oil (MDO). The sulphur content limit decreased from 3.0% for HFO to 0.1 % for ultra-low sulphur fuel oil (ULSFO) and MGO [87]. Because of its high energy density, common availability wide use in the marine industry, diesel has also often been investigated for SOFC systems. Fuels with low sulphur content are easier to handle for SOFC systems, since it reduces the stress on the desulphuriser. SOFCs may even be able to operate stably on ULSFO without desulphurization, albeit with a small performance drop caused by sulfur poisoning [88]. However, low sulphur fuels are more expensive, since additional catalysts and chemical additives are used in the refining process [89]. Biodiesel has also been successfully used in SOFCs, externally and internally reformed [90]. However, it is expected that biodiesel will not be widely available since its production competes with food production [4, 91]. The production and distribution infrastructure, as well as regulations of diesel fuels, are in place. Due to these advantages, diesel-type fuels were often considered for SOFCs in marine applications [29, 30, 92, 93]. However, diesel is inconvenient for SOFCs, since it requires a complex and large fuel processing plant [28], which lowers the power density and efficiency of the SOFC system.

Hydrogen

Recently, the many initiatives by companies and governments illustrate an increasing interest in hydrogen for marine applications. The most common storage options for hydrogen are compressed or cryogenic. Cryogenic storage (at -253 °C) is currently the most energy-dense option [94], making it most suitable for marine applications [28] and will be referred to as LH2 in this study. However, cryogenic storage requires insulation to keep the fuel in liquid phase at low temperature and it requires cylindrical tanks to handle pressure gradients. Both increase the required ship volume for fuel storage; the volumetric energy density of LH2 storage is the lowest compared with other alternative fuels. The cooling of hydrogen to cryogenic stage also requires much energy [94]. Liquefied hydrogen is currently the most expensive alternative fuel for marine applications [37].

Although hydrogen can be used in SOFCs with satisfactory efficiency [95], it is not a straightforward choice. The main advantages of SOFC compared with LT-PEMFC are the possibility of internal reforming as well as its high tolerance to carbon monoxide (CO) and CO_2, which become obsolete for hydrogen. Moreover, CO is even used as fuel in SOFCs, further increasing efficiency. On top of that, internal reforming cools the SOFC stack, since heat is needed for the reaction. When using hydrogen, a larger airflow is needed to cool the stack, which increases the parasitic blower power. Although it seems counter intuitive, hydrogen-fuelled SOFCs often lead to lower system efficiencies than hydrocarbon-fuelled SOFCs [96, 97]. Due to the lower power density, the lower dynamic capability, and the higher cost per kW of SOFCs, LT-PEMFC would be the preferred option for hydrogen.

NATURAL GAS

Natural gas's most common storage for marine applications is in cylindrical tanks at -162 °C, also called liquefied natural gas (LNG). The volumetric and gravimetric energy density for stored LNG is significantly lower than for diesel but higher than for hydrogen. Natural gas is increasingly being used in the marine industry, meaning its fuel infrastructure and production capacity is expanding [98, 99]. Initially, it was concluded that LNG-fuelled marine engines can meet Tier III NO_X and SO_X emission regulations without emission abatement, as well as achieving significant CO_2 reduction [100]. However, more recently, methane slip in natural gas-fuelled engines is recognized as a serious concern due to its high global warming potential [5].

Most SOFC research and commercially available SOFC systems use natural gas as the main fuel, and high efficiency has been demonstrated [35, 84, 101]. Natural gas can be directly used in an SOFC after desulphurization, but a pre-reformer is often applied to promote steam methane reforming to reduce the stress on the fuel cell catalyst. Opposed to an LNG-fuelled engine, methane slip is negligible [102]. Biogas-fuelled SOFC has shown comparable performance to hydrogen in terms of power production [103].

METHANOL

Methanol can be stored in liquid form at room temperature, omitting the need for insulation and cylindrical tanks. Consequently, methanol is stored at a higher energy density than gaseous fuels. Liquid storage is even more beneficial for marine applications, since irregular ship volumes can be used to store fuel. Moreover, diesel infrastructure can be used for methanol after slight adjustments [104].

Few studies examined SOFC performance fuelled with methanol [28]. In contrast with natural gas, methanol has a relative low reforming temperature, making it convenient to reform the fuel externally [105]. Since internal reforming is usually beneficial for the cells in terms of efficiency and thermal balance, Rechberger et al. [106] added a methanator before the anode outlet, to allow internal reforming of methane in the stacks. Methanol has been investigated to use directly in SOFCs [107], while demonstrating high performance without notable cell degradation [108], but direct methanol SOFC systems are still in the research phase [109].

DIMETHYL ETHER

Within the last five years, dimethyl ether (DME) has received increasing attention as a fuel for the marine industry, since implementation would lead to a reduction in NO_X, SO_X and PM emissions [28, 110, 111]. Above 700 °C, DME can be easily reformed to methane, carbon monoxide, and hydrogen, making it a convenient fuel for high- temperature fuel cells [112]. Murray et al. [113] concluded a high power density for SOFC systems directly fuelled with DME. One practical problem of directly supplying DME to SOFC is coke formation. This can be suppressed by adding CO_2 to the fuel at high temperatures, but this adds extra complexity to the system [112]. Sato et al. [114] investigated the potential of steam reformed DME for SOFC. It was found that DME was easily reformed using a commercial catalyst, no coke was formed and nominal power level and electrical efficiency were reached using DME.

AMMONIA

Ammonia (NH_3) is a much produced chemical commodity that recently received more interest in the marine industry, since it can be used in modified engines and fuel cells [115]. Ammonia can be stored in its liquid form at -33 °C or at a pressure of 10 Bar [116, 117] and its storage is characterized by moderate volumetric energy density, compared with the other discussed fuels. Because it contains no carbon, ammonia can be used in SOFC without the risk of carbon monoxide poisoning or coke formation. Ammonia can be directly fed to the anode, where ammonia is cracked internally, which is beneficial for the heat efficiency of the SOFC system [118]. Carbon dioxide and methane are not emitted, because no carbon is present in the fuel. An ammonia-fuelled engine produces NO_X during the combustion, whereas an SOFC system fuelled by ammonia avoids most NO_X formation by producing N_2 as the main nitrogen-containing product [116]. Several investigations concluded that an SOFC running directly on ammonia shows similar [118–120] or even higher [34, 121, 122] efficiency than hydrogen. Frandsen et al. [123] demonstrated with a multi-physics 3D stack model and cell experiments that internal cracking is very fast at typical operating conditions, anode recirculation appears feasible, and that only negligible reforming in heat exchangers will occur. Ammonia contains no sulphur, so the desulphurization component is not necessarily for an ammonia-fuelled SOFC.

Table 2.1: Performance of different fuels in combination with SOFC for marine applications. Production capacity is global [124–130]. Energy density includes the onboard storage system [28, 37, 77, 94, 131, 132]. Fuel price ranges depend on market volatility and feedstock [22, 27, 32, 126, 128, 131, 133–139]. *Fuel storage price* represents the capital cost of storage system [32, 131, 135, 139–142]. *TRL* is technological readiness level and is rated on the common scale of 1 to 9 [20, 22, 28, 100, 143–145]. The benchmark (MGO) has been compensated for efficiency difference between diesel generators (43%) and SOFCs (55%) for comparison purposes. All data is based on LHV.

	Unit	**MGO** Amb. T	**LH2** -253 °C	**Biodiesel** Amb. T	**LNG** -162 °C	**MeOH** Amb. T	**DME** 5 bar	**NH3** 10 bar
Production capacity	TWh/Y	600	2500	1700	38000	1000	90	1000
Incl. liquefaction	TWh/Y		4		5800			
Vol. energy density	kWh/m^3	6000-7800	1200-2200	7200-8900	3100-3800	3300-4200	3600-3800	2300-2600
Grav. energy density	kWh/ton	6500-7400	2200-3900	7100-8600	7300-8800	3900-4500	5400-5600	2900-3600
Fuel price	€/kWh	0.03-0.19	0.04-0.54	0.08-0.13	0.02-0.18	0.04-0.12	0.01-0.07	0.06-0.16
Fuel storage price	€/kWh	0.03-0.15	1.3-9.0	0.02-0.08	0.14-1.44	0.04-0.16	0.17-0.23	0.23-0.72
Marine TRL of fuel	-	9	4	8	9	5	2	3
TRL of fuel with SOFC	-	-	6	3	8	7	4	5

FUEL COMPARISON

Several fuel possibilities for marine SOFC systems have been presented and a comparison is shown in Table 2.1. The production capacity of DME and LH2 is still very low and would require a large scale-up for marine applications. Hydrogen performs very badly in ship storage, which makes it inconvenient for long-haul applications (see figure 2.4). For marine applications, the fuel cost is often a large contributor to the total cost of ownership and current hydrogen prices are very high. Fuel cost for LNG, MeOH, and DME is similar or even less compared with MGO after compensating for the efficiency difference between diesel generators (DGs) and SOFCs. For conventional fuels, the cost of the fuel storage system is not a large economic driver. However, LH2, LNG and DME require cylindrical or spherical tanks, which significantly increases the cost of the storage system. Especially hydrogen is very costly to store, see Table 2.1. Many ships are powered by diesel-type fuels or LNG, ensuring high technological readiness for marine use. Since hydrogen, methanol, and ammonia are often applied in other industries, there is much knowledge about storage, distribution, system control, and safety, however, they have not been applied at large scale in commercial vessels. Most of these fuels have also been investigated for marine engines, but research points out lubrication, cooling, ignition, knocking, and fuel slip problems [94, 146]. Moreover, the engine efficiency is often not as good as with diesel-type fuels [147, 148]. Consequently, alternative fuels could be used in combination with marine engines to reduce emissions, but the gain is larger with SOFC systems. SOFC research has focused on LNG-fuelled systems and most commercially available systems are LNG-fuelled, resulting in a high technological readiness. Most alternative fuels have been theoretically verified or simulated for SOFC cells, stacks and systems, however, modifications to the reforming process and the system control are often necessary and not yet commercialized. When comparing the different fuels, no clear favourable candidate appears and the choice would depend on the ship type and operational profile, and should be considered in combination with the power generation system. When considering SOFC systems for long-haul ships, hydrogen seems an unfavourable option and LNG is in the current situation most economically and technically feasible.

2.3. SOFC IN MARINE APPLICATIONS

SOFC systems are mostly investigated for on-site power generation, for instance, data centres and residential applications, and were initially not considered suitable for mobile applications [64]. Although an SOFC system would be too large and too complex to fit in automotive applications, its research in marine applications has increased. This means the SOFC system must comply with the operational requirements of a marine power plant, which differ much from a residential application. This section explores the requirements of a marine power plant and explores the possibilities of integrating SOFCs into marine power plants. Lastly, the practical lessons from noteworthy research projects of SOFCs in marine applications will be discussed. An overview of SOFC research in marine applications is provided in Tables 2.2 and 2.3. These tables show that most marine literature considers SOFC systems using internal reforming, methanol is not often considered as fuel for marine SOFC applications and that recently, stand-alone cycles are more often investigated than combined cycles.

2

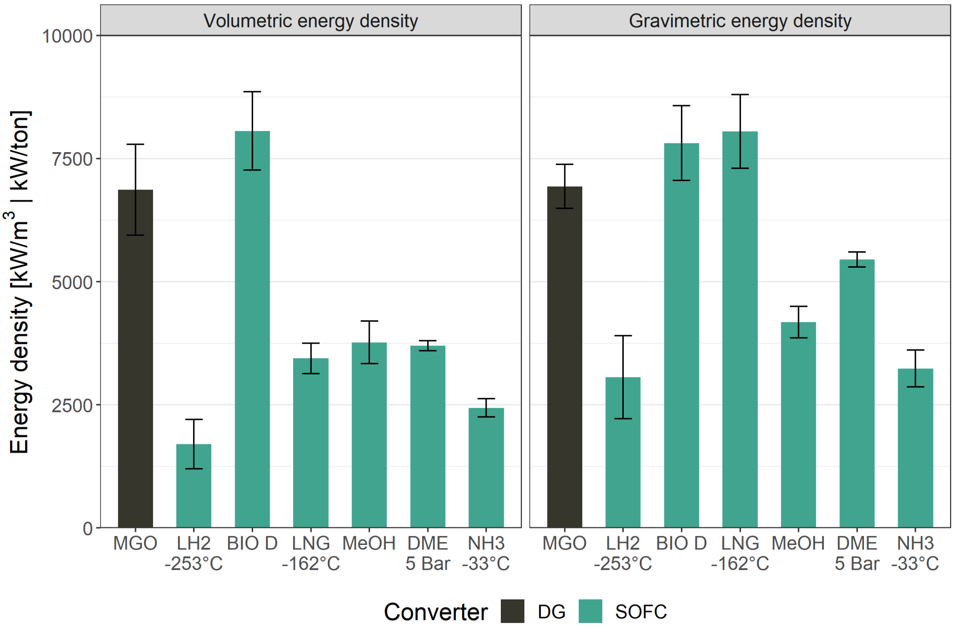

Figure 2.4: Energy density of future fuels including the storage system of the concerned fuel. The benchmark (MGO) has been compensated for the efficiency difference between diesel generators (43%) and SOFC (55%). Based on LHV of fuels. The blue bars show the data ranges found in literature, projects, and supplier specifications [28, 77, 149, 150].

Table 2.2: Chronological overview of research in SOFC for marine applications part I. The SOFC power ratio indicates the power contribution by the SOFC with respect to the total supplied power to the ship at nominal conditions.

Study type	Source	Ship type	Fuel	SOFC system	Marine power plant	SOFC power ratio	System efficiency
Challenge identification	[151]	Several	Several				
Electrothermal simulation	[152]	Navy	Diesel		SOFC-GT	11%	S: 68%
Life cycle analysis	[153]	General	Several		SOFC		
Thermodynamic analysis	[154]	Yacht	Methane	IR Pr.	SOFC-GT & DG	25%	S: 68%
FC comparison	[155]	General	Several				
FC system design	[156]	Seagoing	ULSD				
Ship design	[157]	Arctic	Diesel	ER	SOFC & DG	14%	
SOFC integration	[158]	Naval	Diesel		SOFC+FW & DG	0-100%	
Thermodynamic analysis	[29]	Naval	Diesel	ER Amb.	SOFC+BAT	100%	S: 55%
Thermodynamic analysis	[42]	General	LNG	IR Pr.	SOFC-GT		S: 66%
Thermodynamic analysis	[84]	General	LNG	IR Pr.	SOFC-ST		S: 59%
Concept design	[92]	OSV	Methanol	ER Pr.	SOFC-GT & DG	13%	A: 47%
Review	[159]	General	Several				
Fuel cell review	[28]	General	Several				
SOFC demonstrator	[93]	Multi-purpose	Diesel	ER Amb.	SOFC		D: 55%
Comparison	[47]	General	Several				
Techno-economic optimisation	[160]	Cruise	Hydrogen & LNG		SOFC & HT-PEMFC & GT & BAT	16-29%	S: 70-73%
Thermodynamic & availability analysis	[161]	Carrier	Ethane	IR Pr.	SOFC-GT & DG	30-53%	S: 61%
Energy management strategy	[32]	Cruise	Hydrogen & LNG	IR Amb.	SOFC & DG	APU	A: 55%
Thermodynamic analysis	[95]	Passenger	Hydrogen	Pr.	SOFC-GT	66%	S: 41%
Thermodynamic analysis	[30, 162]	Seagoing	Diesel	ER Pr. AOGR	SOFC	APU	S: 55%
Techno-economic analysis	[144]	Naval	Several	ER	SOFC	100%	A: 45%
Techno-economic optimisation	[27]	Cruise & carrier	LNG	IR	SOFC & DG & GG & BAT		A: 53%
Environmental-economic analysis	[163]	Container	Ammonia	IR	SOFC+BAT	100%	A: 59%
SOFC integration	[77]	Naval	LNG	IR AOG-RE	SOFC-RE	7-100%	A: 45-60%
Techno-economic analysis	[37]	Cruise	Several	IR	SOFC+BAT & DG	62%, 100%	A: 60%
Fuel cell review	[164]	General	Several				
Case study	[165]	Cruise	LNG	IR	SOFC & DG	41%	A: 55%
Comparison	[166]	Ferry	LNG	IR	SOFC	100%	A: 55%

Fuel: LNG = Liquefied Natural Gas and ULSD = Ultra Low Sulphur Diesel.

SOFC system: IR/ER/PR = Internally/Externally/Pre Reformed, Amb. = Ambient, Pr. = Pressurized.

Power plant: DG/GG = Diesel/Gas Generator, RE = Reciprocating Engine, FW = Fly Wheel, BAT = Battery.

SOFC power ratio: APU = Auxiliary Power Unit.

System efficiency: A = Assumed, S = Simulated and D = Demonstrated.

2

Table 2.3: Chronological overview of research in SOFC for marine applications part II.

Study type	Source	Ship type	Fuel	SOFC system	Marine power plant	SOFC power ratio	System efficiency
Feasibility study	[167]	Passenger	LNG	IR	SOFC	100%	A: 55%
Techno-economic analysis	[168]	Cruise	LNG	ER	SOFC+BAT	100%	
Component sizing & energy management	[169]	Dredging	LNG	IR	SOFC+BAT & DG	17-100%	S: 42-59%
Case study	[170]	Cruise	LNG	IR	SOFC & DG	27.5%	A: 60%
SOFC integration	[31]	General	LNG	IR AOG-RE	SOFC-RE		
Feasibility study	[171]	General	Ammonia	IR	SOFC+BAT	100%	
LCA & LCCA	[136]	Ferry	Hydrogen & Ammonia		SOFC+BAT	100%	A: 65%
SOFC integration	[172]	Passenger	HFO & LNG	ER	SOFC & DG	80%	
Spatial optimisation	[173]	Cruise	LNG	IR	SOFC+BAT & DG	35%	A: 54-58%
Thermodynamic analysis	[174]	General cargo	Ammonia	IR	SOFC-GT	100%	S: 65%
Thermodynamic & control analysis	[175]	River cargo	LNG	IR	SOFC-GT	72%	S: 61%
Thermodynamic analysis	[176]	General	Several	PR	SOFC		S: 47-58%
System design	[177]	General	LNG & diesel	PR	SOFC		S: 47-58%

Table 2.4: Performance comparison between off-the-shelf SOFC systems (planar stacks, non-pressurized system and without combined cycles or batteries) and medium-speed 4-stroke marine diesel generators. Derived from [27, 28, 30, 32, 46, 159, 178–180] and supplier information (Table 2.6).

Criteria	Unit	SOFC	DG
Electrical efficiency	-	43% - 65%	30% - 45%
Vol. power density	kW/m^3	2 - 28	30 - 60
Grav. power density	kW/ton	5 - 30	45 - 75
Start-up time (cold-start) Start-up time (hot start)	h h	12 - 24 0.1 - 0.2	0.2 - 0.3 0.02 - 0.04
Load change rate	%/min	2% - 10%	10% - 20%
Noise	dB (A)	40 - 70	80 - 110
Current system CAPEX (2021) Expected system CAPEX (2030)	€/kW €/kW	1,500 - 7,000 500 - 2,000	250 - 400 300 - 500
System lifetime Major maintenance interval	1000h 1000h	100 - 150 30 - 90 (stack replacement)	120-200 40-60 (engine overhaul)

2

2.3.1. MARINE POWER PLANTS

A marine power plant must be assessed on the following criteria [28, 31]:

- Efficiency of marine power plant
- Size and weight
- Load transients and start-up time
- Safety and reliability
- Economics
- Environmental impact

SOFC power plants performs better than conventional marine engines on some of the criteria and worse on others; the technologies are compared in Table 2.4.

SOFC power plants generate energy at high electrical efficiency; suppliers state 43-65% for natural gas-fuelled systems. Additionally, SOFCs maintain high efficiency at part-load conditions, in contrast to diesel engines. SOFC systems generally show a broad optimum between 50% and 80% load [181]. This is especially interesting for many marine applications, where the maximum installed power is only occasionally used [182].

Current SOFC systems perform poorly in terms of power density (see Table 2.4), resulting in a large and heavy power plant. This is a big challenge for marine applications, because high installed power is often required to satisfy the operational profile of a ship. Most vessels (e.g., container ships, cargo ships, and cruise ships) are volume critical, although some vessel design (e.g., high-speed crafts, naval support vessels) is driven by weight requirements [144]. Sapra [77] compared the required space and weight for a hybrid SOFC-RE system with the original diesel-electric architecture for three different ships. The SOFC-RE system was 2 to 3.7 times larger and 1.1 to 2 times heavier with a system efficiency improvement of 9% to 11% and an emission reduction of 35% to 43%.

SOFC systems are characterized by poor transient capabilities [31], because the high temperature requires heating of a large thermal mass [28]. Their relative long startup times (12-24 hours) and slow response in operational power (2-10 % load/min) form a challenge for marine applications, where significant changes in power demand are required, for instance during manoeuvring or crane operations [183]. The transient power requirements surely depend on the ship type and the operational profile, but it is certain that the transient capabilities are not sufficient for most marine applications. Complementary technologies can be used to supply additional power during peak loads [28, 40, 155, 160]. These technologies can be divided in energy storage devices (batteries, supercapacitors and flywheels) and power generation technologies with better transient capabilities (PEMFC or diesel generators).

SOFC power plants are costly, compared with diesel generators, see Table 2.4. However, these prices are expected to decrease with technological advances and production scale-up. Within 10 years, the prices of SOFC systems are expected to be in the range of 500-2000 €/kW at high production capacities above 250 MW/year [46, 179]. On the other hand, the prices of diesel generators are expected to increase. Stricter emission regulations require the addition of complex aftertreatment systems, which increase the capital cost of marine diesel generator systems.

A fuel cell degrades over time, decreasing its power output [184]. Fuel cell suppliers have to tackle this by installing overcapacity, since regulations define that the life of a fuel cell is over when it is not able to deliver its rated power [64]. Although not often stated by suppliers, the electrical efficiency also decreases over the lifetime of the fuel cell stacks, incrementally increasing the fuel consumption. This is important to consider in the early stages of ship design, since it means the size of the required fuel storage increases during the lifetime of the SOFC system. SOFC suppliers demonstrated lifetimes of 30,000 to 90,000 hours at nominal load with a relative system efficiency decrease of 10 to 15% over the lifetime of the fuel cell system [39, 185]. Consequently, the stacks must be replaced regularly, which further drives the already high price of SOFC systems. Nevertheless, operating the SOFCs at part-load conditions increases the stack lifetime, as stated by several fuel cell system suppliers. To put the SOFC lifetime into perspective, medium-speed diesel generators also need major maintenance after 40,000 to 60,000 operational hours [186, 187]. However, such an engine overhaul is not as expensive as stack replacement.

Figure 2.5 compares the nominal emissions for MGO-fuelled diesel generators, LNG-fuelled engines, and LNG-fuelled SOFCs. The figure is based on the data in Appendix A Table A.1. The reduction in carbon dioxide emissions from LNG engines to SOFCs is mainly attributed to efficiency gains. Methane slip does not happen in SOFC, so the CH_4 emissions are virtually zero. In total, the application of SOFC leads to a large decrease in greenhouse gas emissions. In engines, soot (C), CO, NO_X and PM emissions originate from incomplete combustion. Since the main principle of SOFCs is not combustion (only in the afterburner), these emissions are much lower compared to diesel generators. To prevent damaging the stacks, most sulphur is extracted from the fuel before it enters the SOFC, so the SO_X emissions are also virtually zero. As can be derived from the figure, the application of SOFC easily satisfies all emissions regulations and meets the

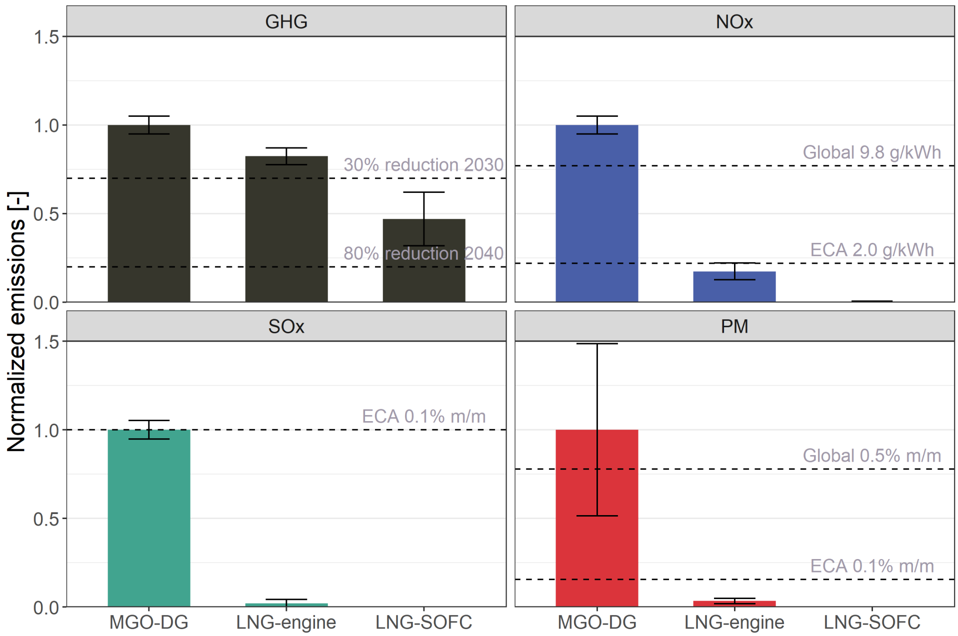

Figure 2.5: Normalized GHG, NO_X, SO_X, tank-to-electricity (TTE) emissions with their targets and regulations by IMO. A range is given based on fuel composition and conversion efficiency of different products. 0.1% S m/m fuel is used to determine the SO_X emissions.

GHG reduction target of 2030. The figure also shows that just LNG-fuelled SOFC systems could not reach the 80% GHG reduction target of 2040. Combining SOFCs with other energy-saving innovations, renewable fuels, or carbon capture technologies would be necessary.

Besides exhaust emissions, marine power plants also produce sound emissions, propagating not only to the cabins but also to the underwater marine life. The consequences of the growing anthropogenic acoustic footprint on marine life are getting more known and are with no doubt negative [188]. Compared with engines, SOFCs strongly reduce the noise radiation from the power plant, see Table 2.4. Quantification of the positive impact on the aquatic environment of noise reduction by SOFCs is still necessary to evaluate how significant this advantage is.

Rivarolo et al. [167] designed an algorithm to effectively compare volume, weight, cost, CO_2 emissions, and NO_X emissions for different marine power plant and fuel storage solutions. The relevance of these criteria differed per ship application and their case study for cruise ships showed that with the current marine regulations and SOFC prices, MGO or LNG-fuelled internal combustion engines still result in the most feasible power plant. However, it also showed, when SOFC cost can be further reduced and more stringent emission regulations will emerge, LNG-fuelled SOFC systems will become the favored candidate.

2.3.2. SOFC SHIP INTEGRATION

Table 2.4 shows that an SOFC power plant is large, heavy, expensive, and is not able to quickly change its power supply. Hybridisation with internal combustion engines can improve the technical and economic feasibility of the power plant by compensating the areas in which the SOFC performs poorly [172]. Moreover, hybridisation often serves as a bridge between established and emerging technologies, with hybrid electric vehicles as a clear example. It familiarises the users and limits the risks to the owners, while also allowing time for manufacturers to further improve their systems. Consequently, hybridisation is suggested, meaning the SOFCs are to be integrated with the current systems onboard. This means it must be connected to the fuel supply, electric systems, and thermal systems. Furthermore, there are new possibilities for the spatial layout, because of the modularity of the SOFCs and the option of decentralisation. Also, the ship regulations might need adaptation for SOFCs. These integration aspects are discussed in the following sections.

HYBRID STRATEGIES

There is a wide range of hybridisation strategies, in which the ratio between installed fuel cell power and total installed power is an important design driver, strongly influencing the dynamic capability, capital cost, overall system efficiency (and thus fuel cost), and reduction in emissions. Evidently, hybridisation reduces the relative efficiency gains and emission improvements [169]. Tables 2.2 and 2.3 show which hybrid SOFC power plants have been investigated for marine applications. The second last column also shows that many researchers do not consider a fully SOFC power ship.

Figure 2.6 illustrates a generic hybrid power plant for an SOFC powered ship. The total power plant must satisfy the following three operational boundary conditions of

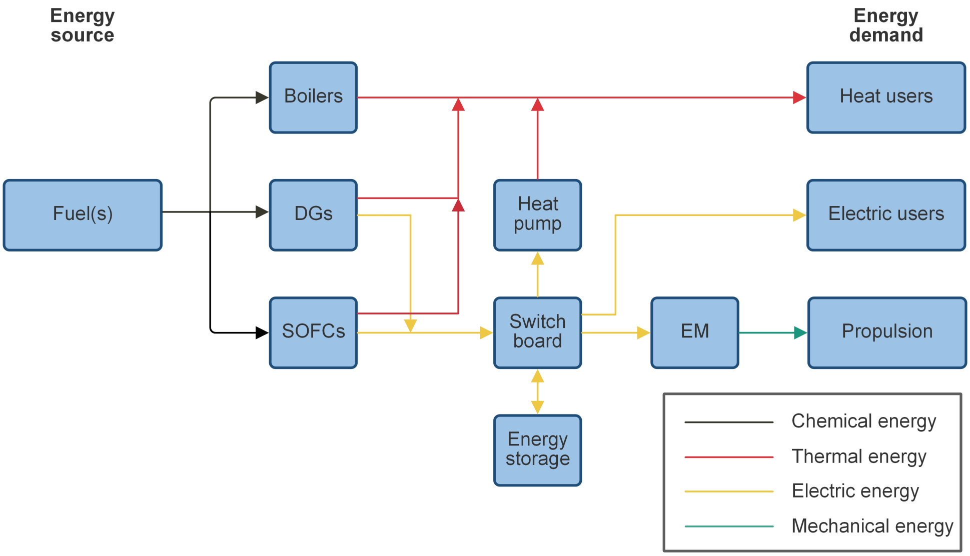

Figure 2.6: Generic hybrid SOFC power plant for marine applications, based on Baldi et al. [27].

the ship while performing optimally on the criteria presented in Section 2.3.1.

1. Maximum thermal and electrical energy demand to complete the voyage.
2. Maximum thermal and electrical power demand for propulsion and auxiliaries.
3. Transient capabilities of power supply.

Veldhuizen [37] investigated two fuel cell hybridisation strategies for an expedition cruise ship using various fuels. The marine power plant consists of SOFC and diesel generators, further supported by batteries to increase transient capability. In the first strategy, the fuel cell is only used to supply power for auxiliary and hotel purposes. This lowered the transient requirements of the fuel cell system and thus the number of required batteries. In the second strategy, the fuel cells were used for main operation (auxiliary and propulsion) and diesel generators were used as range extenders during long transits. This reduced the required size of the fuel storage tanks for the fuel cell, which is especially beneficial when using fuels that require more space in the ship to store, like hydrogen or LNG. It was concluded that the second hybrid strategy results in a smaller ship, lower ship cost, and fewer emissions than the first hybrid strategy.

Díaz-de-Baldasano et al. [92] hybridised diesel generators with methanol fed SOFC in a platform supply vessel. SOFC modules contributed to 7% of the total installed power and during normal operation, the SOFC supplied 12.5% of the total power. The SOFC modules only supply power to auxiliary consumers, due to different voltage requirements of the thrusters. It was concluded that the plant can be implemented without limiting ship performance or operating capabilities.

Archetti et al. [172] investigated a power plant with SOFCs and combustion engines for a fixed CO_2 reduction of 20% in a passenger ship case study. To realize this reduction using LNG as fuel, it was estimated that 57% of the power should be supplied by the SOFCs. Although the analysis showed a potential solution, it was pointed out that this was not suitable for a simple retrofit, because it would load the existing engines under 40%, which is not desirable for longer periods.

Haseltalab et al. [169] researched the SOFC as a primary energy source for a dredger ship. An optimisation-based energy management approach was used to investigate the power split of LNG-fuelled SOFCs, gas engines, and batteries for a DC power plant. They showed that the energy efficiency can be increased by 28% and CO_2 emissions can be reduced by 32% if the size and engine and weight of the engine room remain unchanged compared with a conventional diesel power plant. This corresponded to a SOFC-engine power split of 17% versus 83%, respectively. A fully SOFC powered ship resulted in a power plant size and weight increase of 70% and a CO_2 emission reduction of 53%.

Instead of separately generating power with SOFCs and diesel generators, these could also be integrated into a combined cycle by fueling the engine with anode off-gas of the SOFC (see also Section 2.2.3). Sapra et al. [31] performed experiments on a marine quality engine and recommended a 33-67% SOFC-ICE power split for marine applications, based on the following marine design drivers: efficiency, space and weight, dynamic capabilities, economics, environmental impact and noise reduction.

Evrin and Dincer [95] even explored a power plant where an LH_2-fuelled SOFC is used in combination with solar panels and wind turbines on a small passenger ship. An electrolysis plant is installed to refill the hydrogen storage when the power of solar panels and wind turbines is excessive, which leads to a ship that is powered 100% with sustainable energy. The power plant also supplies potable water to the ship. However, the proposed power plant is said to only be feasible for ships with a refuelling interval up to 10 hours.

FUEL FLEXIBILITY

SOFC systems are particularly attractive for marine applications due to their fuel flexibility [27]. Currently, actors in the marine industry are not sure about the main future fuel, which is problematic since ships are built for a long lifespan. SOFC systems offer resilience and offer the option for a fuel-flexible ship, with the following two options:

- A ship that stores and uses two or more fuels, similar to ships with dual-fuel engines. Although this offers operational flexibility, it leads to many redundant components, since fuel bunkering, storage, and fuel handling must be present in the ship for different applied fuels.

- A ship design that is adaptive to two or more fuels. This can be integrated into the design by applying modular concepts on component level [189, 190]. For an adaptive design, it is convenient to combine fuels that have similar properties in fuel storage and fuel handling, for instance, LNG and ammonia. Both fuels are gases at ambient temperature and ammonia can be stored in LNG tanks without major design changes [191]. Another convenient option is MGO and methanol. Both fuels are stored as a liquid and can be stored in irregular ship volumes such as the double bottom [192]. An adaptive design makes it possible to use a widely used fossil fuel in the short term and a cleaner alternative fuel in the future, when more widely available.

Most marine research projects consider several fuels, but it is unclear which fuel is most effective for an SOFC powered ship in terms of availability, technical feasibility, economics, and environmental impact. Moreover, a fuel-flexible ship powered with SOFCs has not been researched yet.

SHIP DESIGN

Fuel cells are modular, meaning the intrinsic performance of a single cell is not different from a big stack [28]. When well designed, SOFC-systems have no single-point-of-failure, as is the case with internal combustion generator sets. This results in high redundancy and thus high availability, which is an important design driver for marine applications. Ahn et al. [161] used a fault tree analysis to investigate the system availability in a large ethane carrier powered by SOFC-GT and dual fuel DG systems. A high system availability was concluded (98%) of which the turbomachinery was identified as the critical component. Availability could be further increased by increasing redundancy in turbomachinery, but this was deemed unnecessary. The modularity and low noise and vibrations of fuel cells also make it possible to spread energy production throughout the ship with minor scale losses. This decreases the grid size and decreases energy transmission losses because of shorter electricity cables [173, 193]. Decentralised power generation also makes it easier to reach high system redundancy in ships [194], because power generation can be distributed over different fire tight compartments. This brings new opportunities in the general arrangement of the ship. Leites et al. [195] installed the SOFCs decentralised, which enhanced the safety and availability of the ship in case of damage. Weidle et al. [157] designed a concept for an Arctic Patrol Vessel using SOFC to generate power. The SOFCs are located near the bow to easily satisfy air intake demands and allow easy access for repair or stack replacement. The SOFCs are placed in an enclosed and isolated area to be able to shut off the room in case of hydrogen or carbon monoxide leaks. Cohen et al. [158] added that fuel cell rooms must be unmanned and separated from diesel spaces and spaces with electric equipment. They also identified ducting as an important design driver, since the air intake of SOFC is large compared to diesel generators and must be distributed to many modules. It is recommended to arrange the modules in such a way that centralised ducting is possible. Rivarolo et al. [32] studied different operating strategies for SOFC energy management on cruise ships. A distributed energy generation approach is proposed, in which the installed power of the SOFC is equally divided over the main vertical zones in the ship, meaning energy is produced close to the end-users. This offered advantages in energy efficiency and reliability but introduced challenges in control strategy, space usage, and safety requirements. In actual marine power plants, redundancy requirements often lead to oversized ICEs, especially for passenger ships, which have to comply with safe return to port regulations [143]. Kistner et al. [173] state that a decentralised fuel cell plant could minimise this over-sizing and even omit the requirement of emergency power generators. They optimised the spatial layout of decentralised power generation with SOFCs in cruise ships and concluded that the economic cost of transmission losses decreased with 55% compared to a centralised configuration. Nevertheless, it is questioned whether the operational cost savings of a decentralised power system may justify the additional ship building expenses of multiple machine rooms.

Micoli et al. [170] examined the possibility of an SOFC plant to supply the entire hotel load of a large cruise ship, which corresponded to 27.5% of the electrical balance. They proposed to install all fuel cells in the back of the ship, separated from the engine room to be compliant with safe return to port regulations. An increase in weight and volume of the power plant forced them to investigate the floating and stability capacity of the ship. They concluded that their solution meets the weight and stability requirements and could reduce CO_2 emissions by 11%. They did not include heat regeneration, which could further improve the power plant efficiency.

SOFCs produce no noise and vibrations since they contain no moving parts. Moving parts in the balance of plant components produce some, but this is much less then the noise and vibrations produced by diesel engines. This is an especially big advantage for ships that require comfort (e.g., cruise ships) or silent operation (e.g., naval ships).

ELECTRIC INTEGRATION

To integrate fuel cells into current marine systems, SOFC modules must be linked to the main switchboards via a transformer to adjust the voltage and possibly an inverter to convert the power to the required output [158]. Cohen noted that inverter modules can be combined for several fuel cell modules. This reduces the system size and cost, but also reduces redundancy.

Currently, most large ships use an alternate current (AC) electric grid [196], because generators provide AC power and the majority of available power electronics components is AC [197]. However, when the majority of power is supplied by fuel cells or batteries, it can be beneficial to apply a direct current (DC) grid. Fewer transformers and switchboards are needed to supply fuel cell power to a DC grid, saving 1 to 2 % electrical loss per component [198]. Moreover, in current system architectures, many DC auxiliary loads are connected to an AC grid using converters, which are also additional power conditioning components. Consequently, employing a DC network increases the electrical system efficiency and lowers the size, weight, and cost of the system [199]. Even for a hybrid concept with major DG and minor SOFC power generation, a DC distribution could be considered. In contrast to an AC grid, synchronisation of generation units at a specific frequency (50/60 Hz) is not required for a DC grid, enabling the diesel generators to operate at their optimal speeds, reducing fuel consumption [196]. Zahedi et al. [199] estimated 15% fuel savings for offshore supply vessels with energy storage using a DC grid compared with a conventional AC system. Kanellos et al. [200] estimated space and weight savings of 30% mainly due to smaller high-speed generators and elimination of bulky low-frequency transformers. The implementation of DC networks on MW-scale ships is limited [201] and a new design philosophy for circuit architecture would be required to ensure reliability and safety [202]. Nevertheless, there is significant potential to increase the overall electric efficiency. The automotive industry experienced the same trend and already demonstrated significant reductions in the size, weight, and cost of DC system components and an increase in their availability [203].

A power management system is required that successfully distributes the power of the fuel cells, energy storage devices, and any other power generators over the electrical consumers. Since SOFCs have higher efficiency and lifetime at part-load, smart control in the start-up, cool-down and power modulation of the many installed modules gives the opportunity to operate at optimal efficiency at different energy demands, although it is well-known that modulation is not desirable for the lifetime of the cells. Bassam et al. [204] compared different control strategies for a hybrid fuel cell power plant in a passenger ship to reduce energy usage and thus reduce fuel consumption. It was concluded that the fuel consumption can be reduced by 4% over an eight-hour voyage, compared with a classical proportional integral controller. This reduction was achieved by effectively charging the battery pack with the fuel cell by controlling the power plant with a multi-scheme energy management system.

In most marine SOFC studies, a standard electrical loss is assumed and not much attention is paid to the design of the power electronics and power and energy management system. However, DC power supply, modularity, and high efficiency at part-load add opportunities to reduce electric losses and increase the total system efficiency.

Thermal integration

The highly exothermic electrochemical reaction in SOFC makes it very appealing for cogeneration and trigeneration purposes. In marine applications, there is often a significant heating and cooling demand (e.g., heating ventilation and air conditioning (HVAC) system, hot water net, chilled water net, steam production), which is usually met with boilers and refrigeration plants. Since these systems consume energy, the total efficiency can be significantly improved by using the exhaust gas for hot water or steam production [92]. Fang et al. [152] integrated the SOFC power plant with the thermal management system of a combatant ship. For each SOFC-GT module, a thermal port is established on the fresh water network. A total system efficiency of 67.9% was simulated. Tse et al. [154] considered different configurations of electric power, heat, and cooling generation from a methane-fuelled SOFC-GT system for the HVAC system in yachts. In the conventional configuration, the SOFC-GT system generates electricity and supplies it to the air conditioning unit and fan. In an integrated configuration, an absorption chiller cooled the air in the HVAC system. Since the cooling was not sufficient, an extra direct expansion coil was needed to condense the water at saturation. Increases in efficiency of the combined SOFC-GT and HVAC system by 204% for a single-effect absorption chiller and 241% for a double-effect absorption chiller were reported. Duong et al. [174] uses SOFCs for the propulsion of a general cargo ship and extends the system with a gas turbine, Rankine cycle and exhaust gas boiler to provide auxiliary power for machinery and heating for crew accommodation. Their thermodynamic analysis simulates an integrated system efficiency of 64.5%. Although several methods of thermal integration have been investigated, Baldi et al. [27] identified that few SOFC studies in marine applications include, besides electrical energy demand, also thermal energy demand. There seems to be a general assumption that SOFC systems can easily fulfil all thermal demand of the ship, because the stack operates at such high temperatures. However, in an SOFC system, a large portion of the heat is already used to bring the air and fuel to the operating temperature of the fuel cell. Consequently, the outlet temperature of the SOFC system is usually in the range of 80-220 °C, dependent on the amount of heat used in the SOFC system. Ship designers should match the heat demand of the ship with the heat supply of the SOFC power plant.

2

Safety and regulations

Although under development, clear regulations for fuel cells in marine applications are not yet available. ABS [205] published a guide for the implementation of marine fuel cell-powered systems, covering fuel storage, reforming equipment, fuel cell stacks, safety systems (e.g., venting, fire protection, and monitoring), testing and certification. DNV GL [206] assigned a class notation to fuel cell-powered ships. This covers required documentation, ventilation, fire safety, and electrical systems. Overall, the current requirements are still generic and not specific on fuel type, fuel cell type, or ship type. Gianni et al. [165] compared the current regulations by classification societies. Although most regulations cover the same topics, some are contradictory regarding the necessity of double pipes, categorisation of fuel cell spaces as machinery spaces, and categorisation of fuel cell rooms as hazardous zones. Furthermore, none of the regulations state a particular fire extinguishing system for fuel cell rooms. Tronstad and Langfeldt [47] identified leakage in fuel cell modules and failure of electrical conditioning systems as the most critical scenarios. Sharifzadeh et al. [207] pointed out that safety and energy efficiency are competing objectives in SOFC system design. They found a strong trade-off between the profitability and the range of the safe operating window. Taking into account the toxicity and flammability of potential SOFC fuels, gas-tight enclosures of pipelines and fuel stacks, redundant leakage detection, emergency shutdown systems, and high venting capacity are paramount in ensuring a safe system [164]. Although SOFC systems can handle minor contamination, fire smoke could disable the operation of the cells. Moreover, the influence of fire smoke intake on the operation of SOFC systems has not been covered in research and regulations.

2.3.3. SOFC impact

For sustainable power generation technologies, there is a clear trade-off between cost and emission reduction, which is discussed in the two sections below.

Economics

Earlier studies show that technologies with relatively low investment cost are generally favoured over solutions with high initial cost and long-term benefits [208]. This has two main reasons. Firstly, larger loans are harder to acquire and more equity is required. Secondly, the future value of money is higher than the current value of money. When shifting to higher initial costs, this money is unavailable for other investments, resulting in higher opportunity costs. This slows down the introduction of SOFC power plants in marine applications, which are characterized by very high investment costs and savings in operational costs, although the latter is very dependent on the used fuel [37].

Geertsma and Krijgsman [144] executed a case study for the application of fuel cells in navy support ships. They proposed a methodology to review alternative power system designs based on: mass, volume, capital and operational expenditure, technological readiness, fuel availability, and emissions. They concluded that for commercial use, improvements in technological readiness, efficiency, and cost of the fuel cell are necessary.

Baldi et al. [27] optimised an SOFC propulsion plant towards two competing objectives: total cost of ownership and emitted greenhouse gases. The power plant was applied to a cruise ship where it supplied a large share of the total power. A clear trade-off between cost and emissions was identified. It was concluded that LNG is the most cost-optimal fuel for SOFCs, but a significant total cost increase (33%) is required compared with a diesel-electric cruise ship power plant, as was also concluded by Veldhuizen [37]. A 34% GHG emissions reduction was estimated, which is on top of the drastic reduction of NO_X and CO emissions. The sensitivity analysis showed that insecurities and developments in SOFC investment cost, SOFC lifetime, and fuel prices of the fuel cells have the largest influence on the economic feasibility of an SOFC powered ship.

The additional weight or volume of an SOFC power plant practically results in a larger ship, a deterioration of the operational profile, a reduction in cargo, or a combination of those, which all have an economic cost. Micco et al. [171] estimated a 3% cargo reduction for retrofitting a commercial vessel with an ammonia-fuelled SOFC powertrain.

Kim et al. [163] extensively compared the lifetime cost of an ammonia-fuelled SOFC power plant with HFO-fuelled engines for a container ship. They concluded that an ammonia-fuelled SOFC power plant would increase the lifetime cost 5.2 times even without considering the loss of cargo, but could also reduce GHG emissions by 92.1% when ammonia is produced via a sustainable pathway. For the SOFC ship, despite the high cost of the SOFC, the fuel cost remained dominant (57.8%). They concluded that when SOFCs become more cost and space-efficient, ammonia-fuelled SOFC systems would be a good long-term solution to decrease greenhouse gasses. Kistner et al. [168] did a similar comparison for an LNG-fuelled SOFC system. They included the emissions as a societal financial cost and concluded that, despite the larger capital and maintenance cost, an SOFC plant is economically viable. For the LNG-fuelled SOFC plant, they also identified the fuel cost as the largest contributor to the lifetime cost.

Environment

The main purpose of SOFC implementation is emission reduction. However, only some of the considered studies actually indicate the emission reduction. Exhaust gas sample measurements of a 50 kW SOFC demonstrator running on Ultra Low Sulphur Diesel (ULSD) indicate that NO_X emissions are far below the limits for ECA zones and no sulphur nor hydrocarbons were detected [93]. The research results of Baldi et al. [27] indicated that the absence of methane slip in the SOFC system is the strongest driver in reducing GHG emissions, compared with LNG-fuelled engines. In their study, applying an SOFC system reduced the GHG emissions twice as much as the CO_2 emissions. Veldhuizen [37] concluded that an LNG-fuelled SOFC powered expedition cruise ship, hybridised with diesel generators to support during long transits, can meet the CO_2 goal of 2030 and the ECA restrictions on NO_X, SO_X and PM emissions. This was concluded at a 20% increase in total costs over the lifetime of the ship. An ammonia-fuelled SOFC system could also reach these targets, however, the total cost of ownership increases with 69%. For a methanol-fuelled SOFC ship, the carbon dioxide emissions did not reduce sufficiently.

It is evident that the implementation of SOFC reduces ship emissions and makes it possible to comply with upcoming regulations, albeit at a very high cost. However, to judge whether SOFCs are more environmentally friendly than conventional solutions, the environmental impact over the full life cycle of the fuel as well as the fuel cell system must be taken into account. Strazza et al. [153] executed an extensive life cycle analysis

(LCA) for SOFC in marine applications considering hydrogen, LNG, and methanol. The study concluded that the environmental impact of SOFC in marine applications is dominated by the fuel production phase. From a life cycle perspective, bio-methanol and hydrogen (produced from cracking and electrolysis respectively) are the best options to fuel SOFC in marine applications. Finally, SOFCs are recommended over conventional diesel generators, just as the life cycle study of Altmann et al. [209] concluded. Lee et al. [210] and Mehmeti et al. [211] concluded from their life cycle analyses that the manufacturing and disposal of the fuel cell contribute little to the total environmental impact (2-10%), while operating the SOFCs has a large impact (90-98%), driven by the fuel consumption. Bicer and Khalid [212] investigated the environmental impact of heat and power generation with SOFCs for hydrogen, natural gas, methanol, and ammonia. The life cycle analysis included all phases from raw material extraction to operation (only end-of-life scenarios were not included). It was concluded that NG-fuelled SOFCs have a less negative environmental impact than hydrogen, methanol, and ammonia, because these fuels are mostly produced from natural gas, requiring additional conversion processes. However, when hydrogen or ammonia are produced from wind energy, the environmental impact was lower than with natural gas. Perčić et al. [136] did an LCA for SOFCs in ferries considering hydrogen and ammonia, taking into account different production pathways. They considered the manufacturing phase, the well-to-pump phase, and the pump-to-wake phase and used global warming potential, acidification potential, aerosol-forming potential, and fossil depletion as environmental indicators. They concluded that SOFC powered ferries using blue or green hydrogen or ammonia have a lower environmental impact than an equivalent diesel-powered ship. By also including the cost over its lifetime, the authors conclude that the blue ammonia-fuelled SOFC option is the most feasible option. It provides a 65% - 72% reduction in GHG emissions at a cost increase of 37% - 43%, where the range represents three different passenger ship case studies. Most LCAs do not consider any disposal or recycle phase, mainly because there is no information regarding the required methods. Sarner et al. [213] made the first efforts to review which recycle methods are applicable for SOFCs, but more research is needed to evaluate the environmental footprint after its lifetime.

2.3.4. RESEARCH PROJECTS

Over the last 30 years, several research projects of fuel cells in marine applications have emerged. Different ship types, fuels, and fuel cell types have been investigated. At first, most research projects focused on diesel as bunkering fuel, due to the low cost, high availability, and developed infrastructure. However, problems emerged in sulphur contamination of the fuel cells and efficiency of the whole system [28]. In the last 15 years, research projects emerged that are focused on solid oxide fuel cells. An overview of the most noteworthy research projects of SOFC in marine applications is shown in Table 2.5. This section describes these projects and their practical lessons for SOFC marinisation.

FELICITAS

In the FELICITAS project, a methane-fuelled 250 kW SOFC system was marinised. Several power plant integration concepts were investigated, such as gas turbine tri-generation, HVAC integration, and the use of flywheels [154]. A high system efficiency

Table 2.5: Chronological overview of research projects of maritime SOFC applications. GT = Gas Turbine, RE = Reciprocating Engine.

Project	Year	Fuel type	Fuel cell type	Ship type	Capacity of demonstrator [kW]	Reference
FELICITAS	2005-2008	LNG	SOFC-GT	Yacht	250	[214]
METHAPU	2006-2010	MeOH	SOFC	RoRo	20	[215]
SchiBZ	2009-2016	Diesel & NG	SOFC	Multipurpose	100	[156]
GasDrive	2016-2022	LNG	SOFC-RE	Ship	-	[77, 117]
SchiBZ 2	2017-2020	Diesel	SOFC	Multipurpose	100	[30, 162]
Nautilus	2020-2024	LNG	SOFC	Cruise	60	[216, 217]
ShipFC	2020-2025	Ammonia	SOFC	Offshore	2000	[218, 219]
FuelSOME	2022-2026	Ammonia, MeOH, H2	SOFC	Cruise	500	[220]
HELENUS	2022-2027	LNG	SOFC	Cruise, Dredger, Offshore	500	[221]

(>60%) was simulated and verified with experiments, and it was noted that the SOFCs should be operated at constant load while being supported with energy storage devices. The harsh marine conditions proved to be a great challenge for SOFC implementation. SOFC power output and lifetime were adversely affected when operating under high humid and saline conditions, resulting in the research advice to develop cathode materials with higher tolerance to Cr species. Additional investigation into marine vibrations and shocks was conducted. It was concluded that the mechanical integrity of the ceramic stack can be guaranteed with off-the-shelf damped mounting and shock resistance. Furthermore, a 1 MW SOFC plant was developed for an existing yacht design. Since the necessary pipes for fuel and ventilation conflicted with bulkhead positions, it is advised to newly design SOFC powered ships [214].

METHAPU

The METHAPU project focused on validating and innovating a methanol-fuelled SOFC system for cargo vessels. Another major aim was to introduce regulations regarding methanol bunkering, distribution, and storage for commercial vessels. A 20 kW prototype was marinised and tested for five months on the car carrier 'Undine' while sailing. The SOFC unit, methanol tank, and fuel reforming system were placed on open deck because this made it easier to ensure safe operation. The project was technically successful and succeeded in running the SOFC for 700 hours with methanol. From their experience, the consortium established design guidelines, an SOFC installation manual, an SOFC user manual, and a methanol bunker checklist METHAPU [215].

SchiBZ

SchIBZ aimed to develop a diesel-fuelled 500 kW SOFC system for oceangoing ships. The reforming process and a system concept are developed. The researchers paid extra attention to minimising the pressure drop between anode and cathode for which they used an uncommon anode recirculation architecture. They designed a cooled recirculation loop because commercial blowers could not operate at high temperatures. A 27 kW containerised demonstrator was tested in the multipurpose vessel 'MS Forester', which demonstrated an electrical efficiency of 50% on low sulphur diesel [195, 222]. In 2016, the project continued with SchIBZ2 to test the seaworthiness of the individual components, optimise them, and further develop them for operation with LNG [30, 162, 223]. The follow-up project MultiSchiBZ aims to scale-up to a 300 kW system. The diesel or LNG-fuelled system combines 12 fuel cell modules with one central fuel processing module in a 40-foot container. Low temperature anode recirculation and a model predictive control strategy are positively evaluated to increase the performance of the SOFC system Hollmann et al. [177].

GasDrive

The Gasdrive consortium proposed a novel NG-fuelled power generation system, where SOFCs are integrated with an internal combustion engine. The anode off-gas of the SOFC fuels the internal combustion engine. The optimal power split between the SOFC and the engine is investigated by Sapra et al. [31]. Carbon deposition indication is researched as a diagnostic tool to define safe operating conditions and appropriate control strategies for the SOFC system. Additionally, the effect of different pre-reforming concepts on the electrochemistry and temperature gradients in a commercial stack was investigated. The highest system efficiency was obtained with a system using allothermal pre-reforming and water recirculation. They learned that both stack and system operation need to be simultaneously considered to design the most efficient SOFC system.

Nautilus

The Nautilus Project aims at developing, evaluating, and validating a highly efficient and dynamic integrated marine energy system fuelled by LNG for long-haul passenger ships. This energy system, responsible to cater for all heat and power needs of a vessel, consists of a SOFC-battery hybrid system and Internal Combustion Engine (ICE) based generators [224]. During the SOFC system design, the target efficiency could not be reached with a simple system architecture. 40% anode off-gas recirculation is applied to increase the projected electric efficiency from 59% to 64% [217]. The consortium develops a complete design concept and digital demonstrator of a fully integrated onboard energy system for cruise ships. It was learned that combining several off-the-shelf SOFC products into a marine power plant brings many new considerations. Centralizing air supply, fuel supply, reforming, exhaust streams, and power electronics could improve the power density and cost when scaling a kW plant to a MW plant, but there are technical limits to the size of these components and using combined components decreases reliability. Furthermore, extra analysis was necessary to design the exhaust ducting because it was not known whether the backflow of exhaust gas (for instance, when one operational module is shut down) would cause issues in the SOFC modules. Additionally, a 60 kW containerized proof-of-concept demonstrator will be developed and tested to validate the design and operational strategies. A direct current busbar (400 V) is used to combine ten 6 kW SOFC modules and one 20 kW battery, because this required less power conditioning equipment, resulted in lower electric losses, and ensured scalability and modularity. This project is still in progress [216].

ShipFC

The ShipFC consortium is going to demonstrate the first marine ammonia-fuelled SOFC system. Instead of an afterburner, they intend to use a catalytic converter to decrease the emission of nitrogen oxides. Offshore vessel 'Viking Energy' will be retrofitted with a 2 MW SOFC system, aiming at a carbon-free operation of 3000 hours annually. The biggest challenge will be to scale the 100 kW Prototech module to an ammonia-fuelled 2000 kW power plant, which is aimed to be installed in 2023. Additionally, the consortium aims to develop certification schemes for the use of green ammonia to prevent carbon emissions in the supply chain [218]. From the first lab experiment was concluded that a high operational temperature should be chosen to promote ammonia cracking and thus prevent ammonia slip.

FuelSOME

Building on the insecurity of the future fuel mix, the project FuelSOME steps into the demand of fuel-flexible power plants and aims at the development and demonstration of a multi-fuel SOFC system. The system will be designed to operate with ammonia, methanol, hydrogen, and mixtures of those. Their focus is on long-distance shipping. This project still has to start.

HELENUS

HELENUS is a recently accepted European Union Horizon research project. It strives to enable full integration of SOFCs in ship design using co-generation and combined cycle solutions for increased efficiency with multiple fuels. A 500 kW fully integrated SOFC will be demonstrated on an ocean cruise vessel. The project also aims to improve fuel flexibility by demonstrating operation with renewable maritime fuels (e.g., ammonia, methanol, Fischer-Tropsch diesel, or hydrogen). A technological and regulatory roadmap will be created to scale-up the SOFC capacity to 20 MW [221].

Lessons learned

LNG is dominantly researched in demonstrator projects, since it is the most used fuel in available systems, but methanol and diesel have also been successfully demonstrated. Recent projects such as Nautilus and HELENUS also include many alternative fuels in their theoretical evaluation and the attention for ammonia-fuelled SOFC demonstrators is increasing.

SOFC demonstration experiments showed that the heat losses in the SOFC system are very relevant. Heat losses in different system components are often inaccurately taken into account in theoretical analysis, which causes deviations between theoretical and demonstrated efficiency. This topic requires more attention in future research.

Although several projects demonstrated a marine SOFC system and contributed to identifying the practical challenges of marinising SOFC systems, no large-scale SOFC system has been physically integrated with shipboard systems yet. The biggest challenges for SOFCs to achieve this are reaching higher power density, lower capital cost, and manufacturing capacity. It is also not known how the power density and cost scale when going from a kW scale plant to a MW scale plant. However, there is an increase in the rated power of demonstrators and the degree of ship integration for current and planned projects. Moreover, several ship types have been investigated, yet an evaluation of the most suitable vessel remains absent.

2

2.4. ADDRESSING MARINE CHALLENGES

This section provides an overview of possible developments in marine SOFC power plants that can address its main challenges, which are operation in marine conditions, low power density, limited lifetime, low transient capability, and high capital cost. The purpose is to indicate the prospects of SOFCs for marine applications from the technical and economic perspective. This section discusses possible improvements separated on cell level, stack level, module level, and marine power plant level. To relate possible improvements to the current status, an overview of all commercially available SOFC systems is provided in Table 2.6. Most are fuelled with natural gas and have a relatively small rated power. Figure 2.7 shows which manufacturers perform best on volumetric power density and electric system efficiency, which are considered important parameters for ship applications.

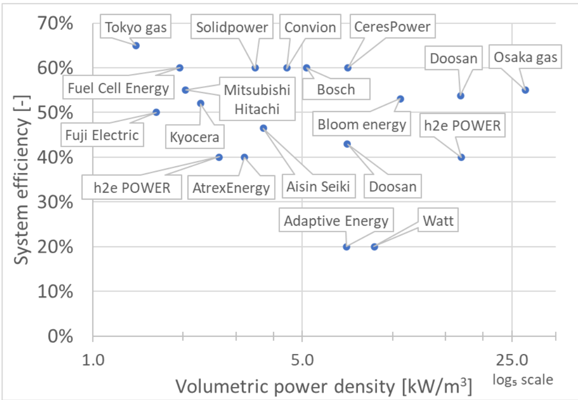

Figure 2.7: Rated efficiency and volumetric power density of commercially available SOFC systems.

Table 2.6: Overview of relevant commercial SOFC systems that are currently or almost available. The proven lifetime is not the lifetime that the supplier expects but what they actually demonstrated.

Supplier	Model	Fuel	Rated power	Electrical efficiency	Total efficiency	Power density		Proven lifetime	Source
			kW			kW/m3	kW/ton	h	
Adaptive Energy (NA)	Endurance	LPG	1	20%	-	7.0	36.8	15000	[225]
Aisin Seiki (Asia)	Ene Farm	NG	0.7	47%	90%	3.7	7.3	-	[226]
AVL (EU)	SOFC CHP	HC	10	60%	95%	-	-	>80000	[227]
AtrexEnergy (NA)	-	JP-8	1.5	40%	-	3.2	9.2	>10000	[226]
Bosch (EU)	FC505	NG/H2	10	60%	85%	-	-	-	[228]
Bloom energy (NA)	Energy server 5	NG	300	53%	-	10.6	19.0	5000	[229]
CEA (EU)	-	NG	15	55%	-	-	-	>8000	EFCF2020
Convion (EU)	C60	NG	60	60%	83%	4.4	-	>13700	[230]
Delphi (NA)	B-level	HC	2	30%	-	-	-	>10000	[231]
Doosan (Asia)	CHP	NG	10	54%	90%	16.8	-	-	[232]
Doosan (Asia)	PureCell 400	NG	440	43%	90%	7.1	-	-	[233]
Fuel Cell Energy (NA)	SureSource4000	NG	3700	60%	-	2.0	-	-	[234]
Fuji Electric (Asia)	-	NG	50	50%	80%	1.6	-	>3000	EFCF2020
h2e POWER (Asia)	Leonardo	NG	1.3	40%	95%	2.6	-	>40000	EFCF2022
	Galileo 1000N	NG	1	40%	95%	17.0	4.8	>40000	[235]
Hitachi Zosen (Asia)	-	NG	20	52%	-	-	-	>4000	EFCF2020
Huaqing Energy (Asia)	-	NG	25	47%	-	-	-	-	EFCF2020
Kyocera (Asia)	-	NG	3	52%	90%	2.3	8.0	>89000	[185]
Mitsubishi (Asia)	MEGAMIE	HC	210	55%	73%	2.0	7.6	>4100	[236]
Miura (Asia)	FC-5B	NG	4.2	50%	90%	-	-	-	[237]
Osaka gas (Asia)	192-AS1	NG	0.7	55%	87%	27.8	8.2	-	[238]
Solidpower (EU)	BG-60	NG	5.2	60%	90%	3.5	9.2	>40000	[239]
Tokyo gas (Asia)	-	NG	5	65%	-	1.4	-	-	EFCF2020
Upstart Power (NA)	Upgen NXG	LPG/NG	1.25	-	-	16.0	30.6	-	[240]
Watt (NA)	Imperium	LPG/NG	0.50	20%	-	8.7	24.0	-	[241]

Fuel: H2 = Hydrogen, HC = several hydrocarbons, JP-8 = Jet fuel, LPG = Liquefied Propane Gas, and NG = Natural Gas.

2

2

2.4.1. SOFC OPERATION

Thus far, SOFC systems have mainly been applied in stationary applications, such as residences and centralised power generation. In contrast to these applications, the power plant of a ship is exposed to sea wave-induced inclinations and accelerations. These could lead to lower accuracy of level sensors by sloshing of liquids, pressure variations in gas streams, increased mechanical stress in stacks and structural components, and failure of rotor pumps and compressors. Moreover, the propeller and internal combustion engines produce vibrations, travelling through the ship structures. It has not been extensively researched whether current SOFC systems can be safely operated when exposed to these conditions, and how these conditions influence the operation and durability.

Moreover, the saline and humid air conditions introduce challenges for SOFCs. The influence of air humidity on the performance and durability of state-of-the-art cathodes (LSM and LSCF) has been researched by Liu et al. [242]. The cathodes were stable when feeding air with typical water vapour concentrations (3 vol%) and even concluded to be better than using dry air, because the surface exchange reaction rate increased. However, cell degradation greatly increased for higher water vapour concentrations (5-20 vol%). In a 1500h durability test, Hagen et al. [243] showed that humid air (4 vol%) makes LSM cathodes perform worse and less durable when the polarization is sufficiently large. For seas and oceans, humidity of 0.5% to 3% is common, imposing no large performance or durability reductions of the SOFC. However, humidity in the air stream will accelerate corrosion from Cr and Si to the cathode. For this reason, Yang et al. [244] recommend to supply the cathode with dry air. Liu et al. [245] investigated the influence of salt content in the air feed for the same cathode materials. At 30 mg/L NaCl, the increase in cell degradation was negligible for LSM cathodes while LSCF cathodes showed decomposition of the cathode material. Thambiraj et al. [246] performed single cell experiments with 1.6 and 250 mg/L NaCl content in the cathode air. 1.6 mg/L salt content during 850 operational hours leads to a 200 mV drop because of delamination, whereas clean air only leads to a voltage drop of 25 mV in 660 hours. They conclude that air filters are needed to avoid NaCL reaching the cathodes. Besides effects on the fuel cell itself, salinity also corrodes other parts in the SOFC system, such as metal cell interconnects or compressors [247]. Luckily, air desalinisation is not new for marine applications, since it has been used for many years for marine gas turbines [248].

The long start-up and cool-down times of the SOFCs introduce challenges for practical operation. In applications where much unanticipated power is needed, a backup system should deliver the required power when the SOFC is still heating up. From this perspective, it would be favorable to use SOFC systems in applications with very constant operational profiles that are known in advance. The design rationale of the operational requirements for marine power plants might be reconsidered when applying SOFC power plants. A defined amount of power might be continuously delivered by SOFCs to reduce start-up and cool-down in order to limit cell degradation. Many ships always require some power for auxiliary functions, even when berthed. In port, low-emission energy could be delivered, where currently high investment shore power infrastructure is needed. When the energy demand of the auxiliaries is low, the excess power can be used to charge the support batteries or even delivered to the electricity net.

2.4.2. POWER DENSITY

Power density can be improved at each level of an SOFC system. For example, starting from improvement of the active layers in a single cell, up to reducing the size of or omitting specific BOP components. Moreover, not all system weights and volumes scale proportionally to the rated power, hence a scaling effect may be expected: large SOFC systems may achieve higher power densities than smaller systems employing the same technology [249].

The power density achieved at cell level is determined primarily by the electrolyte and electrode materials selected, their conductivity and thicknesses, active electrode and catalyst area, operating temperature, and pressure [250]. While the majority of commercially available systems rely on robust thick electrolyte supported cell types, designs with thin electrolytes supported on anode or metal substrates feature potential power density improvements. The potential power density improvements may be significant. For example, metal-supported designs achieve 2.8 A/cm^2 at 0.7 V and 650 °C [251] which is a factor 10 higher than the first generation based on the same concept. However, structural integrity remains a challenge for anode-supported designs, as is the use of metals at high operating temperature [252].

Flat-tubular SOFCs have the tubular stack advantages of easy gas-tight sealing, thermal robustness, and ease of fabrication while also profiting from planar advantages such as low ohmic resistance and high power density. The fuel flows through anode-supported, extruded channels. Parameters such as the number of air channels, wall thickness, width, and height of these air channels can be varied to optimise cell performance and mechanical strength. A review of Khan et al. [253] showed that the performance of these cells increased three to four times since their introduction in Kim et al. [254] by using different materials and architectures. Ilbas et al. [255] proved a 20% increase in power density compared with tubular stacks using a 3D cell model. Although this cell build is still in the research phase, its developments are also put into practice by Kyocera, Japan, and KIER, South Korea [253].

Large power density improvements may be achieved through stack design as well. The Compact Solid Oxide Architecture (CSA) Stack by Fuel Cell Energy, for example, is reported to achieve up to six times the power to weight and eight times power to volume compared with previous stack design, achieving 467 kW/ton and 778 kW/m^3 at only 0.29 A/cm^2 [256]. Although the power density of even today's stack technology is sufficiently high for most applications, the relatively large BOP of SOFC systems paints a very different picture. In fact, the BOP can easily make up as much as 90% of the total system mass and volume. For example, a 200 kW proof of concept built by Fuelcell Energy is reported to fit in a 20-foot container, thus achieving a power density of about a factor 10 lower than the power density reported at stack level [256]. Nevertheless, power density has not been as large of a design driver for most commercial SOFC systems as it would be for marine applications. It would be beneficial to tailor the design process to the marine requirements, rather than adapting existing designs with different initial requirements to the marine conditions.

For large-scale marine power plants, the desulphurisers, filtering equipment, blowers, and control architectures could be centralised for a multitude of SOFC modules, which would positively influence the power density and specific cost of the system with a slight reduction in system reliability. Moreover, air ducting is expected to require much ship volume. The specific air flows required for SOFCs are four to six times higher than those of diesel engines, because of the high air excess ratio that is required to cool the stack internally. Cathode air recirculation may reduce overall oxygen utilisation and thus limit the primary airflow and consequently the size of air ducting channels [53]. Cathode air recirculation could also increase the heat recovery capacity due to a higher flue gas temperature [176]. A more novel concept to reduce air intake uses SOFC stacks with liquid cooling, which has the additional advantage of a smaller parasitic power consumption. This was researched by Promsen et al. [257] for tubular and planar cells, who concluded that liquid cooling improved the temperature distribution inside the stack, improving the electrochemical performance. Nevertheless, this requires a completely new stack and system design, new operating principles, and a coolant suitable for high-temperature operation.

While sometimes overlooked, it is indispensable to consider the entire system when designing a compact and lightweight SOFC system. This calls for a holistic design approach, since choices at system level affect stack and cell performance, and vice versa. For example, the removal of a pre-heater or pre-reformer may reduce the size of the BOP, but reduce both the power density and the lifetime achieved by the stack [258].

2.4.3. LIFETIME

Lifetime is an important aspect of maritime power generation, as the number of annual operational hours is typically high in many ship types. In contrast to the low-temperature fuel cell types, SOFCs are primarily considered for stationary applications and uninterrupted power supply, for example data centres [259]. As these applications require the system to deliver for many hours per annum, lifetime and reliability have been major aspects of product development. First of all, high temperatures increase sintering speeds, creep, and crack growth, which alter the microstructural morphology of the cells and affects their electrochemical performance. In addition, high operating temperatures affect the chemical stability of the materials, including the electrolyte, the electrodes, and especially the interconnect. Therefore, material selection and microstructural design play a key role in reducing degradation at cell level [260]. The development of new materials for SOFCs is continuously evolving, for example bilayer electrolytes and new electrode morphologies [261].

Secondly, large internal temperature gradients are established over the stack to avoid a large airflow for cooling. These temperature gradients may be even higher locally, due to the differences in the magnitude of the exothermic electrochemical reaction. The presence of internal endothermic fuel reforming or cracking reactions may worsen the situation even further [262]. Temperature gradients result in thermal stress and potential delamination of the individual layers in the cells. Matching of thermal expansion coefficients helps to mitigate this issue, for which interlayers and composite electrodes may be applied [263]. In addition, researchers have proposed to adjust the catalyst loading spatially to control internal fuel conversion rates [264].

Carbon deposition may be encountered in case hydrocarbon fuels are used due to unwanted side reactions on the anode catalyst. Although carbon deposition may be suppressed through the supply of excess reforming agents, this generally negatively impacts cell life and efficiency. Alternatives for the nickel catalysts that have a low selectivity for solid carbon formation may be used instead, such as ceria-based anodes [265]. Both fossil fuels and biofuels typically contain small quantities of contaminants that may poison or react with SOFC electrodes, such as sulphur, chlorine, and potassium [266]. In addition, poisonous substances may migrate or evaporate from other parts of the system.

Chromium evaporation is commonly encountered in high-temperature alloys, which leads to irreversible performance loss at the cathode [267]. This issue can be addressed by applying surface coatings or modifications to the used alloys [268]. Ammonia, seen as a potential future fuel in the marine industry [269], does not contain carbon or these other contaminants. However, recent stack experiments showed that ammonia causes nitridation of the separator steel and the nickel catalyst. Although initial nitridation did not negatively influence cell performance, long-term nitridation deforms the stack components and causes local alternations or even blockage to the fuel channels [118]. Methods should be investigated to reduce or prevent nitridation.

It is generally acknowledged that dynamic operation influences the lifetime of SOFCs negatively [270, 271]. Effectively controlling SOFCs and other power generation components can stabilize the operation of the fuel cells, reducing cell degradation [164]. Parhizkar and Hafeznezami [272] optimised the operation of SOFC systems taking into account several degradation mechanisms and simulated a 7.4% increase in system productivity. Lai et al. [273] compared a stand-alone dynamic operated SOFC plant with a steady-state operated SOFC supported with combined cycles delivering power to the transient loads. They concluded that steady-state operation of the SOFCs is beneficial for the levelized cost of energy because of the reduced number of stack replacements. Marzooghi and Raoofat [274] proposed to use a Fuzzy-PI controller to reduce SOFC degradation of dynamically operated SOFC systems, which turned out to be a satisfactory control strategy. Although research in control of SOFC systems to increase lifetime has been increasing, very few degradation experiments have been performed on system level [275]. Moreover, most degradation experiments were executed in steady-state on nominal conditions. For marine implementation, it would be beneficial to investigate the differences in lifetime when the stacks are operated at part-load or with transient loads.

Improving lifetime remains an important aspect of SOFC development. There is a large number of mechanisms affecting degradation at cell, stack, and system level. Consequently, the lifetime can be improved through a large variety of developments, but often there is a trade-off versus system efficiency and power density. The lifetime of existing SOFC products is already sufficient for replacement intervals that are comparable to major overhauls of marine internal combustion engines, but further improvement of SOFC durability will be beneficial for commercialisation.

2.4.4. TRANSIENT CAPABILITIES

SOFC systems that are designed for stationary applications are optimised for load profiles with small and few load changes. However, most marine applications require quicker load changes. The transient response of electrochemical cells is inherently fast due to the small timescales of the electrochemical reactions. Still, the transient response times of SOFC systems are notoriously long, for which the large thermal mass of the system and response times of BOP components are often identified as the culprit

[276]. While these explain the long times required for a cold start, neither provides a satisfactory explanation for the slow response once the system has reached its operating temperature.

Transient limitations in a hot and operating system originate primarily from thermal management challenges. SOFCs are usually cooled by cathode air, thus avoiding the need for high-temperature coolants. Although this simplifies the system, it leads to large airflows and thermal gradients due to the limited heat capacity of air [277]. The actual amount of cooling needs to be carefully controlled during transients to prevent local subcooling, overheating, or thermal stresses. However, the combination of solid materials with a high thermal mass and gaseous coolant with a low thermal mass causes long stabilisation times. Consequently, the point of operation needs to be changed slowly to give the airflow controller time to respond to the delayed change in the air outlet temperature [278].

The transient response may be improved by increasing the safety margin against thermal overloading, for example, by operating the SOFC well below the maximum temperature and maximum temperature gradient. However, both compromise the power density and efficiency as the stack resistance or air stoichiometry are increased. Alternatively, the transient response may be improved through algorithms that control the airflow proactively, for instance, using model predictive control [279]. Wang et al. [175] managed to increase the thermal response time with 50% by using a fuzzy PID controller for power regulation and a feedforward controller for the thermal regulation. Hollmann et al. [177] used a controller that considers electro-chemical and transport characteristics to predict the system behavior over several minutes. The controller successfully increased the transient capability during testing on the operational profile of a cruise and cargo ship.

2.4.5. CAPITAL COST

While the fuel costs will be reduced by SOFC-based power generation, these savings are still not sufficient to justify the high capital cost. The current price of SOFC power plants may vary from 1500 up to as much as 22,000 €/kW depending on the system configuration and size. Although this is at least one order of magnitude higher than heavy-duty diesel generator sets, the cost may be substantially reduced by advanced manufacturing and scale-up. A detailed cost analysis by Scataglini et al. [179] reveals that the expected system cost of SOFC combined heat and power generation products may be reduced from 13000 €/kW for an annual production volume of 100 units of 1 kWe, to 500 €/kW for 50,000 units of 250 kWe. However, the challenge lies in attaining such production volumes at the current price level.

The capital cost of SOFCs may be further reduced through the adoption of more affordable materials or increasing the power density and, thus, reducing the cost of materials (see Section 2.4.2). Harboe et al. [38] identified that optimising the structural design of SOFC stacks to obtain a minimum contact resistance between the stack contacting areas is a key element in achieving cost-efficient stack design by reducing material usage. Various research groups are, for example, working on reducing the operating temperature of SOFCs as this would allow the introduction of cheaper materials, easier assembling methods, and the use of off-the-shelf components [280]. The latter is important as the balance of plant can make up a large part of the total system size, weight, and cost, while the low production volume of SOFCs today makes the development of dedicated BOP components particularly expensive, for instance, high-temperature anode recirculation blowers. Cost analyses point out that stack manufacturing, control architecture, and power conditioning equipment contribute the most to the cost of SOFC systems [46, 281], so cost reduction should initially be aimed at these components.

2.5. OVERVIEW OF SUGGESTED RESEARCH DIRECTIONS

Section 2.3 discussed the integration challenges associated with the efficient and safe operation of SOFCs. Additionally, despite their low emissions, the environmental impact of SOFC systems, particularly regarding the use of alternative fuels and the recycling phase, warrants further investigation. Section 2.4 offered research directions on cell, stack, system and ship levels to improve the operation, power density, lifetime, transient capabilities and capital cost of SOFC systems. An overview of the main challenges and corresponding research directions that were discussed in these sections is provided in Table 2.7, which is offered to guide future endeavours in the marinisation of SOFC systems.

Research objectives 2 to 6 presented in Section 1.5 are selected from the proposed research directions in Table 2.7, with those addressed in this dissertation highlighted in bold. Chapter 3 examines the safe operation of SOFCs on ships by assessing the effects of inclinations and accelerations and offers system improvements to make SOFC systems more resilient to marine conditions. Chapter 4 establishes the potential of SOFC systems across different fuels by evaluating the net electric efficiency and heat recovery capacity, including system improvements with COGR. Chapter 5 addresses the scaling of commercial SOFC systems to higher power ratings and improves power density by centralizing BOP components. Chapter 6 evaluates the size, fuel consumption and emissions of hybrid SOFC systems with gensets and batteries, while taking into account the effect of part-load operation and component degradation. Direct current architectures are implemented where feasible to reduce conversion losses. Finally, Chapter 7 discusses the most suitable ship applications for SOFC systems based on their operational and technical specifications. Together these research objectives evaluate the effective integration of SOFC into ships. This aids researchers and engineers in making informed decisions regarding fuel selection, SOFC system layout, hybridization with other components, and the development of a robust energy management strategy.

Table 2.7: Overview of identified research gaps or research directions in marine SOFC research. Those addressed in this dissertation are highlighted in bold.

Target	Research gap or direction	Level
Efficient operation	Anode off-gas recirculation to increase electric efficiency	System
	Cathode off-gas recirculation to increase heat efficiency	System
	Smart control to operate at optimal efficiency for different energy demands	System & Ship
	Direct current architectures	Ship
	Decentralised power generation	Ship
	Suitability of ship types	Ship
Safe operation	Effect of fire smoke on SOFC operation	Cell & Stack
	Effect of salinity and humidity on SOFC operation	Cell & Stack
	Effect of inclinations and accelerations on SOFC technology	System
	Effect of propeller or equipment vibrations on SOFC technology	System
	Marine fuel cell regulations specific for SOFCs	Ship
Low environmental impact	**Operation of SOFC system with renewable fuels**	All
	Disposal and recycling methods of SOFCs	Cell & Stack
Increase power density	Metal-supported SOFCs	Cell
	Flat-tubular SOFCs	Stack
	Liquid cooling of SOFCs	Stack
	Centralising balance of plant components	System & Ship
	Hybridisation with diesel generators	Ship
Increase lifetime	Spatial catalyst loading to control fuel conversion and thermal gradients	Cell
	Quantification of lifetime enhancement at part-load operation	Cell & Stack
	Long-term degradation behavior for transient operation	Cell & Stack
	Energy management system optimised towards SOFC lifetime	System
Increase transient capabilities	Low-temperature operation	Cell
	Improved flow field design	Stack
	Advanced thermal management and control	System
	PEMFCs fuelled with anode off-gas of SOFC	System
	Hybridisation with batteries	Ship
Decrease capital cost	Development of new materials and manufacturing methods	Cell & Stack
	Decrease cost of control architecture and power electronics	System

2.6. CONCLUSION

Research regarding SOFCs for marine applications has been reviewed. These electrochemical devices could be used to reduce NO_X, SO_X, PM, and GHG emissions. Developments in SOFC power plants and fuel possibilities are discussed, followed by the research efforts regarding ship integration, which cover hybrid strategies, fuel flexibility, spatial layout, thermal and electric connection, operating strategies, and safety. Compared to land-based systems, the marinisation of SOFC systems introduces new challenges in design and integration. The SOFC systems must be able to withstand accelerations and inclinations which most commercial systems are not designed for. Moreover, air salinity and humidity potentially deteriorate power production and increase degradation. On top of that, ships often require higher load transients. Thus, SOFCs should be combined with energy storage devices or components with higher transient capabilities.

2

Implementing SOFC in ships is currently difficult because of low power density, short lifetime, slow transient behaviour, and high capital cost. However, these disadvantages could be outweighed by the high efficiency of SOFCs and the reduced emissions, which would be even more favourable in case an emission tax is introduced. Nevertheless, hybridisation with internal combustion engines and batteries is suggested to increase the feasibility in terms of size, cost, and transient capabilities.

On SOFC system level, several developments are indicated that can potentially address the challenges for marine implementation, such as cathode off-gas recirculation. When considering whole marine power plants, DC grid architectures, centralised BOP components, and decentralised power generation can offer improvements in efficiency and power density. The matching of heat supply and demand, the matching of transient capabilities and the ship's operational profile, hybridisation strategies, and the effects of marine conditions on SOFC operation are suggested as important topics for further research. These topics are addressed in the remaining chapters.

LNG-fuelled SOFCs allow ship owners to meet the IMO regulations for NO_X and SO_X emissions and the 2030 GHG target, when SOFCs deliver the majority of shipboard energy. Renewable fuels and other energy-saving technologies would be necessary to reach the IMO's GHG target of 2040 using SOFC systems. Carbon-free ship operation should not be the main goal; converting renewable fuels with high efficiency over the whole life cycle should gain the focus. Although implementing SOFC in ships still faces technical, economic, and design challenges, it is a promising solution for the marine industry to decrease NO_X, SO_X, and PM emissions while benefiting from noise reduction and increased reliability.

3

The influence of inclinations and accelerations on SOFC systems

In the middle of difficulty lies opportunity.

Albert Einstein

This chapter has been published in the Journal of Power Sources **585**, 5163448 (2023) [282].

3

3.1. INTRODUCTION

Many ships make deep-sea itineraries with the possibility of encountering large waves and heavy weather. However, most SOFC systems are designed for stationary applications such as domestic, power plants or data centres [44]. All shipboard equipment and machinery must be designed to function properly even when exposed to these inclinations and motions. The conditions the equipment might be exposed to and the regulations currently in place for shipboard machinery are summarised in Appendix A.2. This is particularly relevant for SOFC systems because one of the benefits is their ability to be installed in a decentralised manner, reducing the size and losses of the power grid, and increasing system reliability [173]. However, this also increases the distance of the SOFC from the centre of rotation of the ship, resulting in increased accelerations that the SOFC system may experience. Despite the growing interest in using SOFCs as a power source for marine vessels, to our knowledge, no other researchers published regarding the effect of ship motions on SOFC systems. There is a need to assess the impact of tilted movements on SOFC systems in order to safely and effectively integrate them into ships.

An initial inclination test campaign was performed to develop solid test procedures [283]. A 1.5 kW SOFC system was inclined statically and dynamically up to angles of 30 degrees. The dynamic inclination test resulted in forced oscillation behaviour of the operational parameters of the SOFC stack. It was concluded that a larger range of test conditions and longer test durations are needed to determine the cause and the potential harm of the forced oscillation behaviour. The findings of the initial test campaign are used to define an improved second test campaign, which is presented in this chapter.

The goal of this chapter is to evaluate the influence of marine conditions in terms of static and dynamic inclinations on the operation, safety and lifetime of SOFC systems. The results will be used to identify safety risks, in order to propose design improvements for SOFC systems and develop well-founded class rules. Using a one-axial oscillation platform, ship motions are emulated up to 30 degrees of inclination. The main contributions can be summarised as follows:

- This chapter introduces a design for a test bench capable of evaluating inclinations and accelerations for fuel cell systems across a wide spectrum of seagoing ship types.
- To the best of our knowledge, this study is a first-of-its-kind assessment of the operability of SOFC systems under inclinations and accelerations.
- This chapter gives insight into the possible consequences for the SOFC technology and its Balance of Plant (BOP) components and identifies which components are most critical for inclined operation.
- The present study provides evidence that SOFCs can operate successfully in the marine environment after minor design adjustments and indicates that ship motions have no significant impact on the system's lifetime.

First, the test set-up, test procedures and data acquisition are explained in Section 3.2. Next, the results and their interpretation for the different tests are shown in Section 3.3. Then, improvements are proposed for the design of SOFC systems, and for fuel cell regulations in Section 3.4. Finally, conclusions and recommendations further investigation are given in Section 3.5.

3.2. METHODOLOGY

3.2.1. TESTED SOFC SYSTEM

The tests are conducted with a 1.5 kW SOFC system manufactured by SolydEra S.p.A. The fuel cell module comprises of a stack composed of 70 anode-supported planar cells, an integrated heat exchanger, a pre-reformer, and a combustor. The cold balance of plant is made up of a desulphurizer, an air supply system, a water treatment system, power conditioning equipment, and a waste heat recovery unit, see Figure 3.1. The fuel channels through the stack follow the negative Y direction, while the gas, water, and air channels follow various directions towards the stack. It is an integrated independent system, meaning that the control architecture and safety mitigation are included in the module. The main characteristics of the module can be found in Table 3.1. The system is designed for stationary applications and was not yet operated before while exposed to dynamic inclinations.

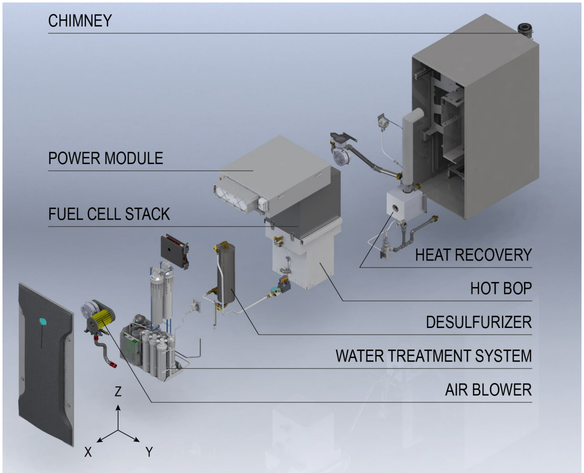

Figure 3.1: Visualisation of main components in tested SOFC system and the defined X, Y and Z axes.

3.2.2. EXPERIMENTAL SET-UP

A uniaxial harmonic oscillation platform induces both static or dynamic inclinations, enabling a wide range of ship motions to be simulated by adjusting the inclination and oscillation period. The SOFC system is secured to the inclination platform using a steel frame and lashing straps. Fuel, water, electricity, and exhaust piping are mounted flexibly. The process air is directly extracted from the environment. The hydraulic platform is electrically controlled, and the operating data of the SOFC module and BOP components are recorded every second. An inclination sensor is installed to also record the instantaneous angle every second. The SOFC module and its connections can be rotated with

Table 3.1: Main characteristics of tested SOFC system.

Characteristic	Value	Unit
Width	1200	mm
Depth	550	mm
Height	1014	mm
Mass	250	kg
Electrical output	0.5 to 1.5	kW
Nominal net electric efficiency	57	%
Heat loss to environment	0.1	kW

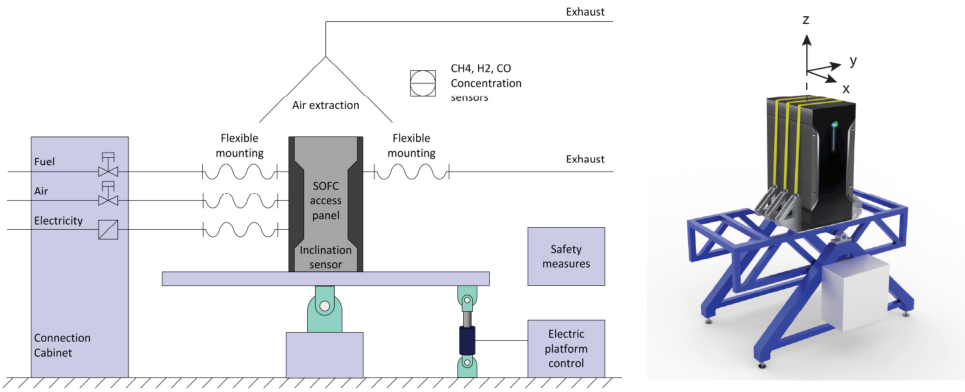

Figure 3.2: Schematic overview of used test setup.

respect to the platform to be able to test rotations around the X and Y-axis of the module. The experimental setup is illustrated in Figure 3.2.

3.2.3. TEST CONDITIONS

Table 3.2 shows the conditions that are used for the different tests. The test conditions are based on an analysis of possible ship motions and, although not limited to, current regulations on motions and accelerations of shipboard equipment, see Appendix A.2.

Table 3.2: Test conditions of different experiments.

	Axes [-]	Inclination Setting [°]	Roll period OR COG acceleration [-]	Steps [-]	Duration per step [min]	Total duration [h]
Static test	X, Y	-30 to 30	-	13	12	5.2
Dynamic tests						
- Full load test (100%)	X, Y	15, 22.5, 30	≈ 8 to 80 s	19	10	19
- Part load test (50%)	X, Y	30	≈ 8 to 80 s	19	10	6.3
- Degradation test	X	30	8 s	-	-	190
- Acceleration test	X	30	0.16 to 0.88 m/s^2	12	3	0.6

Room temperature during testing varies from 15-20 °C.
Pressure of natural gas line is 17 mbarg.
Volumetric composition of used natural gas: 94.3% CH_4, 3.2% C_2H_6, 0.8% C_3H_8, 0.2% C_4H_{10}, 0.5% CO_2, 1.0% N_2

3

The static test subjects the SOFC system to an inclination range spanning from -30°to 30°, with a step size of 5°, with each inclination lasting 12 minutes. The static inclination test is performed around the X and Y axis.

The dynamic testing employs harmonic oscillations, as an electric motor with a crank connection drives the platform. For the full load and part-load test 19 oscillation periods between 8 and 80 seconds are used, to include a wide variety of ship types (see Appendix A.2 Table A.2). The full-load test is conducted at inclinations of 15°, 22.5°, and 30°, while the part-load test is solely performed at an inclination of 30°. The SOFC is operated for a duration of 10 minutes at each distinct combination of test conditions. Because power modulation is time intensive, solely one part-load condition is taken into account, namely 50% power production. The full-load and part-load tests are also executed for two rotational axes.

In order to investigate the impact of dynamic inclinations on the lifetime of the SOFC system, the module is operated under nominal conditions for a total of 190 hours, of which 64 hours are under dynamic inclinations. The dynamic inclinations are solely performed around the X-axis, with an outer inclination setting of 30 degrees. The shortest motion period of 8 seconds is used because this results in the highest number of cycles and impose the highest structural loads.

When the SOFC system is positioned far from the centre of rotation on a ship, roll and pitch motions can expose the system to significant accelerations. To assess the suitability of the system for decentralised power production, it is subjected to high acceleration testing. It is noteworthy that current regulations for fuel cell testing do not mandate any acceleration tests. Consequently, the acceleration test parameters are based on prior studies that reported simulated or measured accelerations, as indicated in Appendix A.2 Table A.3, although the maximum acceleration was limited by the capability of the platform. The accelerations range from 0.1 to 0.88 m/s^2, distributed over 12 discrete steps.

3.2.4. DEGRADATION RATE PREDICTION

The SOFC module is designed to maintain constant power output. Therefore, as voltage decreases due to degradation, the current increases to compensate and deliver the same power output. This in turn further decreases voltage along the polarization curve of the

SOFC stack. Hence, the absolute degradation rate (as expressed by Equation 3.1) is determined based on the decrease in system efficiency and not voltage, as this is a more representative parameter for system-level testing [284].

$$deg\,[\eta_{net}/kh] = \left(\eta_{net,start} - \eta_{net,end}\right) \cdot \frac{1000}{t_{end} - t_{start}} \tag{3.1}$$

Accurate estimation of the degradation rate in the SOFC module requires extensive testing hours, owing to small variations in its operation, continuous deviations by control feedback, and noise generated by sensors. According to Gemmen and Johnson [284], operation for at least 10,000 hours is required for reliable results when the experimental noise is 1% and the nominal voltage degradation rate is 0.5 %/kh, which is typical for commercial stacks. In this research, Gaussian process regression (GPR) is used to predict the net electric efficiency to estimate the range of degradation rates that can be concluded from this relatively short degradation experiment. GPR makes use of a probability distribution over an infinite number of functions that coincide with the used data points. The mean and covariance of all these functions form the prediction, which makes it possible to reflect the uncertainty in the prediction. GPR has also been successfully used by Zhu and Chen [285] and Deng et al. [286] to predict the degradation of fuel cells. The net electric efficiency is estimated by $f(x)$ and a noise term:

$$\eta_{net} = f(x) + \epsilon \tag{3.2}$$

of which the signal term $f(x)$ is a collection of functions, following a Gaussian process:

$$f(x) \sim \mathcal{GP}(m(x), k(x_i, x_j)) \tag{3.3}$$

The noise term reflects the inherent randomness in the observations, which is assumed to be normally distributed:

$$\epsilon \sim \mathcal{N}(\mu, \sigma^2) \tag{3.4}$$

The kernel is a function that measures the similarity of two inputs. A suitable kernel needs to be selected to calculate the covariance matrix of the Gaussian process. Because cell degradation is often simplified to a quasi-linear process over time, a combined linear and constant kernel is used for the GPR model, as expressed by Equation 3.5. Some other composite kernels were also tested, such as RBF (Radial basis function) + periodic + linear and linear + RBF·periodic + RBF, but these combined kernels matched the measurement data less well.

$$k = k_C(x_i, x_j) + k_L(x_i, x_j) = \sigma^2 x_i^\top x_j + C \tag{3.5}$$

where x_i and x_j are input vectors. The variance σ^2 and constant C form the hyperparameters of the model, which are used to tune the kernel. These are optimised using maximum likelihood estimation to achieve an accurate fit of the measurement data. The measurement data during the 190 hours of the degradation experiment are used to train the model to estimate a 95% confidence interval for the net electric efficiency after 10,000 hours of operation, from which the expected degradation rate can be derived.

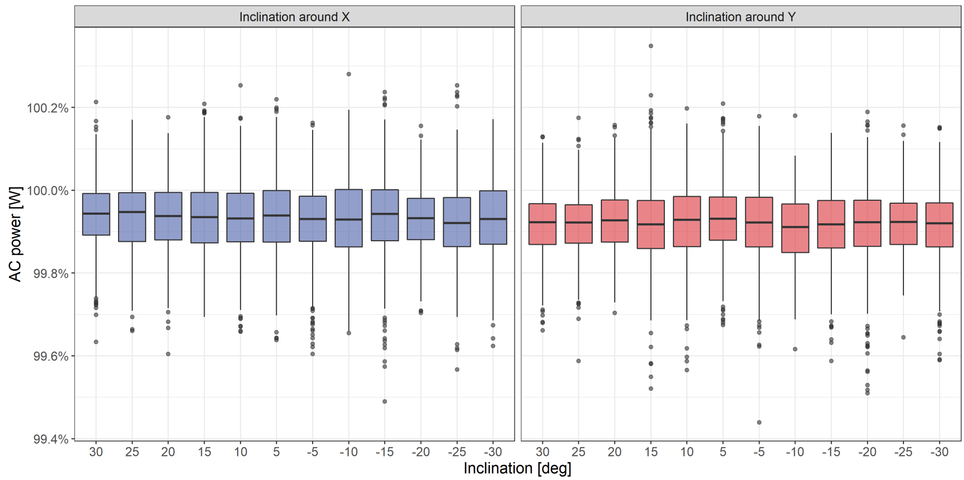

Figure 3.3: Normalised delivered AC power during static test.

3.3. RESULTS & DISCUSSION

The SOFC module delivers power over the full test duration, and no gas leakages or safety hazards are detected. Moreover, there is no indication of cell defects or delamination of the air electrodes. Nevertheless, small water leakages occur at inclined positions, possibly due to the overflowing of the condensate discharge system. Furthermore, some level sensors measure values that differ from the actual values due to the inclined or sloshing level surface.

3.3.1. STATIC INCLINATION TEST

In the static experiment, no extraordinary observations are made, and the system operation does not significantly differ from non-inclined operation. Figure 3.3 illustrates the power production measurements taken during the experiment at various static inclination angles. The power production remains highly stable and shows minimal variance for higher inclination angles.

3.3.2. DYNAMIC INCLINATION TESTS

Dynamic inclinations have a significant influence on the operational parameters of the SOFC module. Figure 3.4(a) illustrates that upon the onset of platform oscillations (indicated by the blue vertical line), the stack voltage shows forced oscillation with the same period as the platform. The magnitude of these oscillations surpasses the noise level observed during normal operational conditions.

FULL LOAD

The stack voltage measurements in full load under varying test conditions are presented in Figure 3.5(a). The deviations are most prominent at a combination of large inclinations and rotation around the X-axis. This forced oscillation behaviour is also observed

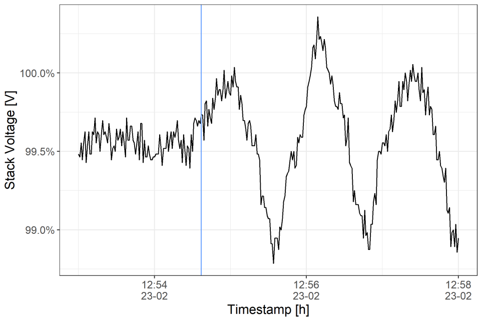

(a) Normalised stack voltage during dynamic inclinations with period of 78 seconds around the X axis up to 30 °C.

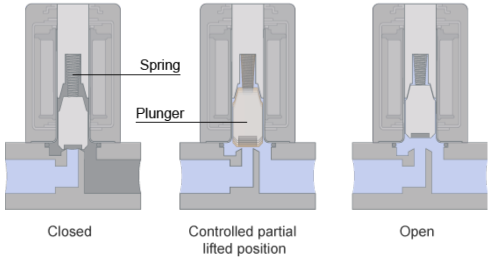

(b) Principle of a proportional solenoid valve that regulates fuel flow [287].

Figure 3.4: Effect of oscillation motion and cause forced oscillation behaviour.

for stack current, burner temperature, fuel utilisation, fuel flow, and steam flow. Consequently, these variations also occur in power production and electric efficiency. This also results in significant changes in the steam-to-carbon ratio, ranging from 1.6 to 2.2, although no carbon deposition is observed. Ultimately, it is discovered that the forced oscillation behaviour in system parameters is caused by the fuel regulation valve. The used proportional solenoid valve acts as a mass-spring-damped system as shown in Figure 3.4(b). The forced oscillation of the plunger leads to variations in the fuel feed. According to the Nernst equation below, variations in $y_{H_2,an}$ and $y_{H_2O,an}$ have a direct effect on the reversible cell voltage at position x along the fuel channel. Because the module's control architecture is aimed at producing a constant power, these voltage fluctuations result in a response by the before-mentioned system parameters.

$$V_{rev,x} = V_{rev,0} + \frac{RT}{2F} \ln\left(\frac{\sqrt{y_{O_2,ca}} \cdot y_{H_2,an}}{y_{H_2O,an}} \cdot \sqrt{p_{cell}} \right) \tag{3.6}$$

where $V_{rev,0}$ is the standard reversible voltage, R the universal gas constant, T the temperature, F is the Faraday constant, y_j the molar concentration of species j, and p_{cell} the cell pressure.

During rotation around the X-axis, the plunger experiences the largest acceleration, hence the larger deviations for this direction. Figure 3.5(b) illustrates that the deviations in stack voltage are largest in the 16 to 26-second period range, which indicates that the natural frequency of the valve is in this range. It is confirmed that the valve causes the forces oscillation behaviour by temporarily positioning the valve such that the plunger has no acceleration component during oscillations. This completely eliminates the enhanced deviations in fuel flow and consequently in all operational parameters.

For the motion periods with high deviations (16 to 26 seconds), the forced oscillation in operational parameters results in a gradual but significant power decrease. The oscillations in fuel flow result in changes in the fuel utilisation of ±2%. As excessive fuel utilisation could oxidise the nickel catalyst, this is undesirable in the SOFC system. Therefore, a safety mechanism is built into the system to prevent high fuel utilisation. The stack current is promptly reduced whenever the fuel utilisation limit is surpassed, as

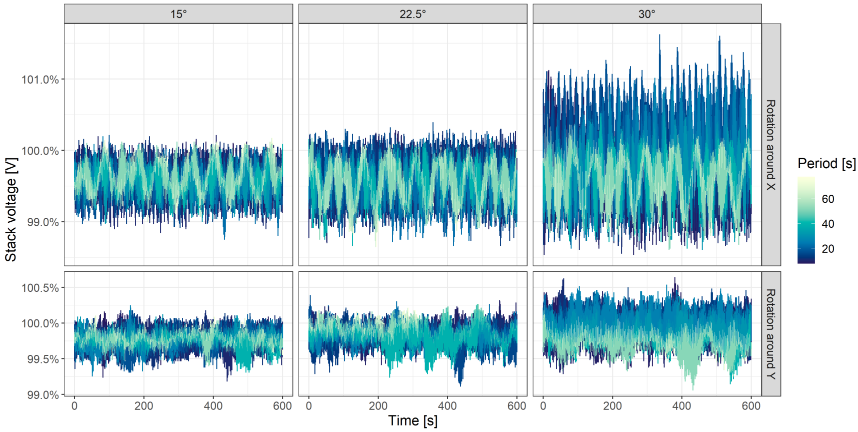

(a) Normalised stack voltage of full load dynamic experiment plotted over testing time for different combinations of test conditions.

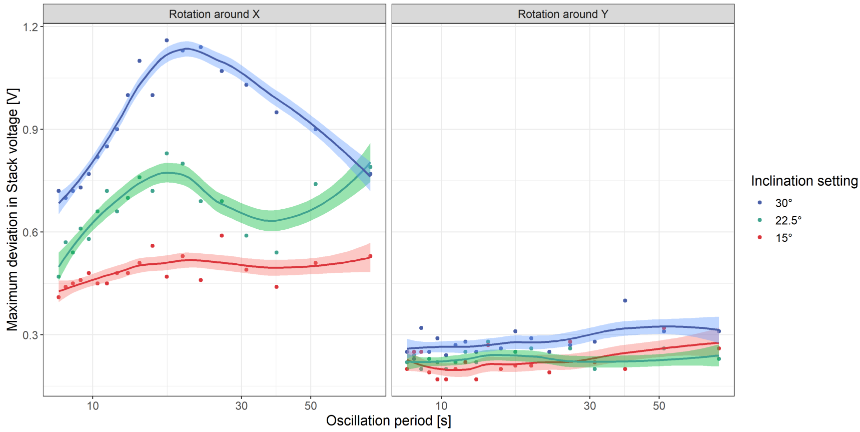

(b) Maximum deviation in stack voltage caused by platform oscillations. The solid line shows a trendline including a 75% confidence interval.

Figure 3.5: Main results of full load static and dynamic test.

shown by the red line in Figure 3.6. However, during oscillations, the limit is periodically exceeded, allowing insufficient time for the current to recover. As a result, the current and subsequently the power gradually decline. Given that the necessary stack current regulates the amount of fuel supplied to the stack, the reduction in current does not alleviate the fuel utilisation quickly enough, leading to a continued decrease in power. Moreover, the effect was tested over a 40-minute period, demonstrating a sustained reduction in power, albeit at a diminishing rate of decline up to a decrease in power of 7%.

PART-LOAD

To investigate whether the oscillation effects are similar or whether new phenomena emerge under partial load conditions, the 30°dynamic inclination experiment is also conducted at 50% part load. Regulation valves typically exhibit non-linear responses to changes in their opening, which can also alter their response to different periods. Therefore, the absolute deviations in fuel flow and air flow are not expected to reduce proportionally with the power. Subsequently, part load conditions may yield distinct behaviour. The deviations in fuel utilisation (±3%) are larger than in full load (±2%), as is visualised with density plots of the measurement data in Figure 3.7. This phenomenon can be attributed to the fact that an absolute deviation in fuel flow would represent a larger proportion of the fuel utilisation at lower fuel flow rates. This is especially relevant since it was pointed out in the previous section that changes in fuel utilisation can have a significant impact on the operation of the system. Nevertheless, the power reduction observed in Figure 3.6 is absent under part-load conditions. This is the case because, at 50% load, the SOFC system operates at 75% fuel utilisation (see Figure 3.7) instead of 85% fuel utilisation. This strategy is used by the SOFC system manufacturer to increase the amount of fuel in the anode off-gas flowing into the afterburner. This ensures that the burner receives sufficient fuel to maintain the temperature of the stack, which can be a challenge at 50% part-load operation. At 75% fuel utilisation with deviations of ±3%, the fuel utilisation limit is never exceeded.

3.3.3. DEGRADATION TEST

Repositioning the fuel regulation valve to eliminate acceleration components during platform motion prevents the oscillation behaviour of system parameters in this particular experimental setup. However, ship motions are more intricate, and accelerations may arise in various directions. Consequently, it is necessary to evaluate whether extended exposure to forced oscillation behaviour results in SOFC damage or accelerated degradation.

During the 190h of the degradation test the module produced power stably and nothing extraordinary is observed besides the forced oscillation behaviour. Figure 3.8 shows the prediction of the net electric efficiency from the degradation experiment using GPR. The estimated net electric efficiency after 10,000 hours of operation is 53.55% ± 1.37%, corresponding to a degradation rate of 0.30 ± 0.14 %./kh. The figure also shows the anticipated net electric efficiency in red according to the nominal degradation of this system, which is roughly 0.2%./kh. Nevertheless, the nominal degradation also varies slightly per SOFC stack, especially at the beginning of the lifetime of the stack. Consequently, it

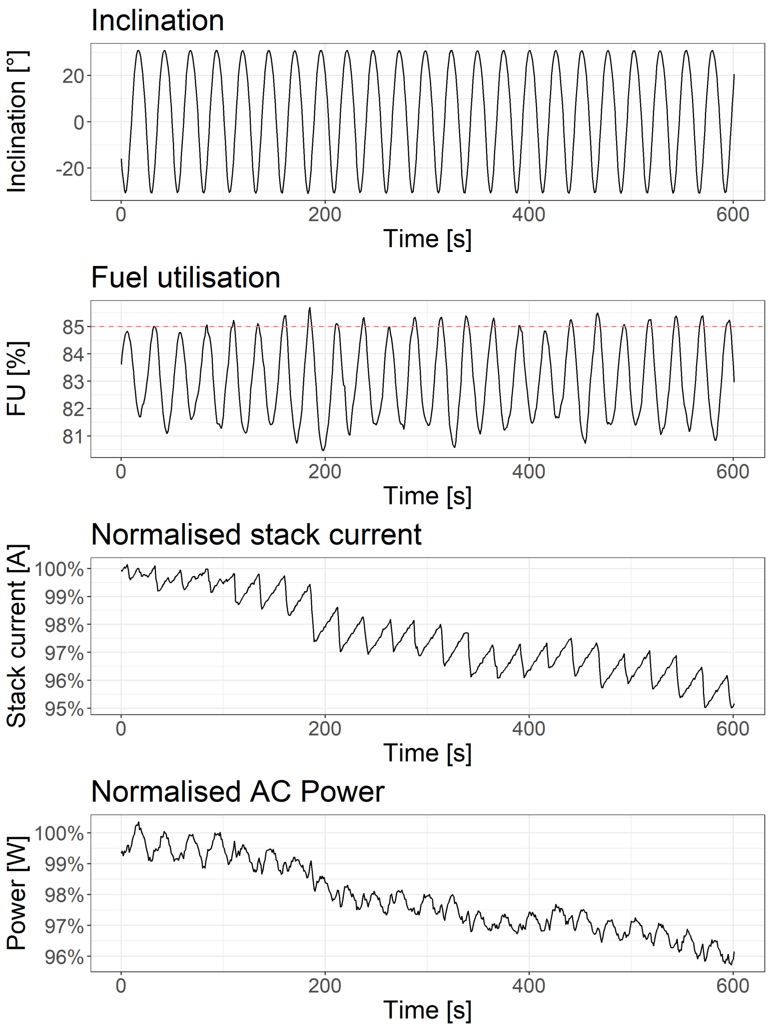

Figure 3.6: Inclination, fuel utilisation, stack current and AC Power over testing time for the dynamic experiment using rotation around X-axis, an angle of 30 degrees and a period of 27 seconds. The stack current and AC power are given as a percentage of their nominal value.

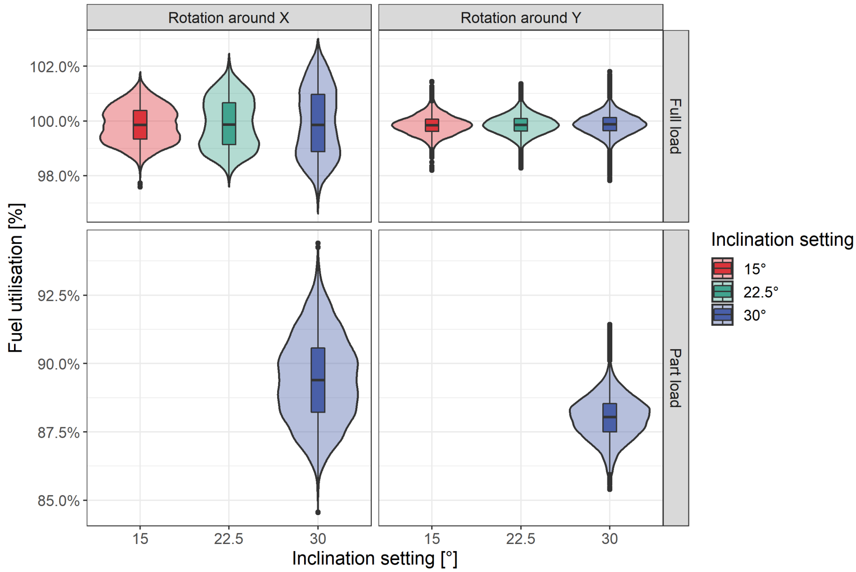

Figure 3.7: Fuel utilisation at full load and part load for two rotation directions and different outer angles.

can only be concluded from this test that the degradation during oscillations with a fast period of 8 seconds and an outer angle of 30º is in the same order of magnitude as in normal operation. Nevertheless, there is an indication of enhanced degradation. Thus, it is recommended to do long-term dynamic inclination experiments to accurately quantify the degradation rate to make sure the lifetime of the system will not be shorter when the system is operated on a ship.

3.3.4. ACCELERATION TEST

For this test, the platform is oscillated at high speeds to let the SOFC system experience high accelerations. The acceleration test is completed without noticeable safety hazards. The frequency of the oscillations in voltage becomes high for high acceleration speeds, because of the forced oscillation behaviour of the fuel regulation valve. However, the amplitude of the deviations in voltage and power production remains steady at high accelerations, see Figure 3.9. At high accelerations, the deviations in power production are smaller than at slower accelerations. This is the case because, at high accelerations, the motion frequency deviates more from the natural frequency of the fuel regulation valve, resulting in a smaller amplitude for the variations in fuel feed.

3.3.5. COMPARING NORMAL AND INCLINED OPERATION

As indicated in the preceding sections, the oscillations of the platform cause deviations in several system parameters. In normal operation, there are also small fluctuations in system parameters due to the noise of the sensors and continuous feedback from the control system. Figure 3.10 compares the amplitude of the fluctuations during normal

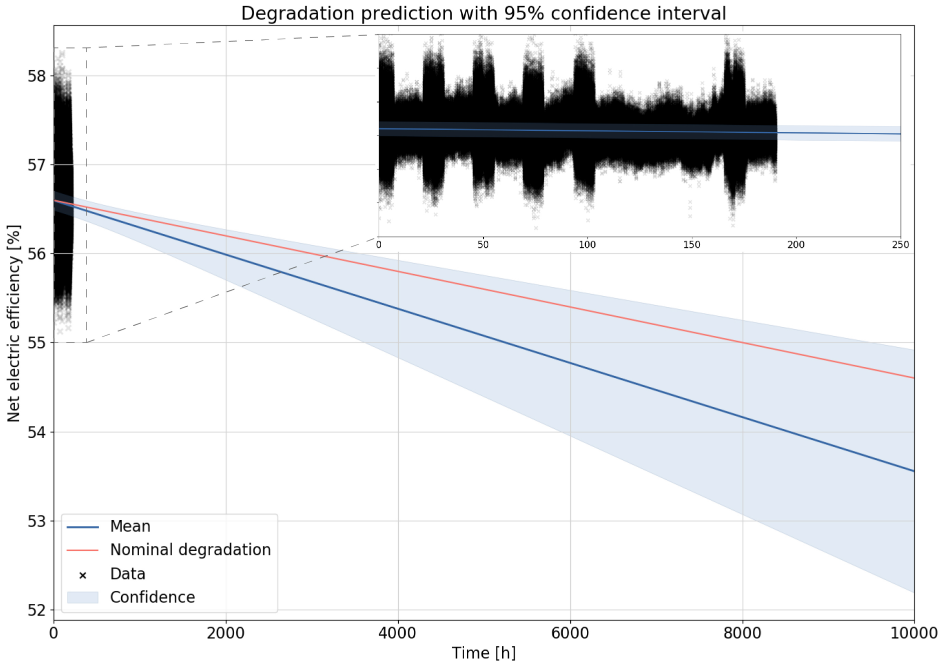

Figure 3.8: Net electric efficiency during degradation experiment with oscillation around X axis at a period of 8 seconds up to 30 degrees. The red line shows the nominal degradation rate in system efficiency during its lifetime, which is 0.2%./kh.

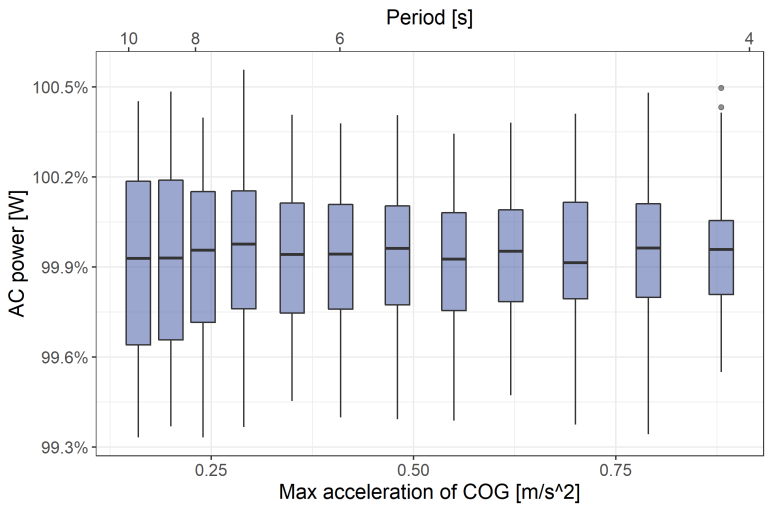

Figure 3.9: Normalised power production during acceleration experiment for different acceleration speeds. The acceleration speed represents the maximum acceleration during the given oscillation period as experienced by the centre of gravity (COG). AC power is given as a percentage of its nominal value.

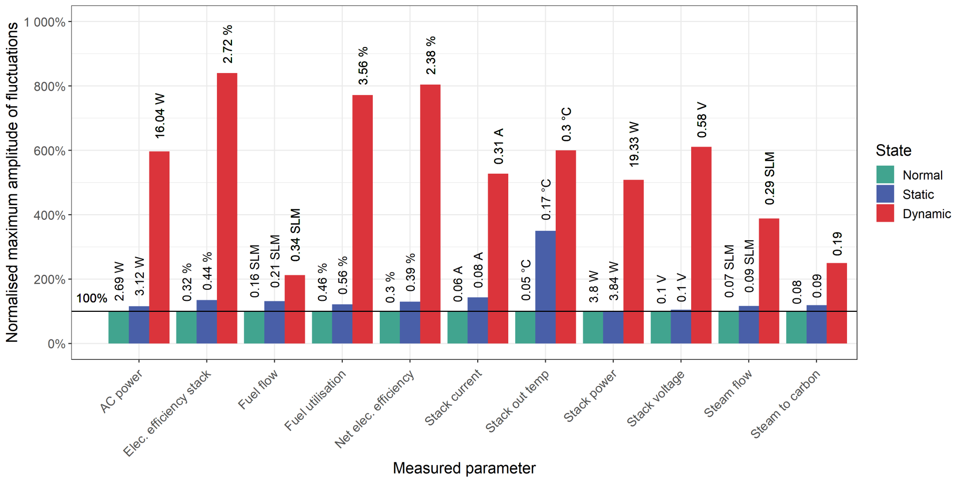

Figure 3.10: Comparison in the maximum amplitude of system parameter measurements between normal operation, static and dynamic operation. The data labels are absolute values of the amplitude while the vertical axis is normalised to be able to show the different parameters on one axis.

operation with those observed during the presented test conditions. The figure shows that the static inclinations do not lead to a significant increase in the amplitude of the fluctuations compared with normal operations for most system parameters. However, dynamic inclinations result in a substantial amplification of the amplitude in all of the shown system parameters.

3.4. GUIDANCE FOR DEVELOPMENT AND REGULATIONS

The results of the inclination experiments are used to propose design improvements for SOFC systems and develop well-founded class rules. First, it is discussed how representative the testing of this specific SOFC system is for SOFC systems in general. Following, guidance is given to stack developments to withstand inclinations and accelerations. Next, improvements to the design and control of SOFC systems are proposed to make them less prone to marine inclination conditions. Finally, the test results are compared with current marine fuel cell regulations to identify current gaps. The recommendations are summarised in Table 3.3.

3.4.1. GENERALIZABILITY OF EXPERIMENT

The presented results are specific to the tested system and its operational and control strategies. For instance, the natural frequency period of fuel oscillations observed in the system could manifest differently in other systems. However, the test methods and design recommendations are applicable to SOFC systems in general, because the system components are very similar. This holds as well for larger high-power systems, which are expected for marine applications. Although, it might be more difficult to expose the whole system to dynamic inclinations.

3.4.2. IMPLICATIONS FOR STACK DEVELOPMENT

The exposure of SOFCs to inclinations and accelerations presents opportunities for the development of cell materials and SOFC stacks. It becomes essential to design materials that can withstand these dynamic conditions while maintaining their electrochemical performance. Optimising the microstructure of the anode material can enhance its stability and prevent the formation of cracks or degradation during inclination or acceleration conditions [288]. The interconnect, which connects individual fuel cells in a stack, should also be designed to withstand increased mechanical stresses. Anode materials with enhanced mechanical properties, such as higher fracture toughness and resistance to mechanical deformation, can help withstand the stresses.

Because the ship motions can result in fuel feed fluctuations, the tolerance of high fuel utilisation in SOFCs could be enhanced. For instance, Futamura et al. [289] achieved high performance and stability at fuel utilisation up to 95% by co-impregnating noble metal catalyst nanoparticles with a conventional cermet anode. Moreover, this stimulates the development of anodes that are less prone to re-oxidation, such as perovskite oxide supported cells [290]. The fluctuations in fuel utilisation also offer an interesting topic for future research. Extensive understanding and modelling of the effect of fluctuations in oxidants and fuel flow fields in stack models are necessary to predict the effect of fuel feed fluctuations. The effect of recurring variations in fuel utilisation on the microstructure of SOFCs is to the knowledge of the authors not yet investigated and could be tested with SOFC cells and short stacks.

3

Table 3.3: Recommendations on stack, system and ship level for reducing negative consequences of marine inclinations conditions to SOFC systems.

Level	Aim	Recommendation
Stack development	Improve resistance to motions	Development of anode materials with higher fracture toughness and resistance to mechanical deformation
	Improve tolerance to temporary increased fuel utilisation	Co-impregnating noble metal catalyst nanoparticles with a conventional cermet anode
		Use of anodes that are less prone to re-oxidation such as perovskites
	Improve knowledge on effect of fuel utilisation fluctuations	Including fluctuations in fuel reactants and oxidants in flow field modelling for stacks
		Stack testing on the effect of fuel utilisation fluctuations on SOFC microstructure
System operation and control	Prevent fuel flow fluctuations	Tune natural frequency of fuel regulation valve
		Use valve that is not affected by accelerations, such as stepper motor valve
	Limit effect of fuel fluctuations on system operation	Increase fuel utilisation limit
		Use advanced control of fuel utilisation to reduce the effect of fuel fluctuations, such as: time-delayed feedback, feedforward control, or model predictive control
		Maintain fuel flow rate when current is reduced bysafety mechanism
	Prevent leakage or backflow of liquids	Use non-gravity based check valves
		Adapt level sensors to inclined or sloshing level surfaces of liquids
Ship design and regulations	Limit acceleration experienced by SOFC	Evaluate the acceleration experienced by the SOFC in relation to the distance to the centre of rotation of the ship
	Improve marine fuel cell regulations	Mandate dynamic inclination test on full range of motion periods of dedicated application
		Mandate to test the effect of inclinations on stack and BOP

3.4.3. IMPLICATIONS FOR SYSTEM OPERATION

FORCED OSCILLATION BEHAVIOR

Although the tests did not result in experimental evidence that the instability of the fuel regulation causes direct damage to the cells, the degradation test did indicate the possibility of an enhanced degradation rate. Fuel fluctuations and stack instabilities are often concluded as causes of accelerated degradation [291]. Fluctuations in fuel utilisation and current result in increased local temperature variations. Moreover, fuel starvation and nickel oxidation can subsequently increase mechanical stress in the cells. In case of fuel overconsumption, it can lead to a significant drop in cell potential, possibly modifying the anode microstructure irreversibly by re-oxidisation. Irreversible damages in the microstructure often result in an accelerated degradation rate. In short, it would be preferred to prevent or limit fluctuations in the fuel feed as much as possible.

During the experiment, forced oscillation behaviour in the system parameters is eliminated by repositioning the fuel regulation valve. However in a ship, completely removing the acceleration component may not be feasible due to its motions in different directions. As an alternative, the spring stiffness of the fuel regulation valve could be modified, changing the natural frequency to prevent a response at the motion periods in the dedicated ship applications. Alternatively, a fuel regulation mechanism that is unaffected by any accelerations, such as a motor stepper valve, could be used. This was tested at the end of the test campaign for different dynamic inclination conditions. During this test, there were no increased fluctuations in operational parameters compared to normal operation, meaning that the fluctuations in fuel feed were completely resolved.

GRADUAL POWER DECREASE

The gradual power decrease that results from periodical exceedance of fuel utilisation is induced by the system's control software. In the case periodical fluctuations in system parameters by ship motions cannot be prevented, there should be a robust control system in place that ensures the effects do not propagate through the whole system. In this specific case, there are several possibilities to prevent this:

- Increase the fuel utilisation limit for which the current is reduced. It is commonly acknowledged that 85% single-pass fuel utilisation is a feasible limit for the operation of planar SOFC stacks. At 90% fuel utilisation, there is a much higher contribution of concentration polarization and a significant risk of fuel starvation, causing oxidation mainly at the end of the fuel channel [292]. In practice, SOFC systems have a fuel utilisation limit between 85% and 90% at which the current is reduced to prevent damage to the cells. However, the consequence of shortly exceeding this limit might not be that high, meaning there is some leeway in the setting of the fuel utilisation limit when experiencing quick fuel flow deviations, as in this experiment. Especially when combined with anode with materials that tolerate higher fuel utilisation (as discussed in section 3.4.2), the fuel utilisation limit could be increased.

- Use of more sophisticated control strategies for fuel utilisation. A time-delayed feedback control would make sure that a very short exceedance of the fuel utilisation limit does not immediately lead to a change in the operation of the fuel cell system. Time-delayed feedback is an easy and effective method to maintain stability and prevent unnecessary actions in systems with complex dynamics and disturbances. Alternatively, feedforward control or model predictive control could be used to limit the fluctuations by using the ship motions to predict fuel feed fluctuations. However, this would lead to complex control architecture and it might be easier to prevent the fuel feed fluctuations.

- Maintain fuel flow rate when current is reduced as a response to the fuel utilisation exceedance. This approach would marginally lower fuel utilisation, thereby avoiding repeated breaches of the fuel utilisation limit. Nevertheless, such an approach would result in a decrease in the nominal system efficiency during scenarios where the stack current is reduced. In order to address this issue, a distinct control loop could be established that identifies instances where current reduction occurs as a safety mechanism rather than intentional power regulation. However, implementing such a control loop would generally be complex, as it would require handling special cases where the loop is always active.

Flow of liquids

Liquid flows and tanks should be designed such that they do not overflow or backflow during inclined operation. Especially gravity-based components to prevent backflow, such as air gaps or siphons can cause problems when the system is inclined. Level sensors and their control architecture should be designed such that they work properly for inclined or sloshing level surfaces. For large inclinations, the low-level sensor could be positioned higher than the high-level sensor, which the control architecture should be able to understand. Moreover, intakes should be designed such that the inflow of the liquid is guaranteed under the inclination conditions.

Structural support

The implications of static and dynamic inclinations should be integrated early in the design process of the system. Although there were no structural failures in the tested system, the SOFC stack is a heavy component which can exert significant forces on the structural components during accelerations. The supporting structural components should be designed for these loads, especially if the direction of these loads change to the lateral direction.

3.4.4. Implications for ship design and regulations

Although there are static and dynamic inclination regulations in place for marine fuel cell systems, the results of this research show that they need further development. According to the regulations, a single motion period is prescribed for dynamic inclination testing. Nonetheless, our experiment reveals that the system's response is significantly influenced by the motion period. Therefore, it is advisable to conduct the dynamic inclination test with the motion periods present in the dedicated application or to perform the test within the range of 8 to 50 seconds for type approval purposes, thus encompassing a broad spectrum of seagoing ships.

Given the expected high power output of marine solid oxide fuel cell (SOFC) power plants, the imposition of static and dynamic inclinations presents a challenge due to the potential size and weight of the systems. As a consequence, recent regulations mandate inclination tests solely for the stack technology [293]. Nevertheless, the experiment results prove that the BOP components and their interface with the stack have a considerable influence on the operational performance of the stack. Hence, it is suggested that type approval testing includes the response to marine conditions by the SOFC stack and BOP as well as their mutual influence. Further development of marine fuel cell regulation could include guidelines for the design of the system including suitable components, regulators and materials to withstand marine inclination conditions.

Finally, although high accelerations did not result in direct damage or operational troubles to the SOFC system, locating the SOFC system far away from the centre of rotation of the ship might result in even larger accelerations than are tested in this study. The position of SOFC systems in the ship should be evaluated with respect to the experienced and allowable accelerations of the SOFC system.

3.5. CONCLUSION

SOFC systems could reduce emissions from seagoing ships, but, it is unknown whether motions from waves or other sources influence the safety, operability, and lifetime of SOFC systems. In this research, a 1.5 kW SOFC module is operated on an inclination platform that emulates ship motions, to evaluate the influence of marine conditions in terms of static and dynamic inclinations on the safety, operation and lifetime of SOFC systems. The module is inclined statically and dynamically around two horizontal axes of rotation up to an outer angle of 30°, including motion periods between 8 to 50 seconds.

The module is tested successfully without any notable hazards during all different test conditions. Furthermore, there is no indication of cell defects or cathode delamination. While static inclinations do not impact the operation of the SOFC module, dynamic inclinations result in adverse effects. The fuel regulation valve acts as a mass-spring system, causing significant fluctuations in fuel flow to the fuel stack and resulting in deviations in fuel utilisation, power production, and efficiency. These deviations are largest at motion periods between 16 and 26 seconds, where fuel utilisation deviations of ±2% cause a gradual decrease in power output as the fuel utilisation limit is periodically exceeded. From the 190-hour degradation test, the degradation rate is estimated to be 0.32 ± 0.14 %./kh. This degradation rate indicates an enhanced degradation rate when compared to the nominal degradation rate (0.2 %./kh), although long-term testing is needed to accurately determine how much the degradation increases.

Based on the experimental results, the following recommendations are proposed for the design and regulation of marine SOFC systems:

- Besides the stack technology, the exposure of BOP components to static and dynamic inclinations and their influence on the SOFC system should be evaluated. The use of flow regulation valves that are affected by accelerations should be avoided or, alternatively, verify that their natural frequency is adequately distant from the anticipated periodic motion that can occur at the application site.

- Control feedback should be designed to mitigate expected forced periodical deviations in operational parameters from affecting the proper operation of the system.

- Liquid-containing systems should be designed to prevent overflow or leakage during inclination, and level sensors should take into account any inclined or sloshing surface level.

- Power producing systems should be tested over a wide range of dynamic motions with periods between 8 and 50 seconds.

Some practical engineering solutions are proposed to prevent the negative consequences on SOFC systems by ship motions. Nevertheless, future research is needed to understand the effect of fluctuations in oxidants and fuel reactants on the microstructure of the cells and stack. Furthermore, it should be confirmed whether motions result in an amplified degradation rate by exposing the system to motions for a long continuous period. For accurate degradation tests, it is recommended to do this testing on stacks instead of an integrated SOFC system. Additionally, forthcoming demonstration projects of SOFC systems on ships present an opportunity to collect data to evaluate the SOFC system's performance under actual ship motions in six degrees of freedom.

Although dynamic inclinations affect the operation of the tested SOFC module, these issues can be addressed through relatively simple design changes. Therefore, inclinations and ship motions do not pose a significant challenge to the integration of SOFCs in seagoing vessels.

4

Fuel efficiency of SOFC system with COGR for alternative fuels

Necessity is the mother of invention.

Translated from Plato

This chapter has been published in Energy Conversion and Management **276**, 116598 (2023) [294].

4.1. Introduction

Many alternative fuels (e.g., LNG, methanol, FT-diesel, ammonia, and hydrogen) are under consideration to reduce ship emissions [94]. However, using alternative fuels in marine engines is not a straightforward choice. Firstly, there are still significant NO_X emissions due to the combustion process. Secondly, the use of alternative fuels in internal combustion engines can cause lubrication, cooling, ignition, and knocking problems, introducing new challenges to combustion engine design [99, 146]. The high operating temperature of SOFCs offers flexibility in terms of fuel choice [295], which is perceived as a key aspect for the transition from fossil to renewable fuels in ships [296]. State-of-the-art SOFC systems can be fuelled with natural gas or hydrogen, but the conversion of ammonia, methanol, and diesel has also been positively evaluated with cell experiments [295]. However, it is not known which fuel could be converted most efficiently in marine applications.

4.1.1. Heat integration of SOFC systems

Many researchers investigated use of the high temperature outlets streams of SOFCs to further increase the conversion efficiency, for instance, with gas turbines [297], steam turbines [298], or ranking cycles [299]. Although many combined cycle studies predict high efficiency, it results in a more complex power plant with large control challenges and reduced part-load performance [36]. Ships often have a significant heat demand, which is usually met with exhaust gas recovery supported by fuel or electric boilers. Baldi et al. [160] demonstrated the significance of the heat demand in passenger ships, which can be over 25% of the total yearly energy demand. The exhaust streams of SOFCs contain much heat. Moreover, the waste heat recovery from conventional diesel generators is limited by a minimum exhaust gas temperature. The exhaust gas of sulphur-containing fuels should not be cooled below 150 °C, because the formation of sulphuric acid would corrode the exhaust system [300]. This means significant heat is present in the emitted exhaust gas. All in all, applying SOFC systems to ships fuelled with a sulphur-free fuel has the potential for high heat recovery. However, the heat integration is barely covered in studies into marine SOFC power plants [27].

4.1.2. Cathode off-gas recirculation

Cathode recirculation can be used to increase the heat efficiency of SOFC systems. Mehr et al. [301] and Chen et al. [302] proposed cathode off-gas recirculation (COGR) to preheat the inlet air of the SOFC, thus increasing the heat efficiency. Liso et al. [53] mentioned that the recycle loop reduces the primary airflow and thus reduces the air preheater dimensions. Air blowers can be used to recirculate the air and overcome the pressure loss of the SOFC [303]. However, the use of a high-temperature air blower introduces design challenges [30], and are not commercially available at operational temperatures above 300 °C [66]. Nevertheless, Tomberg et al. [304] recently demonstrated successful operation of a high-temperature blower in an anode recirculation configuration. Wang et al. [97] applied a low-temperature cathode recirculation loop to avoid the HT-COGR challenges, but cooling and reheating add to the thermal losses and system size. Alternatively, ejectors can recirculate the cathode off-gas [302], but they are difficult to control [59]. In the system analyses of Kazempoor et al. [96] and Jia et al. [57], the lower primary airflow due to COGR increased the net electric efficiency due to a decrease in blower power, but no blower was used in the recirculation loop.

In this chapter, COGR is investigated to enhance the heat quality of the exhaust stream to improve the heat regeneration capacity for ship auxiliary systems. COGR reduces the primary airflow, which limits the amount of heat needed for air preheating and improves the air-fuel ratio in the combustor. This subsequently increases the temperature of the flue gas, which is beneficial for heat regeneration. Moreover, a smaller primary airflow is desirable in ships since it decreases the volume required for air and exhaust piping.

4.1.3. OBJECTIVE & OUTLINE

This study compares the performance of a marine SOFC power plant for methane, methanol, diesel, ammonia, and hydrogen in terms of electrical and thermal efficiency. COGR is investigated with the aim of increasing the amount and quality of heat regeneration. The main contributions are as follows:

1. One of the main novelties of this chapter is applying cathode off-gas recirculation to increase the heat recovery capacity in an application where heat can be used efficiently. The effects of COGR on oxygen utilisation and flue gas temperature are quantified. The study shows that COGR strongly increases the magnitude and quality of heat recovery and reduces the size of the air pre-heater. Evaluation of COGR for five different fuels showed that the benefits are the largest for methanol and hydrogen.

2. This chapter provides a systematical comparison of the conversion efficiency of an SOFC power plant for five alternative marine fuels. Comparing existing studies with different fuels was not sufficient, because the results of other studies depend much on the system architecture and operational parameters of the SOFC.

3. Suitable system architectures for a marine SOFC power plant are generated for different fuels, taking into account the reforming process and efficient heat regeneration.

4. The validation includes an extensive comparison of the present study with thermodynamic analyses of comparable systems. Besides validating the present study, this gives insight into what assumptions other researchers used and how it influenced their results.

The system designs for the selected fuels are described in Section 4.2. Potential fuels for marine SOFC systems have been selected in earlier research based on production capacity, stored energy density, technological readiness, safety, fuel cost, cost of the fuel storage system, and environmental impact [305]. Section 4.3 explains the thermodynamic modelling of the SOFC system. The results are presented in Section 4.4 with and without COGR. Verification and validation are provided in Section 4.5, by reflecting on the model limitations, analysing the model sensitivity, and comparing the results with comparable thermodynamic analyses. Conclusions are drawn in Section 4.6.

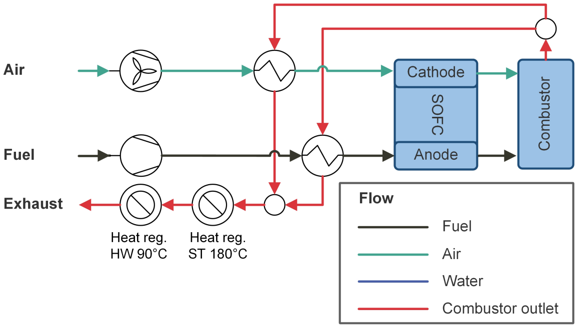

(a) Simple system layout.

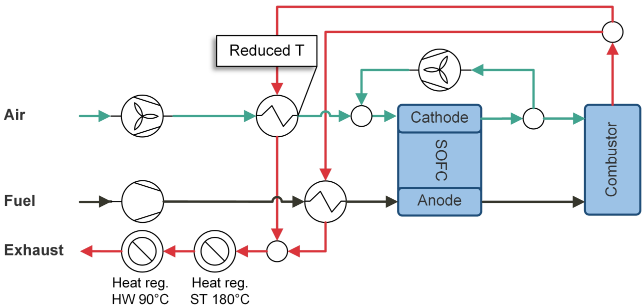

(b) System layout with cathode off-gas recirculation.

Figure 4.1: Reference SOFC systems.

4.2. DESCRIPTION OF SELECTED SOFC SYSTEMS

A general reference model is defined based on system configurations by Jia et al. [57], Kazempoor et al. [96], and Liso et al. [53], see Figure 4.1(a). The fuel is supplied by a pump, compressor, or blower and is preheated before entering the anode. Air is supplied with a blower and preheated. Co-flow planar SOFCs converts the fuel into power and flue gas. The anode and cathode outlets flow directly into a combustor. Its exhaust leads through the counterflow heat exchangers that preheat the fuel and air. The flue gas flow is split to make sure the fuel and air can both reach the required temperature at the SOFC inlets. This is especially relevant for the carbon fuels, because additional heat is required at the fuel side, since steam is necessary to prevent carbon deposition and additional heat is needed for the reforming process. Finally, the remaining heat is recovered from the exhaust stream to the saturated steam net (180 °C at 9 bar) and the hot water net (90 °C at ambient pressure). These are common temperatures and pressures for ship applications [300, 306]. Additional components for the specific fuels (e.g., evaporators, reformers, and heat exchangers) are added in the order of required heat quality. For the COGR configuration, a variable air blower is used in the recirculation loop to control the recirculation ratio, see Figure 4.1(b).

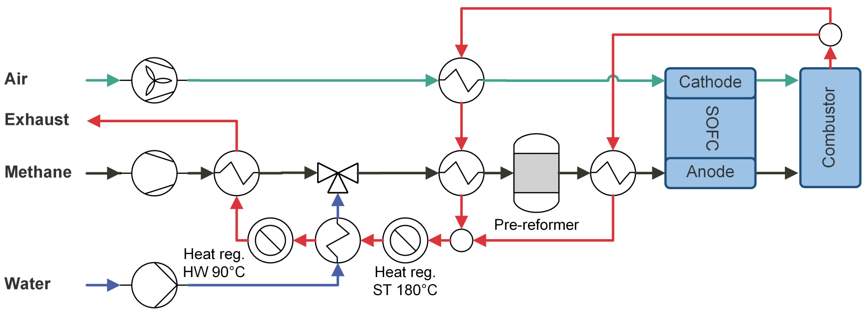

(a) Methane-fuelled SOFC system.

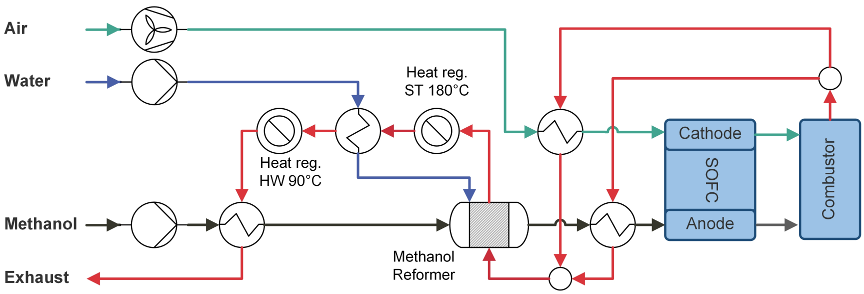

(b) Methanol-fuelled SOFC system.

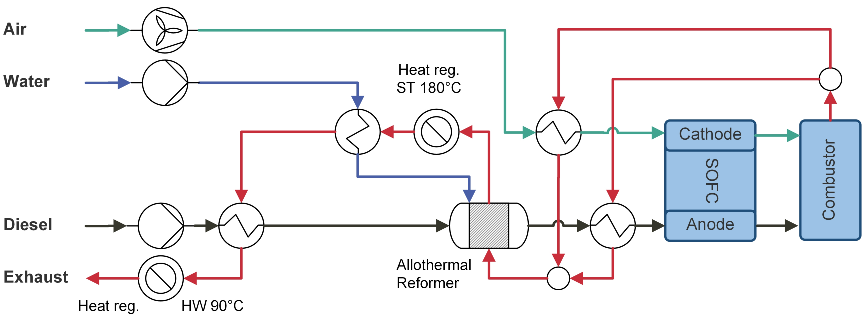

(c) Diesel-fuelled SOFC system.

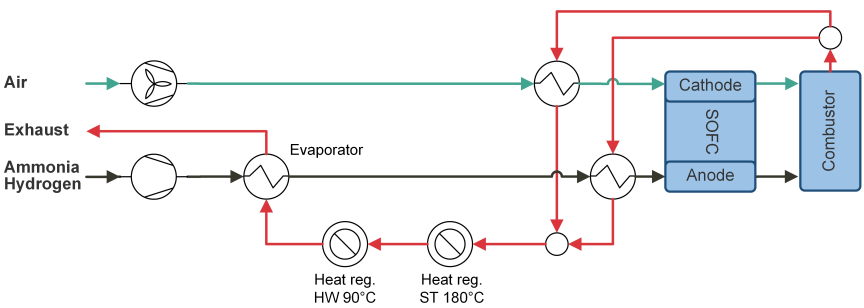

(d) Ammonia-fuelled SOFC system and hydrogen-fuelled SOFC system.

Figure 4.2: SOFC system layout of SOFC for various fuels.

4.2.1. METHANE SYSTEM

The methane system layout is very similar to the configuration presented by Jia et al. [57], see Figure 4.2(a). Methane steam reforming and the water gas shift (WGS) reaction convert part of the methane to a hydrogen-rich gas (Equations 4.1 and 4.2). An adiabatic pre-reformer is applied to reduce stress on the fuel catalyst in the SOFC. The pre-reform ratio is defined in Equation 4.3 [72]. Much internal reforming results in a higher net electric efficiency since less blower power is required for air cooling. For this reason, the minimum pre-reform ratio as stated by the SOFC supplier is used, which is 20%. The anode supply contains CH_4, H_2O, H_2, CO, and CO_2. Water is required for the reforming, which is heated and added as steam. A constant steam to carbon ratio (S/C) of 2.3 is used to prevent carbon deposition.

4

$$CH_4 + H_2O \rightleftharpoons CO + 3H_2 \tag{4.1}$$

$$CO + H_2O \rightleftharpoons H_2 + CO_2 \tag{4.2}$$

$$a_{PR} = 1 - \frac{(\chi_{CH_4} \cdot \dot{M})^{out}_{reformer}}{(\chi_{CH_4} \cdot \dot{M})^{in}_{reformer}} \tag{4.3}$$

where χ is the molar fraction and $\dot{M}$ the molar flow rate. An additional heat exchanger is added to the exhaust stream after the reformer, because the adiabatic pre-reformer reduces the fuel temperature. The exhaust stream is also used to generate the required steam. Since the fuel is usually stored cryogenically at -162 °C, remaining heat in the exhaust stream is used to evaporate and preheat the fuel.

4.2.2. METHANOL SYSTEM

Methanol is stored as a liquid at ambient temperature, so the methanol is supplied with a pump and evaporated by using heat of the exhaust stream, see Figure 4.2(b). Xu and Ni [109] positively evaluated direct feed of methanol to SOFC, however, it is often concluded that extremely high temperatures are necessary for adequate methanol conversion [107, 307]. In order to use comparable operational conditions to the other fuels, the methanol is decomposed in an external reformer (Equations 4.4 and 4.2), similar to the configuration by Cocco and Tola [105]. It is assumed that the gaseous methanol is fully converted to H_2, H_2, CO, and CO_2. After the exhaust stream of the combustor preheats the fuel and air, heat is fed into the methanol reformer. Subsequently, heat is used for steam generation, hot water generation and finally to evaporate the methanol. The generated steam is fed to the methanol reformer.

$$CH_3OH \rightleftharpoons H_2 + CO \tag{4.4}$$

4.2.3. DIESEL SYSTEM

A diesel pump feeds preheated diesel into an allothermal reformer, see Figure 4.2(c). Although, autothermal reformers are often considered in combination with SOFCs for being relatively compact in terms of size and weight, higher electric efficiencies can be reached with an allothermal reformer [308, 309]. In this reformer, the diesel is converted to a hydrogen-rich gas with steam reforming (Equation 4.5) and WGS reaction. Similar to the methanol model, steam and exhaust heat are fed to the reactor.

$$C_nH_m + nH_2O \rightarrow (n + \frac{m}{2})H_2 + nCO \tag{4.5}$$

4.2.4. AMMONIA SYSTEM

The ammonia layout is based on the configurations of Farhad and Hamdullahpur [310] and Barelli et al. [121] and is shown in Figure 4.2(d). The ammonia is evaporated, preheated and fed directly into the SOFC stack, where the ammonia is internally cracked (Equation 4.6). Direct feed of ammonia is mostly assessed at single cell level [255, 311, 312], but recently Barelli et al. [121] showed with stack experiments that external ammonia decomposition has a minimum influence on electric efficiency and is disadvantageous for the system size. They concluded that internal cracking is a feasible solution. All ammonia is converted because the operational temperature of the SOFCs is above 590 °C, the temperature of complete conversion [103]. Since ammonia is stored as a liquid at -33 °C, remaining heat is used to evaporate and heat up the fuel.

4

$$2NH_3 \rightleftharpoons N_2 + 3H_2 \tag{4.6}$$

4.2.5. HYDROGEN SYSTEM

The hydrogen system is similar to the basic system layout of Peters et al. [62]. The difference is that their configuration preheats the fuel with the anode off-gas instead of the flue gas, as was done by Sadeghi et al. [313]. Naturally, hydrogen is fed directly to the SOFC, see also Figure 4.2(d). Similar to the ammonia system, remaining heat is used to evaporate and preheat the fuel from its liquid storage temperature (-253 °C).

4.3. METHODOLOGY

A flow-sheet software (Cycle-Tempo) is used for thermodynamic analysis of the fuel cell systems. Cycle-Tempo contains models for the relevant system components, such as pump, compressor, evaporator, reformer, fuel cell, combustor, and heat exchanger. Together, these components form a system matrix of mass and energy equations, which is used to calculate the mass flow, pressure, temperature and composition in all components. The ideal gas law and no losses in piping are assumed. The used parameters for the thermodynamic simulation are shown in Table 4.1.

4.3.1. SOFC MODEL

The fuel cell and combustor use a Gibbs free energy minimisation routine to calculate the chemical equilibrium composition. In the SOFC model, the equilibrium compositions of the inlet gasses determine the electrical current and electrical power output, for which the internal temperature and pressures are assumed constant. Next, the required fuel flow for this current is calculated with the following equation [314]:

Table 4.1: Used parameters for thermodynamic analysis.

General	**Symbol**	**Value**	**Unit**
Environment temperature	p_{amb}	25	°C
Environment pressure	T_{amb}	1.013	bar
SOFC			
Temperature both inlets	T_{SOFC}^{in}	680	°C
Temperature both outlets	T_{SOFC}^{out}	760	°C
Average cell temperature	T_{CELL}	720	°C
Pressure difference anode	Δp_{anode}	0.02	bar
Pressure difference cathode	$\Delta p_{cathode}$	0.015	bar
Nominal fuel utilisation	U_f	80%	-
Nominal cell voltage	V	0.8	V
Heat dissipation	Φ_{SOFC}	1.5	kW
DC-AC conversion	$\eta_{DC\|AC}$	0.96	-
Nominal AC power output	$P_{SOFC,AC}$	100	kW
Equipment			
Pressure loss across equipment	Δp	0.01	bar
Isentropic compressor efficiency	$\eta_{is,comp}$	0.7	-
Mechanical compressor efficiency	$\eta_{m,comp}$	0.8	-
Isentropic pump efficiency	$\eta_{is,pump}$	0.85	-
Mechanical pump efficiency	$\eta_{m,pump}$	0.6	-
Methane system			
Storage temperature	$T_{storage}$	-162	°C
Pre-reform ratio	a_{PR}	0.2	-
Steam reforming temperature	T_{reform}	725	°C
Steam to carbon ratio	S/C	2.3	-
Methanol system			
Reformer outlet temperature	T_{reform}^{out}	500	°C
Diesel system			
Reforming temperature	T_{reform}	540	°C
Ammonia system			
Storage temperature	$T_{storage}$	-33	°C
Hydrogen system			
Storage temperature	$T_{storage}$	-253	°C

$$m_{an}^{in} = \frac{I \cdot M_{an}}{2F\left(y_{H_2}^{in} + y_{CO}^{in} + 4y_{CH_4}^{in}\right)U_F} \tag{4.7}$$

where m_{an}^{in} is the mass flow of the anode inlet, M_{an} is the molar mass of the anode gas, F is the Faraday constant and y_j^{in} the molar concentration of species j at the anode inlet, and U_F the fuel utilisation. A 1D model is used to calculate the current density, voltage and electrical power. This imposes the assumption that temperature, pressure and gas composition are constant over the cross-section perpendicular to the fuel flow. Higher dimension models are more accurate, but they strongly increase the computational time and are most relevant for estimating the dynamic response of SOFCs [270]. Since this research focuses on steady-state operation, a 1D model is sufficient. The particle concentration, reversible voltage, and current density are calculated through the fuel cell stack as a function of position x. The reversible voltage at x is calculated with the Nernst equation [314]:

4

$$V_{rev,x} = V_{rev,0} + \frac{RT}{2F}\ln\left(\frac{\sqrt{y_{O_2,ca}} \cdot y_{H_2,an}}{y_{H_2O,an}} \cdot \sqrt{p_{cell}}\right) \tag{4.8}$$

where $V_{rev,0}$ is the standard reversible voltage, R the universal gas constant, T the temperature, and p_{cell} the cell pressure. The model assumes no voltage losses at the electrode in x direction, resulting in the following current density at x:

$$i_x = \frac{\Delta V_x}{R_{eq}} = \frac{V_{rev,x} - V}{R_{eq}} \tag{4.9}$$

with R_{eq} being the equivalent cell resistance. The current density depends on the fuel utilisation at position x, which is maximum at the inlet and zero at the outlet. The average current in the stack is shown in Equation 4.10 [314]. The average current results from the integration of the local current densities over the dimensionless reaction coordinates λ, which represents the part of the fuel that already has been electrochemically converted.

$$I_{cell} = \frac{U_F \cdot V_{cell} \cdot A_{cell}}{R_{eq}\int_0^{U_F} d\lambda / \left(V_{rev,x} - V\right)} \tag{4.10}$$

where A_{cell} represents the cell area. Following, the power is directly calculated from the current and voltage. From the required electrical power and electrochemical balance, the required fuel flow is determined. The oxygen mass flow from the cathode to the anode is calculated using the determined current. Since the nominal inlet and outlet temperatures were defined, the flow through the cathode depends on the oxygen required for the reaction or the required cooling in the stack. The required cooling was in every case the determining factor for the cathode airflow.

Although SOFC stacks are well-insulated, some heat will dissipate into the environment. A constant heat dissipation Φ_{SOFC} of 1.5 kW is assumed, which resulted from steady-state testing. This assumption can be justified because the stack temperature is kept constant in all simulations in this research, as was done by Liso et al. [53].

4.3.2. BALANCE OF PLANT COMPONENTS

It is assumed that the combustor converts all in-flowing combustible gases [36]:

$$\begin{aligned}&\alpha H_2 + \beta CH_4 + \gamma CO + \left(\frac{\alpha}{2} + 2\beta + \frac{\gamma}{2}\right) O_2 \rightarrow \\ &(\alpha + 2\beta) H_2O + (\beta + \gamma) CO_2\end{aligned} \tag{4.11}$$

For compressors and pumps, the isentropic efficiency is used to estimate the actual power required for the pressure increase, compared with the amount of power required for ideal compression [315].The isentropic and mechanical efficiency are assumed constant (see Table 4.1), and the values are based on literature with similar rated power [36, 66]. The required power is calculated with Equation 4.12 [36].

$$P_{comp/pump} = \dot{m} \frac{h_{out,is} - h_{in}}{\eta_m \cdot \eta_{is}} \tag{4.12}$$

where $h_{out,is}$ represents the enthalpy after isentropic pressure increase, η_m the mechanical efficiency of the equipment, and η_{is} the isentropic efficiency of the equipment.

4.3.3. CATHODE RECIRCULATION SYSTEM

For the SOFC systems with COGR, the recirculation ratio (RR) is defined as the mass flow in the circulation loop divided by the cathode outlet mass flow, see Equation 4.13.

$$RR = \frac{\dot{m}_{recycle}}{\dot{m}_{ca}^{out}} \tag{4.13}$$

The recirculation rate affects the overall oxygen utilisation in the SOFC system, which in this research, excludes the combustion process:

$$(U_O)_{overall} = 1 - \frac{(\chi_{O_2} \cdot \dot{M})^{in}_{combustor}}{(\chi_{O_2} \cdot \dot{M})^{in}_{airblower}} \tag{4.14}$$

where χ is the molar fraction and $\dot{M}$ the molar flow rate. Peters et al. [65] consider oxygen utilisation above 50% to be infeasible, because a high oxygen utilisation reduces the equilibrium potential due to a lower molar oxygen concentration, see Equation 4.8. Ni et al. [316] mentioned 20% as a suitable oxygen utilisation. In this study, the recirculation is set such that the temperature after the combustor does not exceed 900 °C. This limit is used to enable the use of gas-to-gas metal heat exchangers for air and fuel pre-heaters [317], and was also applied by Cinti et al. [122] and Liso et al. [53].

4.3.4. SYSTEM PERFORMANCE

After subtracting the parasitic electrical power losses and converting DC to AC power, the net electrical efficiency of the SOFC system is based on the lower heating value [301]:

$$\eta_{net,AC} = \frac{\eta_{DC|AC} P_{SOFC,DC} - P_{aux}}{\dot{m}_{f,in} \cdot LHV_f} \tag{4.15}$$

where $\eta_{DC|AC}$ represents the electrical conversion efficiency from direct current to alternating current, $P_{SOFC,DC}$ the electrical power generated by the fuel cells, P_{aux} the parasitic power of pumps, blowers and compressors, $\dot{m}_{f,in}$ the mass flow of the dedicated fuel f, and LHV_f the lower heating value of fuel f.

Remaining heat in the exhaust stream is recovered for the hot water (HW) and saturated steam (ST) network with a pinch point temperature of 10 °C. Subsequently, for the saturated steam network, heat is subtracted from the exhaust stream up to 190 °C. For the hot water network, heat is subtracted from the exhaust stream up to 100 °C. The amount of regenerated heat for hot water and saturated steam determines the heat efficiency:

$$\eta_{heat} = \frac{\dot{Q}_{HW} + \dot{Q}_{ST}}{\dot{m}_{f,in} \cdot LHV_f} \tag{4.16}$$

with $\dot{Q}$ being the heat flow that is recovered from the exhaust stream. Heat exchangers are usually bulky and expensive equipment and their size and cost strongly depend on the required heat transmission [53]. Deviations in mass flow influence the amount of transferred heat. Moreover, a higher flue gas temperature positively influences the heat transfer rate. The differences in heat exchanger size for the different fuels and for employing COGR are taken into account in the performance evaluation. The increase in heat exchanger surface area is estimated with the often used LMTD method, see Equations 4.17 and 4.18 [318]. This method assumes no heat loss to the surroundings, steady flow conditions, constant specific heat, and constant overall heat transfer coefficient.

$$A_S[\%] = \frac{\left(\dot{Q}/LMTD\right)_{COGR}}{\left(\dot{Q}/LMTD\right)_{no\,COGR}} \tag{4.17}$$

$$LMTD = \frac{\Delta T_1 - \Delta T_2}{\ln \Delta T_1/\Delta T_2} \tag{4.18}$$

4.4. RESULTS

The results are generated by simulating the presented model with the parameters stated in Table 4.2. The main results regarding the electrical and heat efficiency for the considered fuels without COGR are presented in Figure 4.3(a) and with COGR in Figure 4.3(b). The results without COGR will be discussed in Sections 4.4.1 and 4.4.2 and the effect of COGR will be discussed in Section 4.4.3.

4.4.1. ELECTRICAL AND HEAT EFFICIENCY

Figure 4.3(a) compares the net electrical efficiency, thermal efficiency, and delivered AC power for the different SOFC systems. Methane, diesel, and ammonia resulted in high electrical efficiency. The electrical efficiency for methanol and hydrogen was much lower.

In the presented model, the heat efficiency is defined by the amount of heat that was regenerated for hot water and saturated steam purposes. Subsequently, the heat efficiency depends on the temperature and mass flow of the flue gas and the heat extraction by other components. The diesel-fuelled SOFC system had the lowest heat efficiency.

4

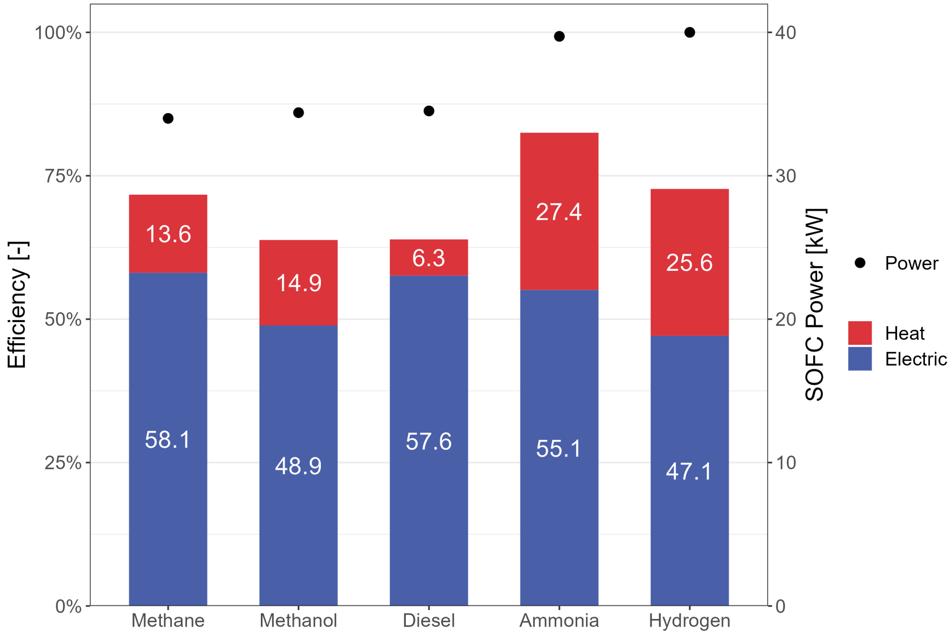

(a) Without COGR

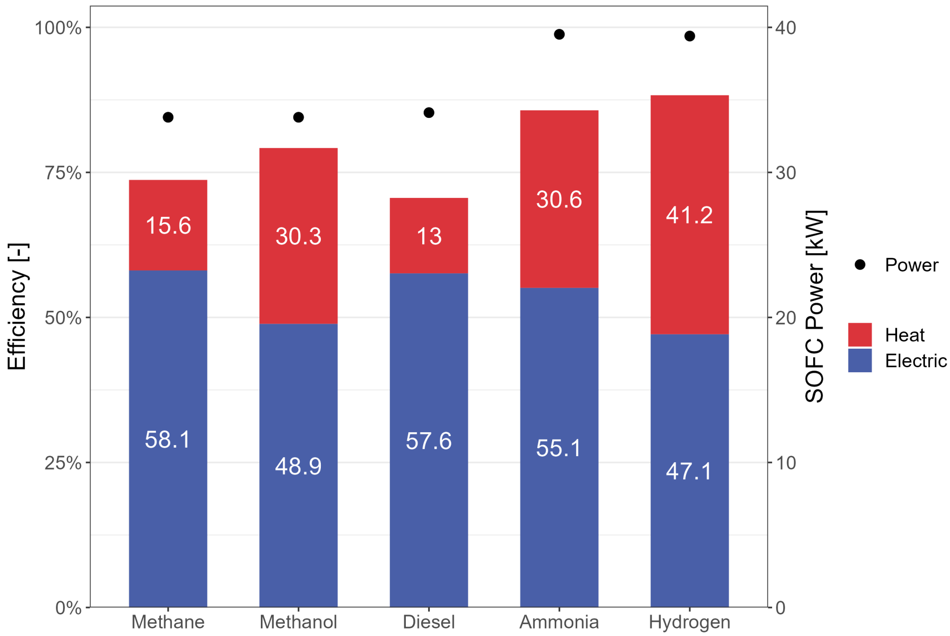

(b) With COGR

Figure 4.3: Net electrical efficiency, heat efficiency and delivered SOFC power for the five selected fuels. Data is generated at nominal operation ($V = 0.8V$ and $U_F = 80\%$).

Table 4.2: Used parameters for simulations of all fuels.

Simulation	Fuel utilisation	Cell voltage	RR
	-	V	-
Nominal	80%	0.8	-
Operating range	70% - 85% $\Delta = 1\%$	0.6 - 0.85 $\Delta = 0.01$	-
COGR	80%	0.8	0 - 0.77 $\Delta = 0.002$

This can be explained by a high heat consumption by the diesel reforming process. Ammonia resulted in the highest heat efficiency, because the ammonia is cracked internally. Moreover, the relatively small airflow resulted in high flue gas temperatures. It must be noted that not all supplied heat was of the same quality. Although hydrogen resulted in high heat efficiency, the temperature of the exhaust stream after fuel and air pre-heating was not sufficient to produce saturated steam.

For the carbon-containing fuels (methane, methanol, and diesel), the power density and thus delivered power was lower than for hydrogen and ammonia, which is illustrated with the yellow line in Figure 4.3(a). Since the equivalent cell resistance, temperature, and cell pressure were assumed constant, the differences in power density can be explained by differences in species concentrations through the cell, influencing the reversible voltage, see Equations 4.8 and 4.9. Although the methane-fuelled system resulted in the highest electrical efficiency, the delivered power was 15% lower than when fuelled with ammonia or hydrogen. This implies more modules would need to be installed to deliver the same power.

4.4.2. OXYGEN UTILISATION AND BLOWER LOSSES

SOFCs are cooled with cathode air. The temperature difference between the cathode inlet and outlet was limited to 80 °C to prevent stress from large thermal gradients. Consequently, the required cooling determined the airflow and thus, the oxygen utilisation, which was generally much larger than the stoichiometric requirements. Large differences were found in the oxygen utilisation and required airflow for the different fuels. This can be explained by heat release differences in the electrochemical and reform reactions in the SOFC for the different fuels. Since the air blower was amply the largest contributor to the parasitic power consumption, oxygen utilisation had a significant impact on the net electrical efficiency. Figure 4.4 shows the net electrical efficiency and the used air blower power over the delivered SOFC power, both as a function of oxygen utilisation. The oxygen utilisation reached fairly low values down to 5%, especially for methanol and hydrogen. For low oxygen utilisation, a large share of the generated power was demanded by the blower, which reduced the net electrical efficiency.

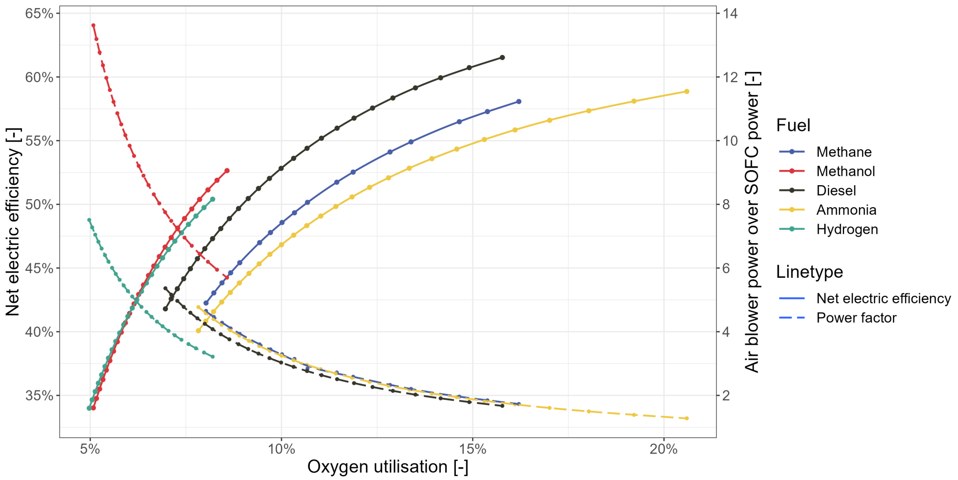

Figure 4.4: Net electrical efficiencies and compressor power divided by delivered AC SOFC power, both plotted as function of the oxygen utilisation for the five selected fuels. Data is generated at $V = 0.6 - 0.85V$ and $U_F =$ 80%.

4.4.3. EFFECT OF CATHODE OFF-GAS RECIRCULATION

Cathode off-gas recirculation is employed to improve the heat regeneration from the exhaust stream. This section investigates the impact of the amount of recirculated air and evaluates the SOFC system with and without COGR.

VARYING THE RECIRCULATION RATIO

Figure 4.5(a) shows the impact of the recirculation ratio (RR) on the overall oxygen utilisation. As was expected, a high recirculation rate strongly increased the overall oxygen utilisation. For the methane, ammonia, and diesel system, the overall oxygen utilisation became particularly high (over 30%) when using recirculation ratios of 0.5 or higher.

Cathode recirculation has additional advantages for the SOFC system. Reducing the primary airflow lowers the required heat transfer in the air pre-heater. The transmitted heat in the air pre-heater exceeded the other heat exchangers by a factor of ten for the considered systems. Consequently, the air pre-heater was the largest and costliest heat exchanger in the system design. The striped lines in Figure 4.5(a) show that the required heat transfer in this heat exchanger decreased linearly for an increasing cathode recirculation ratio. Large reductions in the required heat transfer were found, especially for the hydrogen and methanol system.

The striped lines in Figure 4.5(b) show that a higher recirculation ratio increased the temperature in the exhaust stream. This increased the heat transfer potential for heat recovery. Despite the decrease in flow rate of the flue gas this positively affected the heat efficiency for all different fuels, which is shown with the solid line in Figure 4.5(b).

WITH OR WITHOUT COGR

Table 4.3 shows the recirculation rates when the the temperature in the exhaust stream is kept under 900 °C. Although the recirculation ratio varied much per fuel, the 900 °C

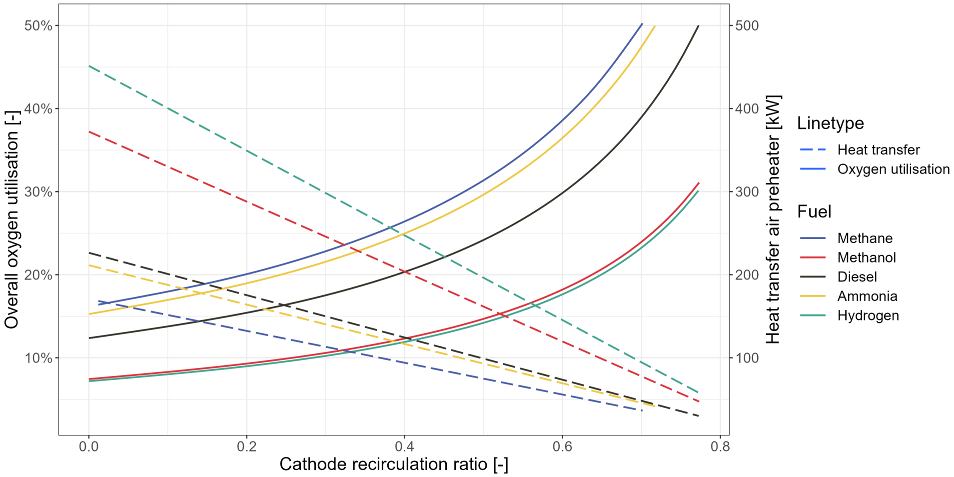

(a) Effect of RR on overall oxygen utilisation and heat transfer in air pre-heater. The oxygen utilisation does not include the consumed oxygen in the combustion process. A higher cathode recirculation, reduces the overall oxygen utilisation, which is accompanied by a lower primary airflow, and ultimately decreases the heat transfer in the air pre-heater.

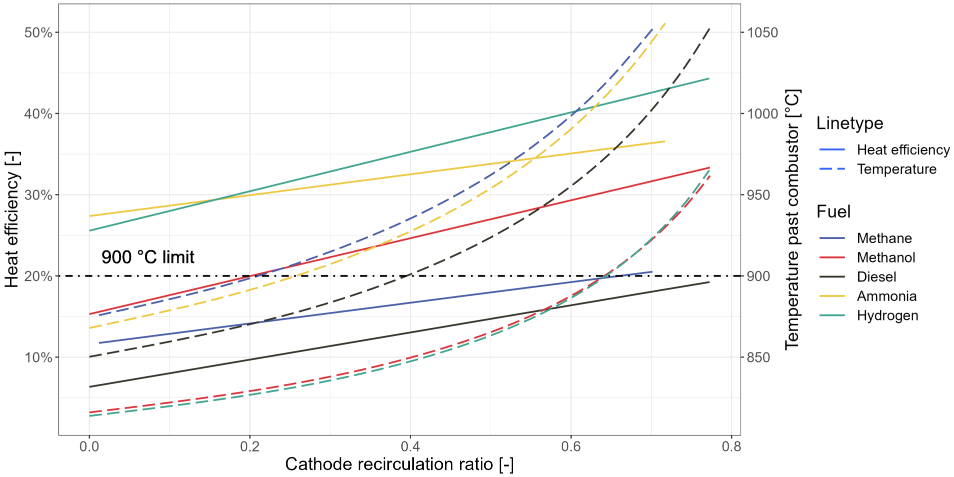

(b) Effect of RR on heat efficiency and flue gas temperature past the combustor. A higher cathode recirculation rate decreases the primary airflow, which increases the flue gas temperature. This ultimately leads to a higher heat efficiency, because more heat can be recovered from the flue gas.

Figure 4.5: Impact of cathode off-gas recirculation ratio for different fuels at a cell voltage of 0.8 V, 80% fuel utilisation, and oxygen utilisation up to 50%.

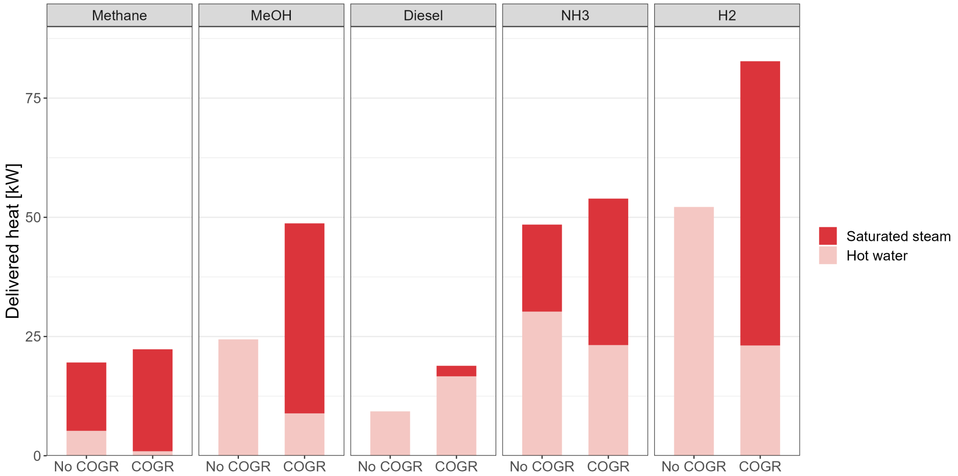

Figure 4.6: Delivered heat to hot water and steam net for original systems and systems including cathode of gas recirculation (COGR). Data is generated at nominal operation ($V = 0.8V$ and $U_F = 0.8$).

limit resulted for all fuels in an overall oxygen utilisation of around 20%.

Figure 4.3(b) shows the net electric efficiency, thermal efficiency, and delivered AC power for the different SOFC systems when COGR is applied with the exhaust temperature limit. Comparing Figure 4.3(a) and Figure 4.3(b) shows that employing COGR increased the heat efficiency by 11.9 to 105.0% for the different fuels. The large increase in thermal efficiency for methanol and hydrogen can be explained by a large increase in oxygen utilisation, which reduced the amount of preheated air. Table 4.3 displays a 2.7 times increase in oxygen utilisation in the system for methanol and hydrogen, for the other fuels this factor is just 1.2 to 1.6. Besides the increase in thermal efficiency, an improvement in the heat regeneration quality of the exhaust stream can be observed in Figure 4.6. For the methanol and hydrogen system without COGR, the quality of the remaining heat after fuel and air preheating was not sufficient to generate any saturated steam. COGR strongly increased the amount of available heat for saturated steam purposes due to a higher flue gas temperature after heat subtraction for fuel and air, especially for the methanol and hydrogen system. A large take-off capacity for saturated steam (dark red in graph) is beneficial, since a surplus of heat can be bypassed and used for the hot water demand, but not vice versa.

The differences in net electric efficiency were minor. The power used by the air blower for the systems without COGR was approximately equal to the used power by the combined primary air blower and the recirculation blower. Moreover, a change in the single-pass oxygen utilisation in the stack only leads to small deviations in the stack's current density. All in all, the addition of COGR resulted in an increase in the total efficiency of 2.7% to 25.1% for the different fuels.

Table 4.4 shows the accomplished decrease in primary airflow and transmitted heat in the air pre-heater for COGR using the 900°C flue gas limit. Moreover, the increase in flue gas temperature positively influenced the heat transfer rate in the air pre-heater.

Table 4.3: Influence of cathode off-gas recirculation on oxygen utilisation and system performance for different fuels at a cell voltage of 0.8 V and 80% fuel utilisation. The recirculating rate is maximised towards an upper limit by introducing a maximum flue gas temperature of 900 °C.

	No COGR	With COGR			Difference			
Fuel	U_O	**RR**	**SP** U_O	**OA** U_O	U_O	**Elec. eff.**	**Heat eff.**	**Total eff.**
Methane	16.2%	19.6%	16.7%	20.0%	1.2x	-0.1%	+14.9%	+2.7%
Methanol	7.5%	64.3%	8.3%	20.3%	2.7x	+1.2%	+103.3%	+25.1%
Diesel	12.4%	39.8%	13.3%	20.3%	1.6x	-0.3%	+106.4%	+10.2%
Ammonia	15.4%	26.7%	16.0%	20.3%	1.3x	-0.1%	+11.9%	+3.9%
Hydrogen	7.2%	64.2%	8.0%	19.6%	2.7x	-0.8%	+61.0%	+21.0%

Table 4.4: Airflow and heat transfer for air pre-heater for SOFC system without and with COGR for different fuels, at a cell voltage of 0.8 V and 80% fuel utilisation. Difference in surface area is estimated with LMTD method.

	Without COGR	With COGR	Difference			
Fuel	**Heat transfer** kW	**Heat transfer** kW	**Airflow** -	**Heat transfer** -	**LMTD** -	**Surface area** -
Methane	171	133	-19.1%	-21.9%	+22.1%	-36.1%
Methanol	373	101	-64.0%	-72.8%	+170.8%	-90.0%
Diesel	227	125	-39.3%	-44.9%	+62.0%	-66.0%
Ammonia	211	151	-25.2%	-28.5%	+32.0%	-45.8%
Hydrogen	451	124	-63.7%	-72.6%	+175.1%	-90.0%

Employing COGR reduced the surface area of the heat exchanger by 36.1% to 90% for the various fuels. Consequently, COGR positively affected the size, weight, and cost of the SOFC system.

4.5. DISCUSSION

This section reflects some of the assumptions in the thermodynamic analysis and discusses why these were made. Furthermore, the model is verified and the results are validated with earlier research.

4.5.1. MODEL LIMITATIONS

During the thermodynamic modelling, several assumptions were made:

- The cell resistance R_{SOFC} is kept constant for different fuels, voltages and fuel utilisation values, because of the unavailability of experimental data for all considered fuels with the same cell architecture. This assumption only holds if the thermal balance in the stack does not change significantly. Although the temperatures of the inlets and outlets stay equal, it could be argued that internal reforming significantly influences the thermal balance in the stack. The kinetics of the electrochemical and reforming reaction are affected by the local temperature and partial pressure of reactants. However, as both reactions in turn affect the spatial distributions of temperature and partial pressures, they are strongly coupled [262].

Nevertheless, this assumption is necessary to fairly compare the performance of the SOFC system for the selected fuels.

- The SOFC model does not consider activation, ohmic, and concentration losses separately, but includes the losses as an average. Activation losses dominate at low current densities and concentration losses start to dominate at high current densities. However, it can be assumed that the presented average loss characteristic is still representative since the SOFC operates in the ohmic region of the polarisation curve for the used input ranges of voltage (0.6 - 0.85 V) and fuel utilisation (70% - 85%).

- Although the SOFC is operated at different voltages, the effectiveness deviations of the balance of plant components at different operational conditions are not included. For instance, air blowers operate at significantly lower efficiency below their operational speed. For most balance of plant components, this has a rather small influence on the net electric efficiency. However, Figure 4.4 shows that the contribution of the air blower to the net electric efficiency is significant. Nevertheless, several configurations and operational modes were investigated for the nominal operation of a marine SOFC system. Different system configurations would require different operational designs of the balance of plant components to ensure they operate as much as possible in their operational conditions. Consequently, this assumption holds for the steady-state operation in this research. When the research would be extended to part-load operation, it would be necessary to include the part-load efficiency of at least the air blower.

- Heat loss in piping and components besides the SOFC are neglected. This is a widely used assumption in SOFC system analyses [85, 319]. Although the system would be well insulated, in practice, some heat would still dissipate. [320] assumed fixed heat loss as a percentage of LHV for reformer, combustor, and piping, which was estimated at only 1.5%. Hollmann et al. [66] estimated significant heat losses by modelling all geometric and insulation properties in ANSYS. However, they argued that the high heat losses were caused by separate insulation of all components to ensure quick accessibility during testing and would be less significant in a commercial system.

- Pressure losses across all BOP components are simplified by assuming a constant pressure drop as was done by Liso et al. [53], which is well-accepted in thermodynamic analyses. An underestimation of the pressure drop across equipment could to an overestimation of the net electrical efficiency, because more parasitic power would be necessary for compressors or pumps. Some researchers formulate the pressure drop as function of the mass flow and a pressure drop correlation parameter [65, 79]. However, the influence on the net electric efficiency is minor and [75] even neglect pressure drop across equipment. The assumption that the pressure drop in piping is negligible is widely used [313] and is valid because the distance between all components is short [53].

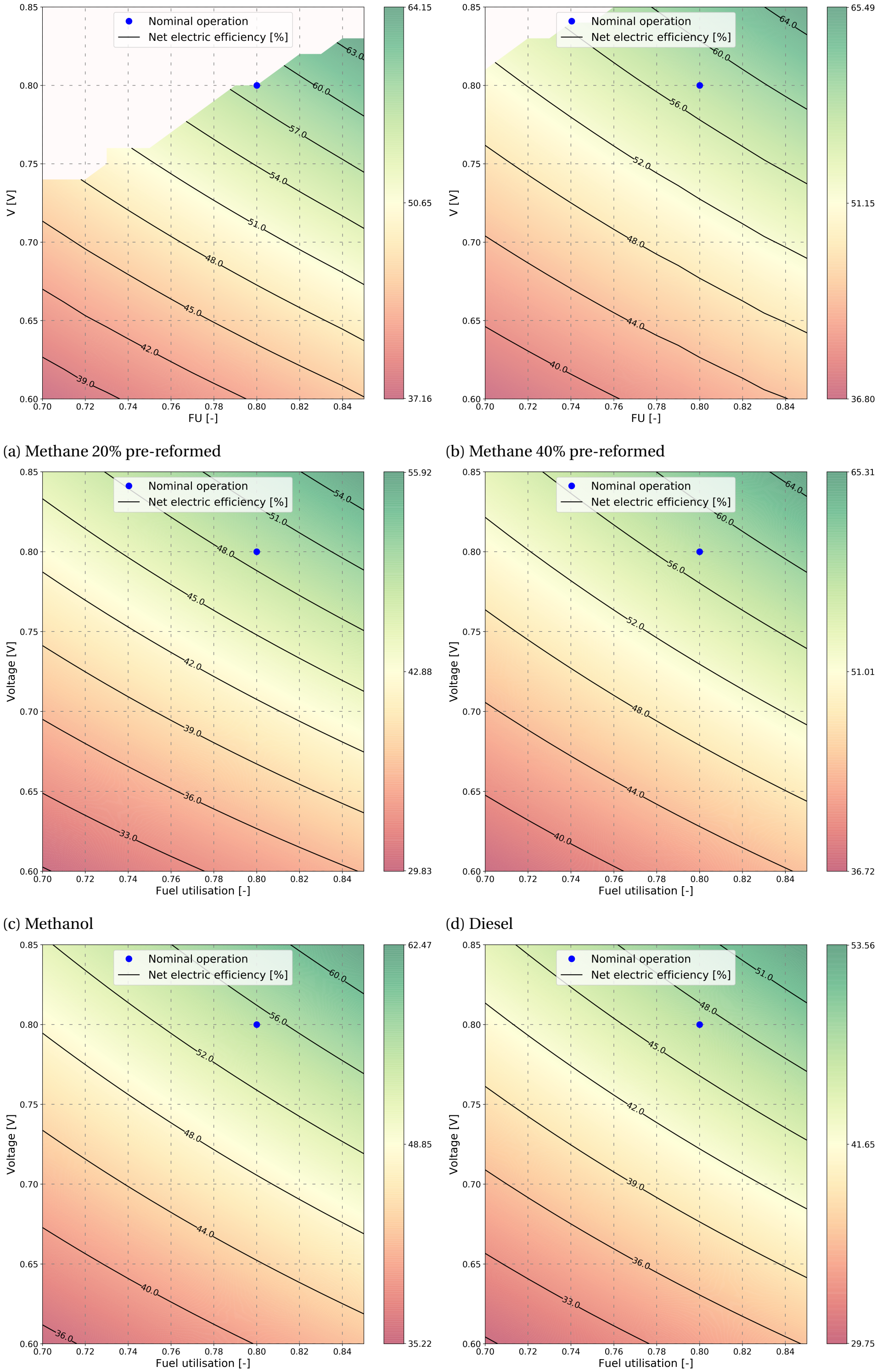

(a) Methane 20% pre-reformed

(b) Methane 40% pre-reformed

(c) Methanol

(d) Diesel

(e) Ammonia

(f) Hydrogen

Figure 4.7: Net electrical efficiency for systems without COGR at cell voltages of 0.6 - 0.85 V and fuel utilisation of 70 - 85%

4.5.2. MODEL VERIFICATION

A sensitivity analysis is performed for the operational conditions of the SOFC to verify whether the model behaves similar to a real SOFC system according to methods provided by Sargent [321]. The voltage and fuel utilisation are varied from 0.6 to 0.85 and 70% to 85%, respectively, see Figure 4.7. The results are in line with theory and other thermodynamic analyses for all modelled systems. The net electrical efficiency increases for higher fuel utilisation and voltages, within the operational constraints of the SOFCs. Naturally, the highest electrical efficiency is also accompanied by the lowest current density.

The net electrical efficiency of the SOFC system is approximately linear to the voltage as to the fuel utilisation, since the stated ranges are in the ohmic region of the polarisation curve of the SOFC. Apparently, the other components in the system do not influence the system efficiency sufficiently to deviate much from this linear SOFC relation, taking into account that part-load effectiveness of the balance of plant components is not included.

The sensitivity analysis showed that the methane-fuelled system was not feasible for higher voltages, see Figure 4.7(a). At higher voltages (i.e., lower current density), less heat is produced in the stack. Heat is required for the internal reforming of methane, and for high voltages, this results in a heat deficit in the SOFC. The pre-reform ratio could be increased to reduce the required heat in the stack and consequently improve the operational range of the stack. This is shown in Figure 4.7(b) for a pre-reform ratio of 40%. Although this results in a slight reduction in electrical efficiency and a significant reduction in heat efficiency at equal operational conditions, the operational range is widened. The small decrease in net electrical efficiency is the consequence of a decrease in the endothermic internal reforming, which increases the cooling requirement by the cathode air, subsequently increasing the parasitic power of the blower [53, 102]. For the other fuels, the SOFC system is feasible over the full considered operational range, see Figures 4.7(c) to 4.7(f).

4.5.3. RESULT VALIDATION

The results are validated by comparison with other research. Specifically, the net electrical efficiency, since the actual heat efficiency is not often stated and depends much on the defined temperature at which heat regeneration is deemed feasible. The net electric efficiencies are as much as possible compared with research using similar process design, plant size, and SOFC operating conditions. Although some significant discrepancies were found, they can all be explained by differences in operating parameters or model assumptions. The comparison is, without and with COGR, summarized in Tables 4.5 and 4.6, respectively. The main parameters that influence the net electrical efficiency are also listed in Appendix A, which are voltage, current density, fuel utilisation, stack temperature, blower efficiency, and inverter efficiency [102]. Moreover, the appendix shows which systems use anode off-gas recirculation (AOGR). AOGR is often proposed to increase the electrical efficiency and reduce the steam generator requirements, and can be used in combination with COGR [82].

Table 4.5: Comparison of SOFC system analyses without COGR. Only comparable studies are included, which means planar O^{2-} conducting SOFCs operated on atmospheric pressure. All efficiency data is based on LHV.

		SOFC operation		Performance
Fuel	**Reference**	**Voltage**	**Fuel utilisation**	**Net electric efficiency**
		V	-	-
Methane	Kazempoor et al. [96]	0.7	80%	49.5%
	Liso et al. [53]	?	80%	61.0%
	Jia et al. [57]	?	85%	41.0%
	Mehr et al. [301]	0.62	85%	41.8%
	Ahmadi et al. [322]	?	80%	47.8%
	This study	0.80	80%	58.1%
	This study	0.80	80%	57.7%
Methanol	Sangtongkitcharoen et al. [323]	0.62	80%	45.0%
	Cocco and Tola [105]	?	85%	50.0%
	Leone et al. [307]	?	80%	51.0%
	Rokni [324]	?	80%	51.9%
	This study	0.80	80%	48.9%
Diesel	Ezgi et al. [29]	0.80	90%	55.3%
	Nehter et al. [93]	0.75	73%	55.0%
	Huerta et al. [30]	0.75	85%	56.0%
	This study	0.80	80%	57.6%
Ammonia	Farhad and Hamdullahpur [310]	0.73	80%	41.0%
	Rokni [324]	?	80%	51.8%
	Cinti et al. [122]	?	80%	55.0%
	Barelli et al. [121]	0.78	80%	52.1%
	Selvam et al. [34]	0.855	80%	59.8%
	This study	0.80	80%	55.1%
Hydrogen	Kazempoor et al. [96]	0.78	80%	37.5%
	Botta et al. [325]	0.75	75%	40.0%
	Peters et al. [62]	0.86	80%	48.0%
	Sadeghi et al. [313]	0.85	85%	49.6%
	This study	0.80	80%	47.1%

Table 4.6: Comparison of SOFC system analyses with COGR. Only comparable studies are included, which means planar O^{2-} conducting SOFCs operated on atmospheric pressure. All efficiency data is based on LHV. For diesel and ammonia, no representative studies with COGR were found.

		SOFC operation				Performance
Fuel	**Reference**	**COGR type** -	**COG RR** -	**Voltage** V	**Fuel utilisation** -	**Net electric efficiency** -
Methane	Kazempoor et al. [96]	EJ	0.6	0.69	80%	53.7%
	Liso et al. [53]	EJ	0.75	0.80	80%	58.0%
	Jia et al. [57]	?	0.5	?	85%	51.0%
	Mehr et al. [301]	?	0.3	0.60	85%	40.2%
	Wang et al. [97]	BL	?	0.83	90%	65.9%
	This study	BL	0.2	0.80	80%	58.0%
Methanol	Wang et al. [97]	BL	?	0.83	90%	60.2%
	This study	BL	0.64	0.80	80%	49.5%
Hydrogen	Kazempoor et al. [96]	EJ	0.6	0.78	80%	40.3%
	Wang et al. [97]	BL	?	0.859	90%	58.3%
	This study	BL	0.64	0.80	80%	46.8%

COGR type: BL = Air recirculation with blower, EJ = Air recirculation with ejector.

METHANE

Liso et al. [53] studied natural gas-based combined heat and power (CHP) systems in various configurations. When using steam reforming and no recirculation streams, they found a net electrical efficiency of 61% for a pre-reform ratio of 40%. This is similar to the 58% electrical efficiency found in the present study for the same pre-reform ratio, see Figure 4.7(b). The stack temperature is also similar in both studies (750 °C and 720 °C). Other studies have also found various electrical efficiencies within the range of this study, which is 37% to 65% for voltages from 0.6 to 0.85 V. In a thermodynamic analysis for residential applications using 30% pre-reforming and 60% anode off-gas recycling, Kazempoor et al. [96] simulated a net electrical efficiency of 49.5% at 0.7 V and 80% fuel utilisation. Using direct internal reforming and no recirculation, Jia et al. [57] found 41% electrical efficiency at 85% fuel utilisation, but the operating voltage is not given. Without employing a pre-reformer, Mehr et al. [301] found a much lower electrical efficiency (exergy) of 41.8% at 85% fuel utilisation, but the fuel cell was operated at 0.62 V. Ahmadi et al. [322] simulated a CHP plant without a pre-reformer, operating at a lower temperature (640 °C) and 80% fuel utilisation, which resulted in a net electrical efficiency of 47.8%.

Opposed to this study, in the work of Liso et al. [53], Kazempoor et al. [96] and Jia et al. [57] the net electrical efficiency strongly improved when COGR was applied, which was a direct consequence of a smaller air blower power. However, in their studies, no blower was used in the recirculation loop, which explains the difference from the present study. Wang et al. [97] studied energy storage systems using reversible solid oxide cells using cathode off-gas recirculation. Their net electrical efficiency ranged from 60.2% to 62.4% for current densities of 4000 to 3000 A/m^2, which is slightly higher than 58.0% at 3465 A/m^2 in this study. This can be explained since the cathode is fed with pure oxygen, which results in a smaller airflow and thus a lower blower power.

METHANOL

Cocco and Tola [105] studied an SOFC-GT system fuelled by methanol. Although combined cycle systems often result in higher efficiencies, the SOFC efficiency was reported separately at 50%. This is similar to the nominal electrical efficiency found in the present study, which is 49%. Leone et al. [307] thermodynamically analysed a CHP SOFC plant, which also resulted in a very similar efficiency of 51% at 80% fuel utilisation. Wang et al. [97] have again reported higher efficiencies in the range of 54% to 64%, compared with 30% to 55% in the present study. Sangtongkitcharoen et al. [323] found a lower net electrical efficiency of 45% for a reformed methanol-fuelled SOFC at similar fuel utilisation and current density as the present study. This difference can be explained, since they operated the SOFCs on 0.62 V. Although Rokni [324] employed a methanator and anode off-gas recirculation with an RR of 3%, their net electrical efficiency (51.9%) was still very similar to the present study.

DIESEL

Most studies on diesel-fuelled SOFC systems report electric efficiencies similar to the present study (58%). Ezgi et al. [29] thermodynamically modelled an SOFC system for auxiliary power generation on a naval ship using autothermal reforming. They reported an electrical efficiency of 55.3% at the same voltage as our study (0.8 V) and a slightly higher operating temperature of 775 °C. The slightly lower electrical efficiency at even higher temperatures can be explained by the use of autothermal reforming. Nehter et al. [93] and Huerta et al. [30] both use steam reforming and anode off-gas recirculation, reporting efficiencies of 55% and 56% respectively at a slightly lower voltage of 0.75 V.

AMMONIA

Cinti et al. [122] studied an ammonia-fuelled system with internal cracking. At an operating temperature of 750 °C and fuel utilisation of 80%, they found net electric efficiency in the range of 38% to 67% depending on the power output. This is similar to the range found in the present study (35% to 62%) for similar operating conditions. Rokni [324] and Selvam et al. [34] Also found efficiencies in the same range. The results of Barelli et al. [121] were most in line with the present study, they found a net electrical efficiency of 52.1 % at a slightly lower voltage (0.78 V) compared with 55.1% at 0.8 V of the present study. Their model was also validated with short stack experiments. Farhad and Hamdullahpur [310] studied a portable power system with a similar process design as this study. They found an efficiency of 41 % at a voltage of 0.73 V and a fuel utilisation of 80%. Under the same conditions, the present study found an efficiency of around 50%, see Figure 4.7(e). In the study of Farhad and Hamdullahpur [310], 20% parasitic power take-off was assumed for the control system since it is only a small system (100W) and DC power is delivered. Together, this explains the 18% difference in net electrical efficiency compared with the present study. Wang et al. [97] used an external cracker and pure oxygen to feed the cathode, finding net electric efficiency in the range of 58.2% to 61.6% for current densities of 4000 to 3000 A/m^2. This again is significantly higher than 55.1% at 4075 A/m^2 of the present study.

Hydrogen

The present study found electrical efficiencies in the range of 30% to 53% for a fuel utilisation of 80% and a stack temperature of 720 °C, with a nominal efficiency of 47.1% at 0.8 V. Botta et al. [325] have found an energy efficiency of 40% at an average cell temperature of 850 °C but at a lower fuel utilisation of 75% and a voltage of 0.75 V. They did not use a combustor, but that should not affect the electrical efficiency as long as preheating needs are met by recuperation. Peters et al. [62] found a similar electrical efficiency of 48% at 80% fuel utilisation and a slightly higher voltage. The analysis of Sadeghi et al. [313] resulted in a slightly higher efficiency (49.6%), but they assumed a fuel utilisation of 85% and used no inverter. Wang et al. [97] again found higher net electric efficiencies in the range of 51% to 60% using pure oxygen instead of air.

4.6. Conclusion

This study compared the thermodynamic performance of a marine SOFC power plant for methane, methanol, diesel, ammonia, and hydrogen. A reference model was established, which was extended with the necessary components for the different fuels. Additionally, cathode off-gas recirculation (COGR) is investigated with the purpose of improving heat regeneration. The thermodynamic model is verified with a sensitivity analysis and validated by comparing the results with thermodynamic analyses of similar SOFC systems.

The difference in electrical and heat efficiency between the fuels was significant. At a cell voltage of 0.8V and a fuel utilisation of 80%, the highest net electrical efficiency (LHV) was found for methane (58.1%), followed by diesel (57.6%) and ammonia (55.1%). The air blower had a major influence on the net electrical efficiency, especially for low oxygen utilisation. The carbon fuels (methane, methanol, and diesel) resulted in a 15% lower power density, compared with ammonia and hydrogen. The highest heat efficiency was found for ammonia (27.4%), followed by hydrogen (25.6%). For both the methane and ammonia system, the heat quality in the exhaust was sufficient for the generation of hot water and saturated steam. Practically, this saves additional fuel or electricity for boilers.

Without COGR, the heat quality was insufficient to generate saturated steam for methanol, diesel, and hydrogen. COGR was used to increase the oxygen utilisation and thus increase the temperature in the exhaust stream. Increasing the recirculation ratio improved the heat efficiency and reduced the required heat transfer in the air pre-heater. Comparing the systems without and with COGR resulted in similar net electrical efficiencies, but the systems with COGR demonstrated a large increase in the quantity and quality of the heat efficiency. This resulted in an increase in the heat efficiency of 11.9% to 105.0% for the different fuels. A smaller primary airflow also resulted in a decrease of heat transfer in the air pre-heater of 21.9% to 72.6%, reducing the size, weight, and cost of this heat exchanger.

Further research will be needed to tackle the design problems of a high-temperature cathode recirculation loop, for which low-temperature COGR or specialised high-temperature blowers are possible strategies. Nevertheless, COGR offers a promising method to increase heat recovery, improving the total efficiency of the power plant. The results of this study can be used to evaluate the fuel choice of a marine SOFC power plant and to improve heat recovery, with the overarching goal to reduce ship emissions.

5

SCALING OF SOFC SYSTEMS TO HIGH RATED POWER

The best way to predict the future is to design it.

Buckminster Fuller

This chapter has been published in the conference proceedings of the International Marine Conference 2023. [326].

5.1. INTRODUCTION

Many ship integration studies consider SOFC systems for small auxiliary power units [30, 32], while very few studies consider an SOFC system that takes the largest share of the onboard energy conversion [27]. Nevertheless, multi-MW SOFC systems could offer significant scale advantages. For large-scale marine power plants, balance of plant components such as the desulphurisers, filtering equipment, blowers, and control architectures could be centralized for a multitude of SOFC units, which would positively influence the power density and specific cost of the system at a slight reduction in system reliability [1]. However, smart centralisation is necessary because it could also increase the amount of piping. Large-scale production of SOFC systems could also improve the market position of SOFC systems. A detailed cost analysis by Scataglini et al. [179] reveals that the expected system cost of SOFC combined heat and power generation products can strongly reduce the production cost. Current SOFC systems cost 1500 – 5000 €/kW whereas diesel generators are in the range of 250 – 500 €/kW, so a cost reduction is needed for economic competitiveness [1, 327]. In short, there is a need to scale small kW systems to the MW scale for marine applications to improve the power density and specific cost of SOFC systems. The scaling effects from current commercial systems to MW scale power plants are not yet quantified for ships.

5

This research aims to identify the scale advantages of high-power SOFC systems. This objective is pursued by conceptualizing a scalable high-power SOFC unit and comparison with existing commercial systems.

The design constraints of a marine SOFC unit are defined in consultation with shipbuilders and marine regulators. This chapter focuses on the benefits of scaling current stack designs to a higher-power system. Other emerging developments in SOFC technology that improve power density, such as metal-supported cells, novel cell materials or novel stack manufacturing techniques are not included.

5.2. SOFC SYSTEM

This chapter briefly introduces the layout of the SOFC system that is selected in this study and highlights potential benefits of scaling SOFC systems to high power.

5.2.1. SYSTEM DEFINITION

The used SOFC system layout (Figure 5.1) is similar to the concept layout used in earlier work by Jia et al. [57] and was already shortly introduced in Metten et al. [224]. The fuel is supplied by a pump, preheated and evaporated. Next, it is mixed with steam and partially converted in the pre-reformer before it enters the anode. Much internal reforming results in a higher net electric efficiency since less blower power is required for air cooling. For this reason, the minimal pre-reform ratio of 20% is used [294]. Air is supplied with a blower and preheated. Co-flow planar SOFCs convert the fuel and air into electricity and heated flue gas.

Part of the anode off-gas is recirculated (AOGR), while the rest is combusted with the air coming from the cathode. In the work by Metten et al. [224], AOGR increased the net electric efficiency from 59% to 64% (LHV) at a recirculation rate of 40%. Furthermore, it omits the need for water feed during nominal operation. After the remaining fuel is

Table 5.1: Qualitative comparison of cold and hot recirculation. HE = heat exchanger.

	Advantages	**Disadvantages**
Hot recirculation	Lower number of HEs Lower HE area Higher flue gas temperature	Higher energy consumption Higher cost of blowers
Cold recirculation	Lower energy consumption Less power use by blowers	Higher number of HEs Higher HE area More complicated piping network More valves for flow and temperature control Lower flue gas temperature

combusted, heat in the exhaust stream is recovered for the saturated steam net of 180 °C at 9 bar and the hot water net of 90 °C at ambient pressure [300, 306].

5

In earlier research (Chapter 4), Veldhuizen et al. [294] positively evaluated the use of cathode off-gas recirculation (COGR). COGR decreases the primary airflow because the overall oxygen utilisation increases. Since SOFC systems require large airflows, the application of COGR could strongly reduce the amount of space required for air and exhaust ducting through the ship. However, it is not yet investigated how big the positive impact of COGR is for design integration in ships. For this reason, this study considers both SOFC systems without and with COGR, see Figure 5.1(a) and Figure 5.1(b) respectively. The cathode off-gas recirculation stream is added just before the cathode inlet to reduce the flow through the air pre-heater. This significantly reduces the size of the largest heat exchanger in the system [294]. A supplementary air stream is added at the burner inlet which can be used in case the burner or the exhaust stream temperatures are reaching their limits.

The AOGR and COGR are evaluated for a hot recirculation loop using hot recirculation blowers [294], as well as a cooled recirculation loop using regular blower [62, 97]. The trade-off is summarised in Table 5.1. For the cold recirculation loop additional heat exchangers are needed to cool the recycle loop increasing heat losses, size and cost of the system. However, high-temperature air blowers are still in development and are costly. Moreover, they usually operate on lower electric efficiency and have higher heat losses. Nevertheless, Tomberg et al. [304] demonstrated successful operation of a high-temperature blower for AOGR. If hot recirculation blowers are further developed and reliably applied to AOGR and COGR loops it would result in a more efficient system, explaining the choice to use a hot recirculation loop, as shown in Figure 5.1(b).

5.2.2. Scaling of SOFC system

Table 5.2 shows the power density of commercial SOFC systems. The rated power of commercial SOFC systems is steadily increasing, as stack manufacturing is increasing and since it results in more cost-effective systems. In general, it is easier to reach high power density with high-power systems. The power derived from an SOFC stack scales

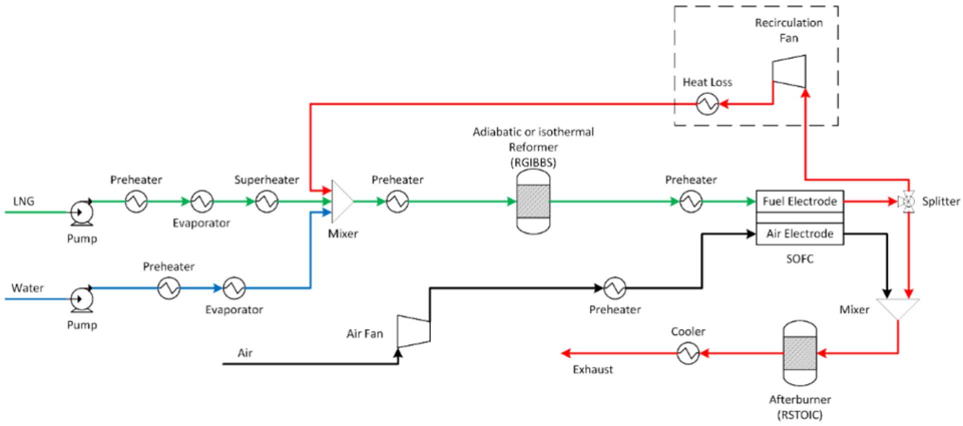

(a) System layout including AOGR without COGR.

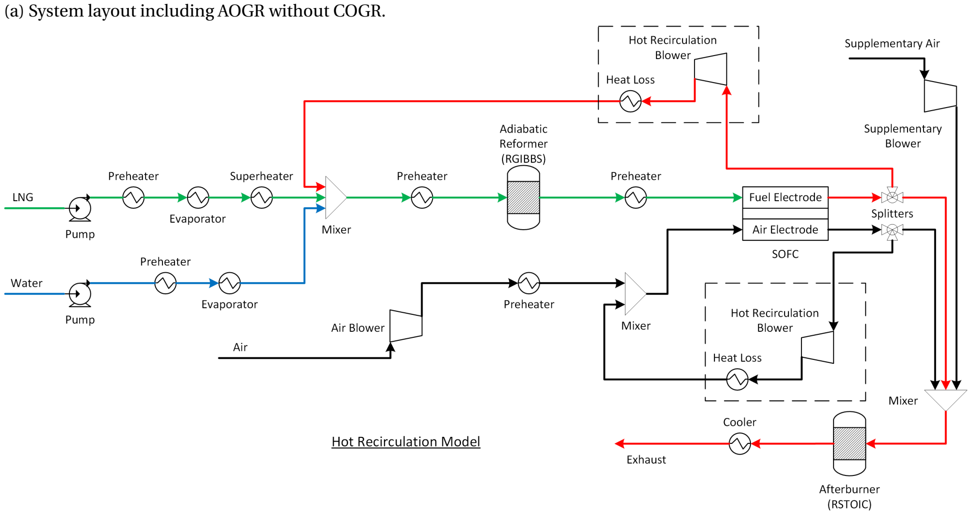

(b) System layout including AOGR with COGR.

Figure 5.1: System layouts of used SOFC system.

Table 5.2: Recently developed SOFC systems. Systems include hot and cold BOP. Ordered on rated power.

Company	**System**	**Power [kW]**	**Power density [kW/m^3]**	**Source**
SolydEra	BG-15	1.5	2.27	[329]
Bosch	FC505	10	5.2	[228]
Convion	C60	60	4	[230]
Fuel Cell Energy	250kW FC	250	4.4	[234]
Bloom	Energy server 5	300	10.6	[229]
Doosan	Purecell 400	440	7.1	[233]

linearly with the number of cells that are used in the stack. Subsequently, the power density of the stack itself is not expected to improve much when increasing the rated power of the system. However, on a system level, there are many scale effects that can improve the power density and specific cost for high-power systems. Combining many stacks closely packed in one system, will reduce the heat loss to the environment because there is also thermal transfer between the stacks and the size of the surface area reduces relatively to the volume of the stacks [328]. This reduces the amount of insulation needed, which usually takes up much space because of the high operational temperature. Moreover, combining balance of plant (BOP) components for many stacks and SOFC modules also has the potential to improve the power density and specific cost of the full system. Especially components that are not directly integrated with the hot part of the system are easy to combine for many SOFC modules, for instance, air blowers, air filters, desulphurisers, water treatment, and heat regeneration. Centralisation does reduce system reliability, so single points of failure in the system should be avoided.

A sizing model has been developed that optimises the 3D configurations of the stacks, pre-reformer, combustor, and high-temperature heat exchangers as functions of the rated power, based on a stack platform of SolydEra. Figure 5.2 shows the resulting power density of this model for different power ratings. The increase in power density in this figure is attributed to an increase in the size and number of stacks, positive scale effects of heat exchanger and combustor for higher rated power, a relative decrease in heat loss, and a relative decrease of the required volume for insulation. The data points represent different configurations, based on the size of the components for the dedicated rated power. By adding a trend line through these configurations, it is visible that the power density improves for a higher-rated power of the hot part of the SOFC system.

5.3. DESIGN OF SCALED SOFC SYSTEM

This section presents the concept design of a scalable SOFC unit. First, the design constraints that were set from the ship perspective are presented. Following, some considerations during the conceptualization of the unit are discussed. Next, the concept of the SOFC unit is shown including its main characteristics, connections, and operational concept. Finally, a concept is presented on how this unit can be scaled to a MW SOFC room.

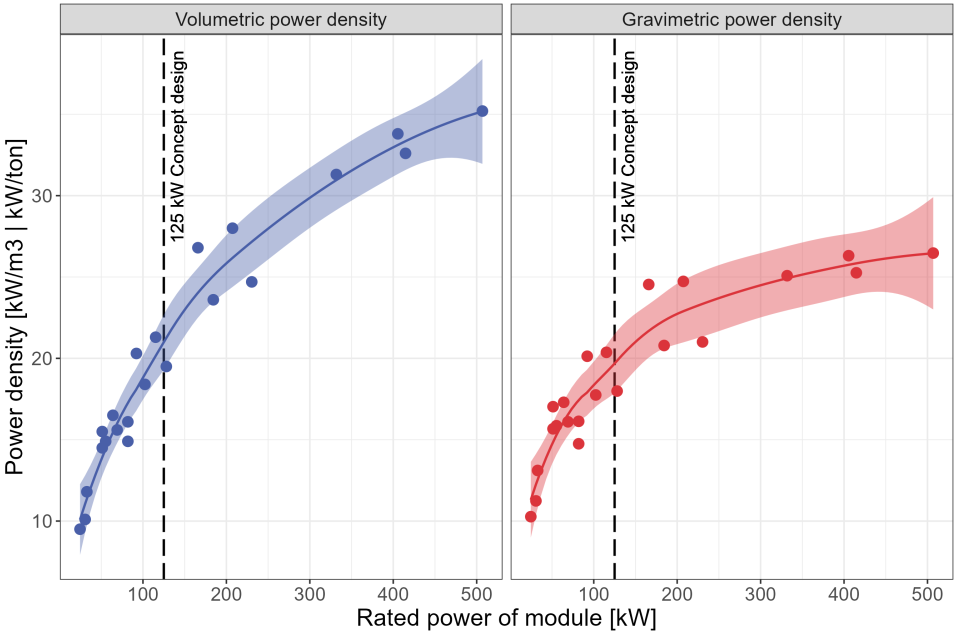

Figure 5.2: Expected power density SOFC module for rated power (Stacks + hot BOP). The estimations are derived from stack platform developments and the reduction of heat loss when scaling hot BOP modules. The vertical line shows the extent to which the scaling effects are utilised in the concept design of this chapter.

5.3.1. DESIGN CONSIDERATIONS

Although the power density increases with the rated power of the system, there are limitations to these scale effects. Introducing SOFC systems in ships presents multiple constraints at various system levels, especially because market introduction is easiest when the system has a small impact on standard ship design procedures and operation.

To evaluate these constraints, two design workshops were organised with R&D specialists and naval architects of Meyer Werft and Chantiers d'Atlantique. In these workshops, different general arrangements of cruise ships between 50,000 and 200,000 GT range were reviewed to identify limits in the dimensions of SOFC systems and their required components. In these workshops, the focus was to limit the dimensions of SOFC systems and components to general spacing dimensions in the ship's structure, because this ensures easy integration without drastic changes to the ship's structure. Moreover, since SOFC stacks need to be replaced regularly, the focus was placed on easy handling of the replaceable parts. The defined constraints are specific to ship types and practices of the shipbuilders, although general applicability to large ocean-going vessels and their regulations is also considered.

The constraints for the replaceable part and the SOFC power plant set during the design workshops are summarized in Table 5.3. First of all, the replaceable part should be easy to handle by the crew and should be able to be transported through the ship. The main dimensions of replaceable parts in the machine room are often limited by the height of watertight doors (which are limited by regulations), and the space that is needed to move the part through gangways and corridors. Furthermore, it is preferred that the weight of the replaceable part is below two metric tons to be able to make use of regular hand forklifts.

Moreover, to maintain flexibility in the onboard location of fuel cell rooms, it would be best to limit the size of the fuel cell rooms to general spacing dimensions in the ship's structure. The shipbuilders point out that the length is limited to the spacing of the watertight compartments, which is maximum 14 meters for the evaluated vessels. Over the width of the ship, there are usually longitudinal strengtheners (walls or columns) with a spacing of 5 meters. The deck height is generally 2.3 meters, excluding the additional height of the main stiffeners. Engine rooms generally do not comply with these limits and are sometimes even two or three decks high. Since this compromises the structural strength of the ship, it would be better to avoid this and use standard-height rooms for fuel cells. The weight of the fixed components is generally not a limiting factor, because the strength of floor plating is adapted to the weight it needs to carry.

5.3.2. DESIGN CONSIDERATIONS

Within the presented constraints many concepts were designed and evaluated. They will not all be presented, but the most important design considerations are listed:

1. According to marine fuel cell regulations [330], fuel cells and parts that convert gas to hydrogen or contain hydrogen such as the pre-reformer are defined as a fuel cell space and must be in gas-tight compartments. For this reason, several SOFC modules and their hot BOP are combined in a single gas-tight unit.

2. All piping containing fuel passing through enclosed spaces is to be double-walled.

Table 5.3: Design constraints. Derived from consultation with Meyer Werft GmbH and Chantiers de l'Atlantique.

(a) Replaceable part.

Measure	Maximum	Unit	Constraint by
Width	1.6	m	Width of standard outside entry minus margin
Depth	2.0	m	Moving and rotating of part through corridors
Height	1.8	m	Height of entry and watertight doors minus space for lifting device
Mass	2.0	mt	Use of cranes and hand forklift

(b) Fuel cell room.

Measure	Maximum	Unit	Constraint by
Length	14	m	General length of watertight compartments
Width	5	m	General space between longitudinal strength units
Height	2.3	m	Deck height minus height of main stiffeners
Mass	-	mt	The stiffening of the floor plating is generally adaptable

5

So, the cascading fuel supply to the SOFC units must also be double-walled. The pipes between hot BOP components in the fuel cell space are not double-walled.

3. The connections are placed at the top or bottom of each module to be able to place the modules back-to-back, which saves space. This means the module should also be designed in such a way that all maintenance can be done from one side. Supply and exhaust pipes can be put below the floor or in the ceiling.

4. Although replacement of an entire integrated stack module including hot BOP and insulation would be easier, such a large heavy module is very hard to replace regularly in a ship. The decision is made to use high-power stacks that are replaced individually. Nevertheless, this introduces additional challenges in applying insulation and assuring gas tights connections during stack replacement.

5. In the room there should be enough space for opening the cabinet, removing the stack, and transporting it through the room, requiring significant pathways in the SOFC room. Besides easy access to the stacks, the other BOP components should also be accessible in case of damage.

6. Any batteries that are usually needed to support the dynamic capabilities of SOFCs should be placed in a different room as defined by regulations because the batteries are perceived as a fire hazard.

7. The process air could be supplied directly to the system, or the air could be supplied to the room and the units would suck the air directly from the room. For the second option this results in less piping to all the SOFC units. However, this still requires a blower and filter in every unit to make sure the unit retrieves air. Since the

goal is to centralise BOP components to reach higher power density it is chosen to supply the air directly to the units.

5.3.3. Concept design SOFC unit

The design constraints are met with an SOFC unit containing six 22.5 kW stacks. The net rated power of the unit is 125 kW. The six stacks produce more power but part of it is used for the parasitic power of the blowers. This power rating of the stacks and unit is selected because it makes use of the scale effect (see vertical line in Figure 5.2), while still ensuring suitable sizes for integration and reasonable weights for stack replacement. Moreover, the rated power of the stacks is something that can be expected in the near future. Although currently commercially available SOFC stacks range up to 10 kW, short stack tests have been successfully completed for the platform of the 22.5 kW stack at SolydEra.

The gastight cabinet (see Figure 5.3) includes the stacks and the hot BOP and is 1 meter wide, 4 meters long and 1.8 meters high (without connections), resulting in a power density of 17.4 kW/m^3 or 31.3 kW/m^2. One unit weighs 6.8 tons. The main system dimensions are summarized in Table 5.6.

5

System components

Table 5.4 shows which system components are included in the cabinet and which components still need to be placed in the ship. The SOFC unit contains the hot BOP components, see Figure 5.3(b), such as the air preheater, the fuel pre-heater, the pre-reformer, and the combustor. The cabinet also houses an AOG recirculation loop and optionally a COG recirculation loop and a water evaporator to supply water for the steam reforming. Because of the decrease in process air when employing COGR, the reduction of the air preheater size compensates for the additional space to include the piping and blower of the COGR piping. Against all the outside plating 15 cm insulation material is added to limit heat loss.

The compression system, the current collection and the ventilation blower for accumulated gases are located under the stacks. Cold balance of plant components like the air blower, waste heat recovery and inverters should still be placed outside of the unit, with the aim to centralise them for several units, reducing the volume of the total system. The stacks are put in series to reach a voltage level of 535V, which means in principle no DC/DC boosters are needed to convert the power to AC. Outside air is dehumidified, desalinated, and distributed directly to the SOFC units. Because the system employs AOGR, the steam supply is only necessary during start-up. A separate steam generator will be added to the units because the onboard steam net generally does not satisfy the contamination limit of the SOFC stack. Heat recovery can be added per unit, but it is also possible to cascade the exhaust ducting and have a centralised heat recovery. Nitrogen purging is used as safety concept during start-up and shut-down.

Operation

Since the voltage of the system degrades over its lifetime, the power, the efficiency, or a combination of both decrease over its lifetime. According to shipyards, it is a strict requirement that the SOFC can deliver nominal power over the total lifetime of the system.

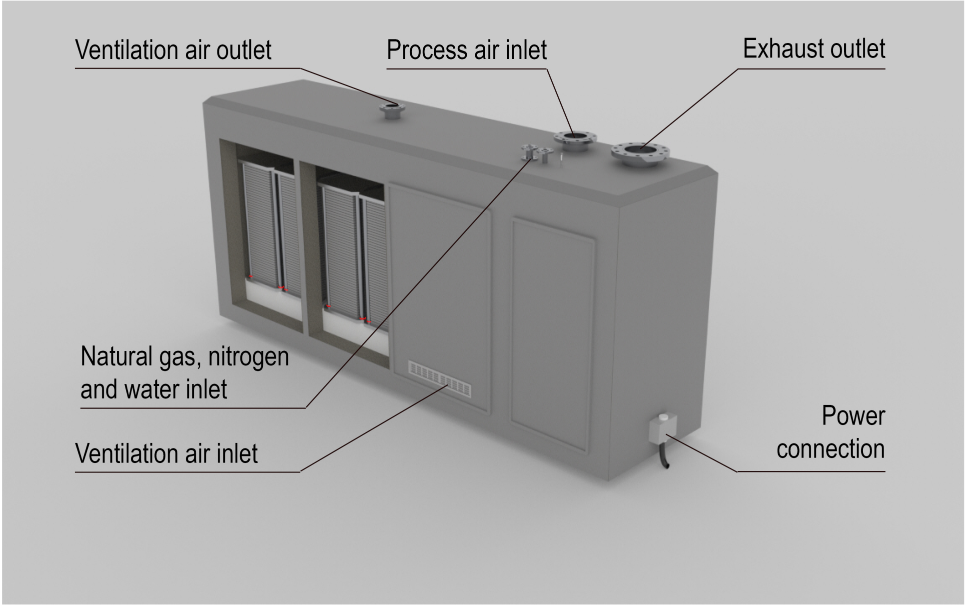

(a) SOFC cabinet including physical and electrical connections.

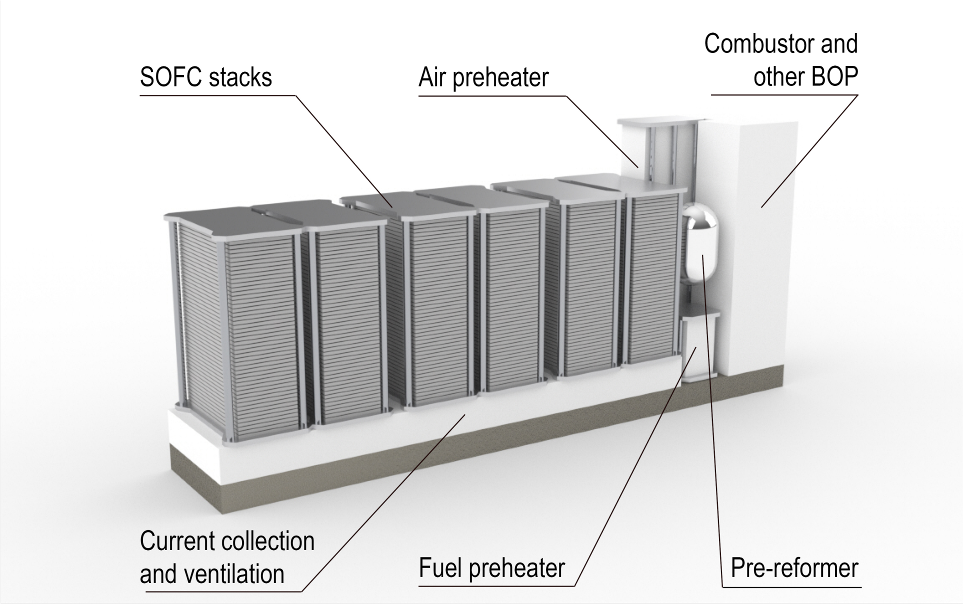

(b) Orientation of components in cabinet.

Figure 5.3: Renders of 125 kW SOFC unit with COGR.

Table 5.4: Distribution of main system components for design concept of 125kW SOFC unit.

Components included in unit		Components not included in unit	
Component	**Included in unit**	**Component**	**Included in SOFC room**
6 SOFC Stacks	Yes	LNG evaporator	No
Compression system	Yes	Desulphuriser	Yes
Current collection	Yes	Air blower	Yes
Insulation	Yes	Air filter	Yes
Fuel preheater	Yes	Exhaust heat recovery	No
Pre-reformer	Yes	(DC/DC booster)	No
Air preheater	Yes	AC/DC inverter	Yes
AOG recirculation loop	Yes	PLC	No
(COG recirculation loop)	Yes	Energy management system	No
Start-up evaporator/boiler	Yes	Battery	Yes
Ventilation blower	Yes		

5

To achieve this considering the cell degradation, the efficiency of the system decreases over its lifetime, which also means that the required flows of the system increase over the lifetime, see Table 5.6. Consequently, the piping and ducting must be sized for the end-of-life conditions of the system.

The SOFC units will function as an integrated system, necessitating modulation and activation of the entire unit. Modulating individual stacks independently would enhance the complexity and hardware demands of the control architecture. Additionally, if only a subset of stacks within a unit was operating at high temperatures, excessive heat transfer would occur to the remaining stacks due to the insulation being placed at the unit's boundaries and not per stack. For this reason, it would be difficult to maintain the operational temperature of the stacks.

When many of these units are combined the operation of the units can be controlled towards an optimum in the total conversion efficiency of all the units. Unlike combustion engines, SOFCs have high efficiency at part-load, so when the ship demands a fraction of the installed power it might be favourable to run all units on part-load instead of some on nominal load. Moreover, in part-load, steady-state degradation is slightly lower. Nevertheless, load transients and start-stop cycles strongly increase the degradation and thus the conversion efficiency of the SOFC units over their lifetime. It might be best to operate the SOFCs on a constant load as much as possible. This operational trade-off between conversion efficiency and degradation needs more investigation and will be investigated in future work.

The replaceable stack has a footprint of 0.75 by 0.45 meters, is 1 meter high and weighs 370 kg, making the modules relatively easy to handle and transport through the ship, without the need for complex towing or lifting equipment. When one stack is replaced, the whole unit should be turned off, so it would be best to replace stacks simultaneously.

Table 5.5: Piping connections of SOFC unit.

Connection	Maximum allowable velocity [m/s]	Without COGR	With COGR
Process air inlet	10	DN 250	DN 150
Fuel inlet (double walled)	18	DN 25	DN 25
Nitrogen inlet	-	DN 25	DN 25
Water inlet	3	DN 6	DN 6
Exhaust outlet (insulated)	10	DN 300	DN 200
Ventilation air outlet	10	DN 100	DN 100

5

System connections

The piping connections are at the top of the unit above the BOP components. The process air and the ventilation air streams are separated. The required ventilation airflow is substantial and since this flow is not heated to the operational temperature of the SOFC stack, it would lower the temperature of the exhaust stream, reducing the heat regeneration capacity. The process air is directly supplied via the piping at the top while the ventilation air is sucked in at the bottom of the units via ventilation grids, see Figure 5.3(a). The ventilation air is removed at the top of the stacks, where a gas sensor is placed to detect any potential leakage. The nitrogen flow is sized to be able to purge the fuel lines. Figure 5.3(a) shows the location of the connections. The electric connection is placed at the bottom since the current collection takes place at the bottom of the SOFC stacks. Using Equation 5.1, the piping connections of the SOFC unit are sized from the required volumetric flow rate and maximum allowable velocity of the medium. The used allowable velocity and the size of the piping connections are shown in Table 5.5.

$$d = \sqrt{\frac{4}{\pi} \cdot \frac{Q}{v_{max}}} \tag{5.1}$$

System performance and characteristics

The presented concept design is modelled in Aspen [224]. This thermodynamic model, containing all components shown in Figure 5.1, is used to determine the required flows and the performance of the SOFC system, see Table 5.6. Especially at the beginning of life, the SOFC units convert fuel to electricity at very high efficiency of 62%. Conversion losses to AC power should be added if the power is supplied to the electrical grid of the ship. Over its lifetime of 40,000 to 50,000 operational hours, the net electric efficiency decreases with 12%. This high decrease is caused by the requirement to deliver 125kW during its lifetime. When the voltage decreases due to degradation, the SOFCs must be operated on a point on the I-V curve with higher power density to maintain 125kW, further decreasing the voltage and thus the conversion efficiency.

Table 5.6 shows that the use of COGR strongly decreases the required flows for process air and exhaust air by 55-57%, which makes it easier to fit the ducting and piping through the ship. Moreover, the exhaust air temperature is higher with COGR resulting in a higher quality exhaust stream to use for exhaust heat recovery. Especially if heat

Unit characteristics	**Without COGR**		**With COGR**		**Unit**
	Begin life	End life	Begin life	End life	
Net electric efficiency at nominal load (DC; LHV)	62%	50%	62%	50%	-
Net rated power	125				kW
Length	4				m
Width	1				m
Height	1.8				m
Weight	6.8				ton
Mechanical interfaces	**Without COGR**		**With COGR**		**Unit**
Fuel	Begin life	End life	Begin life	End life	
Required fuel flow (85% global fuel utilisation)	320	400	320	400	SLM
Process air					
Airflow	17108	22811	7281	9686	SLM
Required air quality (salt in air)	<0.2				micron
Water					
Water flow (only during start-up)	0.56	0.71	0.56	0.71	L/min
Flue gas					
Exhaust flow	16749	22332	7501	10001	SLM
Temperature of exhaust after hot BOP	150-200	150-200	250-300	250-300	°C
Ventilation					
Ventilation airflow	5000				SLM
Electric interfaces	**Without COGR**		**With COGR**		**Unit**
	Begin life	End life	Begin life	End life	
Voltage of module	535	425	535	425	V
Current of module	258	325	258	325	A

Table 5.6: System characteristics of 125 kW SOFC unit. The required flows are determined using thermodynamic system simulations in Aspen [224].

is required for the saturated steam net of the ship (generally at 9 bar and 180 °C), this increase in exhaust temperature is very relevant.

5.3.4. CONCEPT DESIGN OF SOFC ROOM

Although the last section showed the design of a scalable unit, more components are needed to supply power to the electric grid of the ship. This section shows a concept with several of the presented SOFC units combined with an additional room for the centralised cold BOP components, see Figure 5.3. Nine units are placed in the SOFC room and supply 1125 kW of power. There is sufficient space between the units to take out and replace the stacks. The SOFC room and the cold BOP room are 5 meters wide, 2.3 meters high, and respectively 14 and 3.1 meters long. The rooms combined result in a power density of 5.7 kW/m^3 or 13.1 kW/m^2.

In the cold BOP room (see Figure 5.4), a desulphuriser reduces the sulphur content in the natural gas to acceptable contents. Outside air is desalinated, filtered, and supplied

Table 5.7: Size of piping and ducting in SOFC room and cold BOP room for 1125kW. The piping in the last column are the sizes used for the shown concept design.

Connection	**Type of piping**	**Without COGR**	**With COGR**
Ventilation air supply	Rectangular ducting	350x250 mm	350x250 mm
Process air supply	Rectangular ducting	1200x300 mm	500x300 mm
Fuel supply	Double-walled pipes	DN 80	DN 80
Nitrogen supply	Regular pipes	DN 80	DN 80
Water supply	Regular pipes	DN 8	DN 8
Flue gas exhaust	Insulated pipes	DN 800	DN 450
Ventilation air exhaust	Regular pipes	DN300	DN300

directly to the units with a blower. One central exhaust line gathers the exhaust from the units. The exhaust pipe is insulated because the flue gas will be supplied to a central heat regeneration unit elsewhere in the ship. The ventilation air is supplied via ducting to the SOFC room while the SOFC units suck the air from the room. Since the ventilation air exhaust can contain hydrogen or methane, it is gathered in one central pipe. The piping and ducting are sized by multiplying the flows in Table 5.6 with the number of units in the room and are shown in Table 5.7.

DC/AC inverters convert the power to the requirements of the ship grid and a battery rack is used for peak shaving, ramp-up, and ramp-down. The battery rack is based on the Corvus Orca and is sized to be able to deliver sufficient power and energy for load-following behaviour but does not contain sufficient capacity to support a cold-start. The cold start-up time of SOFC systems of 12-24h is very long [1] and unreasonable battery capacity would be needed to meet the energy demand during start-up. Timely switching on and off the SOFCs is required to make sure there is enough power available to meet the demands of the ship. To size the battery, it is assumed that the SOFC and the battery combined should have the same transient capability as a diesel genset. In that case, the battery capacity can be calculated with Equation 2 to 4. One 124 kWh vertical pack was sufficient to fulfil the transient requirements.

$$E_{bat,req} = \frac{P_{SOFC,installed}}{2a_{trans,SOFC}} - \frac{P_{SOFC,installed}}{2a_{trans,DG}} \tag{5.2}$$

$$P_{bat,req} = \left(a_{trans,DG} - a_{trans,SOFC}\right) \cdot \frac{P_{SOFC,installed}}{a_{trans,DG}} \tag{5.3}$$

$$E_{bat,installed} = \max\left[E_{bat,req}; \frac{P_{bat,req}}{C_{rate}}\right] \tag{5.4}$$

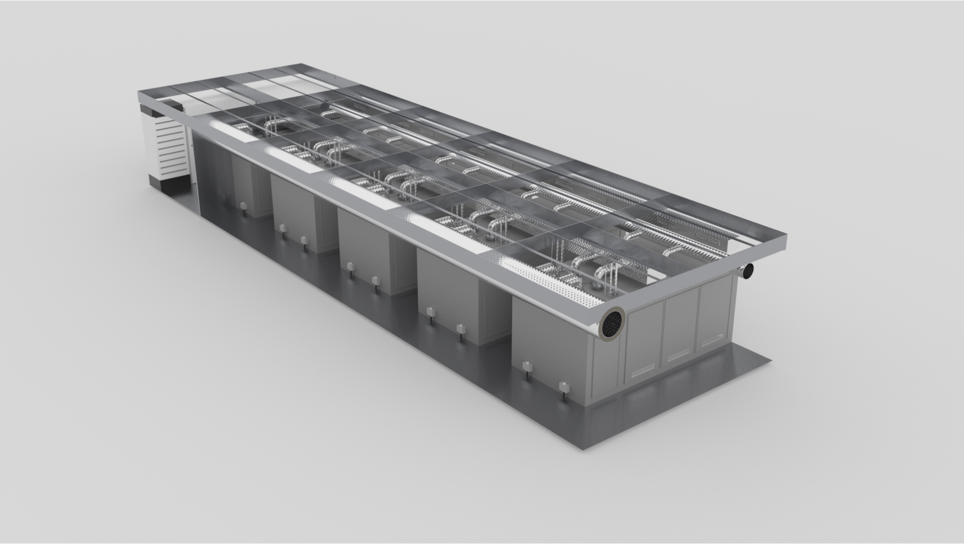

(a) Render of concept design.

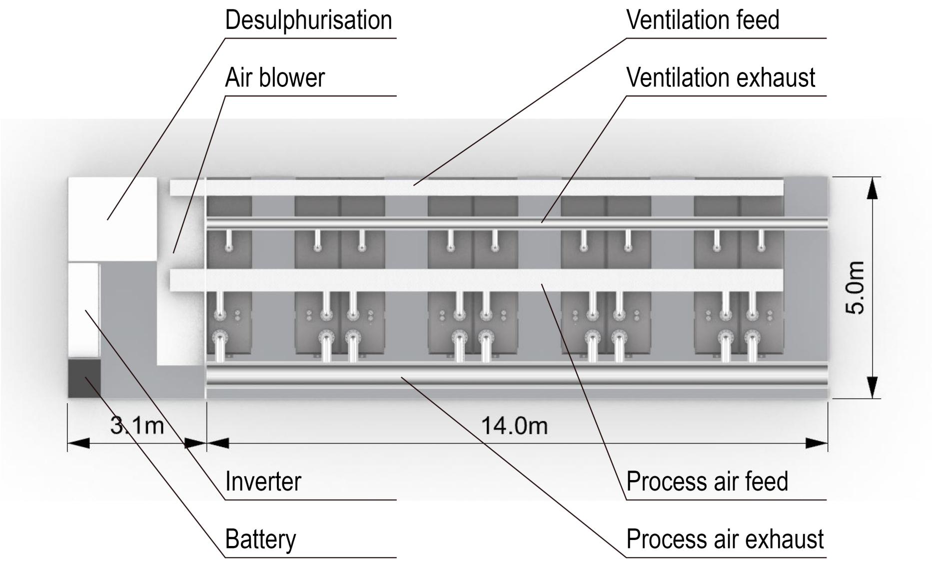

(b) Orientation of components in SOFC room and BOP room.

Figure 5.4: Renders of 1.125 MW SOFC room with COGR.

5

5.4. CONCLUSION

SOFC systems are considered a promising option to reduce ship emissions. However, they need to be scaled from low kW systems to the MW scale for marine applications while improving the power density and specific cost of SOFC systems. It is important to design a system that exploits potential scale effects. Such a scaled system should offer flexibility for ship types and operation, and have a limited effect on ship design practices, while also ensuring high system efficiency and reliability.

After setting several constraints from the ship and fuel cell development perspective, a 125kW SOFC unit with six replaceable stacks and hot BOP components was designed. Nine of these units are placed in an SOFC room and combined with a cold BOP room to result in an SOFC power plant that can directly supply power to the electrical grid of the ship. During the design phase, the following lessons were learned:

1. Size and weight limitations of stack replacement are a limiting factor to the design of marine SOFC systems.

2. It is important to take SOFC degradation into account during system design. Since the required flows increase over the lifetime, the end-of-life conditions must be used for sizing.

3. The high air-fuel ratio of the SOFC system which is needed for the cooling of the stack during operation leads to very high air and exhaust flows. The piping through the ship would occupy a considerable amount of space. COGR should be applied to marine SOFC systems to reduce the ducting size. In this system, COGR resulted in a 55 to 57% reduction of the process airflow resulting in much smaller piping.

A higher power density is achieved by combining several large stacks and the hot BOP in an integrated gas-tight unit. This unit reaches a power density of 17.4 kW/m^3 or 31.3 kW/m^2 which is a significant improvement compared with current commercial systems, ranging up to 10.6 kW/m^3 (see Table 5.2). However, the cold BOP components that also require significant volume, such as the inverter, the air blower and the heat recovery are not included in the unit. These components are centralised for several SOFC units, to further increase the power density of the total systems due to scale effects. A concept is developed of a 1.125 MW SOFC room containing nine SOFC units and a separate cold BOP room. This results in a power density of 5.7 kW/m^3 or 13.1 kW/m^2, which already includes maintenance paths and space for ducting. Several of these SOFC rooms can be used to scale to a multi-MW power plant for seagoing ships while being competitive in terms of space and efficiency, while strongly reducing ship emissions.

6

DYNAMIC SIMULATION OF HYBRID SOFC POWER PLANT

Time-domain simulations allow us to peer into the future and adjust the present for better outcomes.

Anonymous

This chapter has been published in Energy Conversion and Management **326**, 119477 (2025) [331].

6.1. INTRODUCTION

In 2022, international shipping accounted for approximately 2% of global CO_2 emissions [6]. Liquefied Natural Gas (LNG) has been implemented as bunker fuel to reduce emissions in the short term and constitutes 15% of newly ordered vessels [332]. However, recent emission measurements on LNG-fuelled vessels report a higher than anticipated methane slip, especially for 4-stroke engines. Comer et al. [333] recommends that a default methane slip of 6% should be considered for policymaking. For the longer term, the marine industry is considering fuels that can be produced renewably, such as hydrogen, ammonia and methanol to reduce carbon emissions over their life cycle [94]. Besides greenhouse gases (GHG), the combustion of marine fuels emits large amounts of nitrogen oxides (NO_X), carbon monoxide (CO), sulphur oxide (SO_X) and particulate matter (PM). The International Marine Organisation (IMO) forces ship operators to reduce greenhouse gas emissions with the Energy Efficiency Existing Ship Index (EEXI) and the Carbon Intensity Indicator (CII) [10]. These regulations contribute to the IMO targets of 30% GHG emission reduction by 2030 and 80% by 2040 [9]. Moreover, strict limits are set to emissions of nitrogen oxides, carbon monoxides and sulphur oxides, especially in dedicated emission control areas [11].

6

Solid oxide fuel cell (SOFC) systems are a potential solution to reduce greenhouse and pollutant emissions [327]. The high electrical efficiency of 50% to 60% results in fuel savings and thus in a reduction of carbon emissions, compared to marine combustion engines. Moreover, unused fuel is burned in a catalytic after-burner to maintain the temperature of the stack, removing any methane slip, which Baldi et al. [27] identified as the strongest driver of GHG emission reduction. Since power is generated by electrochemical conversion instead of combustion, SOFCs emit almost no NO_X and CO emissions. In the NAUTILUS project, PM emissions are even reported to be lower than ambient conditions, improving the air quality of the direct environment.

SOFC systems offer additional benefits for maritime vessels. SOFCs can operate on different fuels. Natural gas, hydrogen and ammonia can be directly fed to SOFCs [34], while other carbon fuels can be used after reforming. Moreover, SOFC systems are silent, do not produce vibrations, and offer high redundancy [167]. Nevertheless, SOFCs are not widely applied in ships yet. Currently, their capital costs are much higher and the volumetric and gravimetric power density is much lower than for internal combustion engines [1]. Moreover, the long start-up and shut-down time introduce challenges in operating these systems, especially for ships with dynamic operating profiles. For these reasons, most studies only include SOFCs as an auxiliary power unit resulting in hybrid SOFC-engine-battery power plants [27]. Nevertheless, researchers and industry acknowledge the potential of SOFC systems to reduce ship emissions, especially for ocean-going vessels, for which hydrogen- or battery-based propulsion cannot fulfil the range demands due to low energy density [27].

SOFC systems are often praised for their high combined heat and power efficiency, ranging up to 90% [334], from which applications with a significant thermal load can benefit, such as cruise ships [160]. Although SOFCs operate at temperatures around 700 °C, high-temperature heat recovery is limited because much heat is used internally to bring the air and fuel to the operating temperature of the fuel cells [37]. Baldi et al. [27] points out that few studies also include the thermal balance between the SOFCs, engines and boilers, and the heat users. Rivarolo et al. [32] studied the thermal integration of SOFCs for a cruise ship and concluded that SOFC systems cannot fulfil all the heat demands of the ship. In this study, the thermal balance is also tackled. Boilers are employed and sized accordingly to supply the heat deficit of the other power plant components. Thus, components with low heat recovery capacity directly increase fuel consumption.

SOFC systems operate on high electrical efficiency, with peak efficiency at part-load. This fundamentally differs from internal combustion engines (ICEs) which often operate most efficiently at their rated power. High part-load efficiency can be exploited for ships, because they do not usually sail at their maximum speed. Nevertheless, most integration studies operate SOFCs constantly at full power because of their slow modulation [27], but this results in suboptimal fuel conversion. Haseltalab et al. [169] simulated a hybrid power plant of a dredger with SOFCs, ICE-generator sets (gensets) and batteries. They used load curves to estimate the fuel consumption but neglected the load-dependency of emissions. For combustion, NO_X and CO emission factors are higher at part-load conditions [335]. Furthermore, methane slip up to 12% was measured at part-load conditions [333]. Load-dependent emissions of commercial SOFC systems are not widely published, but a recent measurement campaign reports emission factors for different load cases [336]. Although often neglected in earlier power plant simulations, this study includes the efficiency as well as emissions of power plant components under different load conditions.

SOFC systems typically respond slower to load transients than combustion engines [31]. Rapidly increasing the current introduces hot spots in the stack, which can cause permanent damage [337]. Moreover, the SOFC system and its hot balance of plant components exhibit notable thermal inertia in response to alterations in operational temperature [28]. For this reason, SOFCs are often coupled with batteries for ramp support, load smoothing and/or peak shaving [27]. Simple methods assume a fixed ratio between SOFC and battery capacity [338] and Haseltalab et al. [169] sized the battery capacity as a function of the transient capabilities of the installed SOFCs and engines. However, the required power and energy capacity of the battery is highly dependent on the function it should fulfil and the load profile. In this study, the operational profile of a specific ship application is used to validate the estimated battery capacity and adapted if necessary.

Cell degradation decreases the performance of SOFC systems over their lifetime. Consequently, the stacks need replacement every 40k [27] to 50k [339] running hours. This is often included in techno-economic assessments [168] but not usually considered for power plant simulations. The degradation of SOFCs is a combination of different mechanisms, and models are complex combinations of electrochemistry mechanics and mass transport [340]. Comprehensive degradation simulation includes physics-based models for nickel coarsening and oxidation, conductivity changes of electrolyte and electrodes, sulphur poisoning, and delamination [341]. Such models are too computationally heavy to include in a long-term power plant analysis. Moreover, empirical data for degradation in part-load or even transient operation is not available in the literature. Nevertheless, degradation influences the operational conditions of the SOFC system; an effective degradation model is needed for dynamic simulations. For consistency, performance degradation of engines and batteries should also be considered, especially because reducing the transient load of one component will increase the cycling of the other power-producing components of a hybrid power plant. Cichowicz et al. [342] indicate that the fuel consumption of engines increases with 4.5% over 100k running hours due to wear and fouling of its components. The degradation of lithium-ion batteries varies widely for different battery chemistries but is usually modelled as a combination of calendar ageing and cycling loading [343]. This study includes methods to incorporate component degradation effectively in long-term power plant simulation.

A suitable control strategy is essential to operate a hybrid power plant efficiently. Rule-based control strategies can be employed to distribute the load over the components considering operating points with low fuel consumption or low emissions [344]. More complex strategies, such as model predictive control can be used to further improve energy efficiency, however, for such strategies, a predictable or repetitive load profile is often required [345]. Furthermore, health-aware energy management strategies for hybrid power generation adapt the load distribution based on the associated degradation effects [346]. Energy management strategies that use batteries for load support typically base the required load of the SOFCs on the state of charge (SOC) of the battery [347]. This enables sufficient charge and discharge capacity to compensate the SOFC at any moment. Although energy management for hybrid power generation on ships is studied extensively, few manuscripts consider power plants with SOFCs, gensets and batteries [169]. This study implements an energy management strategy considering efficient operation and lifetime preservation of the different power plant components.

To the authors' knowledge, the size, mass, fuel consumption, GHG emissions, and pollutant emissions of hybrid SOFC plants have not been integrally evaluated for cruise ships. Although Li et al. [338] extensively studied the performance of a SOFC, engine, and battery power plant for cargo ships, degradation effects and emissions were not considered in the evaluation, which are included in this study. A dynamic simulation model combining electrical and heat demand, and allocating power among power plant components considering part-load operation, is required for a detailed estimation. Additionally, a low-computational method is necessary to account for the effects of degradation on the operation of SOFC systems.

This research aims to compare the volume, mass, fuel consumption, and emissions of different hybrid SOFC power plants for cruise ships. A dynamic power plant model is developed to simulate the control and operation of the needed components. The model can be used to find the right hybridisation strategy for the dedicated ship application. The main scientific contributions of this chapter can be summarised as follows:

- The development of a dynamic power plant simulation model that includes component sizing, part-load behaviour, and emissions for the main components that generate electricity or heat.
- Component degradation and its effect on operation is included, which is often neglected in power plant analyses.
- An extensive comparison of power plant size and weight, fuel consumption, and emissions for different hybrid design scenarios.
- Validation and eventually adaption of the required battery and boiler capacity, preventing over- or under-sizing.

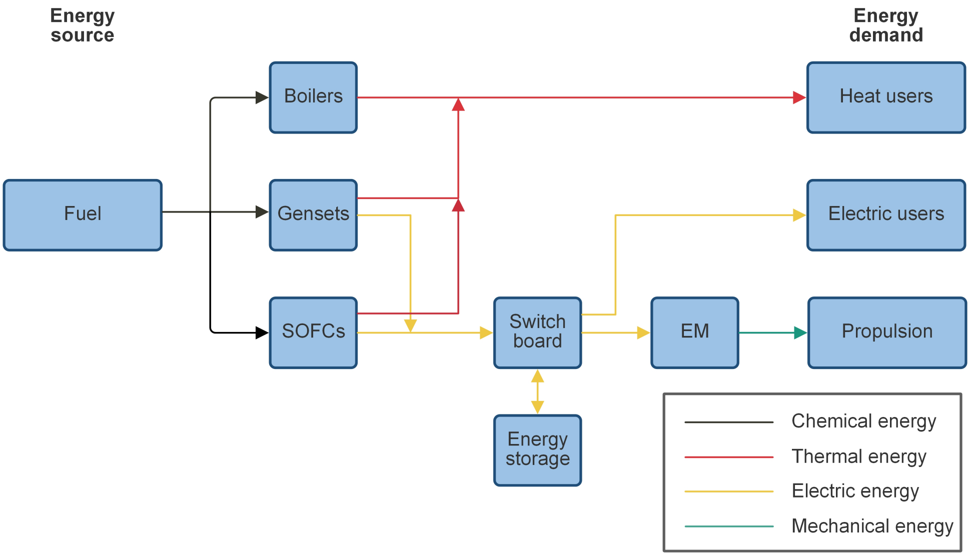

Figure 6.1: General system layout of onboard components.

- A simple but robust control strategy for the operation of SOFC systems paired with batteries and engines.

6.2. METHODOLOGY

The component sizing and power plant simulation is based on the general layout described in Figure 6.1. Electrical power is supplied by natural gas-fuelled SOFCs and ICE generator sets, running on marine gas oil (MGO) or natural gas. Batteries are used to support the load-following capability. A waste heat recovery system retrieves heat if needed from the gensets and the SOFCs, which the boilers can complement. An energy management system ensures all electrical and heat demand is met. This section describes how this system is sized and how the different components are modelled in the dynamic simulation model. This model is used to compare different design scenarios quantitatively on the main performance indicators of power plants: volume, weight, fuel consumption, and emissions [28]. CO_2 and CH_4 are included as GHG emissions NO_X, SO_X, PM, and CO as toxic airborne pollutants, further referred to as pollutants, all taking into account well-to-tank (WTT) and tank-to-wake (TTW) processes.

6.2.1. DESIGN SCENARIOS

Multiple reference design scenarios (1-3) and SOFC design scenarios (A-D) are defined in correspondence with two cruise shipyards. Although this does not ensure an optimally sized power plant, these are plausible scenarios from a functional perspective.

- Scenario 1 represents a conventional ship fully powered with MGO-fuelled diesel generators (DGs).

Table 6.1: Overview of installed components and fuel dimensioning for considered design scenarios. AUX = auxiliaries, MAN = manoeuvring.

DS	Design scenario	Installed power split		Fuel tank dimensioning	
		SOFC	GEN	MGO	LNG
1	DG	0%	100% (4 DGs)	All operations DG	-
2	DFG	0%	100% (4 DFGs)	Pilot fuel Range extender	Main operations
3	GG	0%	100 % (4 GGs)	-	All operations
A	SOFC AUX	P_{AUX}	Remainder (3 DFGs)	Pilot fuel Range extender	Auxiliaries SOFC Propulsion DFG
B	SOFC MAN	P_{AUX}+P_{MAN}	Remainder (3 DFGs)	Pilot fuel Range extender	AUX & MAN SOFC Remainder DFG
C	SOFC CRUISE	P_{AUX}+P_{PROP}	Remainder (3 GGs)	-	All operations
D	SOFC FULL	100%	0%	-	All operations

- Scenario 2 has a state-of-the-art power plant with dual fuel gensets (DFG) on MGO and LNG.
- In scenario 3, the use of MGO is eliminated and the ship is fully powered by gas generators (GG).
- Scenario A - SOFC AUX uses SOFCs solely for hotel and auxiliary power demands. The auxiliary (AUX) load is more continuous, even when the ship is berthed. This prevents the need to turn off the SOFCs and limits the required battery capacity.
- Design scenario B - SOFC MAN incorporates sufficient installed power for berthing and manoeuvring (MAN) operations, enabling navigation in ports or fjords with stringent pollutant emission regulations.
- In design scenario C - SOFC CRUISE, sufficient SOFC power is installed to accommodate power requirement for the propulsion and auxiliaries for regular cruise operations, while additional GGs are installed for high-speed cruising and to meet the overall power demand.
- Design scenario D - SOFC FULL fully relies on SOFCs for all operational requirements.

Consequently, design scenarios 3, C and D are LNG-only ship designs. An overview of the power split and required fuel storage is provided in Table 6.1.

Figure 6.2 shows which grid architectures correspond with the design scenarios. In this study, the grid architecture selection mainly influences the electrical conversion losses. For the reference scenarios, a conventional AC net has been selected as shown in Figure 6.2(a). For the full SOFC scenario, a DC architecture is selected, as shown in Figure 6.2(c). Fewer transformers and switchboards are needed to supply fuel cell power to a DC grid, improving system efficiency and lowering the size, weight, and cost of the system [199]. For the hybrid scenarios, the two architectures are combined, as shown in Figure 6.2(b). This makes it possible to avoid conversion losses for DC users, while still relying on off-the-shelf AC components for the main net. An AC-DC conversion efficiency of 96% is assumed while the DC-DC conversion is assumed at 98%.

6.2.2. COMPONENT SIZING MODEL

The installed capacity of the power-producing components is already presented in Table 6.1. An initial battery capacity is estimated assuming conservatively that the total power plant should have the same transient capabilities as dual-fuel gensets. Since the batteries should support energy as well as power supply, the battery capacity is established from both, see Equations 6.1 to 6.3.

$$E_{BAT,req} = \frac{P_{SOFC,installed}}{2 \cdot T_{trans,SOFC}} - \frac{P_{SOFC,installed}}{2 \cdot T_{trans,ENG}} \tag{6.1}$$

$$P_{BAT,req} = \left(T_{trans,ENG} - T_{trans,SOFC}\right) \cdot \frac{P_{SOFC,installed}}{T_{trans,ENG}} \tag{6.2}$$

$$E_{BAT} = \max\left(E_{BAT,req}; \frac{P_{BAT,req}}{C_{rate}}\right) \tag{6.3}$$

Where E_{BAT} is the battery capacity, P is the power, and T_{trans} is the transient capability of the power-generating component in percentage of total power per second. The C_{rate} is the rate at which the battery is charged or discharged, where 1C corresponds to discharge in an hour and 2C in two hours. The derivation of this equation can be found in the supplementary materials. The required heat-producing capacity of the boilers $\dot{Q}_{BOIL}$ is sized from the required heat demand and the heat produced by the SOFCs and gensets for every sail mode:

$$\dot{Q}_{BOIL} = \max\left(\dot{Q}^{s}_{load} - \dot{Q}^{s}_{ENG} - \dot{Q}^{s}_{SOFC}\right)_{s=sailmode} \tag{6.4}$$

Both the battery capacity and boiler capacity will be adapted to the actual requirements of the load profile using the dynamic simulation, which is described in Section 6.2.4.

The required fuel capacity is estimated using the end-of-life efficiency η_{EOL} of the power plant components and a 10% margin S_{fuel}. The estimation includes MGO and LNG consumption for gensets (also including pilot fuel), SOFCs and boilers. A generalised formulation of the calculation is shown in Equation 6.5.

$$E_{fuel} = \left(1 + S_{fuel}\right) \cdot \left(\frac{\frac{P_{component}}{P_{installed}} \cdot E_{max,fuel}}{\eta_{component,EOL}}\right) \tag{6.5}$$

Where $E_{max,fuel}$ is the energy required of the dedicated fuel to fulfil the range and endurance requirements as derived from the load profile.

The capacity of the various components is combined with an elaborate database of power density and energy density to estimate the required volume and mass of the different components according to Equations 6.6 to 6.7. The database (see Table 6.2) is

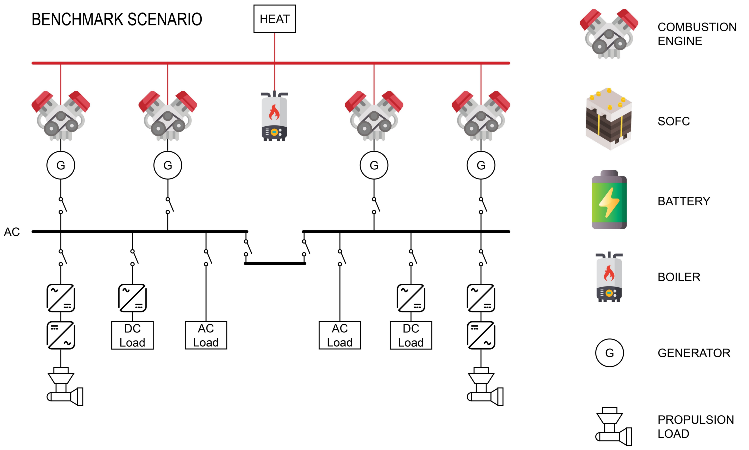

(a) Conventional AC grid architecture for design scenarios 1-3.

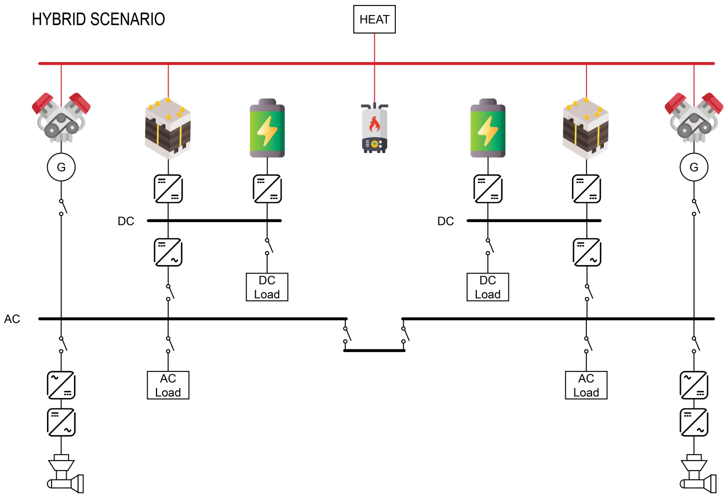

(b) Mixed grid architecture for hybrid power plant in design scenarios A-C.

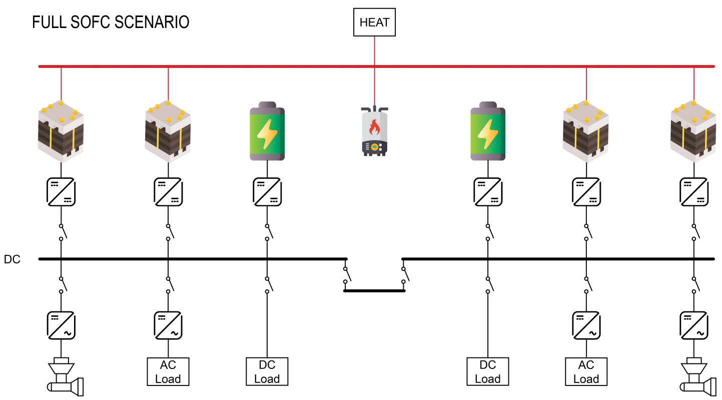

(c) DC grid architecture for fully fuel cell powered ship in design scenario D.

Figure 6.2: Grid architectures for all the different design scenarios.

6

Table 6.2: Used data to estimate component size and weight. The energy density of the fuel also includes storage equipment.

Variable	Component	Fuel	Value	Unit	Source
p_{vol}	SOFC	LNG	15	kW/m^3	[1, 169, 326]
p_{grav}	SOFC	LNG	25	kW/ton	[1, 169]
p_{vol}	DG	MGO	45	kW/m^3	[1]
p_{grav}	DG	MGO	60	kW/ton	[1]
p_{vol}	DFG	Both	40	kW/m^3	Wartsilla, MAN, CSI
p_{grav}	DFG	Both	50	kW/ton	Wartsilla, MAN, CSI
p_{vol}	GG	LNG	40	kW/m^3	Same values as DFG
p_{grav}	GG	LNG	50	kW/ton	Same values as DFG
p_{vol}	BOIL	MGO	104	kW/m^3	[27]
p_{grav}	BOIL	MGO	360	kW/ton	[27]
p_{vol}	BOIL	LNG	75	kW/m^3	Alfa Laval
p_{grav}	BOIL	LNG	310	kW/ton	Alfa LAval
e_{vol}	BAT (Li-ion)	-	90	kWh/m^3	[27]
e_{grav}	BAT (Li-ion)	-	80	kWh/ton	[27]
e_{vol}	-	MGO	8200	kWh/m^3	[28]
e_{grav}	-	MGO	8300	kWh/ton	[28]
e_{vol}	-	LNG	3443	kWh/m^3	[348]
e_{grav}	-	LNG	8050	kWh/ton	[348]

established from literature and supplier data. To ensure the integrity of this dataset, a consistent scope of the needed auxiliary components was essential.

$$V_{component} = \frac{P_{component}}{p_{vol,component}} \tag{6.6}$$

$$m_{component} = \frac{P_{component}}{p_{grav,component}} \tag{6.7}$$

6.2.3. POWER PLANT SIMULATION MODEL

This section describes how the power plant components and the energy management strategy are modelled. Matlab Simulink© is used for the time-domain simulations.

SOFC MODEL

Haseltalab et al. [169] used an isothermal plug flow reactor to calculate the current-voltage characteristics and fuel consumption of the SOFC stack for different loads. They modelled the transient response by limiting the rate of change of the stack current. Constant and load-dependent loss terms account for the parasitic consumption of auxiliary components. This model is adapted by including differences in heat loss and fuel utilisation in part-load conditions. Because of a difference in stack temperature, the heat losses cannot be assumed constant. Moreover, SOFC systems are often operated at lower fuel

Table 6.3: Used parameters for simulation model.

General	Parameter	Value	Unit
Lower heating value MGO	LHV_{MGO}	42800	kJ/kg
Lower heating value LNG	LHV_{LNG}	50000	kJ/kg
CO_2 equivalent methane	$CO_2\text{-}eq_{CH4}$	25	-
Safety margin fuel capacity	S_{fuel}	10%	-
SOFC			
Nominal voltage at BOL	$V_{cell,BOL}$	0.85	V
Nominal voltage at EOL	$V_{cell,EOL}$	0.71	V
Max current change rise	R	2% of P	/min
Max current change fall	F	8% of P	/min
Transient threshold	T_{thold}	0.03%	/min
Transient factor	a_{trans}	1.5	-
Nominal stack lifetime	L_{SOFC}	30000	h
Genset			
Transient capability on MGO	$T_{trans,MGO}$	2.7% of P	/s
Transient capability on LNG	$T_{trans,LNG}$	1.4% of P	/s
Generator efficiency	η_{gen}	95%	-
Amount of pilot fuel for DFG	p_{DFG}	3%	-
Lower load limit	LL	10%	-
Battery			
Charge efficiency	η_{ch}	90%	-
Discharge efficiency	η_{dis}	95%	-
Max C-rate	C_{rate}	3	-
Initial SOC	SOC_{init}	0.55	-
Upper bound SOC	SOC_{UB}	0.9	-
Lower bound SOC	SOC_{LB}	0.2	-
Safety margin	S_{BAT}	10%	-
Boiler			
Boiler efficiency - MGO	η_{MGO}	85%	-
Boiler efficiency - LNG	η_{LNG}	90%	-
Other			
Converter efficiency DC|DC	$\eta_{DC\|DC}$	98%	-
Inverter efficiency AC|DC	$\eta_{AC\|DC}$	96%	-

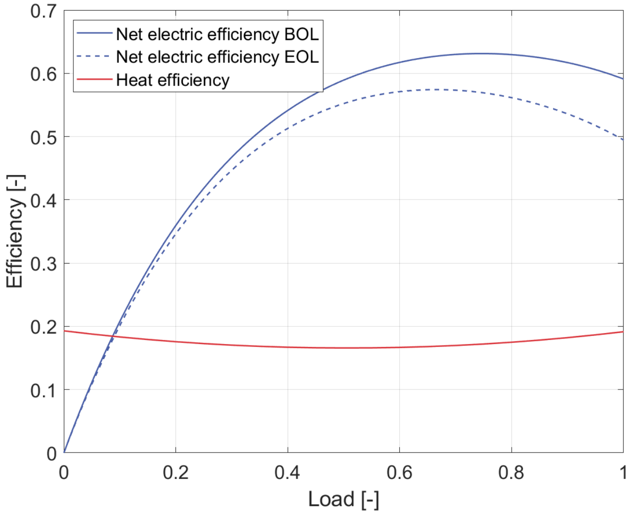

Figure 6.3: Net electricalefficiency (DC) and heat efficiency of SOFC system at beginning-of-life and end-of-life. The model of this study (green) is adapted from Haseltalab et al. [169], which is shown in blue.

utilisation at part-load in order to feed additional fuel to the burner to ensure sufficient heat supply to the stack. This adaptation makes the net-efficiency curve (see Figure 6.3) correspond better with published data of commercial SOFC systems [349]. Additionally, a distinction is made between the allowed current density rate during ramp-up and ramp-down, which is formulated in Equation 6.8. Transient SOFC experiments showed a four times higher ramp-down rate (see Table 6.3), because the temperature change in the cells is more uniform than during ramp-up [350] The heat efficiency is based on supplier data of the available heat in the exhaust stream. Although the heat efficiency is assumed to be constant over its lifetime (see Figure 6.3), the delivered heat increases, because more fuel is fed to the SOFC due to the decrease in electrical efficiency. It is assumed that heat can only be recovered up to 100 °C for the hot water and steam net [294], which explains why the heat efficiency is slightly lower than reported by SOFC system manufacturers. The specific emissions of the SOFC are based on literature and reported in supplementary materials.

$$u(t) = \begin{cases} u(t) = \Delta t \cdot R + i(t-1) & \text{if i'> R} \\ u(t) = -\Delta t \cdot F + i(t-1) & \text{if i'< F} \\ u(t) & \text{else} \end{cases} \tag{6.8}$$

Where i is the input, u the output, t the time, R the rising slew rate, and F the falling slew rate.

A novel approach is used to include the degradation effects. Decreasing cell voltage reduces the rated power and efficiency at a specific current density. However, when constant power output is required, the current density must be increased along the i-V curve, further decreasing voltage and thus efficiency [273]. Moreover, a rise in current density increases the degradation rate [351]. To incorporate this, a degradation resistance term is added to calculate the power of the fuel cell:

$$P = V_{cell} \cdot I = \left(V_0 - I\left(R + R_{deg}\right)\right) \cdot I \tag{6.9}$$

Where V_{cell} is the cell voltage, R is the cell resistance, and R_{deg} is the additional resistance due to degradation effects. Solving for the current I yields,

$$I = \frac{V_0 + \sqrt{4P\left(R + R_{deg}\right) - V_0^2}}{2\left(R + R_{deg}\right)} \tag{6.10}$$

Load cycles reduce lifetime, while degradation is lower at part-load operation since the SOFC is operated at a lower current density. The load-dependent degradation formulation is retrieved from Abreu-Sepulveda et al. [352], who define the degradation rate as a function of the current density i. The function is fitted to the lifetime projected by the SOFC system manufacturer. The degradation model also detects whether the change rate of the current is above the threshold for transient operation T_{thold}, which adds a multiplication factor a_{trans} to the degradation rate, see Equation 6.11.

$$r_{deg} = a_{trans} \cdot 0.0573 \cdot e^{1.25i} \quad \left[\%.\eta_{net}/1000h\right] \tag{6.11}$$

6

The degradation rate is integrated over time to find the increase in cell resistance needed for Equation 6.10. The state of health SOH is defined from the current cell voltage V_{cell} and the voltage at beginning of life (BOL) and end of life (EOL), see Equation 6.12. SOH is usually defined for a constant current density. In this research, SOH is defined at nominal load P_{nom}, since the current density increases over its lifetime to maintain constant power.

$$SOH = \frac{V_{cell}\left(P_{nom}\right) - V_{cell,EOL}\left(P_{nom}\right)}{V_{cell,BOL}\left(P_{nom}\right) - V_{cell,EOL}\left(P_{nom}\right)} \tag{6.12}$$

GENSET MODEL

The ICE genset is modelled with look-up tables for the efficiency and emissions as a function of the load, see Figure 6.4(a) and the supplementary materials respectively. The efficiency and emissions include a constant generator efficiency of 0.95. The dynamic behaviour is captured with a rate limiter (Equation 6.8) on the load and a minimum load of 10% per engine is implemented. The performance depends on the engine type, as defined by the design scenario (Table 6.1). For the DFG model, 3% pilot fuel is assumed. The allowable load changing rate of gas engines is usually lower than diesel-fuelled engines, see Table 6.3. For this reason, DFGs usually switch to MGO operation during rapid load changes, which is included with the following logic:

$$u = \begin{cases} \text{MGO mode} & \text{if i'>T}_{trans,LNG} \\ \text{Gas mode} & \text{else} \end{cases} \tag{6.13}$$

Wear and fouling of engine components is included in the simulation model as an increase in fuel consumption during running hours, as prescribed by Cichowicz et al. [342] in Figure 6.4(b).

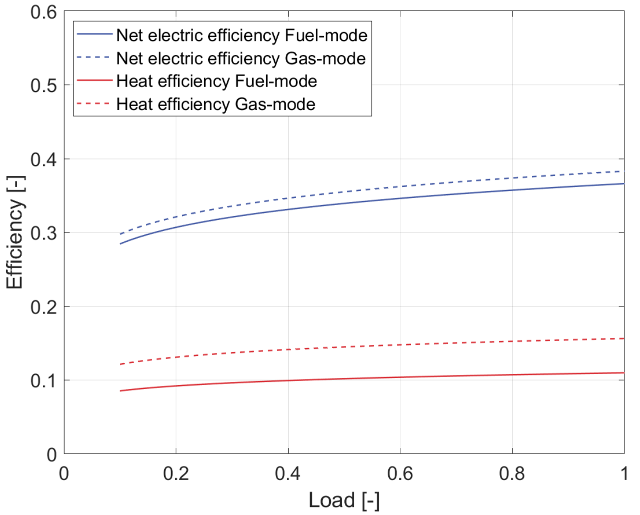

(a) Electrical efficiency of gensets for MGO and LNG, based on Wärtsilä 34DF [169]. Electrical efficiency includes generator efficiency. Heat efficiency retrieved from Sheykhi et al. [353]

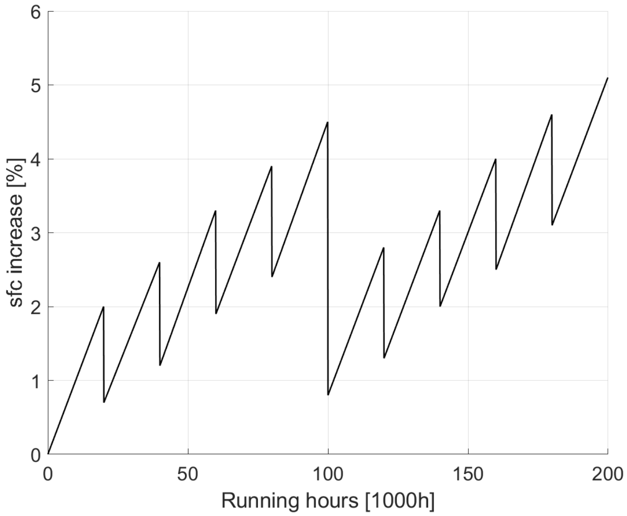

(b) Increase in specific fuel consumption due to wear and fouling of engine components. The small and large peaks are due to small and large engine overhauls [342].

Figure 6.4: Engine performance maps.

6

Table 6.4: Number of cycles in battery life for depth of discharge and charge rates [355].

DoD	**Cycles in battery life**			
	0.5C	**1C**	**2C**	**3C**
0.2	2127	2540	-	-
0.6	1634	1654	-	-
1	429	429	739	571

BATTERY MODEL

The battery model is based on a power and energy balance model that includes cycle efficiency and degradation effects. The available power is denoted as the current battery capacity times the maximum C_{rate}:

$$P_{BAT,max} = C_{rate} \cdot E_{BAT} \tag{6.14}$$

This equation neglects the decrease in battery capacity at higher C-rates but this is usually small. The battery degradation is modelled as a superposition of cyclic ageing and calendar ageing. The calendar ageing is independent of the battery current [343]. An algorithm detects whether the battery is in use or idle and applies the cyclic ageing data or the calendar ageing data respectively. Ali et al. [354] proposed a calendar ageing model based on temperature and SOC, substantiated by literature and an extensive experimental campaign. The degradation rate is defined with the derivative of the calendar ageing for NMC Li-ion batteries, as shown in Equation 6.15.

$$r_{deg,cal} = 0.03304e^{0.5036SOC} \cdot 385.3e^{-2708T} \cdot 0.51\,t^{-0.49} \tag{6.15}$$

Where T is the temperature in Kelvin and t is the time in days. The degradation due to cycling is based on a multi-year study for 18650 commercial battery cells [355]. The equivalent full cycles for 20% capacity reduction are formulated as a function of the depth of discharge (DOD) and the C_{rate}, as shown in Table 6.4. The equivalent cycles are calculated with the rainflow algorithm, which is often used for battery degradation with varying DODs [356]. Finally, the capacity degradation is estimated at every timestep by superposition of the degradation rate for calendar ageing and cycle effects. This is used to estimate the number of required battery replacements.

BOILER MODEL

Three boiler models are implemented: oil-fired, gas-fired, and dual-fuel boiler, dependent on the bunker fuels in the dedicated design scenario (see Table 6.1). The boiler is modelled as an instantaneous heat source supplying the difference between the load and the heat-producing components, as defined in Equation 6.16.

The heat efficiency and specific emissions are assumed to be load-independent, which can be justified because the boilers are only responsible for a minimal share of fuel consumption and ship emissions. Furthermore, no load transients are applied to the boiler.

$$\dot{Q}_{BOIL} = \dot{Q}_{load} - \dot{Q}_{ENG} - \dot{Q}_{SOFC} \tag{6.16}$$

ENERGY MANAGEMENT STRATEGY

The SOC-based energy management strategy has been adapted from Ünlübayir et al. [357] and is shown in Figure 6.5(a). It has been implemented to divide the load over the SOFCs, gensets and batteries. The hierarchical sequence of the control system prioritises the SOFC, followed by the gensets, with the battery as the third priority. A low-pass filter is applied to the load of the SOFC system. It only passes signals below the cut-off frequency, removing rapid load demand changes. The cut-off frequency is determined based on the transient capabilities of the SOFC and gensets and implemented with transfer function 6.17.

$$T(s) = \frac{1}{1 + \frac{1}{\omega_0}} \tag{6.17}$$

The SOFC load is also limited to the installed power of the SOFCs and the remaining higher frequency signal is the resulting load for the gensets (see Equation 6.18). The SOFC model and genset model include the transient behaviour of both components. The actual produced power is compared with the load and the difference is requested from the batteries (see Equation 6.19). The load is artificially increased or decreased to attain the desired SOC for the battery. The initial and target value is set at 0.55, giving the greatest flexibility for discharging or charging the battery at any specific moment. The load is increased with Equation 6.20, increasing proportionally with the deviation from the target SOC. Meanwhile, a double hysteresis control has been implemented to prevent rapid cycling of the SOFC around the charge limits of the battery. For instance, for low SOC, the battery starts charging at SOC_{L1} and stops charging at SOC_{L2}. Figure 6.5(b) demonstrates the power distribution between the SOFCs, the engines, and batteries during berthing, manoeuvring and cruising for design scenario SOFC MAN. The SOFC (green) slowly follows the load up to the maximum installed power, and is compensated by the battery (blue). The gensets (black) are only used when needed and supply power above the installed power limit of the SOFC.

$$P_{ENG,req} = P_{load} + P_{add} - P_{SOFC,req} \tag{6.18}$$

$$P_{BAT,req} = P_{load} + P_{add} - P_{SOFC,act} - P_{ENG,act} \tag{6.19}$$

$$P_{add}(t) = (SOC_{L2} - SOC(t)) \cdot a_{SOC} \cdot E_{BAT} \cdot C_{rate} \tag{6.20}$$

The recoverable heat produced from SOFCs and gensets is compared with the heat load and complemented by firing the boilers. Excess heat is expelled from the ship through the exhaust stream.

6

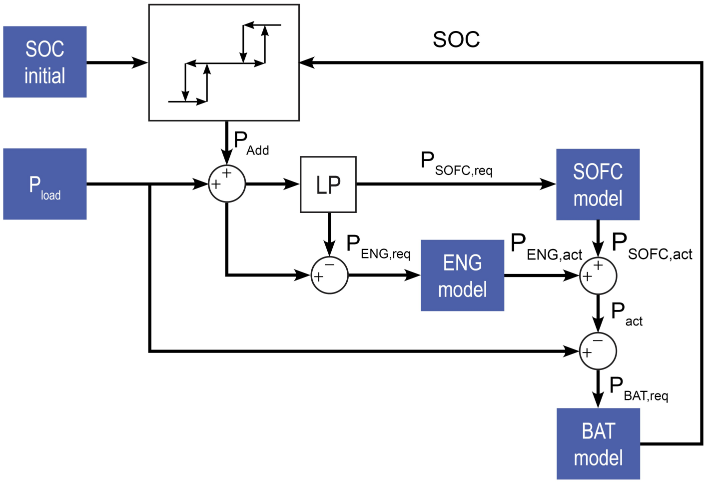

(a) Control architecture of energy management strategy.

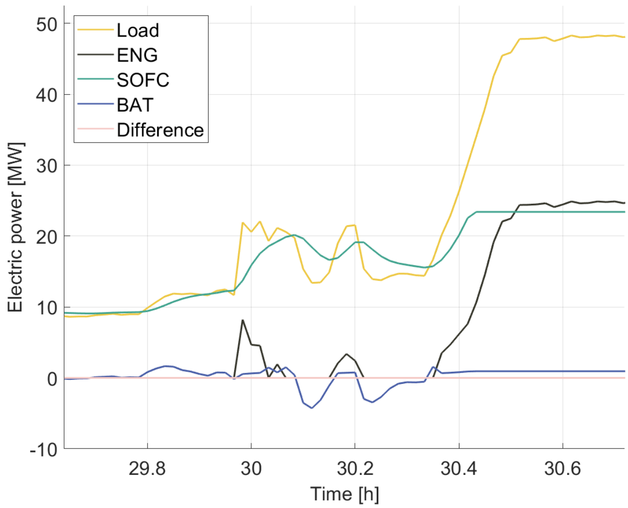

(b) Demonstration of energy management strategy during short interval of operational profile for design scenario B - SOFC MAN.

Figure 6.5: Control of SOFC systems, gensets, and battery SOC management.

6.2.4. ADAPTATION OF BATTERY AND BOILER COMPONENTS

The initial sizing of both the battery and the boiler is necessary to run the simulation. Subsequently, the simulation outcomes are used to validate the precision of these estimations. The required power and energy capacity of the battery and boiler are compared with the constraints imposed by the installed components (Equations 6.21 and 6.23 for the battery). This comparison yields a utilisation ratio u, which is used to resize the battery, including a 10% safety margin as shown in Equation 6.24. A similar formulation is used to resize the boiler.

$$u_{SOC,LB} = \frac{\min(SOC(t)) - SOC_{target}}{SOC_{LB} - SOC_{target}} \tag{6.21}$$

$$u_{SOC,LB} = \frac{\min(P_{BAT}(t))}{E_{BAT,init} \cdot C_{rate}} \tag{6.22}$$

$$u_{BAT} = \max\left(u_{SOC,LB};\ u_{SOC,UB};\ u_{P,LB};\ u_{P,UB}\right) \tag{6.23}$$

$$E_{BAT,adapted} = (1 + S_{BAT}) \cdot E_{BAT,init} \cdot u_{BAT} \tag{6.24}$$

6.3. RESULTS

6

The component sizing model and power plant simulation model are applied to a cruise ship. The main particulars and load profiles are supplied by a shipyard and scaled to the size of a fictive cruise ship for confidentiality purposes using the cruise ship database presented in Veldhuizen [37]. Its main particulars are summarised in Table 6.5. The load profile consists of a week of cruise operation with daily port calls. Yearly the ship performs 48 cruise travels and two transatlantic journeys. First, one week is simulated to assess the initial sizing of the battery and boiler, followed by a five-year simulation to fully account for the degradation effects within one dry docking maintenance interval. All time-domain simulations use a step size of 60 seconds and Figure 6.6 shows an overview of the inputs, simulation order, and outputs. The applied component models, energy management strategy, and degradation formulations provide a relatively low-computational model. Five years of power plant operation are simulated in 10.4 hours.

6.3.1. VOLUME AND MASS OF POWER PLANT

This section contains the results of the component sizing model. Figures 6.7(a) and 6.7(c) show that increasing the number of installed SOFC systems requires more space and mass for power-producing components due to a lower power density, which is similar to results presented by Li et al. [338]. However, when including volume for fuel storage, the volume increase diminishes for higher installed SOFC power, see Figure 6.7(b). The power plant of SOFC FULL is 162% larger than the DFG power plant, while the total volume for the power plant and fuel storage is 27% higher. The power plant of SOFC FULL is 104% heavier compared to DFG, but when fuel storage is included the weight is 14% less. This is due to the high conversion efficiency of SOFCs, which reduces the required fuel storage size to meet range requirements. It is also interesting to note

Table 6.5: Main particulars of ship used for case study.

	Cruise ship	Unit
Length	292	m
Width	38.3	m
Draft	8.7	m
Passengers	4000	-
Crew	1600	-
Installed power	75000	kW
- Auxiliaries	13125	kW
- Manoeuvring	23400	kW
- Main operations	38400	kW

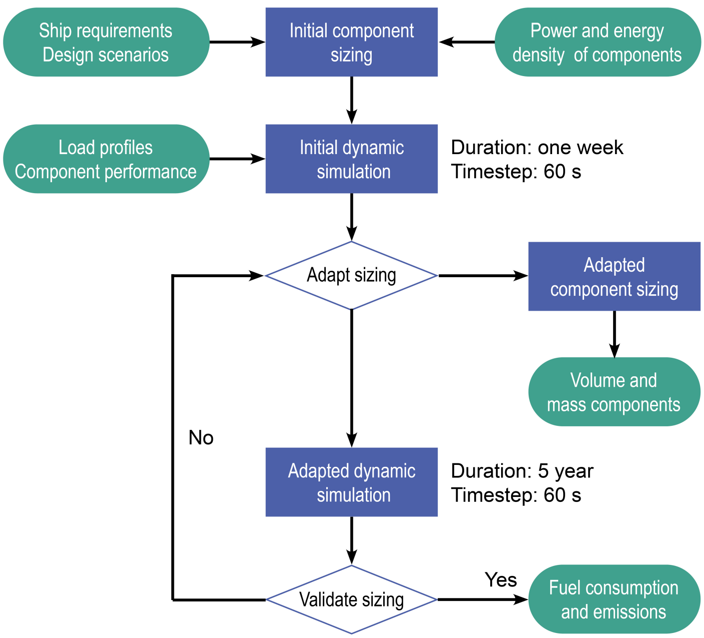

Figure 6.6: Flowsheet of simulation steps including timestep and duration.

Table 6.6: Reduction in battery capacity with respect to initial estimation.

DS	Design Scenario	Initial BAT capacity [kWh]	Adapted BAT capacity [kWh]	BAT reduction
A	SOFC AUX	4210	2200	48%
B	SOFC MAN	7506	5465	27%
C	SOFC CRUISE	18321	10444	43%
D	SOFC FULL	24059	7736	68%

that all SOFC scenarios have a smaller power plant than a fully LNG-powered ship using solely gas engines. Moreover, the mass of the total power plant of design scenarios SOFC CRUISE and SOFC FULL is lower than the conventional options as shown in Figure 6.7(d), due to the weight of MGO.

The presented results are generated using the adapted battery and boiler capacity (see Section 6.2.4). The change in battery capacity is shown in Table 6.6. Large reductions in battery capacity are realised using dynamic simulations. This highlights the importance of a detailed power plant simulation model to prevent over or under-dimensioning of auxiliary components. The change in mass and volume of the power plant was minor, as the boiler capacity partially offset the alteration, and the boiler and battery constitute only a small portion of the overall power plant.

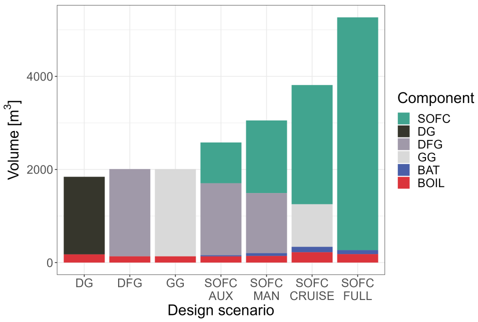

(a) Volume of power plant.

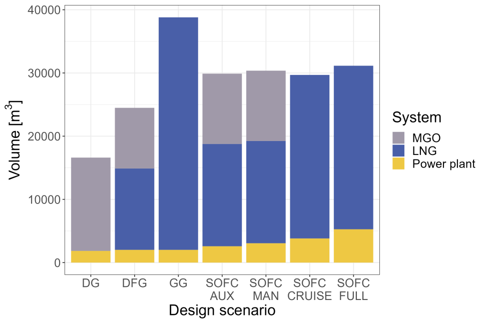

(b) Volume of power plant and fuel storage.

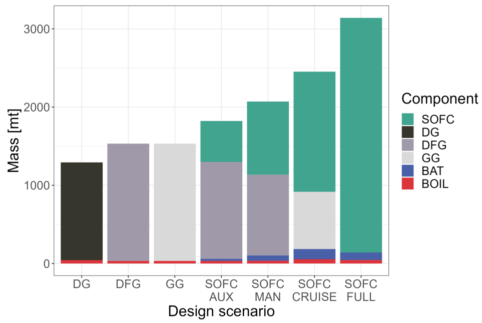

(c) Mass of power plant.

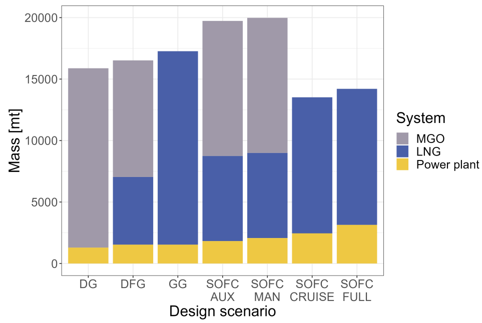

(d) Mass of power plant and fuel storage.

Figure 6.7: Sizing of power plant after adapting boiler and battery capacity. The left graphs form the yellow part of the right graphs.

6.3.2. POWER AND ENERGY BALANCE

The first week of the adapted simulation is visualised in Figure 6.8 and 6.9. Figure 6.8 illustrates the power output of the components. In 6.8(a) and 6.8(b), the SOFCs follow the load and gensets supplement power beyond the SOFCs' capacity. For design scenario SOFC CRUISE, the gensets are required intermittently during significant fluctuations in propulsion demand. The variation in battery power is much lower when the SOFCs are only used for the auxiliary power, which corresponds with the smallest required battery capacity of design scenario SOFC AUX in Table 6.6. Figures 6.8(c) and 6.8(d) clearly illustrate a distinction between the load and the produced power. These represent the power conversion losses, which are lower for design scenario SOFC FULL, because a full DC grid is used.

Notably, the largest peaks in battery power occur when the ship slows down, storing power in the batteries, despite the SOFCs' allowable ramp-down current rate being four times higher than the ramp-up limit. The used load profile is derived from an engine-operated ship and is managed accordingly. Reducing the speed more gradually could lower the required battery capacity. The implications of changing ship requirements are discussed extensively in Section 6.4.1.

When the transient capability is insufficient to meet a change in the load profile, batteries provide additional power. As can be seen in Figure 6.9(a), batteries are consistently used for load-smoothing, with significant demand only during changes in ship speed. Consequently, battery cycling is limited and battery lifetime is preserved. The effectiveness of the energy management strategy is evident, SOC of the batteries remains mostly between 0.4 and 0.6.

The heat load and production are shown in Figure 6.9(b). Although the full boiler capacity is rarely used, a significant amount of boiler capacity is needed throughout the cruise operation, as the SOFCs and gensets do not generate enough heat to fulfil the load profile. Occasionally, there is a large amount of unused heat, but it is not consistent enough to justify additional heat recovery systems.

For all simulated design scenarios, the modelled power plant fully meets the electrical and heat load profile.

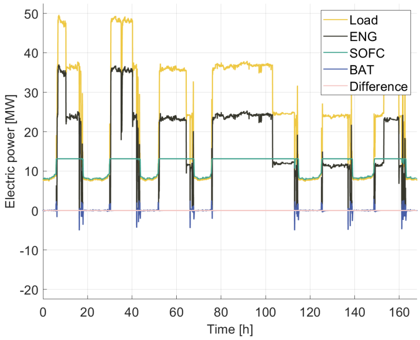

(a) Design scenario SOFC AUX.

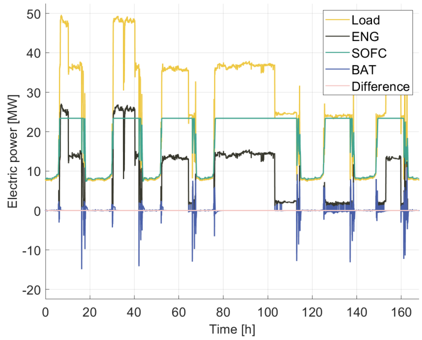

(b) Design scenario SOFC MAN.

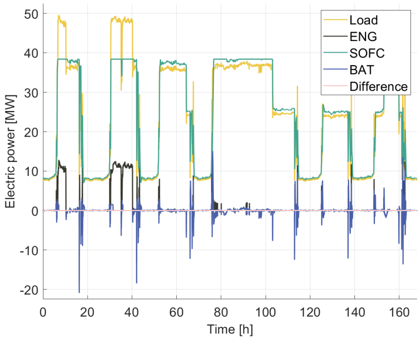

(c) Design scenario SOFC CRUISE.

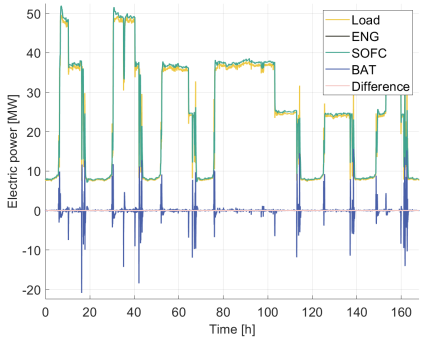

(d) Design scenario SOFC FULL.

Figure 6.8: Delivered power by components for SOFC scenarios during the first week of the simulation.

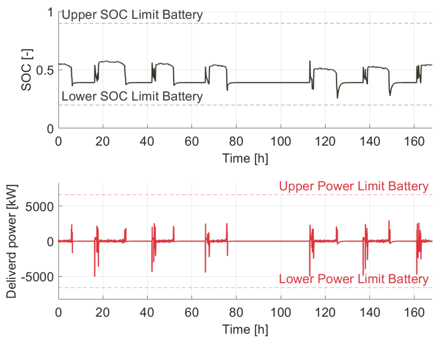

(a) Battery Power and SOC for design scenario SOFC AUX.

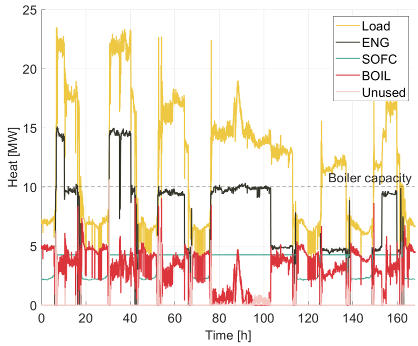

(b) Delivered heat by components for design scenario SOFC AUX.

Figure 6.9: Battery operation and heat balance for design scenario SOFC AUX during the first week of simulation.

Table 6.7: Overview of SOFC and battery degradation after 5-year simulation.

DS	Design scenario	SOFC SOH	BAT replacements
A	SOFC AUX	0.08	1.49
B	SOFC MAN	0.19	1.65
C	SOFC CRUISE	0.19	0.90
D	SOFC FULL	0.47	1.10

6.3.3. DEGRADATION EFFECTS

The degradation speed of SOFCs and batteries varies with loading and cycling conditions across the design scenarios. Table 6.7 and Figure 6.10 show the degradation of these components after five years. The remaining SOH of the SOFCs is 0.47 for design scenario SOFC FULL, which is the highest among the design scenarios. This is the case because the degradation is a function of the current density (see Equation 3.1) and the SOFCs are mostly operated at part-load. Although the load of SOFC AUX is more stable, the remaining SOH of 0.08 is the lowest for this scenario. Apparently, the load-dependent degradation dominates the consequences of transient operation. For all design scenarios, the observed degradation of SOFCs accelerates over their lifetime, because the current density gradually increases to maintain the rated power. The degradation analysis reveals that all scenarios finish five years of operation before stack replacement, although thermal cycles are not considered. Implementing additional power capacity, as in the SOFC FULL design scenario, can extend the overall system's lifespan by operating the stacks at a lower current.

6

The battery requires replacement 0.9 to 1.65 times within five years across different design scenarios. This exceeds expectations, as marine battery suppliers typically claim a lifespan of 5 to 10 years, corresponding to 2000 to 3000 equivalent cycles [358]. However, this holds only for low C_{rate}, while the SOFC system's slow transient response needs high battery power output. Installing additional batteries could reduce the required C_{rate}, therefore extending the battery's cycle life, although this increases volume and cost. The fastest degradation occurs in the SOFC MAN design scenario, due to high C_{rate} and large DOD during manoeuvring operations. The SOFC CRUISE scenario reaches the five-year operational interval.

6.3.4. FUEL CONSUMPTION AND EMISSIONS

Figure 6.11 shows the fuel efficiency and consumption across the design scenarios during five years of operation. For design scenarios DFG, SOFC AUX, and SOFC MAN, there is some MGO consumption as pilot fuel. The average fuel efficiency increases with greater use of SOFCs. Nevertheless, the fuel consumption is higher for the fully SOFC-powered ship. This is the case because all SOFCs are operated on the same load. With a higher installed SOFC power, especially in berth, this leads to a significantly lower conversion efficiency. This limitation of the simulation model will be further discussed in Section 6.4.2. Overall, all four SOFC scenarios result in a major fuel consumption reduction, compared to the reference scenarios. Although the boiler's fuel consumption slightly increases with more SOFC usage, this is negligible compared to the gains in elec-

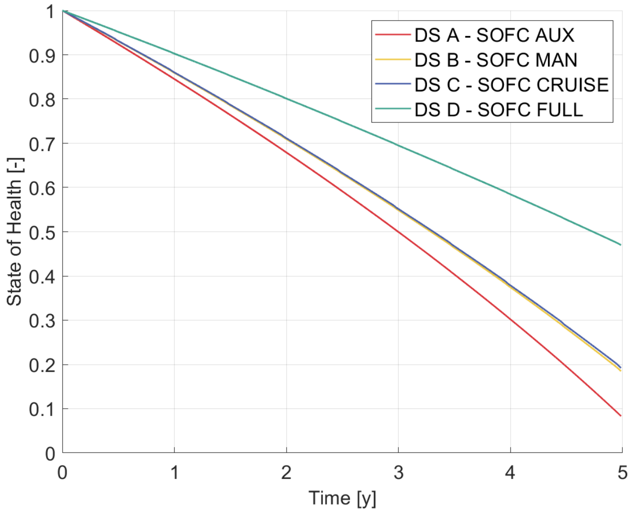

Figure 6.10: State of health of SOFC stacks for different design scenarios during 5-year simulation.

6

trical efficiency, as shown in 6.11(b).

Figure 6.12 illustrates the GHG, NO_X, SO_X, PM and CO emissions for the design scenarios during 5 years of operation. WTT emissions are also included if reliable data was available. Figure 6.12(a) shows that adapting to LNG only reduces GHG emissions by a little compared with MGO-fuelled gensets. Although the WTT emissions are lower for LNG, methane slip in current engines is high, especially at part-load conditions. Using SOFCs solely for auxiliary loads significantly reduces GHG emissions. Additionally, the reduction in fuel consumption leads to a decrease in WTT emissions. However, in design scenario SOFC FULL, GHG emissions increase, corresponding with the rise in fuel consumption. Compared with diesel generators, all SOFC scenarios result in a GHG reduction of over 30%, complying with the IMO target to reduce GHG emissions by 30% by 2030 [9]. None of the SOFC scenarios reach the 80% reduction target set for 2040. Renewable fuels could be applied to further decrease GHG emissions.

LNG-fuelled gensets emit significantly less NO_X and particularly SO_X emissions compared to MGO-fuelled gensets, although dual-fuel and gas engines produce higher PM and CO emissions. All pollutant emissions of SOFCs are minimal, thus the NO_X, SO_X, PM and CO emissions in design scenarios SOFC AUX, SOFC MAN and SOFC CRUISE mainly originate from the gensets. In design scenarios SOFC CRUISE and SOFC FULL most pollutant emissions are eliminated.

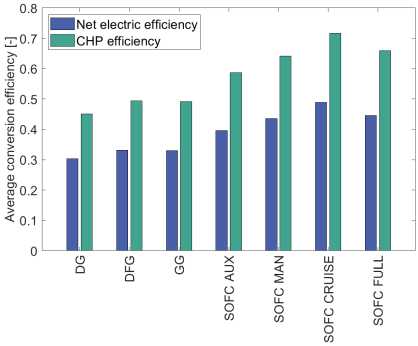

(a) Fuel efficiency.

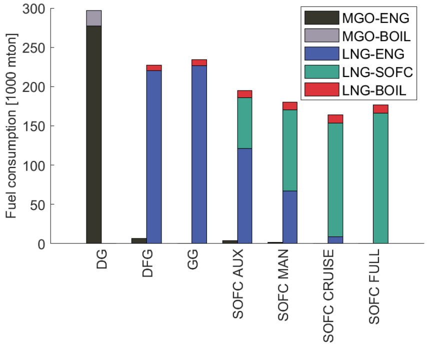

(b) Fuel consumption.

Figure 6.11: Fuel efficiency and consumption of simulated power plants for five years of operation.

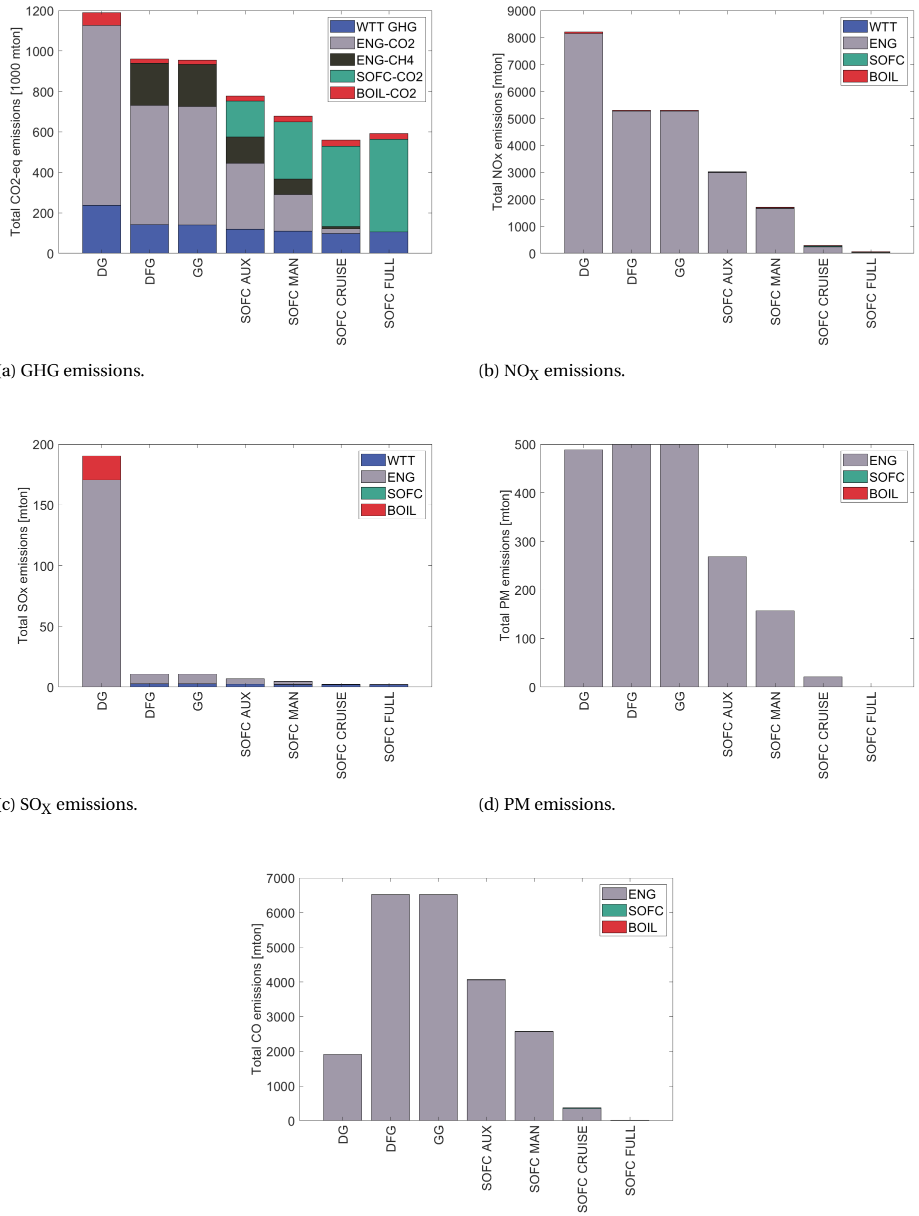

(a) GHG emissions.

(b) NO_X emissions.

(c) SO_X emissions.

(d) PM emissions.

(e) CO emissions.

Figure 6.12: Greenhouse gas and pollutant emissions of simulated power plants for defined design scenarios.

6.4. Discussion

This section reflects on the validity of the simulation model. First, potential changes in the ship's requirements for an SOFC ship are discussed. Subsequently, the limitation of the model concerning part-load operation is addressed. Finally, the applicability of the model to other ship types and load profiles is assessed.

6.4.1. Range and installed power requirements

The analysis of various design scenarios revealed that accommodating the proposed power plant would be challenging without sacrificing valuable space. Introducing low-power-density technologies, like SOFCs, and low-energy-density fuels, often stored in large cryogenic tanks, leads to a reevaluation of ship design requirements. Conventional ships typically have tank storage designed for high range and endurance, yet in practice, much of this space remains unused. In this study, it was found that only 20% to 60% of the stored fuel across the design scenarios, as estimated based on a 20-day endurance criterion, was required to fulfil the operational profile. The sensitivity analysis in Figure 6.13 shows that the volume of the whole power plant strongly reduces for lower endurance requirements.

Moreover, maximum installed power requirements are often based on redundancy needs. For example, with four engines divided between two main vertical zones, losing one zone still requires sufficient power for a safe return to port. Fuel cells, when installed in a decentralised manner, can enhance redundancy and potentially reduce the overall installed power requirements. Additionally, the battery SOC approached its limit during slowdown phases, as SOFCs temporarily produced excess power. To address this, reducing speed earlier and more gradually could decrease the necessary battery capacity.

In this study, operational requirements were kept constant to ensure a fair comparison of design scenarios. However, aligning ship requirements more closely with the operational profile and power plant components could significantly reduce the size and cost of the power plant. This approach, though, would diminish the operational flexibility of the ship. Ship owners must carefully consider whether reduced ship requirements would render the vessel less versatile for varying scenarios.

6.4.2. Advanced energy management

In scenario D, where only SOFCs are installed, fuel efficiency is lower compared to scenario C, which has just enough power to fulfil all main operations. This inefficiency arises because all SOFCs operate at the same load. Higher installed power at part-load results in lower conversion efficiency (Figure 6.3), particularly at berth, where the electrical load represents only 10% to 15% of the installed power. Although these results align with the simulation model, this is unlikely to reflect real power plant operations. To avoid low conversion efficiency at low loads, a fully SOFC-powered plant would likely control groups of SOFC modules, turning them on or off as needed. Optimising this control strategy is an interesting area for future research, focusing on fuel consumption, emissions, and lifetime conservation. However, cold starts take up to 24 hours and thermal cycles impact lifespan significantly [359]. Alternatively, groups of SOFC modules could run on hot stand-by, avoiding thermal cycles but consuming some parasitic fuel to maintain temperature. Consequently, such a control strategy would require complex

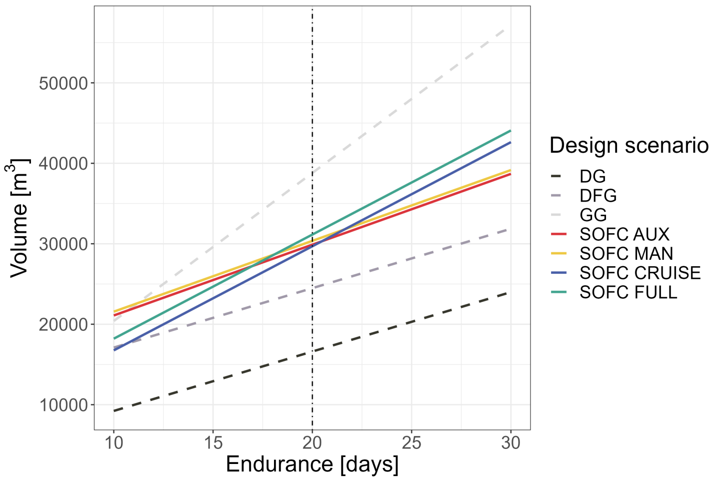

Figure 6.13: Sensitivity analysis of ship endurance on and volume of the power plant and fuel storage combined.

optimisation with many decision variables, warranting a separate study. Once developed, this control could be implemented in the power plant simulation.

6.4.3. APPLICABILITY OF SIMULATION MODEL

Since the simulations are executed for a specific ship, the transferability of the results is questionable. Nevertheless, the scientific relevance lies in the method, which can be directly applied to other cruise ships. Cruise ships are investigated due to their significant thermal load and relatively high and constant auxiliary load. However, the developed framework and simulation model are adaptable to other ship types. The study's findings indicate that heat recovery does not offer improvements over gensets, suggesting that high thermal demand is not a prerequisite for efficient SOFC operation. Nevertheless, other ship types differ in their load profile. For example, dredgers have highly variable auxiliary load profiles and frequently use flywheels for energy storage. Such components can be incorporated into the simulation framework, though the results should be invalidated. The research further demonstrated that the required battery capacity and SOFC degradation are smaller when operating under a relatively constant load profile, as in scenario SOFC AUX. Therefore, ship applications with a stable load profile, such as deep-sea cargo and container ships are recommended for SOFC integration.

The study also shows that significant emission reductions are achievable with LNG-fuelled SOFCs. Nevertheless, LNG remains a fossil fuel with considerable carbon emissions. The marine industry is exploring several alternative fuels, such as methanol, hydrogen, and ammonia, as green alternatives. These could be integrated into the simulation framework if reliable sizing, efficiency, and emission data of SOFCs fuelled with alternative fuels are available. This study excluded these fuels due to the lack of such data.

6.5. CONCLUSION

The performance of a marine SOFC power plant is evaluated on size, weight, fuel consumption, and emissions. Four LNG-fuelled SOFC design scenarios are compared using an iterative component sizing and time-domain power plant model. The power plant components (SOFC, gensets, battery, and boilers) and their degradation are modelled in Matlab Simulink© and an SOC-based control strategy is used to allocate the requested power. A large cruise ship serves as case study, using five years of electrical and heat load profiles. The applied iterative sizing and dynamic simulation method emphasises the importance of time-domain simulation for adequate power plant sizing. The battery capacity was reduced by 27% to 68% while the boiler capacity had to be increased. Simulations confirm that the degradation rate of the SOFC system depends greatly on its operation. The remaining state of health was lowest for design scenario SOFC AUX, meaning the degradation is more heavily influenced by the load level than the fuel cell's modulation for the evaluated load profile.

Installing more SOFCs strongly increases the size and mass of the power installation. However, this increase is partly offset by a reduction in fuel storage due to the high conversion efficiency. This becomes most relevant for ships with high range and endurance requirements. Compared with the reference scenarios, the SOFC scenarios increase fuel efficiency by 19% to 59%. All design scenarios result in significant emission reductions. Design scenario SOFC AUX minimally impacts capital costs and power plant design, making it economically advantageous. Compared with dual-fuel gensets, a 21% GHG reduction and 38% to 46% reduction across the reported pollutants is obtainable with only 17.5% of installed SOFC power. This is possible because of improved fuel efficiency and methane slip reduction. Moreover, using the SOFCs mainly for the more stable auxiliary load limits the required battery capacity. Design scenario SOFC MAN has operational advantages. With 31% SOFC power, it is possible to operate at low speeds in low-emission zones while reducing GHG emissions by 33% and pollutants with 60% to 70%. Using SOFCs for all the main cruise operations is recommended from an environmental perspective, resulting in 49% GHG reduction and pollutants by 94% to 96% at 51% installed SOFC power. Pollutants can be eliminated to negligible levels with a fully SOFC-powered ship, although an advanced energy management strategy is required to ensure high conversion efficiency at part-load.

This chapter shows that large emission reduction is possible even without fully optimising the operation of the SOFC modules. All considered SOFC scenarios meet the IMO target to reduce GHG emissions by 30% by 2030, and more importantly, with available technology and fuel infrastructure. To further decrease emissions for future emission targets, the SOFC power plant model should be extended for renewable fuels and grouped modulation control should be implemented for optimal fuel conversion at part-load. An energy management strategy that optimises towards fuel consumption, emissions, and lifetime could be used to improve component operation. Furthermore, only four SOFC scenarios are defined in this study. An optimal architecture could be assessed from a wide range of hybrid configurations by combining the power plant volume, weight, fuel consumption, and emissions into an objective function.

7

Application discussion

The future belongs to those who see possibilities before they become obvious.

John Sculley

Parts of this chapter have been published in the conference proceedings of the International Marine Conference 2023 [326].

7.1. POWER PLANT PERFORMANCE

To put the characteristics of SOFC systems in perspective, they are compared with commercially available power-generating systems for marine power plants, namely hydrogen-fuelled LT-PEMFC and dual fuel generator sets, see Table 7.1. The comparison focuses on four-stroke engine generator sets as the risk is lower for shipowners to use SOFCs for the auxiliary load than to integrate them into the propulsion system. Additionally, replacing four-stroke generator sets offers a higher efficiency gain than replacing two-stroke main engines, which typically operate at around 48% fuel efficiency [360]. The power density of the 125 kW SOFC concept unit (presented in Chapter 5) is used for fair comparison since gensets often take up a limited amount of space in a machine room because of maintenance space and space for auxiliary equipment.

Table 7.1: Comparison of SOFC system (concept design form Chapter 5) and other commercially available power generation systems for ships [1, 27, 32, 117, 212, 327, 361, 362]. The data ranges for PEMFC is based on commercial marine approved systems from Nedstack, Bloom, Corvus, and Ballard.

	Unit	**Concept design SOFC system**	**Marine LT-PEMFC**	**DF GENSET**
Fuel supply	-	LNG	Hydrogen	LNG & MGO
Power density	kW/m^3 kW/ton	17 16	25-100 40-200	35-50 45-65
System cost	EUR/kw	1500-5000	2500-3500	250-500
Net electrical efficiency	-	40%-62%	40%-55%	30%-50%
CHP efficiency	-	80%-90%	40%-65%	60%-80%
TTW NO_X emissions	g/kWhe	0.001-0.003	≈ 0	8-10
TTW SO_X emissions	g/kWhe	≈ 0	≈ 0	0-0.016 (LNG) 0.38 (MGO 0.1% S)

SOFCs perform poorly in terms of volumetric power density. However, a power plant using LT-PEMFC, which relies on hydrogen as its fuel source, requires a substantial volume for hydrogen storage on board. Furthermore, the higher conversion efficiency of SOFC results in a reduction in LNG storage requirements compared to dual-fuel gensets. This is especially advantageous for large ocean-going vessels with large fuel storage tanks due to their high range requirements. The gravimetric power density of SOFC systems is also much lower than for LT-PEMFC and DF gensets, although for most ship types the volume is crucial.

From a cost perspective, both types of fuel cells are associated with high capital costs. Nevertheless, hydrogen is very expensive, while the fuel consumption with SOFCs is lower than with LNG-fuelled gensets. Consequently, in terms of fuel costs, which typically represent the most significant cost component, SOFCs are favoured. Besides the high electric efficiency, SOFCs have a high potential to recover heat from the exhaust stream, especially when using COGR, as shown in this dissertation. Subsequently, SOFCs are especially favourable over LT-PEMFC for ship applications with a high heat demand.

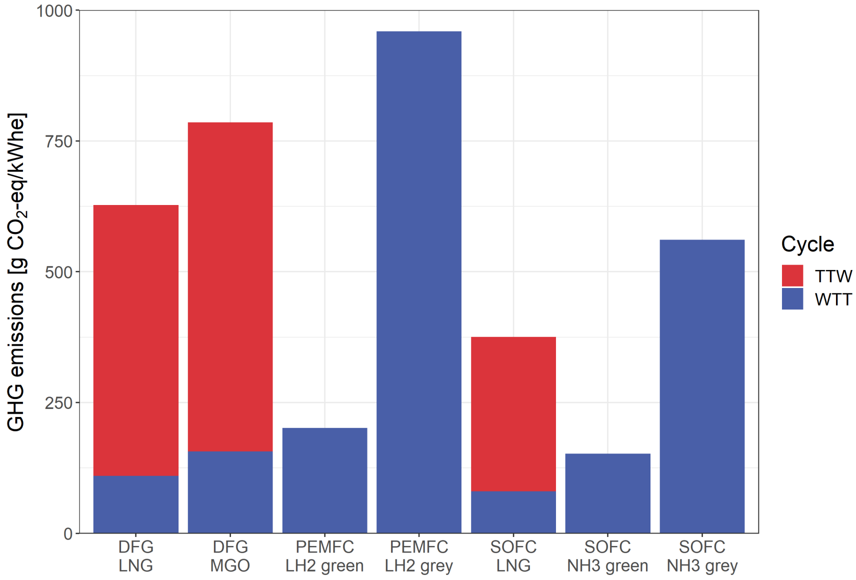

Figure 7.1: Comparison of WTT and TTW emissions for commercially available marine power generation systems. The WTT emissions are based on life cycle analyses and the TTW emissions on supplier specifications and literature [49, 153, 209, 212, 362–364].

Although capital costs and space requirements are expected to be higher than those of dual fuel gensets, the primary motivation for adopting fuel cells is the substantial reduction in emissions. The reduction of NO_X emissions is substantial because of the limited combustion. SO_X emissions are also close to zero for the fuel cell power plants, although this is mainly the case because of the low sulphur tolerance. However, the tolerance of LT-PEMFC to sulphur is much lower, increasing the complexity of the desulphurisation. Transitioning from dual-fuel gensets to LNG-fuelled SOFC systems already yields significant GHG emissions reductions due to the high conversion efficiency and the absence of methane slip, as shown in Figure 7.1. This is also confirmed with the power plants simulation results (Section 6.3.4). While hydrogen-LT-PEMFC powered ships do not emit tail-pipe emissions, other studies indicate that well-to-wake GHG emissions are only decreased when utilising green or blue hydrogen, which is currently not widely available [212]. Using LT-PEMFC with hydrogen produced by steam-reforming natural gas (grey hydrogen) increases the WTW emissions compared with gensets, as shown in Figure 7.1. Using LNG-fuelled SOFCs in the short term and green ammonia-fuelled SOFCs in the long term contributes to the largest GHG reductions from a life cycle perspective.

In short, at the expense of capital cost and volume, LNG-fuelled SOFC systems can be a good alternative for large sea-going vessels to reduce emissions, especially for ships with large range requirements, steady power demand, and significant heat demand. The next section discusses which ship types offer this opportunity.

7.2. Ship applications

SOFCs are typically most suitable for long-range applications, primarily due to the limitations of other low-emission solutions. Batteries are effective for short-range, high-power applications but require excessive energy storage for medium-range needs. For medium-range operations, hydrogen-fuelled PEMFCs are cost- and space-efficient, with high conversion efficiency. However, long-range applications require fuels with higher energy densities, such as natural gas, methanol, or ammonia, where SOFCs are most appropriate due to their limited reforming steps and high conversion efficiency. A predictable load profile is advantageous for SOFCs, allowing for pre-starting or continuous operation, and they perform best with steady power and significant heat demands, which are common in auxiliary loads or long-distance voyages. The different ship types and the applicability of SOFCs are discussed on range requirements, predictability of load profile, and size of auxiliary and heat demand. The discussion is summarised in Table 7.2 in order of range requirements and predictability of the load profile, with the most suitable ship types in the bottom rows.

Tugboats

Tugboats are robust vessels designed to assist larger ships in confined areas like harbours. Equipped with powerful engines and towing equipment, they facilitate safe navigation by assisting in docking, undocking, and towing operations. Tugboats have significant power requirements and experience rapid changes in power demand, making the slower response of SOFCs less suitable. The need for substantial battery capacity to handle power surges during pulling and pushing operations, combined with the short mission durations, suggests that a fully battery-powered plant might be a more appropriate low-emission solution for tugboats.

High-Speed Vessels

High-speed vessels are designed for rapid water transit, incorporating advanced technology and streamlined hull designs. These vessels are often built lightweight to enable planing or even hydrofoil-supported flight, making weight a critical design factor. SOFCs may be too heavy to accommodate these requirements, potentially limiting their applicability in high-speed vessels.

Ferries

Ferries typically operate over short distances between ports or cities and have varying load profiles. Applying SOFCs would lead to a significant required battery capacity. However, given the predictability of their operational profiles, it is conceivable that SOFCs could power both propulsion and auxiliary systems. During berthing, the ferry could potentially return energy to the grid, functioning somewhat like the inverse of a battery-powered ferry. Nevertheless, this is a conceptual application that requires additional investigation.

Inland transport ships

Inland ships are vessels designed for navigating rivers, canals, and other inland waterways. These cargo ships usually have medium-range requirements but face varying and unpredictable power demands due to factors such as stops at locks and navigation through other traffic. They usually have low auxiliary and heat demand. In short, applying SOFCs to this application appears challenging.

DREDGER

Dredgers are specialised vessels designed to excavate and remove sediment to maintain navigable waterways, facilitate port operations, and support construction projects. These vessels typically operate at relatively low and consistent speeds, with dredging activities demanding substantial auxiliary power. This auxiliary load has large fluctuations because of the varying composition of the seabed [169]. To manage these rapid load changes, some dredgers are equipped with flywheels. The vessel's crew has a minor heat load, but this contribution is minimal.

YACHTS

Yachts are luxurious recreational vessels offering a private space for leisure activities, exploration, and relaxation on the water. Although yachts have significant auxiliary and heat demands, their operation is unpredictable and highly variable, largely influenced by the preferences and demands of the owner. Additionally, yachts are frequently idle, leading to numerous thermal cycles of the SOFC system.

OFFSHORE SUPPORT VESSELS

Offshore support vessels (OSVs) play a critical role in supporting operations within the offshore oil and gas industry. These ships deliver essential services, including the transportation of personnel, equipment, and supplies to and from offshore platforms. They typically travel medium distances to offshore sites, either for scheduled maintenance or for ad-hoc tasks as required. As a result, their load profile is highly variable and unpredictable. These vessels also maintain a moderate auxiliary load to support crew, personnel, and onboard machinery. SOFCs could best be applied as a stable auxiliary power supply.

FISHING VESSELS

Fishing vessels are ships designed to harvest fish, playing a vital role in the global seafood industry. These vessels require a medium operating range to remain at sea for several days and are frequently equipped with onboard facilities for processing and storing catches to maintain freshness. Consequently, they have substantial auxiliary power and cooling demands.

NAVAL SHIPS

Naval ships encompass a wide range of military vessels with operational profiles that vary significantly depending on the type of vessel. They must be capable of responding to missions, resulting in highly unpredictable load profiles. These ships also have high cooling demands for weaponry, as well as significant auxiliary and heat demands for crew accommodation. Furthermore, the onboard systems must be resilient to vibrations and impacts, a requirement that needs further research to determine if SOFCs can meet these military specifications.

RESEARCH VESSELS

Research vessels are specialised ships equipped for scientific exploration and data collection. Outfitted with advanced instrumentation and laboratories, they facilitate studies in fields such as oceanography, marine biology, geophysics, and environmental science. Research vessels often undertake long voyages and have significant auxiliary and thermal load to support crew and research facilities. However, their load profiles are unpredictable, as they may need to respond rapidly to specific research operations. Their high range requirements and high and stable auxiliary load opt for applying SOFCs to replace auxiliary generators.

CRUISE SHIPS

Cruise ships are large passenger vessels primarily designed for leisure travel, providing a unique vacation experience with numerous onboard amenities, entertainment, and excursions to multiple destinations. These ships have considerable and steady auxiliary and heat demands. The propulsion load is predictable due to fixed cruise itineraries, although it can vary much when ships berth at multiple ports in a week. Consequently, SOFCs could be effectively utilised for the auxiliary load on cruise ships, as was also concluded in Chapter 6.

CONTAINER SHIPS AND BULK CARRIERS

Known for their high carrying capacities, container ships and bulk carriers play a vital role in the global logistics chain, facilitating the efficient movement of goods between ports. These ships typically operate over long distances at steady speeds, with predictable load profiles all year round. Their auxiliary and heat demands are minimal. SOFCs could be applied for the largest share of the power supply, using a thermal cycle or hot stand-by for the few times the ship is berthing. This category encompasses most trade volume. If SOFCs could be successfully applied for these ship types, substantial emissions reduction from the marine industry could be achieved.

TANKERS

Tankers are designed for transporting liquid cargo, playing a crucial role in the global energy and chemical industries. While their load profiles are similar to those of container ships and bulk carriers, tankers have additional significant heat or cooling demands, depending on the type of chemical or oil they are transporting. SOFCs could be used similar to container ships and bulk carriers for the steady propulsion demand, with additional heat recovery.

GAS CARRIERS

Gas carriers are designed to transport liquefied gases such as liquefied natural gas (LNG), liquefied petroleum gas (LPG), and other chemical gases. Their load profiles resemble those of container ships and bulk carriers, but a unique feature is the ability to use boil-off gas from the transported cargo as fuel for SOFCs. This approach has been applied, for example, in an SOFC system fueled by the boil-off from an ethane carrier [161]. SOFCs could be applied in LNG, hydrogen, or ammonia carriers.

Green corridors and fixed routes

Another potential application that could enhance the feasibility of SOFC technology is in green corridors and ships operating on fixed routes. These scenarios allow for more predictable load profiles, enabling greater optimisation in design. For example, ensuring adequate fuel capacity for a specific route rather than global operations is crucial, particularly for liquefied fuels such as LNG, ammonia, and hydrogen, which occupy significant ship volume. Samskip's hydrogen-fuelled, fuel cell-powered container ship operating between Rotterdam and Norway exemplifies this approach by limiting the required space for fuel storage. Although this reduces the ship's operational flexibility, it is a viable strategy for vessels dedicated to specific routes, potentially making SOFC applications more practical.

Table 7.2: Overview of ship types and relevant qualities for SOFC adaption. The suitability is rated on a scale of 1 to 5, where 1 represents the lowest level of suitability and 5 indicates the highest.

Shiptype	**Range requirement**	**Load profile**	**Propulsion**	**Auxiliary load**	**Heat demand**	**Suitability**
Tugs	Short	Unpredictable	Volatile	Small	Very small	1
High-speed vessel	Short	Unpredictable	Volatile	Very small	Very small	1
Ferries	Short	Predictable	Volatile	Medium and steady	Small	2
Inland transport ships	Medium	Unpredictable	Volatile	Small	Very small	2
Dredgers	Medium	Unpredictable	Volatile	Large and Volatile	Very small	2
Yachts	Medium	Unpredictable	Volatile	Large	Small	3
Offshore support vessels	Medium	Predictable	Volatile	Medium	Small	3
Fishing vessels	Medium	Predictable	Steady	Small	Cooling	3
Naval ships	Long	Unpredictable	Volatile	Large	Heating and cooling	3
Research vessels	Long	Unpredictable	Steady	Large	Heating and cooling	4
Bulk carriers	Long	Predictable	Steady	Small	Very small	4
Tankers	Long	Predictable	Steady	Small	Heating	4
Container ships	Long	Predictable	Steady	Small	Very small	4
Cruise ships	Long	Predictable	Volatile	Large and steady	Large	5
Gas carriers	Long	Predictable	Steady	Small	Cooling	5

7

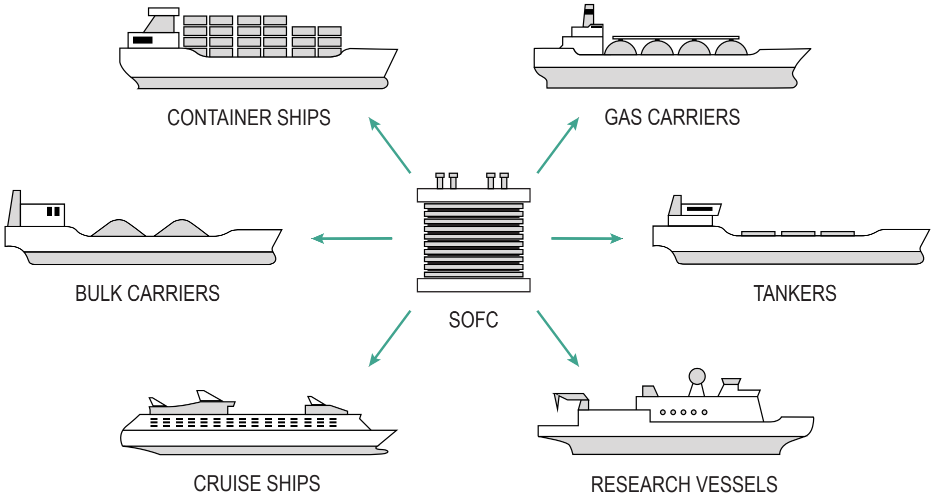

Figure 7.2: Proposed ship types for SOFC application [own image].

7.3. CONCLUSION

The applicability of SOFCs for various ship types is analysed. The assessment considers range requirements, load profile predictability, and auxiliary and heat demands. The qualitative analysis concludes that SOFCs are less suitable for tugs, high-speed vessels, ferries, and inland transport vessels. However, ships with high range requirements and stable, predictable propulsion or auxiliary loads offer the greatest potential for significant efficiency gains without the need for extensive battery capacity or rapid SOFC degradation. Container ships, gas carriers, bulk carriers, tankers, cruise ships, and research vessels are identified as suitable applications for SOFC systems, see Figure 7.2. Green corridors and fixed route contracts are also identified to enable an optimised SOFC power plant.

8

Conclusions and recommendations

It always seems impossible until it's done.

Nelson Mandela

8.1. Conclusions

Global targets and regulations force the marine industry to limit their shipping emissions. SOFCs offer a promising solution because of their high fuel efficiency and very low emission of toxic airborne pollutants. Using SOFCs fuelled by widely available LNG already leads to large emission reductions compared with engine-based solutions. Furthermore, its fuel flexibility makes it possible to adapt fuels that can be produced in a renewable manner, such as hydrogen, ammonia and methanol. Proper electrical and thermal integration is needed to reach high efficiency and power density. Therefore, this research focused on the question: *How can SOFC systems be effectively integrated in ships in order to reduce emissions?* By addressing this question, the following scientific contributions are made, elaborated in the sections below.

- An extensive review of SOFCs for marine applications, resulting in proposed research directions.
- Experimentally testing the influence of static and dynamic inclinations on the safety, operability, and lifetime of SOFC systems.
- Thermodynamic simulation model of an SOFC system with COGR to compare the electrical efficiency and heat recovery capacity across five different fuels.
- Concept design of a modular 1.125 MW SOFC system for ships with centralised BOP components and stack replacement strategy.
- Dynamic simulation model of the electric and thermal balance of a hybrid SOFC power plant considering degradation effects.
- Qualitative overview of the applicability of SOFCs on different ship types.

SOFC for marine applications

The marine application of SOFCs was reviewed, covering power plant components, fuel options and integration opportunities. Using SOFCs in ships introduces challenges compared with land-based systems, such as exposing the system to inclinations and accelerations, air salinity and humidity, and highly varying load profiles. Power density, capital cost, and lifetime improvements are necessary to compete with marine combustion engines. COGR and liquid cooling were proposed as research fields to improve power density. Furthermore, combining numerous stacks into high-power systems with centralised BOP components could further increase space effectiveness. With the current state of the art, hybridisation of SOFC systems with generator sets and batteries is suggested to reach feasibility in terms of cost, size and transient capabilities. Although implementing SOFCs in ships still faces technical, economic, and design challenges, it is a promising solution for the marine industry to decrease GHG and pollutant emissions while benefiting from noise reduction and increased reliability.

Influence of static and dynamic inclinations

A 1.5 kW SOFC module was operated on an inclination platform that emulates ship motions, to evaluate the influence of inclinations on the system's safety, operation, and lifetime. The module is inclined statically and dynamically around two horizontal axes of rotation up to an outer angle of 30°, including motion periods between 8 to 50 seconds. There were no detectable gas leakages or safety hazards during all different test conditions. Nevertheless, dynamic inclinations resulted in forced oscillations in the fuel supply because of the natural frequency of the gas regulation valve's plunger. This propagated through the control system, leading to significant deviations in the operational parameters of the system. Furthermore, a 190-hour degradation test with continuous dynamic inclinations indicated an enhanced degradation rate, although long-term testing is needed to accurately determine the degradation rate. The following is proposed for design practices and regulations: besides the stack technology, BOP components and their interaction with the stacks should also be evaluated on inclinations. Furthermore, the control feedback should be designed such that potential periodical deviations in operational parameters are mitigated. All in all, dynamic inclinations can impact the operation of the SOFC system, but the issues can be resolved with relatively simple design modifications. Thus, ship motions do not form a showstopper for applying SOFCs in seagoing vessels.

FUEL EFFICIENCY COMPARISON ACROSS ALTERNATIVE FUELS AND COGR

The thermodynamic performance of a marine SOFC power plant was evaluated for methane, methanol, diesel, ammonia, and hydrogen. A 1D stack model and the dedicated BOP components were modelled in Cycle Tempo to calculate the mass flow, pressure, temperature and composition between all components. The thermodynamic models are verified with a sensitivity analysis and validated by comparing them with similar studies. The model showed minor deviations in the net electric efficiency compared with other studies. These could be explained by differences in the used parameters, such as voltage, fuel utilisation, stack temperature, blower efficiency, and inverter efficiency. The highest net electrical efficiency (LHV) was found for methane (58.1%), followed by diesel (57.6%) and ammonia (55.1%). The parasitic losses of the air blower had a major influence on the net electrical efficiency. The highest heat efficiency was found for ammonia (27.4%), followed by hydrogen (25.6%). However, fuels with lower oxygen utilisation (methanol, diesel, and hydrogen) required significant exhaust heat to warm the process air, resulting in exhaust temperatures insufficient to produce steam for high-temperature applications on the ship. The carbon fuels (methane, methanol, and diesel) resulted in a 15% lower power density, compared to ammonia and hydrogen. From a thermodynamic perspective, ammonia can reach the highest fuel efficiency in case the ship has a significant heat demand. Otherwise, methane results in the highest fuel efficiency.

An SOFC system using cathode off-gas recirculation was investigated with the developed thermodynamic models to reduce the primary airflow and improve the heat recovery capacity. COGR increased oxygen utilisation, without a significant impact on the electric efficiency. This decreases the primary airflow, requiring less pre-heating. In turn, this increases the temperature in the exhaust and reduces the required heat exchanger area of the air pre-heater. Although further development of high-temperature recirculation blowers is necessary, COGR can be applied to enhance the heat recovery capacity. Furthermore, since SOFC systems require large airflow to cool the stack, the application of COGR could strongly reduce the amount of space required for air and exhaust ducting through the ship.

CONCEPT DESIGN OF A 1.125 MW MARINE SOFC SYSTEM

Commercial SOFC systems are not available on the power scale required for large ships. There is a need to scale SOFC systems from kW-scale modules to MW-scale marine power plants while exploiting scale effects to improve the power density and specific cost. A modular 125 kW SOFC cabinet was designed, containing six replaceable stacks and centralised hot BOP components. Nine of these gas-tight cabinets are combined in one SOFC room with a rated power of 1.125 MW, with a separate room for cold BOP components. The design process learned that the preference for handleable stack replacement forces a limitation in scaling the SOFC system to a high-rated power. Furthermore, performance degradation needs to be taken into account during the design to dimension all components in the power plant for end-of-life conditions. By using a large stack footprint and centralising BOP components on different levels, it was possible to reach a power density of 17.4 kW/m^3 which is a significant improvement compared with current commercial systems which range up to 10.6 kW/m^3. Several of these SOFC rooms can be used to reach a multi-MW power plant for seagoing ships.

SIMULATION OF HYBRID SOFC POWER PLANTS CONSIDERING COMPONENT DEGRADATION

Power plant performance can be quantified by size, weight, fuel efficiency, and emissions. Four hybrid scenarios of an LNG-fuelled SOFC power plant are evaluated and compared with three reference scenarios based on combustion engines. A component sizing model and a time-domain power plant simulation model have been developed to estimate these indicators. The energy and heat balance of the power plant components are simulated, taking into account part-load operation and degradation effects. An energy management system allocates the power demand based on the battery state of charge. The combined component sizing and time-domain model highlights the importance of dynamic simulation for adequate battery sizing. Moreover, the operational strategy of the SOFCs has a significant impact on the degradation rate. The simulation results show that using SOFCs for the auxiliary consumers can reduce GHG emissions by 21% and pollutants by 38% to 46% with only 17.5% installed SOFC power, which has limited consequences for the cost and size of the power plant. With 31% installed power, the ship can operate in low-emission zones while reducing GHG emissions by 33% and pollutants by 60% to 70%. Performing all cruise operations on SOFCs requires 51% installed SOFC power and reduces GHG emissions with 49% and pollutants with 94% to 96%. In conclusion, the study affirms that SOFC technology, when properly sized and operated, meets IMO's GHG reduction target of 30% by 2030.

APPLICABILITY OF SOFCS ON DIFFERENT SHIP TYPES

The applicability of SOFCs on different ship types is discussed considering range requirements, predictability of load profile, and size of auxiliary and heat demand. The qualitative analysis concludes that SOFCs are less suitable for tugs, high-speed vessels, ferries, and inland transport vessels. However, ships with high range requirements and stable, predictable propulsion or auxiliary loads offer the greatest potential for significant efficiency gains without the need for extensive battery capacity or rapid SOFC degradation. Container ships, gas carriers, bulk carriers, tankers, cruise ships, and research vessels are identified as suitable applications for SOFC systems.

8.2. RECOMMENDATIONS FOR FUTURE RESEARCH

This section presents several recommendations for future research, addressing unresolved issues within the time frame of this PhD and newly identified areas. These recommendations aim to further facilitate the integration of SOFCs in maritime applications.

CONDITIONS IN SHIPS AT SEA

Although Chapter 3 already covered one potential challenge of the onboard conditions, namely inclinations and accelerations, other environmental conditions need further research. Firstly, the air blowing over the seas gets saturated with humidity and salt, which both affect the SOFC stacks and its BOP components. Experimental studies are required to determine whether this directly damages or accelerates the degradation of SOFCs. If such effects are observed, air pre-treatment could be integrated into marine SOFC systems. Secondly, vibrations propagate through the structure of the ship, produced by generator sets and propellers. Vibration testing is needed to verify whether this causes harm or safety issues to the SOFC stacks, particularly to the ceramic materials, which are likely most susceptible to damage from vibrations or shock.

ALTERNATIVE FUELS

The marine industry is considering different alternative fuels. Especially hydrogen, ammonia, and methanol are seeing uptake in various applications, from small ferries to the largest container carriers. Although Chapter 4 covered the thermodynamic performance of an SOFC system with these fuels, the concept design and power plant simulation were restricted to methane due to insufficient data on SOFC systems using alternative fuels. To accurately assess the power plant's performance with these fuels, it is essential to determine the volumetric and gravimetric power density, part-load efficiency, pollutant emissions, and transient capabilities. Demonstration projects for SOFCs using alternative fuels are necessary to achieve this. A fuel-flexible SOFC system is also an interesting research topic. While fuel flexibility is often referred to as an advantage of SOFCs, the required BOP components and their dimensioning typically depend on the used fuel, locking in the fuel choice. However, it may be possible to develop a system capable of handling two fuels or one where modular components can be replaced to switch fuels. The potential technical challenges and space and cost implications of such a system should be evaluated to determine its viability.

8

OPERATIONAL STRATEGIES OF SOFCS

Ships predominantly operate at a proportion of their installed capacity. To maintain high conversion efficiency at low loads, an SOFC-powered plant would likely manage groups of SOFC modules by turning them on or off as needed, similar to the operation of marine genset arrays. Nevertheless, SOFCs face additional challenges: the high modularity of SOFCs gives a high degree of freedom in the number of units to be modulated. Furthermore, the long start-up and cool-down time of SOFCs requires anticipation of their use. Lastly, regular modulation and especially thermal cycles decrease the lifetime of SOFCs. Optimising the control of such a power plant involves balancing fuel consumption, emissions, and lifespan conservation. This presents an intriguing area for future research, where model predictive control or other artificial intelligence models could be used to optimise operations.

IMPROVING POWER DENSITY

The review in Chapter 2 and the power plant simulation in Chapter 6 revealed that an integrated SOFC system requires significantly more space than an equivalent genset system. Increasing the power density of SOFC systems is crucial to place SOFCs in ships, where volume is directly tied to cargo capacity. This requires a holistic approach, encompassing cell technology, stack manufacturing, system development, and system integration to minimise spatial requirements. Efforts made in this dissertation include applying COGR to reduce ducting space and air pre-heater size, and centralising BOP components across different levels for greater space effectiveness. Additionally, novel SOFC technologies, such as metal-supported, flat-tubular, or monolithic cells, could reduce the stack's footprint, while optimising the BOP can further minimise the size of the total system and required air and exhaust flows.

A
APPENDIX

A.1. EMISSION DATA REVIEW

The data used to generate Figure 2.5 is shown in Table A.1. For this data, SOFC systems fuelled with LNG and without combined cycles are used, since these are mainly commercially available. The emissions of DG are without after treatment. Presented emissions are just tank-to-propeller emissions and are calculated with 55% SOFC efficiency and 43% DG efficiency.

Table A.1: Tank-to-electricity (TTE) emission comparison between off-the-shelf SOFC systems and medium-speed 4-stroke marine diesel generators fuelled with MGO (1.5% S) or LNG. Derived from [11, 27, 147, 153, 209, 362, 365, 366] and supplier information.

TTW emission		**Targets and regulations**		**Emissions per system**		
		2030 target	**2040 target**	**DG (MGO)**	**DFG (LNG)**	**SOFC (LNG)**
CO2-eq	g/kWhe	70	20%	600 - 660	490 - 550	200 - 390
		Non-ECA 2020	**ECA 2020**	**DG (MGO) 0.1% S**	**DFG (LNG)**	**SOFC (LNG)**
NOx	g/kWhe	<7.7	<1.96	9 - 9.96	1.2 - 2	0.0001 - 0.052
SOx	g/kWhe	<2 (0.5 %m/m)	<0.4 (0.1 %m/m)	0.36 - 0.4	0 - 0.008	0
PM	g/kWhe	<2 (0.5 %m/m)	<0.4 (0.1 %m/m)	0.19-0.54	0.007 - 0.0018	0

A.2. MARINE INCLINATION CONDITIONS AND REGULATIONS

Seagoing ships experience ship motions in all degrees of freedom induced by waves, wind and manoeuvring, which can be significant. The following influence the ship motions [367]:

A

- Ship type and dimensions
- Loading conditions
- Sea state at operating location
- Ship speed and manoeuvring

Generally, the inclinations are the largest in the roll direction. Table A.2 gives an overview of common roll periods for different ship types. The accelerations that the equipment experiences are also dependent on the position on the ship. This is additionally relevant for the evaluation of SOFC for ships, because installing them decentralised is seen as a beneficial option [173]. Table A.3 shows measured or simulated accelerations for different ship types.

Table A.2: Minimum, maximum and typical roll periods for common sea-going ships [368].

Shiptype	**Roll Period [s]**		
	Min	Max	Typical
Bulk carrier	8	16	-
Container vessel	10	40	-
Cruise vessel	14	25	-
Ferry	10	25	15
General cargo	10	20	-
Naval ship	10	15	12
OSV/PSV	8	16	11
Tanker	10	20	-
Overall	8	40	-

Table A.3: Maximum measured or simulated acceleration for different ship types in sea waves up to sea state 8.

Shiptype	**At location**	**Lateral acceleration** m/s^2	**Vertical acceleration** m/s^2	**Study type**	**Source**
OSV	Anywhere	2.58	5.51	Measured	[369]
Large passenger	Passenger area	1.00	2.00	Measured	[370]
Small passenger	Bow	-	1.9	Simulated	[371]
Small passenger	Bow	-	1.62	Simulated	[372]
Cruise	Anywhere	-	1.40	Simulated	[373]
Training ship	After deck	0.49	1.08	Measured	[374]

All shipboard equipment and machinery must be designed to function properly even when exposed to these inclinations and motions. The regulations by different class societies for inclinations for shipboard machinery are summarised in Table A.4. The test conditions in the experiments of this study are derived from the shown marine conditions and regulations.

Table A.4: Requirements for inclination testing of shipboard equipment and machinery for different class societies [205, 375–379].

		Heel angle			Trim angle				
Equipment	**Class**	**Static**	**Dynamic**		**Static**	**Dynamic**		**Simultaneous**	**Minimum time**
		[°]	[°]	[s]	[°]	[°]	[s]	-	[min]
Main and auxiliary machinery	ABS	15	22.5	-	5	7.5	-	yes	-
	BV	15	22.5	10	5	7.5	5	yes	-
	DNV	15	22.5	-	5	7.5	-	yes	-
	LR	22.5	22.5	10	22.5	22.5	10	no	15
	KR	15	22.5	-	5	7.5	-	yes	-
Safety or emergency equipment	ABS	22.5	22.5	-	10	10	-	yes	-
	BV	22.5	22.5	10	10	10	5	yes	-
	DNV	22.5	22.5	-	10	10	-	yes	-
	LR	22.5	22.5	10	22.5	22.5	10	no	15
	KR	22.5	22.5	-	10	10	-	yes	-

The Society may consider deviations from these angles of inclination taking into consideration the type, size and service condition of the ship.
On ships for the carriage of liquefied gases and chemicals, the emergency power supply is to remain operational with the ship flooded up to a maximum inclination of 30°.

A.3. DATA PROCESSING OF INCLINATION EXPERIMENT

CLEANING AND FILTERING OF DATA

The tested system is available for commercial purposes and thus includes operational strategies such as occasional filling of the steam dosing tank, hourly toggling of the airflow, and a 12-hour surge in fuel and air flow to verify their regulation. These strategies and safety operations have a temporary influence on the system's stable operation and are therefore excluded from the collected data.

NORMALISATION OF DATA

Because of intellectual property considerations of the SOFC manufacturer, the shown data is normalised. Some of the shown data is normalised to the nominal conditions of the system at the beginning of the experimental campaign:

$$x'(t) = x(t)/x_{nominal} \tag{A.1}$$

MAXIMUM DEVIATION DETERMINATION

To ensure an accurate comparison between the deviations in operational parameters during normal operation and during the experiment, it is necessary to account for high-frequency noise in the operational data and gradual changes over time. Therefore, a maximum deviation is calculated, which takes into account the variability in the data over a certain time period:

$$\Delta x_{max} = \max(|x_i - x_{i+\frac{1}{2}T}|) \tag{A.2}$$

A

where $x_{i+\frac{1}{2}T}$ is the value of the dedicated variable at half oscillation period after the current time. To prevent the possibility of overlapping different test conditions, Equation A.2 is used for each different combination of inclination setting, rotation direction, and oscillation period.

A.4. SIMULATION PARAMETERS OF VALIDATION STUDIES

The results of the thermodynamic analysis are compared with similar studies in Section 4.5.3. An extended overview of these studies is provided in this appendix, including the assumed model parameters. Table A.5 shows studies without COGR and Table A.6 shows studies that include COGR.

[1] Net electric exergy efficiency
[2] Polytropic efficiency
[3] Overall efficiency
[4] Gross energy efficiency
[5] Overall blower efficiency

Table A.5: Comparison of SOFC system analyses without COGR. Only comparable studies are included, which means planar O^{2-} conducting SOFCs operated on atmospheric pressure. All efficiency data is based on LHV. When no stack temperature is provided, the average between stack inlet and outlet is reported.

		SOFC operation							System characteristics		Performance
Fuel	Reference	Reforming	Pre-reform ratio	Voltage	Current density	AOGR	Overall fuel utilisation	Stack temperature	Isentropic blower efficiency	DC/AC inverter efficiency	Net electric efficiency
		-	-	V	A/m^2	-	-	°C	-	-	-
Methane	[96]	SR	30%	0.7	5000	✓	80%	750	73%	92%	49.5%
	[53]	SR	40%	?	?	-	80%	750	?	92%	61.0%
	[57]	SR	50%	?	?	-	85%	820	70%	98%	41.0%
	[301]	SR	0%	0.62	6000	-	85%	727	85%	97%	41.8% [1]
	[322]	SR	0%	?	5500	-	80%	640	85%	97%	47.8%
	This study	SR	20%	0.80	3483	-	80%	720	70%	96%	58.1%
	This study	SR	40%	0.80	3429	-	80%	720	70%	96%	57.7%
Methanol	[323]	SR	100%	0.62	3230	-	80%	900	?	100%	45.0%
	[105]	SR	100%	?	3000	-	85%	900	82% [2]	95%	50.0%
	[307]	SR	100%	?	6600	-	80%	800	?	?	51.0%
	[324]	ME	100%	?	?	✓	80%	700	70%	97%	51.9%
	This study	SR	100%	0.80	3526	-	80%	720	70%	96%	48.9%
Diesel	[29]	ATR	90%	0.80	4000	-	90%	775	72% [3]	100%	55.3%
	[93]	SR	100%	0.75	?	✓	73%	800	?	?	55.0% [4]
	[30]	SR	100%	0.75	?	✓	85%	775	65%	?	56.0%
	This study	SR	100%	0.80	3538	-	80%	720	70%	96%	57.6%
Ammonia	[310]	IC	0%	0.73	?	-	80%	800	55% [5]	100%	41.0%
	[324]	IC	0%	?	?	-	80%	700	70%	97%	51.8%
	[122]	IC	0%	?	?	-	80%	750	80%	100%	55.0%
	[121]	IC	0%	0.78	5000	-	80%	750	90%	95%	52.1%
	[34]	IC	0%	0.855	2000	-	80%	800	80%	98%	59.8%
	This study	IC	0%	0.80	4075	-	80%	720	70%	96%	55.1%
Hydrogen	[96]	-	-	0.78	5000	-	80%	750	73%	92%	37.5%
	[325]	-	-	0.75	8000	-	75%	850	80%	100%	40.0%
	[62]	-	-	0.86	5000	-	80%	750	60%	95%	48.0%
	[313]	-	-	0.85	10000	-	85%	750	85%	100%	49.6%
	This study	-	-	0.80	4100	-	80%	720	70%	96%	47.1%

General: - = Not applicable, ? = Not reported by author.
Reforming: SR = Steam Reforming, ME = Methanation, ATR = Auto Thermal Reforming, IC = Internal Cracking.
AOGR = Anode Off-gas Recirculation.

Table A.6: Comparison of SOFC system analyses with COGR. Only comparable studies are included, which means planar O^{2-} conducting SOFCs operated on atmospheric pressure. All efficiency data is based on LHV. For diesel and ammonia, no representative studies with COGR were found.

		SOFC operation								*System characteristics*		*Performance*
Fuel	**Reference**	**Reforming**	**Pre-reform ratio**	**COGR type**	**COG RR**	**Voltage**	**Current density**	**Fuel utilisation**	**Stack temperature**	**Isentropic blower efficiency**	**DC/AC inverter efficiency**	**Net electric efficiency**
		-	-	-	-	*V*	A/m^2	-	°*C*	-	-	-
Methane	[96]	SR	30%	EJ	0.6	0.69	5000	80%	750	73%	92%	53.7%
	[53]	SR	40%	EJ	0.75	0.80	?	80%	750	?	92%	58.0%
	[57]	SR	0%	?	0.5	?	?	85%	820	70%	98%	51.0%
	[301]	SR	0%	?	0.3	0.60	6000	85%	727	85%	97%	40.2% [6]
	[97]	SR	80%	BL	?	0.83	4000	90%	710	?	100%	65.9%
	This study	SR	20%	BL	0.2	0.80	3465	80%	750	70%	96%	58.0%
Methanol	[97]	SR	100%	BL	?	0.83	4000	90%	710	?	100%	60.2%
	This study	SR	100%	BL	0.64	0.80	3464	80%	720	70%	96%	49.5%
Hydrogen	[96]	-	-	EJ	0.6	0.78	5000	80%	750	73%	92%	40.3%
	[97]	-	-	BL	?	0.859	4000	90%	710	?	100%	58.3%
	This study	-	-	BL	0.64	0.80	4039	80%	720	70%	96%	46.8%

General: - = Not applicable, ? = Not reported by author
Reforming: SR = Steam Reforming.
COGR type: BL = Air recirculation with blower, EJ = Air recirculation with ejector.

[6] Net electric exergy efficiency

A

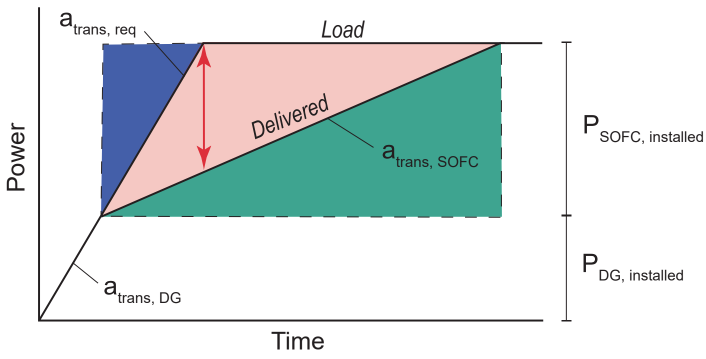

Figure A.1: Illustration for initial estimation of battery capacity based on transient requirements and capabilities.

A.5. DERIVATION OF INITIAL BATTERY CAPACITY SIZING

DERIVATION OF INITIAL BATTERY SIZING

Equation 5.2 in Section 6.2 estimates an initial battery capacity under the assumption that the hybrid power plant must posses transient capabilities equivalent to solely diesel generators. The derivation is given in this section.

In Figure A.1 it is shown in red which energy capacity and power capacity the batteries should have. The slope of the lines represents the transient capability of the power-producing components. The required energy from the batter is calculated with trigonometry. The energy in the green area is:

$$E = \frac{1}{2} \cdot P_{SOFC,installed} \cdot \Delta t \tag{A.3}$$

$$\Delta t = \frac{P_{installed} - P_{DG,installed}}{a_{trans,SOFC} \cdot P_{SOFC,installed}} \tag{A.4}$$

$$E = \frac{P_{SOFC,installed}}{2 \cdot a_{trans,SOFC}} \tag{A.5}$$

Similarly, the blue area can be calculated with:

$$E = \frac{1}{2} \cdot \frac{P_{SOFC,installed}}{a_{trans,DG}} \tag{A.6}$$

The required energy from the battery (red area) can be calculated by subtracting the blue area from the green area:

$$E_{bat,req} = \frac{P_{SOFC,installed}}{2 \cdot a_{trans,SOFC}} - \frac{P_{SOFC,installed}}{2 \cdot a_{trans,DG}} \tag{A.7}$$

The maximum power required from the battery is calculated using the slopes of the lines:

$$P_{bat,req} = \left(a_{trans,DG} - a_{trans,SOFC}\right) \cdot \frac{P_{SOFC,installed}}{a_{trans,DG}} \tag{A.8}$$

Finally, the required battery capacity must fulfil the energy as well as the power requirements for ramp support:

$$P_{bat,installed} = \max\left[E_{bat,req}; \frac{P_{bat,req}}{C_{rate}}\right] \tag{A.9}$$

The limitation is that the sizing is not based on the operational profile. However, this aspect is addressed during the dynamic simulation.

A.6. EMISSION DATA FOR POWER PLANT SIMULATION

The used emission factors for well-to-tank (WTT) and tank-to-wake (TTW) are shown in Table A.7. Some emissions can be directly calculated from the fuel consumption such as GHG emissions and sulphur emissions. The CO_2 emissions for LNG converted in gensets are lower than with SOFC, because not all carbon particles are converted to CO_2 because of the methane slip. In some cases, the specific emissions are load dependent, for instance, methane and NO_X emissions from engines, which are retrieved from published experimental campaigns. Figure A.2 shows the used load curves.

A

Table A.7: Specific emissions for used power plant components. Some emission factors are load dependent, which are shown in in Figure A.2.

Component	Fuel	Emissions	Chain	Value	Unit	Source
-	MGO	GHG	WTT	0,80	kg/kg fuel	[361–363]
-	MGO	NOx	WTT	0	kg/kg fuel	-
-	MGO	SOx	WTT	0	kg/kg fuel	-
-	LNG	GHG	WTT	0,60	kg/kg fuel	[361–363]
-	LNG	NOx	WTT	0,000024	kg/kg fuel	[380]
-	LNG	SOx	WTT	0,000012	kg/kg fuel	[380]
ENG	MGO	CO2	TTW	3,21	kg/kg fuel	[366]
ENG	MGO	CH4	TTW	0	g/kWhe	-
ENG	MGO	NOx	TTW	Load-curve	g/kWhe	[335]
ENG	MGO	SOx	TTW	Load-curve	g/kWhe	[335]
ENG	MGO	PM	TTW	Load-curve	g/kWhe	[335]
ENG	MGO	CO	TTW	Load-curve	g/kWhe	[335]
ENG	LNG	CO2	TTW	2,59	kg/kg fuel	[366]
ENG	LNG	CH4	TTW	Load-curve	g/kWhe	[333]
ENG	LNG	NOx	TTW	Load-curve	g/kWhe	[333]
ENG	LNG	SOx	TTW	Load-curve	g/kWhe	[366]
ENG	MGO	PM	TTW	Load-curve	g/kWhe	[381]
ENG	MGO	CO	TTW	Load-curve	g/kWhe	[333]
SOFC	LNG	GHG	TTW	2,75	kg/kg fuel	[366]
SOFC	LNG	NOx	TTW	0,023	g/kWhe	Gandilgio
SOFC	LNG	SOx	TTW	0	g/kWhe	Gandilgio
SOFC	LNG	PM	TTW	0	g/kWhe	Gandilgio
SOFC	LNG	CO	TTW	0	g/kWhe	Gandilgio
BOIL	MGO	GHG	TTW	3,21	kg/kg fuel	Alfa Laval boiler
BOIL	MGO	NOx	TTW	0,30	g/kWh heat	Alfa Laval boiler
BOIL	MGO	SOx	TTW	0,10	g/kWh heat	Alfa Laval boiler
BOIL	LNG	GHG	TTW	2,75	kg/kg fuel	Alfa Laval boiler
BOIL	LNG	NOx	TTW	0,21	g/kWh heat	Alfa Laval boiler
BOIL	LNG	SOx	TTW	0	g/kWh heat	Alfa Laval boiler

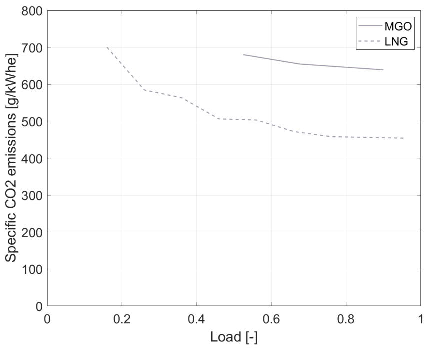

(a) Specific CO_2 emissions.

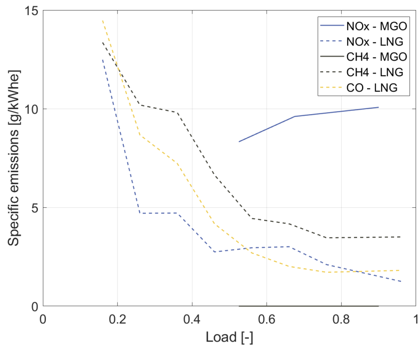

(b) Specific NO_X, CH_4 and CO emissions.

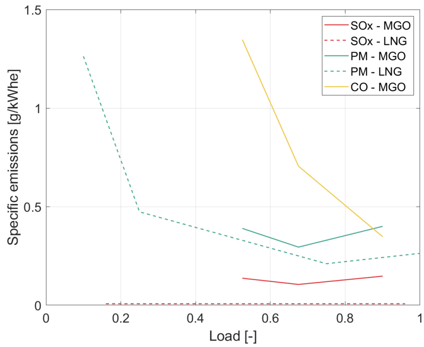

(c) Specific SO_X, PM and CO emissions.

Figure A.2: Used emission maps for gensets [333, 335, 381].

Bibliography

[1] B. van Veldhuizen, L. van Biert, and P. V. Aravind. "Solid Oxide Fuel Cells for Marine Applications". In: *International Journal of Energy Research* (2023).

[2] T. R. Walker et al. "Environmental effects of marine transportation". In: *World Seas: An Environmental Evaluation Volume III: Ecological Issues and Environmental Impacts*. Elsevier, Jan. 2018, pp. 505–530.

[3] IMO. *Introduction to IMO*. 2020. URL: https://www.imo.org/en/About/Pages/Default.aspx.

[4] K. Andersson et al. *Shipping and the Environment, Improving Environmental Performance in Marine Transportation*. Springer, 2016.

[5] IMO. "Fourth IMO GHG Study". In: (2020).

[6] IEA. *International shipping*. 2023. URL: https://www.iea.org/energy-system/transport/international-shipping.

[7] European Environmental Agency. *Emissions of air pollutants from transport*. 2020. URL: https://www.eea.europa.eu/data-and-maps/indicators/transport-emissions-of-air-pollutants-8/transport-emissions-of-air-pollutants-8.

[8] IMO. *UN body adopts climate change strategy for shipping*. 2018. URL: http://www.imo.org/en/MediaCentre/PressBriefings/Pages/06GHGinitialstrategy.aspx.

[9] IMO. *Revised GHG reduction strategy for global shipping adopted*. 2023. URL: https://www.imo.org/en/MediaCentre/PressBriefings/pages/Revised-GHG-reduction-strategy-for-global-shipping-adopted-.aspx.

[10] IMO. *Rules on ship carbon intensity and rating system enter into force*. 2022. URL: https://www.imo.org/en/MediaCentre/PressBriefings/pages/CII-and-EEXI-entry-into-force.aspx.

[11] IMO. *Nitrogen oxides (NOx) – Regulation 13*. 2020. URL: http://www.imo.org/en/OurWork/Environment/PollutionPrevention/AirPollution/Pages/Nitrogen-oxides-(NOx)-%E2%80%93-Regulation-13.aspx.

[12] E. Lindstad and T. I. Bø. "Potential power setups, fuels and hull designs capable of satisfying future EEDI requirements". In: *Transportation Research Part D: Transport and Environment* 63 (Aug. 2018), pp. 276–290.

[13] P. Liu et al. "Development and optimization of dual-mode propellers for renewable energy". In: *Renewable Energy* 119 (Apr. 2018), pp. 566–576.

[14] M. Wen et al. “A multiple ship routing and speed optimization problem under time, cost and environmental objectives”. In: *Transportation Research Part D: Transport and Environment* 52 (2017), pp. 303–321.

[15] J. Zheng et al. “A voyage with minimal fuel consumption for cruise ships”. In: *Journal of Cleaner Production* 215 (Apr. 2019), pp. 144–153.

[16] A. Uusitalo et al. “Numerical analysis on utilizing excess steam for electricity production in cruise ships”. In: *Journal of Cleaner Production* 209 (Feb. 2019), pp. 424–438.

[17] Y. Yan et al. “Multi-objective design optimization of combined cooling, heating and power system for cruise ship application”. In: *Journal of Cleaner Production* 233 (Oct. 2019), pp. 264–279.

[18] M. Al-Falahi et al. “AC Ship Microgrids: Control and Power Management Optimization”. In: *Energies* 11.6 (June 2018), p. 1458.

[19] F. Burel, R. Taccani, and N. Zuliani. “Improving sustainability of maritime transport through utilization of Liquefied Natural Gas (LNG) for propulsion”. In: *Energy* 57 (Aug. 2013), pp. 412–420.

[20] C. W. Mohd Noor, M. M. Noor, and R. Mamat. “Biodiesel as alternative fuel for marine diesel engine applications: A review”. In: *Renewable and Sustainable Energy Reviews* 94 (Oct. 2018), pp. 127–142.

[21] S. Bengtsson, K. Andersson, and E. Fridell. “A comparative life cycle assessment of marine fuels liquefied natural gas and three other fossil fuels”. In: *Proceedings of the Institution of Mechanical Engineers, Part M: Journal of Engineering for the Maritime Environment* 225.2 (May 2011), pp. 97–110.

[22] Y. Zhou et al. *The potential of liquid biofuels in reducing ship emissions*. Tech. rep. International Council on Clean Transportation, 2020.

[23] H. Winnes, E. Fridell, and J. Moldanová. “Effects of Marine Exhaust Gas Scrubbers on Gas and Particle Emissions”. In: *Journal of Marine Science and Engineering* 8.4 (Apr. 2020), p. 299.

[24] M. Feenstra et al. “Ship-based carbon capture onboard of diesel or LNG-fuelled ships”. In: *International Journal of Greenhouse Gas Control* 85 (June 2019), pp. 1–10.

[25] Z. Zhou et al. “A review of energy storage technologies for marine current energy systems”. In: *Renewable and Sustainable Energy Reviews* 18 (Feb. 2013), pp. 390–400.

[26] H. Wang et al. “Comparison of decarbonisation solutions for shipping: hydrogen, ammonia and batteries”. In: *International Marine Design Conference*. 2022.

[27] F. Baldi et al. “The role of solid oxide fuel cells in future ship energy systems”. In: *Energy* 194 (Mar. 2020), p. 116811.

[28] L. van Biert et al. “A review of fuel cell systems for maritime applications”. In: *Journal of Power Sources* 327.February 2018 (2016), pp. 345–364.

[29] C. Ezgi, M. T. Çoban, and O. Selvi. "Design and thermodynamic analysis of an SOFC system for naval surface ship application". In: *Journal of Fuel Cell Science and Technology* 10.3 (June 2013).

[30] G. V. Huerta et al. "Exergy analysis of the diesel pre-reforming solid oxide fuel cell system with anode off-gas recycling in the SchIBZ project. Part I: Modeling and validation". In: *International Journal of Hydrogen Energy* 43.34 (Aug. 2018), pp. 16684–16693.

[31] H. Sapra et al. "Integration of solid oxide fuel cell and internal combustion engine for maritime applications". In: *Applied Energy* 281 (Jan. 2021), p. 115854.

[32] M. Rivarolo, D. Rattazzi, and L. Magistri. "Best operative strategy for energy management of a cruise ship employing different distributed generation technologies". In: *International Journal of Hydrogen Energy* 43.52 (Dec. 2018), pp. 23500–23510.

[33] R. E. Rosli et al. "A review of high-temperature proton exchange membrane fuel cell (HT-PEMFC) system". In: *International Journal of Hydrogen Energy* 42.14 (Apr. 2017), pp. 9293–9314.

[34] K. Selvam et al. "Thermodynamic analysis of 100% system fuel utilization solid oxide fuel cell (SOFC) system fueled with ammonia". In: *Energy Conversion and Management* 249 (Dec. 2021), p. 114839.

[35] A. Buonomano et al. "Hybrid solid oxide fuel cells-gas turbine systems for combined heat and power: A review". In: *Applied Energy* 156 (Oct. 2015), pp. 32–85.

[36] L. van Biert et al. "A thermodynamic comparison of solid oxide fuel cell-combined cycles". In: *Journal of Power Sources* 397 (Sept. 2018), pp. 382–396.

[37] B. van Veldhuizen. *Fuel cell systems Applied in Expedition Cruise Ships - A Comparative Impact Analysis.* Tech. rep. Delft University of Technology, 2020.

[38] S. Harboe et al. "Manufacturing cost model for planar 5 kWel SOFC stacks at Forschungszentrum Jülich". In: *International Journal of Hydrogen Energy* 45.15 (Mar. 2020), pp. 8015–8030.

[39] T. L. Skafte et al. "Quantitative review of degradation and lifetime of solid oxide cells and stacks". In: *EFCF 2016 proceedings* B0501 (2016), pp. 8–26.

[40] C. H. Choi et al. "Development and demonstration of PEM fuel-cell-battery hybrid system for propulsion of tourist boat". In: *International Journal of Hydrogen Energy* 41.5 (Feb. 2016), pp. 3591–3599.

[41] J. Markowski and I. Pielecha. "The potential of fuel cells as a drive source of maritime transport". In: *IOP Conference Series: Earth and Environmental Science.* Vol. 214. 1. Institute of Physics Publishing, Jan. 2019, p. 12019.

[42] Y. M. A. Welaya, M. Mosleh, and N. R. Ammar. "Thermodynamic analysis of a combined gas turbine power plant with a solid oxide fuel cell for marine applications". In: *International Journal of Naval Architecture and Ocean Engineering* 5.4 (Dec. 2013), pp. 529–545.

[43] P. C. Okonkwo et al. “Platinum degradation mechanisms in proton exchange membrane fuel cell (PEMFC) system: A review”. In: *International Journal of Hydrogen Energy* 46.29 (2021), pp. 15850–15865.

[44] A. Choudhury, H. Chandra, and A. Arora. “Application of solid oxide fuel cell technology for power generation - A review”. In: *Renewable and Sustainable Energy Reviews* 20 (Apr. 2013), pp. 430–442.

[45] I. Ritucci et al. “A Ba-free sealing glass with a high coefficient of thermal expansion and excellent interface stability optimized for SOFC/SOEC stack applications”. In: *International Journal of Applied Ceramic Technology* 15.4 (2018), pp. 1011–1022.

[46] Battelle Memorial Institute. *Manufacturing Cost Analysis of 100 and 250 kW Fuel Cell Systems for Primary Power and Combined Heat and Power Applications*. Tech. rep. 2016.

[47] T. Tronstad and L. Langfeldt. *Study on the use of fuel cells in shipping*. Tech. rep. EMSA European Maritime Safety, 2017.

[48] N. Minh, J. Mizusaki, and S. C. Singhal. “Advances in Solid Oxide Fuel Cells: Review of Progress through Three Decades of the International Symposia on Solid Oxide Fuel Cells”. In: *ECS Transactions* 78.1 (May 2017), pp. 63–73.

[49] M. Singh, D. Zappa, and E. Comini. “Solid oxide fuel cell: Decade of progress, future perspectives and challenges”. In: *International Journal of Hydrogen Energy* 46.54 (Aug. 2021), pp. 27643–27674.

[50] S. Roychoudhury and R. Mastanduno. “Balance of Plant”. In: *Fuel Cells: Technologies for Fuel Processing*. Elsevier, Jan. 2011, pp. 517–526.

[51] J. G. Sung et al. “Catalytic combustion of SOFC stack flue gas over CuO and Mn2O3 supported by La0.8Sr0.2Mn0.67Cu0.33O3 perovskite”. In: *AIChE Journal* 64.3 (Mar. 2018), pp. 940–949.

[52] O. van Rheinberg et al. “Selective removal of sulphur in liquid fuels for fuel cell applications”. In: *Fuel* 87.13-14 (Oct. 2008), pp. 2988–2996.

[53] V. Liso et al. “Performance comparison between partial oxidation and methane steam reforming processes for solid oxide fuel cell (SOFC) micro combined heat and power (CHP) system”. In: *Energy* 36.7 (July 2011), pp. 4216–4226.

[54] F. Calise et al. “Full load synthesis/design optimization of a hybrid SOFC-GT power plant”. In: *Energy* 32.4 (Apr. 2007), pp. 446–458.

[55] F. Calise, A. Palombo, and L. Vanoli. “Design and partial load exergy analysis of hybrid SOFC-GT power plant”. In: *Journal of Power Sources* 158.1 (2006), pp. 225–244.

[56] S. H. Chan, H. K. Ho, and Y. Tian. “Modelling for part-load operation of solid oxide fuel cell-gas turbine hybrid power plant”. In: *Journal of Power Sources* 114.2 (Mar. 2003), pp. 213–227.

[57] J. Jia et al. “Effects of gas recycle on performance of solid oxide fuel cell power systems”. In: *Energy* 36.2 (Feb. 2011), pp. 1068–1075.

[58] P. H. Wagner et al. “Experimental characterization of a solid oxide fuel cell coupled to a steam-driven micro anode off-gas recirculation fan”. In: *Applied Energy* 262 (Mar. 2020), p. 114219.

[59] L. van Biert, K. Visser, and P. V. Aravind. “A comparison of steam reforming concepts in solid oxide fuel cell systems”. In: *Applied Energy* 264 (Apr. 2020), p. 114748.

[60] F. Schäfer et al. “Control of oxygen-to-carbon ratio and fuel utilization with regard to solid oxide fuel cell systems with anode exhaust gas recirculation: A review”. In: *Journal of Power Sources* 524 (Mar. 2022), p. 231077.

[61] T. S. Lee, J. N. Chung, and Y. C. Chen. “Design and optimization of a combined fuel reforming and solid oxide fuel cell system with anode off-gas recycling”. In: *Energy Conversion and Management* 52.10 (Sept. 2011), pp. 3214–3226.

[62] R. Peters et al. “Efficiency analysis of a hydrogen-fueled solid oxide fuel cell system with anode off-gas recirculation”. In: *Journal of Power Sources* 328 (2016), pp. 105–113.

[63] F. Zabihian and A. S. Fung. “Thermodynamic sensitivity analysis of hybrid system based on solid oxide fuel cell”. In: *Sustainable Energy Technologies and Assessments* 6 (June 2014), pp. 51–59.

[64] J. Larminie and A. Dicks. *Fuel Cell Systems Explained (Second Edition)*. Wiley, 2003.

[65] R. Peters et al. “Analysis of solid oxide fuel cell system concepts with anode recycling”. In: *International Journal of Hydrogen Energy* 38.16 (May 2013), pp. 6809–6820.

[66] J. Hollmann et al. “System Simulation and Analysis of an LNG-Fueled SOFC System Using Additively Manufactured High Temperature Heat Exchangers”. In: *Energies* 15.3 (Jan. 2022), p. 941.

[67] S. S. Kumar et al. “Grid Tied Solid Oxide Fuel Cell Power Generation System for Peak Load Management”. In: *nternational Conference on Electrical, Computer and Communication Technologies* 3 (2019).

[68] X. Yu et al. “Fuel cell power conditioning for electric power applications: A summary”. In: *IET Electric Power Applications* 1.5 (2007), pp. 643–656.

[69] L. Luckose, H. L. Hess, and B. K. Johnson. “Fuel cell propulsion system for marine applications”. In: *IEEE Electric Ship Technologies Symposium, ESTS 2009*. 2009, pp. 574–580.

[70] J. Ki and D. Kim. “Computational model to predict thermal dynamics of planar solid oxide fuel cell stack during start-up process”. In: *Journal of Power Sources* 195.10 (May 2010), pp. 3186–3200.

[71] U. Bossel. “Rapid startup SOFC modules”. In: *Energy Procedia*. Vol. 28. Elsevier Ltd, Jan. 2012, pp. 48–56.

[72] C. Stiller. *Design, Operation and Control Modelling of SOFC/GT Hybrid Systems*. Tech. rep. Trondheim: Norwegian University of Science and Technology, 2006.

[73] F. Baldi. *ODes aCCSES Report: Optimal design and control of cruise ship energy systems*. Tech. rep. École Polytechnique Fédérale de Lausanne, 2019, pp. 1–28.

[74] L. Tan, C. Yang, and N. Zhou. "Thermoeconomic optimization of a solid oxide fuel cell and proton exchange membrane fuel cell hybrid power system". In: *Journal of Fuel Cell Science and Technology* 11.1 (Feb. 2014).

[75] L. Tan, C. Yang, and N. Zhou. "Synthesis/design optimization of SOFC-PEM hybrid system under uncertainty". In: *Chinese Journal of Chemical Engineering* 23.1 (Jan. 2015), pp. 128–137.

[76] A. Hagen, R. Caldogno, and X. Sun. "Ammonia fueled SOFC for shipping – The Aegir project". In: *15th European SOFC & SOE Forum*. Vol. 445-450. 2022, pp. 5–8.

[77] H. Sapra. "Combined Gas Engine- Solid Oxide Fuel Cell Systems for Marine Power Generation". PhD thesis. 2020.

[78] Y. Kawabata et al. "Practicality Evaluation of Solid Oxide Fuel Cell (SOFC) - Micro Gas Turbine (MGT) Hybrid Power Generation System". In: *Proceedings of 14th European SOFC & SOE Forum*. October. 2020, pp. 132–143.

[79] D. P. Bakalis and A. G. Stamatis. "Incorporating available micro gas turbines and fuel cell: Matching considerations and performance evaluation". In: *Applied Energy* 103 (Mar. 2013), pp. 607–617.

[80] L. Barelli, G. Bidini, and A. Ottaviano. "Part load operation of SOFC/GT hybrid systems: Stationary analysis". In: *International Journal of Hydrogen Energy* 37.21 (Nov. 2012), pp. 16140–16150.

[81] Y. Komatsu, S. Kimijima, and J. S. Szmyd. "Performance analysis for the part-load operation of a solid oxide fuel cell-micro gas turbine hybrid system". In: *Energy* 35.2 (Feb. 2010), pp. 982–988.

[82] J. Chen et al. "Effect of different operating strategies for a SOFC-GT hybrid system equipped with anode and cathode ejectors". In: *Energy* 163 (Nov. 2018), pp. 1–14.

[83] F. D. F. Chuahy and S. L. Kokjohn. "Solid oxide fuel cell and advanced combustion engine combined cycle: A pathway to 70% electrical efficiency". In: *Applied Energy* 235 (Feb. 2019), pp. 391–408.

[84] Y. M. A. Welaya, M. Mosleh, and N. R. Ammar. "Energy analysis of a combined solid oxide fuel cell with a steam turbine power plant for marine applications". In: *Journal of Marine Science and Application* 12.4 (Dec. 2014), pp. 473–483.

[85] A. Arsalis. "Thermoeconomic modeling and parametric study of hybrid SOFC-gas turbine-steam turbine power plants ranging from 1.5 to 10 MWe". In: *Journal of Power Sources* 181.2 (July 2008), pp. 313–326.

[86] Z. Wu et al. "Dynamic modeling and operation strategy of natural gas fueled SOFC-Engine hybrid power system with hydrogen addition by metal hydride for vehicle applications". In: *eTransportation* 5 (Aug. 2020), p. 100074.

[87] Chevron. *Everything You Need to Know About Marine Fuels*. Tech. rep. Ghent, 2012.

[88] P. Boldrin et al. “Strategies for Carbon and Sulfur Tolerant Solid Oxide Fuel Cell Materials, Incorporating Lessons from Heterogeneous Catalysis”. In: *Chemical Reviews* 116.22 (Nov. 2016), pp. 13633–13684.

[89] D. N. Kuimov, M. S. Minkin, and A. D. Lukyanov. “Low-sulfur fuel and oil production”. In: *Materials Science Forum* 870 (2016), pp. 671–676.

[90] Y. Shiratori, T. Quang-Tuye, and K. Sasaki. “Performance enhancement of biodiesel fueled SOFC using paper-structured catalyst”. In: *International Journal of Hydrogen Energy* 38.23 (Aug. 2013), pp. 9856–9866.

[91] A. Kumar and S. Sharma. “Potential non-edible oil resources as biodiesel feedstock: An Indian perspective”. In: *Renewable and Sustainable Energy Reviews* 15.4 (May 2011), pp. 1791–1800.

[92] M. C. Díaz-de-Baldasano et al. “Conceptual design of offshore platform supply vessel based on hybrid diesel generator-fuel cell power plant”. In: *Applied Energy* 116 (Mar. 2014), pp. 91–100.

[93] P. Nehter et al. “Diesel Based SOFC Demonstrator for Maritime Applications”. In: *ECS Transactions* 78.1 (May 2017), pp. 171–180.

[94] L. Van Hoecke et al. *Challenges in the use of hydrogen for maritime applications.* Feb. 2021.

[95] R. A. Evrin and I. Dincer. “Thermodynamic analysis and assessment of an integrated hydrogen fuel cell system for ships”. In: *International Journal of Hydrogen Energy* 44.13 (Mar. 2019), pp. 6919–6928.

[96] P. Kazempoor, V. Dorer, and F. Ommi. “Evaluation of hydrogen and methane-fuelled solid oxide fuel cell systems for residential applications: System design alternative and parameter study”. In: *International Journal of Hydrogen Energy* 34 (2009), pp. 8630–8644.

[97] L. Wang et al. “Reversible solid-oxide cell stack based power-to-x-to-power systems: Comparison of thermodynamic performance”. In: *Applied Energy* 275 (Oct. 2020), p. 115330.

[98] M. M. F. Hasan, A. M. Zheng, and I. A. Karimi. “Minimizing boil-off losses in liquefied natural gas transportation”. In: *Industrial and Engineering Chemistry Research* 48.21 (2009), pp. 9571–9580.

[99] International Gas Union. *2020 World LNG Report.* Tech. rep. 2020, p. 68.

[100] P. Balcombe et al. “How to decarbonise international shipping: Options for fuels, technologies and policies”. In: *Energy Conversion and Management* 182 (Feb. 2019), pp. 72–88.

[101] T. M. Gür. “Comprehensive review of methane conversion in solid oxide fuel cells: Prospects for efficient electricity generation from natural gas”. In: *Progress in Energy and Combustion Science* 54 (May 2016), pp. 1–64.

[102] R. Payne, J. Love, and M. Kah. “Generating Electricity at 60% Electrical Efficiency from 1-2 kWe SOFC Products”. In: *ECS Transactions.* The Electrochemical Society, 2009, pp. 231–239.

[103] S. A. Saadabadi et al. "Solid Oxide Fuel Cells fuelled with biogas: Potential and constraints". In: *Renewable Energy* 134 (Apr. 2019), pp. 194–214.

[104] I. Ridjan. "Integrated electrofuels and renewable energy systems". PhD thesis. Aalborg University, 2015.

[105] D. Cocco and V. Tola. "Externally reformed solid oxide fuel cell-micro-gas turbine (SOFC-MGT) hybrid systems fueled by methanol and di-methyl-ether (DME)". In: *Energy* 34.12 (Dec. 2009), pp. 2124–2130.

[106] J. Rechberger et al. "Development of a Methanol SOFC APU Demonstration System". In: *ECS Transactions* 25.2 (2009), pp. 1085–1092.

[107] N. Laosiripojana and S. Assabumrungrat. "Catalytic steam reforming of methane, methanol, and ethanol over Ni/YSZ: The possible use of these fuels in internal reforming SOFC". In: *Journal of Power Sources* 163.2 (Jan. 2007), pp. 943–951.

[108] M. Liu et al. "Direct liquid methanol-fueled solid oxide fuel cell". In: *Journal of Power Sources* 185.1 (Oct. 2008), pp. 188–192.

[109] Q. Xu and M. Ni. "Modelling of high temperature direct methanol solid oxide fuel cells". In: *International Journal of Energy Research* 45.2 (2021), pp. 3097–3112.

[110] J. Ellis and K. Tanneberger. *Study on the use of ethyl and methyl alcohol as alternative fuels in shipping*. Tech. rep. EMSA, 2016.

[111] K. Moirangthem and D. Baxter. *Alternative Fuels for Marine and Inland Waterways*. Tech. rep. JRC, 2016.

[112] C. Su et al. "Coke formation and performance of an intermediate-temperature solid oxide fuel cell operating on dimethyl ether fuel". In: *Journal of Power Sources* 196.4 (Feb. 2011), pp. 1967–1974.

[113] E. P. Murray, S. J. Harris, and H. Jen. "Solid Oxide Fuel Cells Utilizing Dimethyl Ether Fuel". In: *Journal of The Electrochemical Society* 149.9 (2002), A1127.

[114] K. Sato et al. "Dual fuel type solid oxide fuel cell using dimethyl ether and liquefied petroleum gas as fuels". In: *Journal of Power Sources* 217 (Nov. 2012), pp. 37–42.

[115] M. Cheliotis et al. "Review on the Safe Use of Ammonia Fuel Cells in the Maritime Industry". In: *Energies 2021, Vol. 14, Page 3023* 14.11 (May 2021), p. 3023.

[116] A. Afif et al. "Ammonia-fed fuel cells: A comprehensive review". In: *Renewable and Sustainable Energy Reviews* 60 (July 2016), pp. 822–835.

[117] L. van Biert. "Solid Oxide Fuel Cells for Ships". PhD thesis. Delft University of Technology, 2020.

[118] Z. Wan et al. "Ammonia as an effective hydrogen carrier and a clean fuel for solid oxide fuel cells". In: *Energy Conversion and Management* 228 (Jan. 2021), p. 113729.

[119] Q. Ma et al. "Direct utilization of ammonia in intermediate-temperature solid oxide fuel cells". In: *Electrochemistry Communications* 8.11 (Nov. 2006), pp. 1791–1795.

[120] M. Ni, M. K. H. Leung, and D. Y. C. Leung. "Ammonia-fed solid oxide fuel cells for power generation-A review". In: *International Journal of Energy Research* 33.11 (2009), pp. 943–959.

[121] L. Barelli, G. Bidini, and G. Cinti. "Operation of a solid oxide fuel cell based power system with ammonia as a fuel: Experimental test and system design". In: *Energies* 13.23 (2020).

[122] G. Cinti et al. "SOFC operating with ammonia: Stack test and system analysis". In: *International Journal of Hydrogen Energy* 41.31 (Aug. 2016), pp. 13583–13590.

[123] H. L. Frandsen et al. "Operation and modelling of ammonia fuelled solid oxide fuel cell , stack and systems". In: *15th European SOFC & SOE Forum*. Vol. B. 2022, pp. 314–321.

[124] Food and Agriculture Organization of the United Nations. *World fertilizer trends and outlook to 2022*. Tech. rep. 2019.

[125] IEA. *The Future of Hydrogen*. Tech. rep. 2019.

[126] IEA. *World Energy Outlook 2020*. Tech. rep. 2020.

[127] IEA. *Oil 2021 - Analysis and forecast to 2026*. Tech. rep. 2021.

[128] T. H. Fleisch, A. Basu, and R. A. Sills. "Introduction and advancement of a new clean global fuel: The status of DME developments in China and beyond". In: *Journal of Natural Gas Science and Engineering* 9 (Nov. 2012), pp. 94–107.

[129] Methanol Institute. *Methanol Safe Handling Manual - 5th Edition*. Tech. rep. 2020.

[130] B. Prabowo et al. "State of the art of global dimethyl ether production and it's potentional application in Indonesia". In: *Proceedings of the Pakistan Academy of Sciences: Part B* 54.1B (2017), pp. 29–39.

[131] MARIN. *Sustainable Power Database*. 2021. URL: https://sustainablepower.application.marin.nl/table?.

[132] Neste. *Renewable Diesel Handbook*. Tech. rep. 2020.

[133] M. Al-Breiki and Y. Bicer. "Comparative cost assessment of sustainable energy carriers produced from natural gas accounting for boil-off gas and social cost of carbon". In: *Energy Reports* 6 (Nov. 2020), pp. 1897–1909.

[134] A. Al-Enazi et al. "A review of cleaner alternative fuels for maritime transportation". In: *Energy Reports* 7 (Nov. 2021), pp. 1962–1985.

[135] A. D. Korberg et al. "Techno-economic assessment of advanced fuels and propulsion systems in future fossil-free ships". In: *Renewable and Sustainable Energy Reviews* 142 (May 2021), p. 110861.

[136] M. Perčić et al. "Application of fuel cells with zero-carbon fuels in short-sea shipping". In: *Applied Energy* 309 (Mar. 2022), p. 118463.

[137] U.S. Geological Survey. *Nitrogen (Fixed) - Ammonia*. Tech. rep. 2021.

[138] Ship & Bunker. *World Bunker Prices*. 2022. URL: https://shipandbunker.com/prices.

[139] TNO. *Power-2-Fuel Cost Analysis*. Tech. rep. 2020.

[140] H. Derking et al. "Liquid Hydrogen Storage: Status and Future Perspectives". In: *Cryogenic Heat and Mass Transfer*. 2019.

[141] K. Law et al. "U.S. Department of Energy Hydrogen Storage Cost Analysis". In: *U.S. Department of Energy* (2013).

[142] A. Yang, C. Antrassian, and J. Kurtzman. *Production of Dimethyl Ether (DME) for Transportation Fuel Part of the Biochemical and Biomolecular Engineering Commons*. Tech. rep. 2020.

[143] DNV GL. *Guidance for safe return to port projects*. Tech. rep. 2016.

[144] R. Geertsma and M. Krijgsman. "Alternative fuels and power systems to reduce environmental impact of support vessels". In: (2019).

[145] S. Wang and T. Notteboom. "The Adoption of Liquefied Natural Gas as a Ship Fuel: A Systematic Review of Perspectives and Challenges". In: *Transport Reviews* 34.6 (Nov. 2014), pp. 749–774.

[146] L. Xiang, E. Song, and Y. Ding. "A Two-Zone Combustion Model for Knocking Prediction of Marine Natural Gas SI Engines". In: *Energies 2018, Vol. 11, Page 561* 11.3 (Mar. 2018), p. 561.

[147] K. Cheenkachorn, C. Poompipatpong, and C. G. Ho. "Performance and emissions of a heavy-duty diesel engine fuelled with diesel and LNG (liquid natural gas)". In: *Energy* 53 (May 2013), pp. 52–57.

[148] H. Pan et al. "Effect of hydrogen addition on criteria and greenhouse gas emissions for a marine diesel engine". In: *International Journal of Hydrogen Energy* 39.21 (July 2014), pp. 11336–11345.

[149] S. M. Aceves et al. "High-density automotive hydrogen storage with cryogenic capable pressure vessels". In: *International Journal of Hydrogen Energy* 35.3 (Feb. 2010), pp. 1219–1226.

[150] B. N. van Veldhuizen, R. G. Hekkenberg, and L. Codiglia. "Fuel Cell Systems Applied in Expedition Cruise Ships - A Comparative Impact Analysis". In: *HIPER*. 2020, pp. 170–188.

[151] C. Bourne et al. *Application of fuel cells in surface ships*. Tech. rep. 2001.

[152] R. Fang et al. "System-level thermal modeling and co-simulation with hybrid power system for future all electric ship". In: *IEEE Electric Ship Technologies Symposium, ESTS 2009* (2009), pp. 547–553.

[153] C. Strazza et al. "Comparative LCA of methanol-fuelled SOFCs as auxiliary power systems on-board ships". In: *Applied Energy* 87.5 (May 2010), pp. 1670–1678.

[154] L. K. C. Tse et al. "Solid oxide fuel cell/gas turbine trigeneration system for marine applications". In: *Journal of Power Sources* 196.6 (Mar. 2011), pp. 3149–3162.

[155] Y. M. A. Welaya, M. M. El Gohary, and N. R. Ammar. "A comparison between fuel cells and other alternatives for marine electric power generation". In: *International Journal of Naval Architecture and Ocean Engineering* 3.2 (June 2011), pp. 141–149.

[156] K. Leites et al. “Design of different diesel based fuel cell systems for seagoing vessels and their evaluation”. In: *ECS Transactions* 42.1 (2012), pp. 49–58.

[157] W. S. Weidle, P. Field, and N. Buckley. *Arctic Ship Design Impacts: Green Arctic Patrol Vessel (GAPV) Project*. Tech. rep. Naval Surface Warfare Center, 2012.

[158] L. Cohen, A. Tate, and N. Weinhold. *Investigation into the Implications of Fuel Cell Shipboard Integration into the T-AGOS 19 Class*. Tech. rep. Feb. 2012.

[159] J. J. De-Troya et al. “Analysing the possibilities of using fuel cells in ships”. In: *International Journal of Hydrogen Energy* (2016).

[160] F. Baldi et al. “Energy and Exergy Analysis of a Cruise Ship”. In: *Energies* 11.10 (Sept. 2018), p. 2508.

[161] J. Ahn et al. “Performance and availability of a marine generator-solid oxide fuel cell-gas turbine hybrid system in a very large ethane carrier”. In: *Journal of Power Sources* 399 (Sept. 2018), pp. 199–206.

[162] G. V. Huerta et al. “Exergy analysis of the diesel pre-reforming SOFC-system with anode off-gas recycling in the SchIBZ project. Part II: System exergetic evaluation”. In: *International Journal of Hydrogen Energy* 44.21 (Apr. 2019), pp. 10916–10924.

[163] K. Kim et al. “A Preliminary Study on an Alternative Ship Propulsion System Fueled by Ammonia: Environmental and Economic Assessments”. In: *Journal of Marine Science and Engineering 2020, Vol. 8, Page 183* 8.3 (Mar. 2020), p. 183.

[164] H. Xing et al. *Fuel cell power systems for maritime applications: Progress and perspectives*. Tech. rep. 3. 2021, pp. 1–34.

[165] M. Gianni, A. Pietra, and R. Taccani. “Outlook of future implementation of PEMFC and SOFC onboard cruise ships”. In: *E3S Web of Conferences* 238 (Feb. 2021). Ed. by U. Desideri, L. Ferrari, and J. Yan, p. 04004.

[166] C. Dall’Armi, D. Micheli, and R. Taccani. “Comparison of different plant layouts and fuel storage solutions for fuel cells utilization on a small ferry”. In: *International Journal of Hydrogen Energy* 46.26 (Apr. 2021), pp. 13878–13897.

[167] M. Rivarolo et al. “Multi-criteria comparison of power generation and fuel storage solutions for maritime application”. In: *Energy Conversion and Management* 244 (Sept. 2021), p. 114506.

[168] L. Kistner et al. “Techno-economic and Environmental Comparison of Internal Combustion Engines and Solid Oxide Fuel Cells for Ship Applications”. In: *Journal of Power Sources* 508 (Oct. 2021), p. 230328.

[169] A. Haseltalab et al. “Component sizing and energy management for SOFC-based ship power systems”. In: *Energy Conversion and Management* 245 (Oct. 2021), p. 114625.

[170] L. Micoli, T. Coppola, and M. Turco. “A Case Study of a Solid Oxide Fuel Cell Plant on Board a Cruise Ship”. In: *Journal of Marine Science and Application* 20.3 (Sept. 2021), pp. 524–533.

[171] S. D. Micco et al. “Ammonia-based Solid Oxide Fuel Cell for zero emission maritime power: a case study”. In: *European Fuel Cells*. 2021, p. 06007.

[172] M. Archetti et al. “High temperature fuel cells to reduce CO2 emission in the maritime sector”. In: *European Fuel Cells*. 2022.

[173] L. Kistner, A. Bensmann, and R. Hanke-Rauschenbach. “Optimal Design of a Distributed Ship Power System with Solid Oxide Fuel Cells under the Consideration of Component Malfunctions”. In: *Applied Energy* 316 (June 2022), p. 119052.

[174] P. A. Duong et al. “Energy and Exergy Analysis of an Ammonia Fuel Cell Integrated System for Marine Vessels”. In: *Energies* 15.9 (May 2022), p. 3331.

[175] Z. Wang et al. “Energy, exergy and economy (3E) investigation of a SOFC-GT-ORC waste heat recovery system for green power ships”. In: *Thermal Science and Engineering Progress* 32 (July 2022), p. 101342.

[176] B. V. Veldhuizen, L. V. Biert, and K. Visser. “Comparative thermodynamic analysis of marine SOFC system for alternative fuels”. In: *15th European SOFC & SOE Forum*. Vol. B. 2022, pp. 340–918.

[177] J. Hollmann et al. “Progress in the development of LNG and Diesel-fueled SOFC systems for maritime applications”. In: *15th European SOFC & SOE Forum*. Vol. A. 2022, pp. 253–733.

[178] W. Li et al. “Diagnosis for Timing Gears Noise of a Diesel Generating Set”. In: *Lecture Notes in Mechanical Engineering* (2020), pp. 582–593.

[179] R. Scataglini et al. “A Direct Manufacturing Cost Model for Solid-Oxide Fuel Cell Stacks”. In: *Fuel Cells* 17.6 (Dec. 2017), pp. 825–842.

[180] L. van Biert, K. Mrozewski, and P. ’t Hart. *Public final report: Inventory of the application of Fuel Cells in the Maritime sector*. Tech. rep. Maritime Knowledge Centre, 2021.

[181] S. Campanari. *Full Load and Part-Load Performance Prediction for Integrated SOFC and Microturbine Systems*. Tech. rep. 2000.

[182] K. Levander. *System based ship design*. 2007.

[183] B. Taskar et al. “The effect of waves on engine-propeller dynamics and propulsion performance of ships”. In: *Ocean Engineering* 122 (Aug. 2016), pp. 262–277.

[184] EGG Technical Services. *Fuel Cell Handbook (Seventh Edition)*. 2004.

[185] M. Suzuki, S. Inoue, and T. Shigehisa. “Field Test Result of Residential SOFC CHP System Over 10 Years, 89000 Hours”. In: *ECS*. Vol. 103. 1. 2021, pp. 25–30.

[186] C. M. Milkie and A. N. Perakis. “Statistical methods for planning diesel engine overhauls in the U. S. Coast Guard”. In: *Naval Engineers Journal*. Vol. 116. 2. American Society of Naval Engineers, 2004, pp. 31–42.

[187] D. Woodyard. *Pounder’s Marine Diesel Engines and Gas Turbines*. 2009.

[188] N. Jones. “Ocean uproar: saving marine life from a barrage of noise.” In: *Nature* 568.7752 (Apr. 2019), pp. 158–162.

[189] O. Chaves, M. Nickelsen, and H. Gaspar. “Enhancing Virtual Prototype in Ship Design Using Modular Techniques”. In: *29th European Conference on Modelling and Simulation*. 2015.

[190] S. O. Erikstad. “Modularisation in Shipbuilding and Modular Production”. 2009.

[191] S. Pekic. *GTT’s LNG containment system to be used for ammonia*. 2021. URL: https://www.offshore-energy.biz/gtts-lng-containment-system-to-be-used-for-ammonia/.

[192] D. Sahnen. “Key aspects for new ship fuels”. In: *Methanol Day*. 2020.

[193] C. Bang-Møller et al. “Decentralized combined heat and power production by two-stage biomass gasification and solid oxide fuel cells”. In: *Energy* 58 (Sept. 2013), pp. 527–537.

[194] M. R. Barakat et al. “JADE-Based Multi-agent Decentralized Energy Management System of a Hybrid Marine-Hydrogen Power Generation System”. In: *Lecture Notes in Electrical Engineering*. Vol. 697. Springer, Cham, 2020, pp. 245–257.

[195] K. Leites et al. “SchIBZ – Application of solid oxide fuel cells for oceangoing ships SchIBZ”. In: *Conference on Fundamentals and Development of Fuel Cells*. 5. 2013.

[196] G. Chang et al. “DC Bus Systems for Electrical Ships: Recent Advances and Analysis of a Real Case”. In: *IEEE Electrification Magazine* 8.3 (Sept. 2020), pp. 28–39.

[197] C. Nuchturee, T. Li, and H. Xia. “Energy efficiency of integrated electric propulsion for ships-A review”. In: *Renewable and Sustainable Energy Reviews* 134.110145 (2020).

[198] J. F. Hansen et al. “Increased Operational Performance of OSVs by Onboard DC Grid”. In: *Technology and Operation of Offshore Support Vessels*. 4. 2011, pp. 79–84.

[199] B. Zahedi, L. E. Norum, and K. B. Ludvigsen. “Optimized efficiency of all-electric ships by dc hybrid power systems”. In: *Journal of Power Sources* 255 (June 2014), pp. 341–354.

[200] F. D. Kanellos, G. J. Tsekouras, and J. Prousalidis. “Onboard DC grid employing smart grid technology: challenges, state of the art and future prospects”. In: *IET Electrical Systems in Transportation* 5.1 (Mar. 2015), pp. 1–11.

[201] S. Yadav, N. H. Van Der Blii, and P. Bauer. “Modeling and Stability Analysis of Radial and Zonal Architectures of a Bipolar DC Ferry Ship”. In: *2021 IEEE Electric Ship Technologies Symposium, ESTS 2021* (2021).

[202] IEEE. *IEEE Recommended Practice for 1 kV to 35 kV Medium-Voltage DC Power Systems on Ships*. Tech. rep. New York, 2018.

[203] S. Habib et al. “Contemporary trends in power electronics converters for charging solutions of electric vehicles”. In: *CSEE Journal of Power and Energy Systems* 6.4 (Dec. 2020), pp. 911–929.

[204] A. M. Bassam et al. “Development of a multi-scheme energy management strategy for a hybrid fuel cell driven passenger ship”. In: *International Journal of Hydrogen Energy* 42.1 (Jan. 2017), pp. 623–635.

[205] ABS. *Fuel cell power systems for marine and offshore applications*. Tech. rep. 2019.

[206] DNV GL. “Fuel Cell Installations”. In: *DNVGL Rules for Classification of Ships*. 2019. Chap. Part 6 Cha, pp. 78–97.

[207] M. Sharifzadeh, M. Meghdari, and D. Rashtchian. “Multi-objective design and operation of Solid Oxide Fuel Cell (SOFC) Triple Combined-cycle Power Generation systems: Integrating energy efficiency and operational safety”. In: *Applied Energy* 185 (Jan. 2017), pp. 345–361.

[208] DNV. *Shipping 2020*. Tech. rep. 2012.

[209] M. Altmann et al. “FCSHIP: Environmental Impacts and Costs of Hydrogen, Natural Gas and Conventional Fuels for Fuel Cell Ships”. In: *15th World Hydrogen Energy Conference*. Yokohama, 2004.

[210] Y. D. Lee et al. “Environmental impact assessment of a solid-oxide fuel-cell-based combined-heat-and-power-generation system”. In: *Energy* 79.C (Jan. 2015), pp. 455–466.

[211] A. Mehmeti et al. “Life cycle sustainability of solid oxide fuel cells: From methodological aspects to system implications”. In: *Journal of Power Sources* 325 (Sept. 2016), pp. 772–785.

[212] Y. Bicer and F. Khalid. “Life cycle environmental impact comparison of solid oxide fuel cells fueled by natural gas, hydrogen, ammonia and methanol for combined heat and power generation”. In: *International Journal of Hydrogen Energy* 45.5 (Jan. 2020), pp. 3670–3685.

[213] S. Sarner et al. “Recycling possibilities and strategies for solid oxide cell stacks”. In: *15th European SOFC & SOE Forum*. Vol. B. 2022, pp. 714–718.

[214] FELICITAS. *Publishable Final Activity Report*. Tech. rep. 2009.

[215] METHAPU. *Publishable Executive Summary*. Tech. rep. 2010.

[216] CORDIS. *Nautical Integrated Hybrid Energy System for Long-haul Cruise Ships*. 2020. URL: https://cordis.europa.eu/project/id/861647.

[217] S. A. Ansar et al. “Electrochemical processes and energy systems towards stepwise emission reduction of the marine sector”. In: *15th European SOFC & SOE Forum*. Vol. 1. 2022, pp. 672–678.

[218] C. Bettini et al. “ShipFC project: NH3-SOFC to decarbonise commercial shipping applications”. In: *15th European SOFC & SOE Forum*. Vol. A. 2022, pp. 660–671.

[219] ShipFC. *Green Ammonia Energy System*. 2022. URL: https://shipfc.eu/.

[220] Atena. *FuelSOME*. 2022. URL: https://www.atenaweb.com/en/fuelsome/.

[221] OpenAIRE. *HELENUS*. 2022. URL: https://cordis.europa.eu/project/id/101056784.

[222] Fuel Cells Bulletin. “Sunfire 50 kW SOFC for ship-integrated fuel cell project in Germany”. In: *Fuel Cells Bulletin* 2015.11 (Nov. 2015), pp. 3–4.

[223] Fuel Cells Bulletin. “MultiSchiBZ project on SOFCs for onboard clean power for ships”. In: *Fuel Cells Bulletin* 2019.9 (Sept. 2019), p. 5.

[224] M. Metten et al. “Evaluation of a hybrid SOFC & battery genset for cruise ship applications”. In: *15th European SOFC & SOE Forum*. Vol. A. 2022, pp. 612–620.

[225] Adaptive Energy. *Endurance Series*. Tech. rep. 2022.

[226] S. J. Mcphail, J. Kiviaho, and B. Conti. *Status of SOFC deployment 2017*. Tech. rep. IEA, 2017.

[227] F. Moradi. *AVL Fuel Cell*. Tech. rep. AVL, 2016.

[228] BOSCH. *The stationary fuel cell system by Bosch*. Tech. rep. 2022.

[229] Bloom Energy. *Energy Server 5 Product Datasheet*. Tech. rep. 2022.

[230] Convion. *Products*. 2022. URL: http://convion.fi/products/.

[231] G. D. Blake. *Solid Oxide Fuel Cell Development for Transportation and Stationary Applications:* tech. rep. Delphi, 2010.

[232] R. Leah et al. “Commercialization of Ceres SteelCell ® Technology for Power Generation and Electrolysis”. In: *15th European SOFC & SOE Forum*. Vol. A. 2022, pp. 39–48.

[233] Doosan. *PureCell Model 400*. 2022. URL: https://www.doosanfuelcell.com/en/prod/prod-0103/.

[234] Fuel Cell Energy. *SureSource 4000*. Tech. rep. 2022.

[235] h2e POWER. *Solid Oxide Fuel Cell*. 2022. URL: https://www.h2epower.net/solid-oxide-fuel-cell/.

[236] Power Mitsubishi. *MEGAMIE*. Tech. rep. 2022.

[237] Miura. *Fuel cell FC-5B*. 2022. URL: https://www.miuraz.co.jp/product/thermoelectric/sofc.html.

[238] Osaka Gas Co. *Osaka Gas to Release a New Product*. Tech. rep. 2020, pp. 1–5.

[239] Hexis AG. *Galileo*. Tech. rep. Wintherthur, 2017.

[240] U. Power. *Products*. 2022. URL: https://www.upstartpower.com/products/#upgennxg.

[241] WATT. *Imperium*. 2022. URL: https://www.wattfuelcell.com/portable-power/watt-imperium/.

[242] R. R. Liu et al. “Influence of water vapor on long-term performance and accelerated degradation of solid oxide fuel cell cathodes”. In: *Journal of Power Sources* 196.17 (Sept. 2011), pp. 7090–7096.

[243] A. Hagen, K. Neufeld, and Y. L. Liu. “Effect of Humidity in Air on Performance and Long-Term Durability of SOFCs”. In: *Journal of The Electrochemical Society* 157.10 (July 2010), B1343.

[244] Z. Yang et al. “A short review of cathode poisoning and corrosion in solid oxide fuel cell”. In: *International Journal of Hydrogen Energy* 42.39 (Sept. 2017), pp. 24948–24959.

[245] R. r. Liu, D. j. Wang, and J. Leng. “Influence of NaCl on cathode performance of solid oxide fuel cells”. In: *Chemical Research in Chinese Universities* 29.4 (July 2013), pp. 747–750.

[246] N. Thambiraj et al. “SOFC Cathode Degradation Due to Salt Contamination”. In: *ECS Meeting Abstracts* 78 (2017), pp. 915–925.

[247] J. W. Fergus. “Effect of Water Vapor and Hydrogen on the Oxidation of Metallic Interconnect Materials for Solid Oxide Fuel Cells”. In: *ECS Proceedings Volumes*. 2005, pp. 1806–1815.

[248] K. Yoshimoto, Y. Hirata, and M. Chiba. “Salt in Sea Atmosphere and Its Removal for Gas Turbines.” In: *American Society of Mechanical Engineers (Paper)* 76 -GT-58 (1976).

[249] G. D. Agnew et al. “Scale Up of a Multi-Functional Solid Oxide Fuel Cell to Multi-Tens of Kilowatt Level (MF-SOFC)”. In: *ECS Proceedings Volumes* 2003-07.1 (Jan. 2003), p. 78.

[250] E. Ivers-Tiffée, A. Weber, and D. Herbstritt. “Materials and technologies for SOFC-components”. In: *Journal of the European Ceramic Society* 21.10-11 (Jan. 2001), pp. 1805–1811.

[251] D. Udomsilp et al. “Metal-Supported Solid Oxide Fuel Cells with Exceptionally High Power Density for Range Extender Systems”. In: *Cell Reports Physical Science* 1.6 (June 2020), p. 100072.

[252] A. Hagen et al. “SOFC stacks for mobile applications with excellent robustness towards thermal stresses”. In: *International Journal of Hydrogen Energy* 45.53 (Oct. 2020), pp. 29201–29211.

[253] M. Z. Khan et al. “Flat-tubular solid oxide fuel cells and stacks: a review”. In: *Journal of Asian Ceramic Societies* 9.3 (2021), pp. 745–770.

[254] J.-H. Kim et al. “Fabrication and characteristics of anode-supported flat-tube solid oxide fuel cell”. In: *Journal of Power Sources* 122 (2003), pp. 138–143.

[255] M. Ilbas, M. Asmare Alemu, and F. Mustafa Cimen. “Comparative performance analysis of a direct ammonia-fuelled anode supported flat tubular solid oxide fuel cell: A 3D numerical study”. In: *International Journal of Hydrogen Energy* 47 (2022), pp. 3416–3428.

[256] H. Ghezel-Ayagh. “Progress in SOFC Technology Development at FuelCell Energy”. In: *20th Annual Solid Oxide Fuel Cell (SOFC)*. Project Review Meeting Washington, DC, 2019.

[257] M. Promsen et al. “Feasibility study on saturated water cooled solid oxide fuel cell stack”. In: *Applied Energy* 279 (Dec. 2020), p. 115803.

[258] V. M. Janardhanan, V. Heuveline, and O. Deutschmann. “Performance analysis of a SOFC under direct internal reforming conditions”. In: *Journal of Power Sources* 172.1 (Oct. 2007), pp. 296–307.

[259] M. Gandiglio, A. Lanzini, and M. Santarelli. “Large stationary solid oxide fuel cell (SOFC) power plants”. In: *Modeling, Design, Construction, and Operation of Power Generators with Solid Oxide Fuel Cells*. Springer Verlag, 2018, pp. 233–261.

[260] N. Mahato et al. "Progress in material selection for solid oxide fuel cell technology: A review". In: *Progress in Materials Science* 72 (July 2015), pp. 141–337.

[261] A. Pesaran et al. "Development of a new ceria/yttria-ceria double-doped bismuth oxide bilayer electrolyte low-temperature SOFC with higher stability". In: *Ionics* 25 (2019), pp. 3153–3164.

[262] L. van Biert et al. "Dynamic modelling of a direct internal reforming solid oxide fuel cell stack based on single cell experiments". In: *Applied Energy* 250 (Sept. 2019), pp. 976–990.

[263] M. Kusnezoff et al. "Influence of Electrode Design and Contacting Layers on Performance of Electrolyte Supported SOFC/SOEC Single Cells". In: *Materials 2016, Vol. 9, Page 906* 9.11 (Nov. 2016), p. 906.

[264] O. Aydin et al. "Designing graded catalytic domain to homogenize temperature distribution while dry reforming of CH4". In: *International Journal of Hydrogen Energy* 43.36 (Sept. 2018), pp. 17431–17443.

[265] X. Wang et al. "Experimental and numerical studies of a bifunctional proton conducting anode of ceria-based SOFCs free from internal shorting and carbon deposition". In: *Electrochimica Acta* 264 (Feb. 2018), pp. 109–118.

[266] A. Lanzini et al. "Reporting Degradation from Different Fuel Contaminants in Ni-anode SOFCs". In: *Fuel Cells* 17.4 (Aug. 2017), pp. 423–433.

[267] S. C. Paulson and V. I. Birss. "Chromium Poisoning of LSM-YSZ SOFC Cathodes: I. Detailed Study of the Distribution of Chromium Species at a Porous, Single-Phase Cathode". In: *Journal ofThe Electrochemical Society* 151.11 (2004), A1961–A1968.

[268] C. Laing et al. "Mitigation of Chromium Assisted Degradation of LSM Cathode in SOFC". In: *ECS Transactions*. The Electrochemical Society, 2017, pp. 57–64.

[269] T. Norgaard. "Scenarios for uptake of alternative fuels in the marine industry". In: *World Marine Technology Conference*. 2022.

[270] Y. Bae et al. "Three-dimensional dynamic modeling and transport analysis of solid oxide fuel cells under electrical load change". In: *Energy Conversion and Management* 165 (June 2018), pp. 405–418.

[271] F. Baldi et al. "A cogeneration system based on solid oxide and proton exchange membrane fuel cells with hybrid storage for off-grid applications". In: *Frontiers in Energy Research* 6 (2019), p. 139.

[272] T. Parhizkar and S. Hafeznezami. "Degradation based operational optimization model to improve the productivity of energy systems, case study: Solid oxide fuel cell stacks". In: *Energy Conversion and Management* 158 (Feb. 2018), pp. 81–91.

[273] H. Lai et al. "Design and eco-technoeconomic analyses of SOFC/GT hybrid systems accounting for long-term degradation effects". In: *International Journal of Hydrogen Energy* 46.7 (Jan. 2021), pp. 5612–5629.

[274] H. Marzooghi and M. Raoofat. “Improving the performance of proton exchange membrane and solid oxide fuel cells under voltage flicker using Fuzzy-PI controller”. In: *International Journal of Hydrogen Energy* 37.9 (May 2012), pp. 7796–7806.

[275] J. Peng et al. “Solid oxide fuel cell (SOFC) performance evaluation, fault diagnosis and health control: A review”. In: *Journal of Power Sources* 505 (Sept. 2021), p. 230058.

[276] K. W. Eichhorn Colombo et al. “Transient system-level performance and thermomechanical stress analysis of a solid oxide fuel cell-based power generation plant with a multi-physics approach”. In: *Computers & Chemical Engineering* 140 (Sept. 2020), p. 106972.

[277] M. Fardadi, D. F. McLarty, and F. Jabbari. “Investigation of thermal control for different SOFC flow geometries”. In: *Applied Energy* 178 (Sept. 2016), pp. 43–55.

[278] G. D’Andrea et al. “Dynamic model with experimental validation of a biogas-fed SOFC plant”. In: *Energy Conversion and Management* 135 (Mar. 2017), pp. 21–34.

[279] X. Wu and D. Gao. “Fault tolerance control of SOFC systems based on nonlinear model predictive control”. In: *International Journal of Hydrogen Energy* 42.4 (Jan. 2017), pp. 2288–2308.

[280] E. D. Wachsman and K. T. Lee. “Lowering the temperature of solid oxide fuel cells”. In: *Science* 334.6058 (Nov. 2011), pp. 935–939.

[281] R. Scataglini et al. *A Total Cost of Ownership Model for Solid Oxide Fuel Cells in Combined Heat and Power and Power-Only Applications*. Tech. rep. September. 2015, p. 197.

[282] B. van Veldhuizen et al. “Experimental evaluation of a solid oxide fuel cell system exposed to inclinations and accelerations by ship motions”. In: *Journal of Power Sources* 585 (Nov. 2023), p. 233634.

[283] B. van Veldhuizen et al. “Experimental Evaluation of SOFC System Exposed to Marine Inclination Conditions”. In: *ECS Transactions* 111.6 (2023), pp. 687–698.

[284] R. S. Gemmen and C. D. Johnson. “Evaluation of fuel cell system efficiency and degradation at development and during commercialization”. In: *Journal of Power Sources* 159.1 (Sept. 2006), pp. 646–655.

[285] L. Zhu and J. Chen. “Prognostics of PEM fuel cells based on Gaussian process state space models”. In: *Energy* 149 (2018), pp. 63–73.

[286] H. Deng et al. “Degradation trajectories prognosis for PEM fuel cell systems based on Gaussian process regression”. In: *Energy* 244 (2022), p. 122569.

[287] Tameson. *Proportional Solenoid Valve - How They Work*. 2023. URL: https://tameson.com/pages/proportional-solenoid-control-valve.

[288] S. Zarabi Golkhatmi, M. I. Asghar, and P. D. Lund. “A review on solid oxide fuel cell durability: Latest progress, mechanisms, and study tools”. In: *Renewable and Sustainable Energy Reviews* 161 (June 2022), p. 112339.

[289] S. Futamura et al. “SOFC anodes impregnated with noble metal catalyst nanoparticles for high fuel utilization”. In: *International Journal of Hydrogen Energy* 44.16 (Mar. 2019), pp. 8502–8518.

[290] L. Lu et al. “Demonstration of high performance in a perovskite oxide supported solid oxide fuel cell based on la and Ca co-doped SrTiO3”. In: *Journal of Materials Chemistry A* 4.30 (2016), pp. 11708–11718.

[291] C. Comminges et al. “Monitoring the degradation of a solid oxide fuel cell stack during 10,000 h via electrochemical impedance spectroscopy”. In: *Electrochimica Acta* 59 (Jan. 2012), pp. 367–375.

[292] Q. Fang et al. “SOFC stack performance under high fuel utilization”. In: *International Journal of Hydrogen Energy* 40.2 (Jan. 2015), pp. 1128–1136.

[293] Lloyds Register. *Type Approval System Test Specificaton Fuel Cell Modules*. Tech. rep. 2023.

[294] B. N. van Veldhuizen et al. “The effects of fuel type and cathode off-gas recirculation on combined heat and power generation of marine SOFC systems”. In: *Energy Conversion and Management* 276 (Jan. 2023), p. 116498.

[295] A. Weber. “Fuel flexibility of solid oxide fuel cells”. In: *Fuel Cells* 21.5 (Oct. 2021), pp. 440–452.

[296] B. Lagemann et al. “Optimal ship lifetime fuel and power system selection”. In: *Transportation Research Part D: Transport and Environment* 102 (Jan. 2022), p. 103145.

[297] Z. Hajabdollahi and P. F. Fu. “Multi-objective based configuration optimization of SOFC-GT cogeneration plant”. In: *Applied Thermal Engineering* 112 (Feb. 2017), pp. 549–559.

[298] P. Sarmah, T. K. Gogoi, and R. Das. “Estimation of operating parameters of a SOFC integrated combined power cycle using differential evolution based inverse method”. In: *Applied Thermal Engineering* 119 (June 2017), pp. 98–107.

[299] S. Zhang et al. “An efficient integration strategy for a SOFC-GT-SORC combined system with performance simulation and parametric optimization”. In: *Applied Thermal Engineering* 121 (July 2017), pp. 314–324.

[300] H. Klein Woud and D. Stapersma. *Design of Auxiliary Systems Shafting and Flexible Mounting Systems*. 2011.

[301] A. S. Mehr et al. “Thermodynamic and exergoeconomic analysis of biogas fed solid oxide fuel cell power plants emphasizing on anode and cathode recycling: A comparative study”. In: *Energy Conversion and Management* 105 (Nov. 2015), pp. 596–606.

[302] J. Chen et al. “Control strategy design for a SOFC-GT hybrid system equipped with anode and cathode recirculation ejectors”. In: *Applied Thermal Engineering* 132 (Mar. 2018), pp. 67–79.

[303] J. Chen et al. “Study on control strategy for a SOFC-GT hybrid system with anode and cathode recirculation loops”. In: *International Journal of Hydrogen Energy* 42.49 (Dec. 2017), pp. 29422–29432.

[304] M. Tomberg et al. “Operation of a Solid Oxide Fuel Cell Reactor with Multiple Stacks in a Pressured System with Fuel Gas Recirculation”. In: *Energy Technology* (2022), p. 2101075.

[305] B. N. van Veldhuizen, A. Amladi, and L. van Biert. *Genset Performance with Future Fuels*. Tech. rep. Nautilus Project, 2021.

[306] R. E. Geneidy et al. “Increasing energy efficiency in passenger ships by novel energy conservation measures”. In: *Journal of Marine Engineering & Technology* 17.2 (2018), pp. 85–98.

[307] P. Leone et al. “Operation of a solid oxide fuel cell under direct internal reforming of liquid fuels”. In: *Chemical Engineering Journal* 191 (May 2012), pp. 349–355.

[308] S. Ahmed and M. Krumpelt. “Hydrogen from hydrocarbon fuels for fuel cells”. In: *International Journal of Hydrogen Energy* 26.4 (Apr. 2001), pp. 291–301.

[309] D. Papadias, S. H. D. Lee, and D. J. Chmielewski. “Autothermal Reforming of Gasoline for Fuel Cell Applications: A Transient Reactor Model”. In: *Industrial and Engineering Chemistry Research* 45 (2006), pp. 5841–5858.

[310] S. Farhad and F. Hamdullahpur. “Conceptual design of a novel ammonia-fuelled portable solid oxide fuel cell system”. In: *Journal of Power Sources* 195.10 (May 2010), pp. 3084–3090.

[311] G. Cinti et al. “Experimental Analysis of SOFC Fuelled by Ammonia”. In: *Fuel Cells* 14.2 (Apr. 2014), pp. 221–230.

[312] B. Stoeckl et al. “Characterization and performance evaluation of ammonia as fuel for solid oxide fuel cells with Ni/YSZ anodes”. In: *Electrochimica Acta* 298 (Mar. 2019), pp. 874–883.

[313] M. Sadeghi et al. “Size and exergy assessment of solid oxide fuel cell-based H2-fed power generation system with alternative electrolytes: A comparative study”. In: *Energy Conversion and Management* 228 (Jan. 2021), p. 113681.

[314] P. V. Aravind et al. “Thermodynamic evaluation of small-scale systems with biomass gasifiers, solid oxide fuel cells with Ni/GDC anodes and gas turbines”. In: *Journal of Power Sources* 190.2 (May 2009), pp. 461–475.

[315] CAGI. *Compressed Air and Gas Institute*. 2022. URL: https://www.cagi.org/education/glossary.aspx.

[316] M. Ni, D. Y. C. Leung, and M. K. H. Leung. “Thermodynamic analysis of ammonia fed solid oxide fuel cells: Comparison between proton-conducting electrolyte and oxygen ion-conducting electrolyte”. In: *Journal of Power Sources* 183.2 (Sept. 2008), pp. 682–686.

[317] Y. Mori, A. E. Sheindlin, and N. H. Afgan. “High Temperature Heat Exchangers”. In: *Journal of Pressure Vessel Technology* 109.2 (1987), pp. 264–264.

[318] J. Lienhard. *A Heat Transfer Textbook*. 5th. Cambridge Massachusetts: Phlogiston Press, 2019.

[319] E. Fontell et al. “Conceptual study of a 250 kW planar SOFC system for CHP application”. In: *Journal of Power Sources* 131.1-2 (May 2004), pp. 49–56.

[320] W. L. Becker et al. “Design and technoeconomic performance analysis of a 1 MW solid oxide fuel cell polygeneration system for combined production of heat, hydrogen, and power”. In: *Journal of Power Sources* 200 (Feb. 2012), pp. 34–44.

[321] R. G. Sargent. “Verification and validation of simulation models”. In: *Proceedings - Winter Simulation Conference*. 2010, pp. 166–183.

[322] S. Ahmadi, H. Ghaebi, and A. Shokri. “A comprehensive thermodynamic analysis of a novel CHP system based on SOFC and APC cycles”. In: *Energy* 186 (Nov. 2019), p. 115899.

[323] W. Sangtongkitcharoen et al. “Performance analysis of methanol-fueled solid oxide fuel cell system incorporated with palladium membrane reactor”. In: *Chemical Engineering Journal* 138.1-3 (May 2008), pp. 436–441.

[324] M. Rokni. “Thermodynamic analysis of SOFC (solid oxide fuel cell)-Stirling hybrid plants using alternative fuels”. In: *Energy* 61 (2013), pp. 87–97.

[325] G. Botta et al. “Thermodynamic and Exergy Analysis of Reversible Solid Oxide Cell Systems”. In: *ECS Transactions* 68.1 (July 2015), pp. 3265–3277.

[326] B. van Veldhuizen et al. “Upscaling and Design of an SOFC System for Marine Applications”. In: *International Marine Conference*. 2023.

[327] A. Elkasfas et al. “Fuel Cell Systems for Maritime: A Review of Research and Perspectives”. In: *Processes* 11.97 (2023).

[328] G. Floerchinger et al. “Characterizing the Performance of kW-Scale Multi-Stack Solid Oxide Fuel Cell Modules through Modeling and Experimentation”. In: *ECS Transactions*. Vol. 111. 6. IOP Publishing, May 2023, p. 803.

[329] SolydEra. *Bluegen BG-15 Brochure*. 2022. URL: https://bluegen.eu/wp-content/uploads/2022/09/Brochure_Bluegen_ENG_2022-09_v3_acc.pdf.

[330] IMO. *Interim Guidelines for the Safety of Ships Using Fuel Cell Power Installations*. Tech. rep. 2022.

[331] B. van Veldhuizen et al. “Component sizing and dynamic simulation of a low-emission power plant for cruise ships with solid oxide fuel cells”. In: *Energy Conversion and Management* 326 (Feb. 2025), p. 119477.

[332] SEA-LNG. *Global fleet - SEA-LNG*. 2024. URL: https://sea-lng.org/why-lng/global-fleet/.

[333] B. Comer et al. *Fugitive and Unburned Methane Emissions from Ships*. Tech. rep. 2024.

[334] Fuel Cell Energy. *250 kW Fuel Cell Spec Sheet*. 2022. URL: https://go.fuelcellenergy.com/hubfs/Solid%20Oxide%20Fuel%20Cell%20Spec%20Sheet.pdf.

[335] H. Winnes and E. Fridell. “Particle emissions from ships: Dependence on fuel type”. In: *Journal of the Air and Waste Management Association* 59.12 (2009), pp. 1391–1398.

[336] M. Gandiglio et al. "Energy and environmental performance from field operation of commercial-scale SOFC systems". In: *International Journal of Hydrogen Energy* 85 (Oct. 2024), pp. 997–1009.

[337] S. Sugihara and H. Iwai. "Measurement of transient temperature distribution behavior of a planar solid oxide fuel cell: Effect of instantaneous switching of power generation and direct internal reforming". In: *Journal of Power Sources* 482 (Jan. 2021).

[338] C. Li et al. "Energy and configuration management strategy for solid oxide fuel cell/engine/battery hybrid power system with methanol on marine: A case study". In: *Energy Conversion and Management* 307 (May 2024).

[339] E. A. Pina et al. "A Comparative Techno-Economic Assessment of Alternative Fuels in SOFC Systems for Cruise Ships". In: *ECS Transactions*. 2023, pp. 2459–2472.

[340] F. Alenazey et al. "Degradation Behaviors of Solid Oxide Fuel Cell Stacks in Steady-State and Cycling Conditions". In: *Energy and Fuels* 34.11 (Nov. 2020), pp. 14864–14873.

[341] C. Yang et al. "Degradation mechanism and modeling study on reversible solid oxide cell in dual-mode — A review". In: *International Journal of Hydrogen Energy* 47.89 (2022), pp. 37895–37928.

[342] J. Cichowicz, G. Theotokatos, and D. Vassalos. "Dynamic energy modelling for ship life-cycle performance assessment". In: *Ocean Engineering* 110 (2015), pp. 49–61.

[343] E. Redondo-Iglesias, P. Venet, and S. Pelissier. "Calendar and cycling ageing combination of batteries in electric vehicles". In: *Microelectronics Reliability* 88-90 (Sept. 2018), pp. 1212–1215.

[344] C. Löffler et al. "Optimizing Energy Management for Full-Electric Vessels: A Health-Aware Approach with Hydrogen and Diesel Employing Equivalent Consumption Minimization Strategy". In: *2023 IEEE Transportation Electrification Conference and Expo*. IEEE, Nov. 2023, pp. 1–8.

[345] A. Haseltalab and R. R. Negenborn. "Model predictive maneuvering control and energy management for all-electric autonomous ships". In: *Applied Energy* 251 (Oct. 2019).

[346] A. Oubelaid et al. "Health-conscious energy management strategy for battery/-fuel cell electric vehicles considering power sources dynamics". In: *Journal of Energy Storage* 68 (Sept. 2023), p. 107676.

[347] Y. Bessekon et al. "Simulation of a SOFC/Battery powered vehicle". In: *International Journal of Hydrogen Energy* 44.3 (Jan. 2019), pp. 1905–1918.

[348] B. V. Veldhuizen et al. "Comparative Analysis of Alternative Fuels for Marine SOFC Systems". In: *PRADS*. 2022, pp. 1240–1258.

[349] M. Gandiglio et al. *Performance and emissions of installed systems*. Tech. rep. 2023.

[350] S. Salas Ventura et al. “SOFC & Battery hybrid experimental proof of concept and transient simulation for maritime load following”. In: *16th EUROPEAN SOFC & SOE FORUM*. Lucerne, 2024.

[351] A. Hagen et al. “Degradation of Anode Supported SOFCs as a Function of Temperature and Current Load”. In: *Journal of The Electrochemical Society* 153.6 (2006), A1165.

[352] M. A. Abreu-Sepulveda et al. “Accelerated Degradation for Hardware in the Loop Simulation of Fuel Cell-Gas Turbine Hybrid System”. In: *Journal of Fuel Cell Science and Technology* 12.2 (Apr. 2015).

[353] M. Sheykhi et al. “Performance investigation of a combined heat and power system with internal and external combustion engines”. In: *Energy Conversion and Management* 185 (Apr. 2019), pp. 291–303.

[354] H. Ali et al. “Assessment of the calendar aging of lithium-ion batteries for a long-term—Space missions”. In: *Frontiers in Energy Research* 11 (Feb. 2023).

[355] Y. Preger et al. “Degradation of Commercial Lithium-Ion Cells as a Function of Chemistry and Cycling Conditions”. In: *Journal of The Electrochemical Society* 167.12 (Jan. 2020), p. 120532.

[356] R. D. Deshpande and K. Uddin. “Physics inspired model for estimating ‘cycles to failure’ as a function of depth of discharge for lithium ion batteries”. In: *Journal of Energy Storage* 33 (Jan. 2021).

[357] C. Ünlübayir et al. “Comparative analysis and test bench validation of energy management methods for a hybrid marine propulsion system powered by batteries and solid oxide fuel cells”. In: *Applied Energy* 376.August (2024), p. 124183.

[358] MG Energy Systems. *HE Series*. 2024. URL: https://www.mgenergysystems.eu/en/products/he-series/.

[359] J. S. Shin et al. “Degradation Mechanisms of Solid Oxide Fuel Cells under Various Thermal Cycling Conditions”. In: *ACS Applied Materials and Interfaces* 13.42 (Oct. 2021), pp. 49868–49878.

[360] Maersk Mc-Kinney Moller Center for Zero Carbon Shipping. *Fuel Cell Technologies and Applications for Deep-Sea Shipping*. Tech. rep. 24.

[361] T. P. S. Van Lieshout et al. *Green Maritime Methanol: WP3 factsheet and comparison with diesel and LNG*. Tech. rep. 2020.

[362] O. Schuller et al. *2nd Life Cycle GHG Emission Study on the Use of LNG as Marine Fuel*. Tech. rep. Sphera, 2021.

[363] S. Hwang et al. “Life Cycle Assessment of LNG Fueled Vessel in Domestic Services”. In: *Journal of Marine Science and Engineering 2019, Vol. 7, Page 359* 7.10 (Oct. 2019), p. 359.

[364] M. Perčić, N. Vladimir, and A. Fan. “Life-cycle cost assessment of alternative marine fuels to reduce the carbon footprint in short-sea shipping: A case study of Croatia”. In: *Applied Energy* 279 (Dec. 2020), p. 115848.

[365] IMO. *Sulphur oxides (SOx) – Regulation 14*. 2020. URL: http://www.imo.org/en/OurWork/Environment/PollutionPrevention/AirPollution/Pages/Sulphur-oxides-(SOx)-%E2%80%93-Regulation-14.aspx.

[366] D. Stapersma. *Diesel Engines Volume 4, Emissions and Heat transfer*. Vol. 4. April. 2010.

[367] J. M. J. Journée and W. W. Massie. *Offshore Hydromechanics (Second Edition)*. Tech. rep. TU Delft, 2008.

[368] B. Buchner et al. "Research into container loss above the Dutch Wadden Islands after the MSC ZOE incident". In: *PRADS*. 2022, pp. 1–22.

[369] Jamal, A. Sulisetyono, and W. D. Aryawan. "Review of the seakeeping criteria for the study of a passenger ship criteria in Indonesian water". In: *IOP Conference Series: Materials Science and Engineering*. 2020, p. 012041.

[370] A. Lawther and M. J. Griffin. "The motion of a ship at sea and the consequent motion sickness amongst passengers". In: *Ergonomics* 29.4 (1986), pp. 535–552.

[371] F. Cakici. "Vertical acceleration control using LQG approach for a passenger ship". In: *Ocean Engineering* 241 (Dec. 2021), p. 110040.

[372] I. B. Kucukdemiral, F. Cakici, and H. Yazici. "A model predictive vertical motion control of a passenger ship". In: *Ocean Engineering* 186 (Aug. 2019), p. 106100.

[373] J. Kim and Y. Kim. "Time-domain analysis of passenger comfort on cruise ships under motion responses in waves". In: *Proceedings of the Institution of Mechanical Engineers Part M: Journal of Engineering for the Maritime Environment* 228.4 (2014), pp. 331–347.

[374] R. Shigehiro, T. Kuroda, and Y. Arita. "Evaluation method of passenger comfort for training ships in irregular seas". In: *Proceedings of the International Offshore and Polar Engineering Conference* 4 (2001), pp. 562–569.

[375] ABS. *Rules for Building and classing Marine Vessels - Part4, Vessel Systems and Machinery*. Tech. rep. 2023.

[376] Bureau Veritas. "Part C - Machinery, Electricity, Automation and Fire Protection". In: *Rules for the Classification of Steel Ships*. 2021.

[377] DNV. *Ship rules Pt.4 Ch.1 - Machinery systems - general*. Tech. rep. 2022, p. 289.

[378] Lloyds Register. *Type Approval System Test Specification Number 1*. Tech. rep. 2022.

[379] Korean Register. *Rules for the Classification of Steel Ships Part - Part 5 Machinery Installations*. Tech. rep. 2011.

[380] M. Al-Breiki and Y. Bicer. "Comparative life cycle assessment of sustainable energy carriers including production, storage, overseas transport and utilization". In: *Journal of Cleaner Production* 279 (Jan. 2021), p. 123481.

[381] California Air Resources Board. *Determination of Emissions from a Very Large Crude Carrier Using Two Different Fuels ARB contract #12-425 Disclaimer Acknowledgments*. Tech. rep. 2015.

ACKNOWLEDGEMENTS

For me, the PhD was an exhilarating activity. I would call it an eye-opening experience on so many levels. Doing a project myself for 4 years enabled me to learn a lot about my personality, my qualities and what I really like. Working in a department with PhDs from all around the world, cooperating with international companies, and visiting many countries as part of the research gave me a palpable feeling of appreciation for the world and people around me. On every trip, I returned with renewed inspiration and motivation to put into my research. Nevertheless, all these valuable life lessons would not have been possible without the never-ending support I received during this trajectory.

When I started, Lindert van Biert took me under his wings as his first PhD candidate. In hindsight, it is a risky choice to start a PhD with somebody who does not have an established research group, but you handled it sublimely. I was very quickly amazed by your deep understanding of fuel cells, from which I leared a lot. At the same time, I think we worked very effectively on the Nautilus project, and as two quite pragmatic people we barely disagreed. I greatly appreciate that you prioritised my best interests and gave me the freedom to shape both the research content and my PhD path as I saw fit.

I would like to appoint Klaas Visser as an abundant source of inspiration. In the beginning of the PhD trajectory when we were having a minor issue you said to me: 'Every setback is a chance of improvement'. Seeing you work, I realised this is something you live by, and as a highly optimistic person this truly resonated with me. I also aspire your skills to navigate through complex discussions with many stakeholders and realign everybody's interest. This is a feature within the university.

Professor Aravind, I deeply appreciate your increased involvement in the second part of the PhD, which lifted the scientific quality of the inclination experiment to a higher level. As we both got very excited from the results of the inclination experiment it was a true pleasure to work on this together.

Hans Hopman you always guarded the process of my PhD and made sure that I did not diverge too much from the core topic, which I certainly had a tendency towards.

I would also like to thank Stefano Modena of SolydEra who gave me the opportunity to do lab experiments in the North of Italy for a month. This felt like a crash course on SOFC systems, where Emanuele Zera taught me everything he knew about operation, control, and system design. Other members of the Nautilus project, such as Amandine Thomas, Asif Ansar, Cem Uenluebayir, Daniel Sahnen, Eduardo Pina, Fabian Grimm, Matthias Metten, Santiago Salas Ventura, and Stefan Diethelm, also contributed majorly to the quality and insights of my thesis.

On a more personal note, my roommates, friends, and parents were always deeply intrigued by the research I was doing and their questions kept me reviewing my own work and directions. Especially Kees Fritschy, every time I had the smallest moment of doubt about whether a PhD was the right choice for me, it took you only a few seconds to get me back on track. Nicole Charissi, I loved that you were my office mate, and besides decorating it to be the most stylish office at the TU Delft, you offered a place where we could discuss the more important matters of life.

Finally, to my love Willemijn. Your endless support and encouragement provided me with the needed motivation towards the finish line.

Curriculum Vitæ

Berend Nathan van Veldhuizen

12-03-1996	Born in Delft, Netherlands.

Education

2020-2024	PhD Marine Engineering Delft University of Technology *Thesis:* Marinisation of SOFC Systems
2018-2020	MSc. Marine Technology Delft University of Technology *Thesis:* Fuel cell Systems Applied in Expedition Cruise Ships *Track:* Ship Design, Production and Operation
2013-2017	BSc. Naval Architecture and Marine Engineering Delft University of Technology

Experience

2021-2023	Chair of University PhD Council Delft University of Technology, The Netherlands
2020	Design & proposal internship Damen Shipyards, Gorinchem, The Netherlands
2018-2019	Junior Maintenance Manager Koole Terminals, The Netherlands
2017	Acquisition Manager AIESEC Delft, The Netherlands

RESEARCH VISITS

02/2023	SOFC experiments (5 weeks) SolydEra, Mezzolombardo, Italy
08/2022	SOFC experiments (2 weeks) SolydEra, Mezzolombardo, Italy

CONFERENCE CONTRIBUTIONS

2	Invited talks at international workshops or conferences
11	Contributions to international workshops or conferences
2	Poster presentations at international workshops or conferences

PHD RELATED ACTIVITIES

2	International summer schools
12	Professional courses
4	Supervised MSc theses
2	Supervised BSc theses
4	Journal articles reviewed

List of Publications

Journal publications

4. **B.N. van Veldhuizen**, L. van Biert, C. Ünlübayir, K. Visser, J.J. Hopman, P.V. Aravind, *Component sizing and dynamic simulation of a low-emission power plant for cruise ships with solid oxide fuel cells*, Energy Conversion and Management **326**, 119477 (2025).

3. **B.N. van Veldhuizen**, E. Zera, L. van Biert, S. Modena, K. Visser, P.V. Aravind, *Experimental evaluation of a solid oxide fuel cell system exposed to inclinations and accelerations by ship motions*, Journal of Power Sources **585**, 233634 (2023).

2. **B.N. van Veldhuizen**, L. van Biert, K. Visser, P.V. Aravind, *Solid Oxide Fuel Cells for marine applications*, International Journal of Energy Research **2023**, 5163448 (2023).

1. **B.N. van Veldhuizen**, L. van Biert, A. Amladi, T. Woudstra, K. Visser, P.V. Aravind, *The effects of fuel type and cathode off-gas recirculation on combined heat and power generation of marine SOFC systems*, Energy Conversion and Management **276**, 116498 (2023).

Conference proceedings

7. **B.N. van Veldhuizen**, L. van Biert, K. Visser, J.J. Hopman, P.V. Aravind, *Dynamic simulation of marine SOFC power plant Berend*, EFCF2024: 16th European SOFC & SOE Forum. Lucerne Switzerland. (2024).

6. P.C. Hofste, **B.N. van Veldhuizen**, M. Duinkerken, D. Schott, *Design of an Ammonia Bunker Installation for Sea-going Vessels - A Best Worst Method Approach*, MARTECH2024: 7th International Conference on Maritime Technology and Engineering. Lisbon, Portugal. (2024).

5. **B.N. van Veldhuizen**, S. Diethelm, D. Sahnen, A. Thomas, L. van Biert, K. Visser, *Upscaling and Design of an SOFC System for Marine Applications*, IMC2023: International Maritime Conference. Sydney, Australia. (2023).

4. E.A. Pina, **B.N. van Veldhuizen**, F. Maréchal, J. van Herle, *A Comparative Techno-Economic Assessment of Alternative Fuels in SOFC Systems for Cruise Ships*, ECS Transactions **111** (6), 2459-2472 (2023).

3. **B.N. van Veldhuizen**, E. Zera, L. van Biert, S. Modena, P.V. Aravind, K. Visser, J.J. Hopman, *Experimental Evaluation of SOFC System Exposed to Marine Inclination Conditions*, ECS Transactions **111** (6), 687-698 (2023).

2. **B.N. van Veldhuizen**, L. van Biert, K. Visser, J.J. Hopman, *Comparative Analysis of Alternative Fuels for Marine SOFC Systems*, PRADS2022: 15th International Symposium on Practical Design of Ships and Other Floating Structures. Dubrovnik, Kroatia. (2022).

1. **B.N. van Veldhuizen**, L. van Biert, K. Visser, P.V. Aravind, J.J. Hopman, *Comparative thermodynamic analysis of marine SOFC system for alternative fuels*, EFCF2022: 15th European SOFC & SOE Forum. Lucerne Switzerland. (2022).